

# **UC San Diego**

## **UC San Diego Electronic Theses and Dissertations**

**Title**

Carotenoid biosynthesis and productivity in diatoms

**Permalink**

<https://escholarship.org/uc/item/6c13j7mg>

**Author**

Gaidarenko, Olga Dmitrievna

**Publication Date**

2018

Peer reviewed|Thesis/dissertation

UNIVERSITY OF CALIFORNIA SAN DIEGO

Carotenoid biosynthesis and productivity in diatoms

A dissertation submitted in partial satisfaction of the  
requirements for the degree Doctor of Philosophy

in

Biology

by

Olga Gaidarenko

Committee in charge:

James Golden, Chair  
Eric Allen  
Steven Briggs  
Brian Palenik  
Julian Schroeder  
Maria Vernet

2018

Copyright

Olga Gaidarenko, 2018

All rights reserved

The Dissertation of Olga Gaidarenko is approved, and it is acceptable in quality and form for publication on microfilm and electronically:

---

---

---

---

---

---

---

Chair

University of California San Diego

2018

## **DEDICATION**

I would like to dedicate this dissertation to my advisor, Dr. Mark Hildebrand, who was an incredibly dedicated and generous mentor, and a dear friend.

I would also like to dedicate this dissertation to my beloved, wonderful grandparents Victor, Elena, Raisa, and Vladimir, in no particular order. I admire you all tremendously.

Finally, I would like to dedicate this dissertation to my favorite (not so) little (anymore) human, Layla Michelle Muñozmartin, who has been one of my greatest teachers in life. Shine on and always remember to stop and feel the breeze as you grow, kiddo.

## TABLE OF CONTENTS

SIGNATURE PAGE.....	iii
DEDICATION.....	iv
TABLE OF CONTENTS.....	v
LIST OF FIGURES.....	vii
LIST OF TABLES.....	ix
ACKNOWLEDGEMENTS.....	x
VITA.....	xiii
ABSTRACT OF THE DISSERTATION.....	xiv
<b>INTRODUCTION.....</b>	<b>1</b>
References for the Introduction.....	14
<b>CHAPTER 1:</b> Timing is everything: diel metabolic and physiological changes in the diatom <i>Cyclotella cryptica</i> grown in simulated outdoor conditions.....	19
1.1 Abstract.....	20
1.2 Introduction.....	20
1.3 Materials and Methods.....	23
1.4 Results.....	27
1.5 Discussion.....	34
1.6 Summary and Conclusions.....	49
1.7 Acknowledgements.....	51
1.8 References.....	68
<b>CHAPTER 2:</b> Novel <i>Thalassiosira pseudonana</i> violaxanthin de-epoxidase-like enzyme (VDL2) catalyzes fucoxanthin biosynthesis.....	74
2.1 Abstract.....	75

2.2 Introduction.....	76
2.3 Results.....	78
2.4 Discussion.....	87
2.5 Methods.....	100
2.6 Acknowledgements.....	104
2.7 References.....	125
Appendix 2.A BLAST Results.....	130
Appendix 2.B Alignments and percent identity matrices.....	135
Appendix 2.C Full-length gene models, protein targeting predictions.....	148
Appendix 2.D Additional sequence-based analyses.....	188
Appendix 2.E Plasmid maps and primers.....	217
<b>CHAPTER 3: Enhanced triacylglycerol (TAG) and protein accumulation in transgenic diatom</b>	
<i>Thalassiosira pseudonana</i> with altered photosynthetic pigmentation.....	221
3.1 Abstract.....	222
3.2 Introduction.....	223
3.3 Results.....	226
3.4 Discussion.....	231
3.5 Methods.....	239
3.6 Acknowledgements.....	242
3.7 References.....	256
<b>CONCLUSIONS.....</b>	259
References for the conclusions.....	267

## LIST OF FIGURES

Figure I.1: Light limitation in a dense microalgal culture.....	13
Figure 1.1: Sinusoidal changes in light and temperature.....	55
Figure 1.2: Culture density relative to cell cycle progression.....	55
Figure 1.3: Culture density and OD750.....	56
Figure 1.4: Rate of OD750 increase per cell versus incident light energy intensity.....	57
Figure 1.5: Increase in OD750 per day versus OD750 at dawn. ....	57
Figure 1.6: Dawn dip in OD750.....	58
Figure 1.7: Cellular TAG levels relative to cell cycle progression. ....	59
Figure 1.8: Changes in cellular pigment abundance vs. cell cycle progression or light intensity... .....	60
Figure 1.9: Changes in normalized cellular abundance of Fx, Chl a, Chl c, and $\beta$ -car.....	61
Figure 1.10: Ddx and Dtx cellular abundance and de-epoxidation state.....	61
Figure 1.11: Changes in the Chl a/Fx and Chl a/Chl c ratios.....	62
Figure 1.12: Optimal harvesting times.....	63
Figure S1.1: Daily OD750 changes.....	64
Figure S1.2: Raw cell counts and fitted curves.....	64
Figure S1.3: Correlation between ash-free dry weight (AFDW) and OD750.....	65
Figure S1.4: Biomass at 6am, gained by the end of the light period, and lost at night .....	65
Figure S1.5: Changes in pigment abundance vs. cell cycle progression. ....	66
Figure S1.6: Total TAG vs. cell cycle progression.....	66
Figure S1.7: Changes in normalized cellular Chl a, Fx, and Ddx+Dtx abundance .....	67
Figure 2.1: Putative carotenoid biosynthesis pathway in <i>T. pseudonana</i> .....	116
Figure 2.2: Sequence identity-based phylogenetic trees.....	117
Figure 2.3: Candidate gene silicon starvation microarray expression patterns .....	118

Figure 2.4: RNA-seq gene expression patterns .....	119
Figure 2.5: HPLC-based pigment analysis of VDL2 OE clones.....	120
Figure 2.6: HPLC-based pigment analysis of LTL KD clones.....	121
Figure 2.7: HPLC-based pigment analysis of VDL1 KD clones .....	122
Figure 2.8: HPLC-based pigment analysis of VDL2 KD clones .....	122
Figure 2.9: Model of differential carotenoid biosynthesis regulation in <i>T. pseudonana</i> .....	123
Figure S2.1: RNA-seq carotenoid biosynthesis gene expression during silicon starvation.....	124
Figure S2.2: qRT-PCR screen for VDL2 overexpression.....	124
Figure 3.1: Rapid light curves.....	246
Figure 3.2: Rapid light curve-derived non-photosynthetic quenching values .....	247
Figure 3.3: Wild type and LTL KD morphology.....	248
Figure 3.4: Growth curves.....	249
Figure 3.5: Average BODIPY fluorescence.....	250
Figure 3.6: Average total cellular protein content. ....	251
Figure 3.7: NPQ at cultivation irradiance vs. BODIPY fluorescence.....	252
Figure 3.8: NPQ at cultivation irradiance vs. total cellular protein content. ....	252
Figure S3.1: Cell area-normalized BODIPY, protein, and carbohydrates for HL LTL KD .....	253
Figure S3.2: Average total cellular carbohydrate content. ....	254
Figure S3.3: (Ddx+Dtx)/Tot vs. NPQ at cultivation irradiance.....	255

## LIST OF TABLES

Table 1.1: Average cellular pigment content and ratios.....	52
Table S1.1: Sample to sample variation in photosynthetic pigment content (pg/cell).....	53
Table S1.2: Nightly biomass loss.....	54
Table S1.3 Yields at optimal harvesting times vs. 8:00 h.....	54
Table 2.1: Model IDs of known carotenoid biosynthesis genes/enzymes and corresponding BLAST results.....	105
Table 2.2: Targeting predictions for known carotenoid biosynthesis enzymes and candidates..	107
Table 2.3 Partial sequence identity matches for the Thaps3_263437 C-terminal peptide.....	108
Table 2.4 Functional annotation of <i>T. pseudonana</i> carotenoid biosynthesis enzymes.....	109
Table 2.5 Carotenoid biosynthesis genes in currently available diatom genomes.....	114
Table 3.1 Photosynthetic parameters.....	244
Table 3.2 Average cell and chloroplast (Chl) area measurements, specific growth rates.....	245

## ACKNOWLEDGEMENTS

First, I cannot thank enough my advisor Dr. Mark Hildebrand who was incredibly dedicated to his students and really generous with his time and energy. His support, enthusiasm, patience, and friendship were indispensable throughout this journey, and I am forever grateful.

I am also very grateful to my doctoral committee members for all their support, guidance, and help. Thank you to Dr. James Golden for stepping in as the chair of the committee in the final few months and providing very helpful feedback and advice, as well as for ongoing support throughout my time in the program. Thank you to Dr. Maria Vernet for all the help, mentorship, advice, and support, and for enabling me to do the photopigment work. Thank you to Dr. Steve Briggs for all the support, guidance, help, discussions, and insights. Thank you to Dr. Brian Palenik for all the insightful questions, feedback, suggestions, and support. Thank you to Dr. Eric Allen for all the helpful fresh perspectives, discussions, suggestions, and support. Thank you to Dr. Julian Schroeder for being willing to join the committee in the last couple of months and being very helpful and flexible.

Thank you to all the members of the Hildebrand laboratory, present and past, for being such a wonderful group to be a part of. Thank you especially to Dr. Sarah Lerch, Dr. Roshan Shrestha, Daniel Yee, Corinne Sathoff, Dr. Jesse Traller, and Dr. Eva Sanchez for all the support, especially in the last few months leading up to my defense. Thank you also to Dr. Raffaela Abbriano, Dr. Aubrey Davis, Dr. Orna Cook, Dr. Sarah Smith, Dylan Mills, and Dr. Kalpana Manandhar-Shrestha for all the help, discussions, and being great lab mates, and thank you Maitreyi Nagarkar for being a great honorary lab member.

Thank you also to the Hubbs community and SIO community in general for being such a wonderful part of my experience here and providing a supportive and intellectually stimulating environment. Thank you as well to the members of the Biological Sciences department,

especially Dr. Amy Pasquinelli, Dr. James Posakony, Dr. Don Helinski, and Dr. Kees Murre for mentorship and being so supportive of me. Thank you also to Dr. Susan Golden for encouraging my interest in circadian biology and providing access to her course, which was one of the highlights of my graduate school journey.

Thank you to all the administrative folks who have helped with numerous logistics, especially Annamarie Bryson, Marifel Alfaro, Suzi Harlow, Lien Ngo, Natalie Noles, Cathy Pugh, and Thomas Thomp.

Thank you also to the members of the UC San Diego and Biological Sciences teaching community, especially Dr. Erylynn Heinrichsen – it has been such a pleasure interacting with you, and I learned so much.

Thank you to my family and especially my parents for all the patience, understanding, support, and tremendous sacrifices made so I can be where I am today.

Lots of gratitude also to my wonderful friends who have been so supportive and understanding through this journey, especially Tarsha Stith, Michael Martin, Erica Lo, Nellia Fleurova-Charlton, Duke Allen, Dr. Kelly Beverly, Dr. Eleodora Andreatta, and Katie DiLibero. And, of course, my dearest Layla Michelle Muñozmartin and my sweet kitty-friend CousCous.

Finally, a big thank you to the music community for enriching my life in so many ways and helping me be a stronger, better, and more balanced person.

#### **PUBLISHED/PREPARED FOR PUBLICATION DISSERTATION MATERIAL**

Chapter 1, in full, has been submitted for publication. Gaidarenko, Olga; Sathoff, Corinne; Staub, Kenneth; Huesemann, Michael M.; Vernet, Maria; Hildebrand, Mark. "Timing is everything: diel metabolic and physiological changes in the diatom *Cyclotella cryptica* grown in

simulated outdoor conditions.” Olga Gaidarenko was the principal author on this paper. We thank Dr. Susan Golden and members of her lab for lending us the ePBR used for this work. We also thank Dr. Daniel Wangpraseurt for assistance with data interpolation. Additionally, we thank Dr. James Golden for providing helpful feedback on the manuscript. This work was supported by U.S. Dept. of Energy grant DE-SC0012556.

Chapter 2, in full, is material currently being prepared for submission for publication. Gaidarenko, Olga; Mills, Dylan W.; Vernet, Maria; Hildebrand, Mark. “Novel *Thalassiosira pseudonana* violaxanthin de-epoxidase-like enzyme (VDL2) catalyzes fucoxanthin biosynthesis.” Olga Gaidarenko was the principal researcher and author of this work. We thank Dr. Sarah R. Smith and Dr. Raffaela M. Abbriano for helpful discussions and data that made this work possible, as well as Dr. Roshan P. Shrestha for helpful discussions and providing genetic manipulation tools. Additionally, we thank Dr. Bradley Moore and Dr. Jonathan Chekan for providing valuable perspective and insights. We also thank Dr. James Golden for critically reading the chapter and providing helpful input. This work was supported by U.S. Dept. of Energy grant DE-FOA-0001471.

Chapter 3, in full, is material currently being prepared for submission for publication. Gaidarenko, Olga; Yee, Daniel; Hildebrand, Mark. “Enhanced triacylglycerol (TAG) and protein accumulation in transgenic diatom *Thalassiosira pseudonana* with altered photosynthetic pigmentation.” Olga Gaidarenko was the principal researcher and author of this work. We thank Dr. Andrew E. Allen and members of his lab for providing access to the Water PAM used in this work. We also thank Ms. Corinne Sathoff for assistance with cultivation chamber set-up and ImageStream data analysis. Additionally, we thank Dr. James Golden for critically reading this work and providing helpful input. This work was supported by U.S. Dept. of Energy grant DE-FOA-0001471.

## VITA

2006	Bachelor of Science, Molecular Biology University of California San Diego
2018	Doctor of Philosophy, Biology University of California San Diego

## PUBLICATIONS

**Gaidarenko O.**, Yee D., Hildebrand M. Enhanced triacylglycerol (TAG) and protein accumulation in transgenic diatom *Thalassiosira pseudonana* with altered photosynthetic pigmentation. In prep.

**Gaidarenko O.**, Mills D. W., Vernet M., Hildebrand M. Novel *Thalassiosira pseudonana* violaxanthin de-epoxidase-like enzyme (VDL2) catalyzes fucoxanthin biosynthesis. In prep.

**Gaidarenko O.**, Sathoff C., Staub K., Huesemann M. M., Vernet M., Hildebrand M. Timing is everything: diel metabolic and physiological changes in the diatom *Cyclotella cryptica* grown in simulated outdoor conditions. Submitted.

Wangpraseurt D., You S., Azam F., Jacucci G., **Gaidarenko O.**, Hildebrand M., Kuhl M., Smith A. G., Davey M. P., Deheyen D. D., Chen S., Vignolini S. Bionic 3D printed corals. Submitted.

Traller, J., Lopez, D., Cokus, S., **Gaidarenko, O.**, Smith, S., McCrow, J., Gallaher, S., Podell, S., Thompson, M., Cook, O., Morcelli, M., Jaroszewicz, A., Allen, E., Allen, A.E., Merchant, S.S., Pellegrini, M., and Hildebrand, M. (2016). Genome and methylome of the oleaginous diatom *Cyclotella cryptica* reveal genetic flexibility toward a high lipid profile. *Biotechnol Biofuels* 9:258.

**Gaidarenko, O.** and Xu, Y. (2011). Relationship between regulatory pathways in pluripotent stem cells and human tumors. In Allan, A. (Ed.), *Cancer Stem Cells in Solid Tumors*. Springer.

**Gaidarenko, O.** and Xu, Y. (2009). Transcription activity is required for p53-dependent tumor suppression. *Oncogene* 28: 4397–4401.

Jenkins, L. M., Mazur, S.J., Rossi, M., **Gaidarenko, O.**, Xu, Y., and Appella, E. (2008). Quantitative proteomics analysis of the effects of ionizing radiation in wild type and p53 K317R knock-in mouse thymocytes. *Mol Cell Proteomics* 7:716-27.

## **ABSTRACT OF THE DISSERTATION**

Carotenoid biosynthesis and productivity in diatoms

by

Olga Gaidarenko

Doctor of Philosophy in Biology

University of California San Diego, 2018

Professor James Golden, Chair

Due to their versatility and modest cultivation requirements, microalgae are a promising potential source of sustainable fuel, chemicals, and food. At present, microalgal production at scale is not economically viable. A major hurdle to productivity is the inefficient use of light energy by dense microalgal cultures. Due to extensive photopigmentation, microalgae closest to the light source absorb more light than they can use, and wastefully dissipate the rest. As a result, light penetrance into the culture is steeply attenuated. Reducing light-harvesting or dissipation capacity of microalgal cells is a promising solution to uneven light distribution in mass

cultures. Most efforts to do so have focused on chlorophytes, with some successes. Diatoms are a class of microalgae that is very promising in terms of productivity and has evolved light-harvesting and photoprotective strategies that differ substantially from those utilized by chlorophytes. This dissertation explores the notion of improving diatom productivity through manipulating their light-harvesting and dissipation capabilities. Because microalgal performance in production conditions can differ substantially from what is observed in the laboratory, the responses of a wild-type production candidate diatom to simulated outdoor conditions are examined in Chapter 1. Substantial diel changes in hypothetical product yields were observed and discussed in terms of what variables need to be optimized to maximize productivity. Main light-harvesting and photoprotective carotenoid-derived photopigments were found to respond differently to chloroplast division and changes in irradiance, suggesting differential regulation. Chapter 2 examined carotenoid biosynthesis in diatoms, because diatom carotenoids play major light-harvesting and photoprotective roles. Targets for genetic manipulation were identified, transgenic lines with two distinct altered photopigmentation phenotypes were generated, and a model for how diatom carotenoid biosynthesis may be differentially regulated in response to chloroplast division and irradiance increase was developed. Chapter 3 focused on examining photosynthetic performance, growth, and productivity of two transgenic strains created in Chapter 2 and identified a strategy that may substantially improve diatom productivity. Overall, the dissertation substantially advances the understanding of diatom carotenoid biosynthesis, identifies strategies for improving light utilization efficiency in diatom cultures, and contributes to the understanding of practices to maximize the productivity of commercial microalgal cultivation.

## **INTRODUCTION**

Photosynthetic microalgae are vastly diverse microorganisms that harness light energy and convert it to biochemical energy. Their unique characteristics with respect to cultivation requirements and chemical composition make them attractive for a variety of commercial applications. Different microalgal species can be adapted to grow in diverse environmental conditions. They can be cultivated on non-arable land and may be able to thrive on waste water and factory flue gases. Microalgae utilize CO<sub>2</sub>, light energy, and media with relatively modest nutrient requirements for the biosynthesis of carbohydrates, lipids, proteins, and pigments. Those compounds are exploitable for the purposes of enhancing nutrition for humans and other animals, manufacturing of cosmetics and pharmaceuticals, and providing feedstock for a variety of renewable types of fuel, including biodiesel, hydrogen, methane, and ethanol [Mata et al. 2010, Pultz and Gross 2004, Spolaore et al. 2005].

Given the increasing demand for sustainable and environmentally friendly sources of fuel and food for the ever-growing human population, there have been numerous efforts put forth over several decades in different parts of the globe to domesticate microalgae and take advantage of their modest cultivation requirements and promising production potential. At present, however, the biotechnological efforts remain stymied by the suboptimal performance of microalgae in industrial cultivation conditions [Spolaore et al. 2005]. Microalgal production systems are not yet cost-efficient enough for mass production of microalgal-derived products to be economically feasible [Davis et al. 2011, Stephens et al. 2010]. One of the main factors that limits microalgal productivity in the dense cultures used in commercial settings is the inefficient capture and use of light energy [Goldman 1978, Kok 1960, Neidhardt et al. 1998, Torzillo et al. 2003].

The lack of efficiency with which microalgal cultures utilize light had been noted during early efforts at microalgal biotechnology [Burlew 1953]. Microalgae are only able to utilize approximately 10% of the light energy available to them when exposed to direct sunlight. This

limitation in light utilization is the result of the rate of light absorption at moderate to high photon flux density values greatly surpassing the biochemical conversion rate in microalgal cells [Burlew 1953, De Mooij et al. 2015, Radmer and Kok 1977, Sukenik et al. 1987, Torzillo et al. 2003]. Microalgae assemble extensive pigment-protein complexes known as photoantennae in their thylakoid membranes that harvest light energy and channel it to photosynthetic reaction centers, where it is used to drive photochemistry. Because microalgae are diverse and have complex evolutionary histories, different taxa employ varied strategies to adjust their light-harvesting apparatus in response to light availability. In chlorophytes, for example, the photoantenna size depends on light availability, with larger photoantennae being assembled by cells in more light-limited environments. This increases the surface area available for light absorption and offers a competitive advantage in the wild [Brown and Richardson 1968, Falkowski and Raven 1997, Mitra and Melis 2008, Mussgnug et al. 2007]. Diatoms, brown microalgae of the Stramenopile or heterokont class, do not adjust photoantenna size, but co-regulate the abundance of photoantennae and reaction centers based on cultivation irradiance [Lepetit et al. 2012]. Microalgal cultures that are subject to mixing adjust photopigmentation based on average irradiance. Due to the steep light attenuation in dense cultures (**Fig. I-1**), the average irradiance is lower than that at the surface, which signals for higher light-harvesting pigmentation than is necessary and useful, wasting cellular resources [Sukenik and Falkowski 1986, Torzillo et al. 2003]. As a result, the extensive light-harvesting pigmentation presents a hurdle to overall productivity of commercially-grown microalgal cultures, which tend to be dense and grown with mixing. Cells that are closest to the light source absorb more light than they are able to utilize. Excess photons are wastefully dissipated as heat and fluorescence, meanwhile light-induced stress results in photoinhibition and further decrease in light utilization efficiency and, therefore, productivity [Myers and Burr 1940, Vonshak and Guy 1992]. Cells that are deeper into the culture are shaded, have less light available

for photosynthesis, and are sub-productive as well. Respiratory losses must also be considered when contemplating the light utilization efficiency in dense cultures. The lower the average light intensity experienced by the cells in the culture is, the greater is the fraction of that light energy that will be necessary to compensate for respiration, leaving a smaller fraction of light energy available for biosynthetic gains [Kok 1953, Kok 1960, Radmer and Kok 1977, Torzillo et al. 2003].

Four general types of solutions to the problem of imbalanced light distribution in dense microalgal cultures have been proposed and attempted since the middle of the 20<sup>th</sup> century. One of the solutions entailed using high culture density along with rapid mixing, based on the notion that individual cells would be brought to the surface very briefly, then plunged deep into the culture, where there would be practically no light, long enough to assimilate all the harvested light energy prior to being brought to the surface again. Rapidly alternating light/dark periods proved promising in the controlled environment of the laboratory. However, the high variability of outdoor conditions, along with the technical challenges of designing a system that would provide the appropriate light intermittence to a substantial proportion of cells moving randomly in a dense large-scale culture, render the practical applications of the strategy problematic. Increasing cell density has been shown to decrease photoinhibition in outdoor cultures grown with mixing, but not enough to eliminate it in cultures grown at densities that are below the threshold at which productivity becomes compromised due to factors such as autoinhibitor accumulation and respiratory losses [Burlew 1953, Goldman 1978, Kok 1953, Qiang et al. 1996, Richmond 1996, Torzillo et al. 2003]. Another practical consideration is that before the cultures reach the high density necessary for this approach, they would be at lower densities.

Another idea was to use photobioreactor design to dilute the light that impinges directly upon the surface of the culture, and/or distribute it more evenly throughout its depth. Evenari et al. [1953] were among the first to propose such a design, during their early work on microalgal

cultivation in Israel. They were followed by numerous other groups, whose diverse and creative ideas are reviewed in Torzillo et al. [2003]. Whereas, in principle, some improvements in algal productivity appear to be achievable by employing clever photobioreactor design tactics, those are, at present, overshadowed by the prohibitive costs and engineering challenges associated with the construction, scaling up, deployment, and maintenance of such systems [Torzillo et al. 2003].

A system for growing thin-layer dense microalgal cultures in a cascading photobioreactor was developed in the 1960's [Setlik et al. 1970]. The main advantages of that approach are relatively low equipment costs and greater light availability to all the cells in the culture due to the shorter light path, compared to the more commonly used photobioreactors and raceway ponds (6-8 mm versus 15 cm or deeper). Such systems may be promising in terms of productivity. However, factors such as light saturation, photoinhibition, and overabsorption/wasteful dissipation of photons at moderate to high light intensities are not mitigated by the design and present a challenge to optimizing yields. Additionally, care must be taken when designing the pumping mechanism necessary for the circulation of microalgae through that type of system in order to avoid shear stress, which would negatively impact productivity [Doucha and Livansky 2009, Torzillo et al. 2010]. Again, the practicality of growing the cultures from lower density inoculates to the desired high density must be considered with this approach.

Finally, the reduction of cellular light-harvesting capacity had been suggested as a means to create microalgal strains with improved light utilization efficiency at high culture densities [Radmer and Kok 1977, Sukenik and Falkowski 1987]. In theory, cells with reduced light-harvesting capacity would become light-saturated and risk photoinhibition at greater light intensities than their wild-type (WT) counterparts. In a dense culture of cells with reduced light-harvesting capacity, those closest to the light source would absorb less light energy and process it with higher efficiency. Light penetrance into the culture would increase, allowing for a greater proportion of the cells to be

photosynthetically active. Thus, the culture as a whole would be more productive and waste less light energy through dissipation due to overabsorption. Also, with light availability being less of a limiting factor, mass cultures may be able to achieve higher densities for a given culture depth [De Mooij et al. 2015, Mitra and Melis 2008].

This principle was first experimentally demonstrated by Melis et al. [1999] in the late 1990's. They used high light-adapted *Dunaliella salina* (chlorophyte) as a model system to study the effects of having reduced photoantenna size on a culture as a whole. Compared to low light-adapted cells with substantially more extensive photoantennae, the high light-adapted cells indeed allowed for greater light penetrance into the culture, required much higher irradiance for light-saturation, and had a higher per chlorophyll photosynthetic efficiency. High light-acclimated cells would not be able to sustain their small photoantenna phenotype at higher culture densities, and thus would not be an option for improving productivity in mass cultures. However, these findings encourage genetic manipulation of microalgae as an approach to creating strains with a stable reduction in light-harvesting capacity with the hopes that they will prove to be more productive in mass cultures [Melis et al. 1999, Neidhardt et al. 1998].

Around the same time frame, Nakajima and colleagues published the first studies of a photoantenna mutant. They demonstrated that a *Synechocystis* sp. (cyanobacteria) mutant with diminished photoantennae was less susceptible to photoinhibition, became light-saturated at higher irradiance, and was more photosynthetically active and productive than WT under their cultivation conditions [Nakajima and Ueda 1997, Nakajima et al. 1999, Nakajima and Ueda 1999]. Shortly after, more studies by various groups followed, characterizing various chlorophyte and cyanobacterial strains with the reduced photoantenna phenotype. Additionally, one study featured a photopigment mutant of a *Cyclotella* sp. (diatom) [Huesemann et al. 2009]. The cultivation conditions and parameters assessed varied greatly between the different studies. Cultivation

systems ranged from small laboratory photobioreactors to 7 L hanging-bag photobioreactors grown outdoors. One or more improvements over parental strains, such as greater light penetrance into the culture, light saturation at higher irradiance, increased maximum photosynthetic rate, increased maximum cell density, improved light to biomass conversion efficiency, and decrease in photoinhibition and photon overabsorption were noted for most of the strains [Beckmann et al. 2009, Cazzaniga et al. 2014, Kirst et al. 2012, Kwon et al. 2013, Lea-Smith et al. 2014, Leganes et al. 2014, Mitra and Melis 2008, Mussgnug et al. 2007, Nakajima et al. 1999, Nakajima and Ueda 1997, Nakajima and Ueda 2000, Ort et al. 2011, Polle et al. 2000, Polle et al. 2001, Polle et al. 2002, Polle et al. 2003]. Some groups saw increased growth rates [Beckmann et al. 2009, Mussgnug et al. 2007], while others reported slower growth [Huesemann et al. 2009, Kirst et al. 2012]. Some groups measured higher productivity under their cultivation conditions [Cazzaniga et al. 2014, Nakajima and Ueda 1999, Nakajima and Ueda 2000, Nakajima et al. 2001, Polle et al. 2000, Polle et al. 2003]. One study found that a truncated photoantenna mutant of the chlorophyte *Chlamydomonas reinhardtii* produced hydrogen more efficiently than WT in their experimental setup [Kosorouev et al. 2011]. Others found that the improved photosynthetic characteristics of their lines did not translate to greater productivity in their culture conditions [Huesemann et al. 2009, Lea-Smith et al. 2014, Page et al. 2012]. It is likely that for strains generated through chemical or ultraviolet radiation-induced mutagenesis, multiple other genetic loci were affected, which may have had an adverse impact on the fitness and performance of those strains. Insertional or transposon-mediated mutagenesis, as well as the introduction of a transgene, are substantially safer in terms of the chances of introducing unwanted genetic alterations along with the intended one, since there usually is only one or few insertion sites. Performance of the strains generated using those approaches may have been also affected by unintended consequences of the genetic alterations

that led to the desired phenotypic changes [Cazzaniga et al. 2014, de Mooij et al. 2015, Huesmann et al. 2009, Mitra and Melis 2008].

De Mooij et al. [2015] recently tested the performance of four *C. reinhardtii* photoantenna mutants in simulated mass culture conditions, using a laboratory scale photobioreactor and irradiance of  $1500 \mu\text{mol photons m}^{-2}\text{s}^{-1}$ , approximating that of full sunlight. Despite the promising initial characterization of the mutants [Bonente et al. 2011, Kirst et al. 2012, Mussgnug et al. 2007], higher productivity was not observed in their culture system. Compared to WT, a greater sensitivity to high light and tendency towards photodamage were observed in the four mutant lines. This finding could be attributed to off-target effects of the procedures used to obtain the mutants, a loss of light-responsive regulatory capabilities in the mutant photoantenna complexes [de Mooij et al. 2015], or a general reduction in antioxidant capacity due the decrease in pigmentation, with a concomitant increase in susceptibility to damage caused by reactive oxygen species that are produced in the thylakoid membranes when exposed to high levels of irradiance [Baroli et al. 2004, Li et al. 2012, Torzillo et al. 2003, Vetroshkina et al. 2015].

It is important to note that whereas studies in laboratory conditions are informative, they do not necessarily predict outcomes in mass culture conditions, which can differ substantially with respect to the quality and quantity of available light, light path/culture depth, pond/photobioreactor geometry and its effects on cell mixing, and diurnal light/temperature fluctuations experienced by outdoor cultures. To date, few lines with altered light-harvesting capabilities have been examined in production conditions. The mutant *Cyclotella* sp. (diatom) generated by Huesemann et al. [2009] performed worse than the WT in a raceway pond. However, it was generated by two rounds of mutagenesis, once with ethylmethane sulfonate, then with ultraviolet radiation, and likely harbored numerous other mutations that gave it an overall reduced fitness, as indicated by its slower growth rate and higher propensity for washout in semi-continuous

culture conditions. The mutant was also green rather than golden-brown, suggesting that a substantial loss of carotenoids, critical for photoprotection and reactive oxygen species scavenging, had occurred [Huesmann et al. 2009]. On the other hand, Cazzaniga et al. [2014] reported greater biomass productivity in their mutant chlorophyte *Chlorella sorokiniana* in laboratory conditions as well as outdoors when cultivated in 7 L hanging bag photobioreactors.

Improving productivity in mass cultures by altering cellular light-harvesting properties remains an attractive prospect. The challenges discovered to date are informative and must be taken into account for future work. It will be important to develop methods for reducing the cellular light-harvesting capacity that do not adversely affect overall cellular fitness. Tolerance of high and fluctuating light conditions should also be prioritized [De Mooij et al. 2015]. In addition to modifying light harvesting, reducing light dissipation may be a valuable strategy for improving light utilization efficiency in mass cultures. Berteotti et al. [2016] recently found that downregulating light energy dissipation through non-photochemical quenching (NPQ) in *C. reinhardtii* improved biomass productivity in a small scale photobioreactor.

Parental strain characteristics must be considered when selecting species for further development of these ideas. Cyanobacteria and eukaryotic microalgae have unique advantages and should be developed in parallel. The former are propitious for the production of small molecules that can be secreted, such as ethanol and fatty acids. The latter have desirable attributes for the production of compounds that require more storage space, such as lipids, proteins, and carbohydrates, as well as the expression of heterologous proteins that require eukaryotic post-translational modifications [Wijffels et al. 2013]. Diatoms, which have so far been understudied for the problem of inefficient light utilization in mass cultures, are an attractive class of eukaryotic microalgae for selecting candidates. Due to their distinctive metabolism, high productivity, and environmental success, numerous species of diatoms are expected to be valuable for commercial

applications such as biofuels [Hildebrand et al. 2012, Sheehan et al. 1998]. Based on available studies, transgenes in diatoms appear to be more stable than in chlorophytes [Hildebrand et al. 2012, Kumar 2015]. Diatom photopigment composition, organization of thylakoid membranes and light harvesting complexes, as well as strategies for short- and long-term adaptation to changes in irradiance differ from those in chlorophytes [Wilhelm et al. 2006]. Due to the differences in light-harvesting and photoprotective mechanisms, diatoms are more efficient at dissipating excess energy and more productive than chlorophytes in fluctuating light conditions, such as those that would be experienced in mass cultures [Hildebrand et al. 2012, Wagner et al. 2006]. Additionally, diatoms are more efficient than chlorophytes at absorbing blue-green light, which is important in aquatic environments. This difference is due to the fact that the main accessory photopigment in diatoms enables absorption between 460 and 570nm, a range that is absent in chlorophytes.

The overarching objective of this thesis was to contribute to the understanding of how diatom productivity can be improved. Because the ultimate goal of strain improvement is to increase productivity in production conditions, Chapter 1 explored diel physiological and metabolic changes in the production candidate diatom *Cyclotella cryptica* (WT) under simulated outdoor conditions. A benchtop photobioreactor (**Fig. I-1**) was used to subject it to sinusoidal diel changes in light and temperature. Synchronous cell cycle progression, typical of microalgal cultures grown on a light-dark regime, was observed. Diel changes in optical density (a proxy for biomass), neutral lipid triacylglycerol (TAG, of interest for biofuel production), and photopigments were recorded and discussed in relation to cell cycle progression as well as diel changes in light and temperature. Time of day substantially affected potential product yields. The necessity of taking specific cultivation conditions into consideration when evaluating strain performance, variables that must be optimized to enhance product yields, and differences that may be expected based on microalgal taxa were discussed. Additionally, cellular photopigment abundance was assessed at high

resolution, and the findings suggested that the diatom carotenoid biosynthesis pathway may be differentially regulated in response to chloroplast replication and changes in irradiance.

Chapter 2 focused on elucidating the carotenoid biosynthesis pathway in the model diatom *Thalassiosira pseudonana*. In diatoms, carotenoids play a major role in light harvesting and dissipation. Thus, it is promising to explore manipulating diatom carotenoid biosynthesis in efforts to improve light utilization efficiency in diatom cultures. The identities of multiple enzymes that catalyze key biosynthetic steps, as well as the sequence of final steps leading to the main diatom light-harvesting and photoprotective carotenoids, have not been identified. Therefore, the goal of Chapter 2 was to improve the understanding of diatom carotenoid biosynthesis and identify targets for genetic manipulation. Basic bioinformatic analyses combined with available transcriptomic and physiological data were employed. A major finding of Chapter 2 was the identification of a novel violaxanthin de-epoxidase-like enzyme (VDL2), found to catalyze the biosynthesis of the main diatom accessory light-harvesting pigment fucoxanthin (Fx). Overexpressing VDL2 resulted in an increase of cellular Fx content accompanied by a stoichiometric decrease in the main photoprotective pigment pool, diadinoxanthin (Ddx) and its reversibly de-epoxidized form diatoxanthin (Dtx), which is necessary for the majority of light energy dissipation. Another major finding was that reducing Fx results in a coordinate reduction of all photosynthetic pigments, including chlorophylls, while photopigment ratios are preserved. A model for how the diatom carotenoid biosynthesis pathway may be differentially regulated in response to chloroplast division and irradiance increase was developed.

Chapter 3 examined photosynthetic parameters, growth, carbon partitioning, and productivity in two transgenic *T. pseudonana* lines, one overexpressing VDL2, and the other with a total reduction of photosynthetic pigmentation, as described above. A major finding of this chapter was that reducing photoprotective pigments (Ddx+Dtx) is a promising strategy for increasing diatom

productivity. *T. pseudonana* overexpressing VDL2 accumulated up to 3.4 times as much TAG and twice as much protein as WT during exponential growth. The accumulation of TAG and protein inversely correlated with NPQ, which is mainly a function of Ddx+Dtx content. VDL2 overexpression lines grew up to 7% slower than WT, but harvesting could be timed so as to take advantage of their higher yield potential. Possible reasons for the observed slower growth and potential strategies to improve upon the phenotype were discussed. A more modest increase in TAG accumulation of up to 40% more than in WT was observed in *T. pseudonana* with an overall reduction of photosynthetic pigments, obtained by using antisense to simultaneously silence both copies of the LUT1-like gene. The cells were 5-10% smaller than WT, contained 11-19% less protein, and appeared stressed, possibly due to a cell cycle progression defect, but growth rate in our cultivation conditions was comparable to WT.

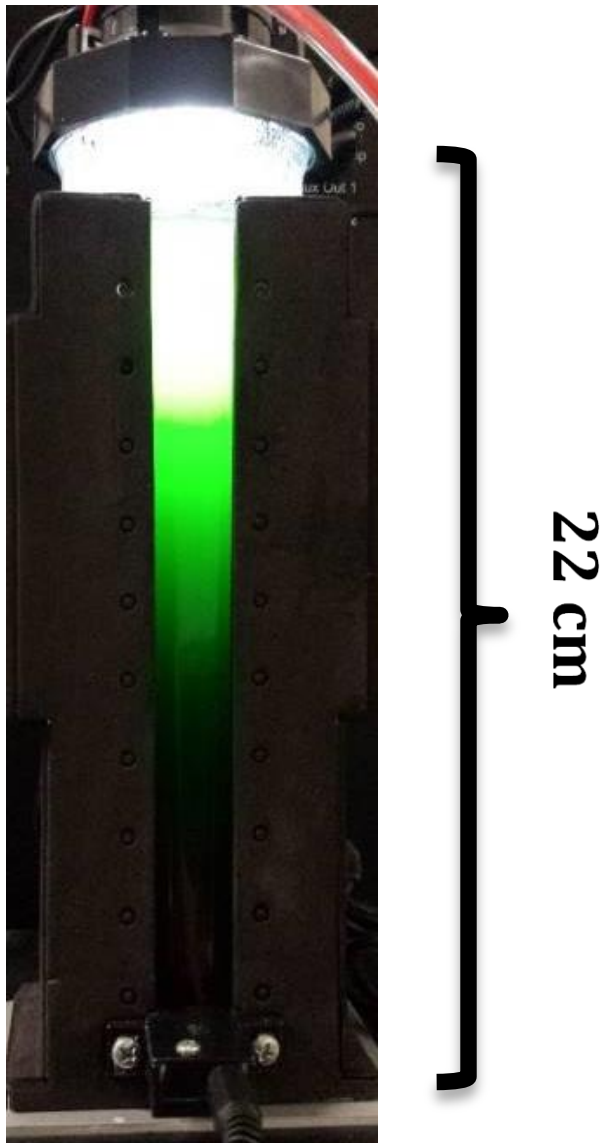


**Figure. I.1.**

22 cm-deep culture of *Chlorella* sp. in a bench-top photobioreactor. Despite the incident light intensity approximating full sunlight, cells at the bottom of the culture are in darkness.

## REFERENCES FOR THE INTRODUCTION

- Baroli I., Gutman B. L., Ledford H. K., Shin J. W., Chin B. L., Havaux M., Niyogi K. K. (2004) Photo-oxidative stress in a xanthophyll-deficient mutant of *Chlamydomonas*. *J Biol Chem* 279(8):6337-6344.
- Beckmann J., Lehr F., Finazzi G., Hankamer B., Posten C., Wobbe L., Kruse O. (2009) Improvement of light to biomass conversion by de-regulation of light-harvesting protein translation in *Chlamydomonas reinhardtii*. *J Biotechnol* 142(1):170-177.
- Berteotti S., Ballottari M., Bassi R. (2016) Increased biomass productivity in green algae by tuning non-photochemical quenching. *Sci Rep* 6:21339.
- Bonente G., Formighieri C., Mantelli M., Catalanotti C., Giuliano G., Morosinotto T., Bassi R. (2011) Mutagenesis and phenotype selection as a strategy toward domestication of *Chlamydomonas reinhardtii* strains for improved performance in photobioreactors. *Photosynth Res* 108: 107-120.
- Brown T. E., Richardson F. L. (1968) The effect of growth environment on the physiology of algae: light intensity. *J Phycol* 4:38-54.
- Burlew J. S. (1953) Current status of the large-scale cultivation of algae. pp 3-23. In: Burlew JS(ed). *Algal Culture: From Laboratory to Pilot Plant*. Carnegie Institution of Washington Publication 600, USA.
- Cazzaniga S., Dall'Osto L., Szaub J., Scibilia L., Ballottari M., Purton S., Bassi R. (2014) Domestication of the green alga *Chlorella sorokiniana*: reduction of antenna size improves light-use efficiency in a photobioreactor. *Biotechnol Biofuels* 7:157.
- Davis R., Aden A., Pienkos P. T. (2011) Techno-economic analysis of autotrophic microalgae for fuel production. *Appl Energ* 88:3524-3531.
- De Mooij T., Janssen M., Cerezo-Chinarro O., Mussgnug J. H., Kruse O., Ballottari M., Bassi R., Bujaldon S., Wollman F. A., Wijffels R. H. (2015) Antenna size reduction as a strategy to increase biomass productivity: a great potential not yet realized. *J Appl Phycol* 27(3):1063-1077.
- Doucha J., Livansky K. (2009) Outdoor open thin-layer microalgal photobioreactor: potential productivity. *J Appl Phycol* 21:111-117.
- Evenari M., Mayer A. M., Gottesman E. (1953) Experiments on culture of algae in Israel. pp197-203. In: Burlew JS(ed). *Algal Culture: From Laboratory to Pilot Plant*. Carnegie Institution of Washington Publication 600, USA.
- Falkowski P. G., Raven J. A. (1997) The molecular structure of the photosynthetic apparatus. pp 163-192. In: *Aquatic Photosynthesis*. Capital City Press, USA.
- Goldman, J. C. (1978) Outdoor algal mass cultures – II. Photosynthetic yield limitations. *Water Res* 13:119-136.

Hildebrand M., Davis A. K., Smith S. R., Traller J. C., Abbriano R. (2012) The place of diatoms in the biofuels industry. *Biofuels* 3(2):221-240.

Huesemann M. H., Hausmann T. S., Bartha R., Aksoy M., Weissman J. C., Benemann J. R. (2009) Biomass productivities in wild type and pigment mutant of *Cyclotella* sp. (diatom). *Appl Biochem Biotechnol* 157:507-526.

Kirst H., Garcia-Cerdan J. G., Zurbriggen A., Melis A. (2012) Assembly of the light-harvesting chlorophyll antenna in the green alga *Chlamydomonas reinhardtii* requires expression of the TLA2-CpFTSY gene. *Plant Physiol* 158(2):930-945.

Kok B. (1953) Experiments of photosynthesis by *Chlorella* in flashing light. pp 63-75. In: Burlew JS(ed). *Algal Culture: From Laboratory to Pilot Plant*. Carnegie Institution of Washington Publication 600, USA.

Kok B. (1960) Efficiency of photosynthesis. pp 566-633. In: Pirson A(ed). *Encyclopedia of Plant Physiology, Vol 5: The Assimilation of CO<sub>2</sub>*. Springer-Verlag Berlin Heidelberg, Germany.

Kosourov S. N., Ghirardi M. L., Seibert M. (2011) A truncated antenna mutant of *Chlamydomonas reinhardtii* can produce more hydrogen than the parental strain. *Int J Hydrogen Energ* 36(3):2044-2048.

Kumar S. (2015) GM algae for biofuel production: biosafety and risk assessment. *Coll Biosaf Rev* 9:52-75.

Kwon J. H., Bernat G., Wagner H., Rogner M., Rexroth S. (2013) Reduced light-harvesting antenna: consequences on cyanobacterial metabolism and photosynthetic productivity. *Algal Res* 2(3):188-195.

Lea-Smith D. J., Bombelli P., Dennis J. S., Scott S. A., Smith A. G., Howe C. J. (2014) Phycobilisome-deficient strains of *Synechocystis* sp. PCC 6803 have reduced size and require carbon-limiting conditions to exhibit enhanced productivity. *Plant Physiol* 165(2):705-714.

Leganes F., Martinez-Granero F., Munoz-Martin M. A., Marco E., Jorge A., Carvajal L., Vida T., Gonzalez-Pleiter M., Fernandez-Pinas F. (2014) Characterization and responses to environmental cues of a photosynthetic antenna-deficient mutant of the filamentous cyanobacterium *Anabaena* sp. PCC 7120. *J Plant Physiol* 171:915-926.

Lepetit B., Goss R., Jakob T., Wilhelm C. (2012) Molecular dynamics of the diatom thylakoid membrane under different light conditions. *Photosynth Res* 111(1-2): 245-257.

Li Z., Kiesling J. D., Niyogi K. K. (2012) Overlapping photoprotective function of vitamin E and carotenoids in *Chlamydomonas*. *Plant Physiol* 158(1):313-323.

Mata T. M., Martins A. A., Caetano N. S. (2010) Microalgae for biodiesel production and other applications: a review. *Renew Sust Energ Rev* 14: 217-232.

Melis A., Neidhardt J., Benemann J. R. (1999) *Dunaliella salina* (Chlorophyta) with small chlorophyll antenna sizes exhibit higher photosynthetic productivities and photon use efficiencies than normally pigmented cells. *J Appl Phycol* 10:515-525.

Mitra M., Melis A. (2008) Optical properties of microalgae for enhanced biofuels production. Opt Express 16(26):21807-21820.

Mussgnug J. H., Thomas-Hall S., Rupprecht J., Foo A., Klassen V., McDowall A., Schenk P. M., Kruse O., Hankamer B. (2007) Engineering photosynthetic light capture: impacts on improved solar energy to biomass conversion. Plant Biotech J 5:802-814.

Myers J., Burr G. O. (1940) Studies on photosynthesis: some effects of light of high intensity on *Chlorella*. J Gen Physiol 24:45-67.

Nakajima Y., Tsuzuki M., Ueda R. (1999) Reduced photoinhibition of a phycocyanin-deficient mutant of *Synechocystis* PCC 6714. J Appl Phycol 10:447-452.

Nakajima Y., Ueda R. (1997) Improvement of photosynthesis in dense microalgal suspension by reduction of light harvesting pigments. J Appl Phycol 9:503-510.

Nakajima Y., Ueda R. (1999) Improvement of microalgal photosynthetic productivity by reducing the content of light harvesting pigment. J Appl Phycol 11:195-201.

Nakajima Y., Ueda R. (2000) The effect of reducing light-harvesting pigment on marine microalgal productivity. J Appl Phycol 12:285-290.

Neidhardt J., Benemann J. R., Zhang L., Melis A. (1998) Photosystem-II repair and chloroplast recovery from irradiance stress: relationship between chronic photoinhibition, light-harvesting chlorophyll antenna size and photosynthetic productivity in *Dunaliella salina* (green algae). Photosynth Res 56:175-184.

Ort D. R., Zhu X., Melis A. (2011) Optimizing antenna size to maximize photosynthetic efficiency. Plant Physiol 155:79-85.

Page L. E., Liberton M., Pakrasi H. B. (2012) Reduction of photoautotrophic productivity in the cyanobacterium *Synechocystis* sp. strain PCC 6803 by phycobilisome antenna truncation. Appl Environ Microbiol 78(17):6349-6351.

Polle J. E. W., Benemann J. R., Tanaka A., Melis A. (2000) Photosynthetic apparatus organization and function in the wild type and a chlorophyll b-less mutant of *Chlamydomonas reinhardtii*. Dependence on carbon source. Planta 211:335-344.

Polle J. E. W., Kanakagiri S., Jin E. S., Masuda T., Melis A. (2002) Truncated chlorophyll antenna size of the photosystems – a practical method to improve microalgal productivity and hydrogen production in mass culture. Int J Hydrogen Energ 27:1257-1264.

Polle J. E. W., Kanakagiri S. D., Melis A. (2003) *tla1*, a DNA insertional transformant of the green alga *Chlamydomonas reinhardtii* with a truncated light-harvesting chlorophyll antenna size. Planta 217:49-59.

Polle J. E. W., Niyogi K. K., Melis A. (2001) Absence of the pigments lutein, violaxanthin and neoxanthin affects the functional chlorophyll antenna size of the photosystem-II but not that of photosystem-I in the green alga *Chlamydomonas reinhardtii*. Plant Cell Physiol 42(5):482-491.

- Pultz O., Gross W. (2004) Valuable products from biotechnology of microalgae. *Appl Microbiol Biotechnol* 65:635-648.
- Qiang H., Guterman H., Richmond A. (1996) Physiological characteristics of *Spirulina platensis* (cyanobacteria) cultured at ultrahigh cell densities. *J Phycol* 32:1066-1073.
- Radmer R., Kok B. (1977) Photosynthesis: Limited yields, unlimited dreams. *BioScience* 27(9):599-605.
- Richmond A. (1996) Efficient utilization of high irradiance for production of photoautotrophic cell mass: a survey. *J Appl Phycol* 8:381-387.
- Setlik I., Veladimir S., Malek I. (1970) Dual purpose open circulation units for large scale culture of algae in temperate zones. I. Basic design considerations and scheme of pilot plant. *Algol Stud* 1: 111-164.
- Sheehan J., Dunahay T., Benemann J., Roessler P. (1998) *A look back at the U.S. Department of Energy's Aquatic Species Program: biodiesel from algae; close-out report*. United States. Doi:10.2172/15003040.
- Spolaore P., Joannis-Cassan C., Duran E., Isambert A. (2005) Commercial applications of algae. *J Biosci Bioeng* 101(2):87-86.
- Stephens E., Ross I. L., King Z., Mussgnug J. H., Kruse O., Posten C., Borowitzka M. A., Hankamer B. (2010) An economic and technical evaluation of microalgal biofuels. *Nat Biotechnol* 28:126-128.
- Sukenik A., Bennett J., Falkowski P. (1987) Light-saturated photosynthesis – limitation by electron transport or carbon fixation? *Biochim Biophys Acta* 891:205-215.
- Sukenik A., Falkowski P. G. (1986) Potential enhancement of photosynthetic energy conversion in algal mass culture. *Biotechnol Bioeng* 30:970-977.
- Torzillo G., Giannelli L., Martinez-Roldan A. J., Verdone N., De Filippis P., Scarsella M., Bravi M. (2010) Microalgae culturing in thin-layer photobioreactors. *Chem Eng Transact* 20:265-270.
- Torzillo G., Pushparaj B., Masojidek J., Vonshak A. (2003) Biological constraints in algal biotechnology. *Biotechnol Bioprocess Eng* 8:338-348.
- Vetoshkina D. V., Borisova-Mubarakshina M. M., Naydov I. A., Kozuleva M. A., Ivanov B. N. (2015) Impact of high light on reactive oxygen species production within photosynthetic biological membranes. *J Biol Life Sci* 6(2):50-60.
- Vonshak A., Guy R. (1992) Photoadaptation, photoinhibition, and productivity in the blue-green alga, *Spirulina platensis* grown outdoors. *Plant Cell Environ* 15:613-616.
- Wagner H., Jacob T., Wilhelm C. (2006) Balancing the energy flow from captured light to biomass under fluctuating light conditions. *New Phytol* 169:95-108.
- Wijffels R. H., Kruse O., Hellingwerf K. J. (2013) Potential of industrial biotechnology with cyanobacteria and eukaryotic microalgae. *Curr Opin Biotechnol* 24:405-413.

Wilhelm C., Buchel C., Fisahn J., Goss R., Jakob T., LaRoche J., Lavaud J., Lohr M., Riebesell U., Stehfest K., Valentin K., Kroth P. G. (2006) The regulation and nutrient assimilation in diatoms is significantly different from green algae. *Protist* 157(2): 91-124.

## CHAPTER 1

**Timing is everything: diel metabolic and physiological changes in the diatom *Cyclotella cryptica* grown in simulated outdoor conditions**

## **1.1 ABSTRACT**

Microalgal cultures grown on a light-dark cycle experience diel patterns in metabolic and physiological processes, including cell cycle synchronization, but the implications for productivity in terms of biomass and commercially-appealing molecules are not commonly appreciated. Despite a long history of diel response studies, only recently have photobioreactor technology advances enabled the use of sinusoidal light and temperature to more accurately mimic outdoor conditions. The present study investigates cell cycle progression and dynamic changes in optical density as a proxy for biomass, triacylglycerol (TAG), and photosynthetic pigments on a 24-hour scale in the diatom *Cyclotella cryptica* grown using a sinusoidal light and temperature regime. Cell division synchronized to occur predominantly in the middle of the light period and biomass started to increase several hours earlier, as the cells prepared to divide. TAG levels increased during the day and decreased at night, with a mid-day dip corresponding to the time when lipid needs for cell division-associated membrane biosynthesis would be high. For the first time, photosynthetic pigment dynamics data, obtained with higher temporal resolution than previously reported for microalgae, was overlaid with cell cycle progression, indicating that while some photosynthetic pigments respond primarily to light, others are influenced by the cell cycle. Additionally, our results indicate that in a synchronized culture, potential product yields change substantially throughout the day. This may inform harvest timing to significantly increase yield.

## **1.2 INTRODUCTION**

Microalgae are a large and very diverse group of unicellular photosynthetic organisms that occupy a wide variety of environmental niches and have major ecological significance [Ebenzer et al. 2012, Sumi 2009]. They are also of interest commercially and can be used to obtain biomass and

a variety of products such as lipids, proteins, carbohydrates, pigments, and other functional nutrients, which can be used for diverse applications such as biofuels, food supplementation, cosmetics, and bioplastics [Khanra et al. 2018, Matos et al. 2017]. With the exception of polar dwellers, natural populations of microalgae typically experience regular and predictable light-dark cycles and concomitant changes in temperature. In response, individual cells exhibit cyclical patterns in metabolic and physiological processes and there is population-level synchronization, allowing for efficient use of resources [Falkowski and Raven 2007]. A major event in a cell's life that influences the timing of many of those changes is division, and most microalgal species synchronize their cell cycles when exposed to light-dark regimes. Several microalgal lineages, including green and red algae, appear to have the cell cycle gated by an endogenous circadian mechanism, restricting division to certain times of day (typically night) [Miyagishima 2017]. This has been found to not generally be the case with diatoms [Chisholm and Brand 1981], which may divide at different times of day and in some cases exhibit no periodicity in division, depending on the species and the cultivation conditions [Chisholm et al. 1980, Nelson and Brand 1979, Paasche 1968, Williamson 1980]. The cyclic nature of the various processes has important implications for work with microalgae, from the field, where timing of measurements and sample collection must be taken into consideration, to the laboratory, especially when evaluating and/or developing strains for outdoor production, to production systems, where the optimal timing of dilution, nutrient addition, and harvest should be determined. There have been numerous informative studies examining growth, productivity, and metabolism of microalgal cultures entrained to various light-dark regimes in the laboratory, but the majority of them have been carried out in constant temperature and using a square-wave (on/off) light regime [Anderson and Sweeney 1977, Chauton et al. 2013, Chisholm et al. 1980, Clark et al. 2002, Cuhel et al. 1984, Darley and Volcani 1971, Eppley et al. 1967, Hoogenhout 1963, Humphrey 1979, Joseph and Villareal 1998, Kohata and Watanabe 1988,

Kohata and Watanabe 1989, Nelson and Brand 1979, Owens et al. 1980, Paasche 1968, Post et al. 1984, Ragni and d'Alcala 2007, Raimbault and Mingazzini 1987, Rivkin 1985, Sukenik and Carmeli 1990, Varum et al. 1986, Williamson 1980]. Whereas those studies greatly advanced the general understanding of the effects of light-dark cycling on microalgae, they did not accurately mimic the sinusoidal light and temperature conditions microalgae experience in the wild and in outdoor cultivation systems. Orefice et al. [2016], utilizing the diatom *Skeletonema marinoi*, demonstrated that a square-wave light regime results in significant differences in cell physiology and metabolism when compared to a sinusoidal light regime. Additionally, a difference of 10°C affects an approximately twofold change in metabolic reaction rates in microalgae [Raven and Geider 1988], and it has been demonstrated that diel temperature variation has an impact on microalgal growth and productivity [Bonnefond et al. 2016, Edmundson and Huesemann 2015, Ogbonna and Tanaka 1996, Yang et al. 2016]. Recently, several groups have taken advantage of technological advances and examined various responses of different microalgal species to sinusoidal light and in some cases temperature, beginning to forge a better understanding of what happens outdoors, but under more controlled conditions [Bonnefond et al. 2016, Jallet et al. 2016, Lacour et al. 2012, Tamburic et al. 2014]. The present study is the first to apply sinusoidal temperature changes along with a sinusoidal light regime to a diatom, examining diel metabolic and physiological changes in *Cyclotella cryptica* in a bench-top photobioreactor. Triacylglycerol (TAG) abundance, optical density as a proxy for biomass, and photosynthetic pigments were tracked over a 24-hour period and related to cell cycle progression. This allowed a distinction to be made between the effects of the cultivation regime and cell cycle progression on some of the parameters, such as TAG content and the abundance of different photosynthetic pigments, and identified different optimal times for harvesting to maximize productivity.

## 1.3 MATERIALS AND METHODS

### 1.3.1 Cultivation Conditions

*C. cryptica* CCMP332, collected in 1956 from West Tisbury Great Pond, Martha's Vineyard, Massachusetts USA, was used in this study. The lab stock culture was maintained in 125 mL Erlenmeyer flasks at 18°C under continuous cool-white fluorescent illumination of 150  $\mu\text{mol m}^{-2}\text{sec}^{-1}$  in artificial sea water (ASW) medium [Darley and Volcani 1969]. The stock was inoculated into 750 mL ASW at  $1.0 \times 10^5$  cells/mL for Experiment 1 (Exp. 1) and  $1.5 \times 10^4$  cells/mL for Experiment 2 (Exp. 2), for cultivation in the Phenometrics environmental photobioreactor (ePBR) 1.1 [Lucker et al. 2014] with continuous stirring set to 400 rpm and gently bubbled air. The ePBR was programmed for a 12h:12h light-dark cycle, with a sinusoidal light regime maximizing at 2000  $\mu\text{mol photons m}^{-2}\text{sec}^{-1}$ , approximating full sunlight, and a sinusoidal temperature regime spanning 14-28°C, a range comfortable for *C. cryptica* (**Fig. 1.1**). The offset between changes in light and temperature was determined automatically by the software.

For equilibration to the growth conditions prior to intensive sampling and to ensure maintenance of synchronization [Hoogenhout 1963], the cultures were diluted nightly based on cell counts to maintain a slightly past mid-exponential phase once the inoculum had reached the desired cell concentration (**Fig. S1.1**). The appropriate volume of culture was removed and replaced with fresh ASW through an opening in the lid using a sterilized cannula. The concentration was chosen to be high enough to allow for efficient sampling while maintaining exponential growth of the culture, and mimics the dense cultures used in production systems. For Exp. 1, the total pre-sampling equilibration period was 9 days, with dilutions performed for the last 7 days,  $4.3 \pm 0.8$  hours into the dark period. For Exp. 2, the total pre-sampling equilibration period was 11 days, with dilutions performed  $2.9 \pm 0.2$  hours into the dark period for the last 7 days. After the equilibration

period, the cultures were intensively sampled for 24 hours without dilution, starting 1 hour prior to dawn.

### *1.3.2 Cell Concentration and Curve Fitting*

Cell counts were performed with the MUSE® Cell Analyzer (EMD Millipore, Billerica, MA) and spot-checked with a hemocytometer. For the intensive sampling periods, curve fitting was performed using online software available from MyAssays Ltd. at <https://www.mycurvefit.com>. Four-parameter logistic fit was used, except for the last 3 and 2 points of Exp. 1 and Exp. 2, respectively. Those points reflect cell concentration increase due to a subpopulation of cells that divided at night, and were fitted with a straight line (**Fig. S1.2**).

### *1.3.3 OD750 Measurements*

Optical density at 750 nm (OD750) was automatically and continuously measured at approximately 10 min intervals by the ePBR. Because the intervals were not exactly 10 min, the timing of measurements varied slightly from day to day. For dawn and dusk analyses (1.4.3.4 and 1.4.3.5), values for exactly 10 min intervals were interpolated from the raw data using Origin software (OriginLab, Northampton, MA).

### *1.3.4 OD750 as a Proxy for Biomass*

Cultivation experiments with *C. cryptica* in climate simulation raceway ponds at the Pacific Northwest National Laboratory [Huesemann et al. 2017, 2018], indicated a strong correlation

between OD750 and ash-free dry weight (AFDW), a measure of biomass (**Fig. S1.3**). Duplicate samples were taken from replicate ponds at least twice a day over a 6-day period where the cultures ranged from lag phase, through exponential, to the beginning of stationary phase. Some of the samples were taken at night, and intensive sampling days during which cell division synchronization was observed were included in the analysis. The robust linear relationship was observed despite the presumable differences in cellular characteristics at different sampling points, suggesting that for actively growing *C. cryptica*, OD750 is a reliable proxy for AFDW.

#### *1.3.5 Cell Cycle Analysis*

One mL of culture was taken for cell cycle analysis at various times throughout the intensive sampling days and processed as previously described [Abbriano et al. 2018].

#### *1.3.6 Cellular TAG Content Analysis*

One mL of culture was taken for relative cellular TAG content analysis via the fluorescent dye 4,4-difluoro-4-bora-3a,4a-diaza-s-indacene (BODIPY 493/503, Molecular Probes) staining at various times throughout the intensive sampling days and processed as previously described [Traller and Hildebrand 2013]. The approach was chosen over gravimetric methods because doing *in situ* analysis allows direct measurement of cellular lipid content in real time, which eliminates errors due to extraction non-specificity, measurement of small weights, and losses during multi-step procedures, and is thus more accurate [Bono et al. 2015]. Additionally, the ePBR does not hold enough culture volume to sample for analysis by gravimetry.

### *1.3.7 Photosynthetic Pigment Analysis*

The cultures were sampled for photosynthetic pigments at various times throughout the intensive sampling days, with more frequent sampling around dawn and dusk. Between  $1.5\text{-}3 \times 10^6$  cells per timepoint were harvested by filtration through a GF/F filter and immediately frozen and stored in liquid nitrogen. Pigments were extracted and analyzed by high-performance liquid chromatography (HPLC) as previously described [Kozlowski et al. 2011]. Cellular pigment content was calculated by normalizing HPLC-derived concentrations by the number of cells harvested using the fitted curves described in 1.3.2.

### *1.3.8 Statistics*

Our study employed two replicate cultures. OD750 measurements were performed automatically approximately every 10 min, resulting in continuous curves that did not present outlier data points. For cell cycle and cellular TAG content analyses,  $10^4$  cells were interrogated. Due to typical high cell-to-cell variation in TAG (e.g., Traller et al. 2013), using standard deviation (SD) to evaluate error is not useful, whereas standard error gives an accurate measure of the mean. Given the large number of cells evaluated, standard error is extremely small. Cell counts performed with the MUSE® Cell Analyzer used the average of  $1 \times 10^3$  cells in triplicate to determine concentration. Spot-checking with a hemocytometer ensured accuracy. As described in 1.3.2, curve fitting was used to smooth the curves and ensure consistent values for the analyses. Due to sampling frequency limitations, only one pigment sample per time-point was obtained; however, as detailed in 1.5.5, differences in the patterns of change between different pigments provide an internal control, demonstrating that the observed dynamics were not due to sampling or processing error. Additionally, to assess error that may occur as a result of sampling and processing, we performed a

control experiment in which a culture of *C. cryptica* was sampled five times successively and processed the same way as the rest of the photosynthetic pigment samples in this study. The results had a SD of less than 5% from the mean for all photosynthetic pigments examined (**Table S1.1**). HPLC analysis employed an internal control of including the same sample in two different quantities to ensure precision in pigment quantification, which scaled accordingly.

## 1.4 RESULTS

### 1.4.1 OD750/Cell Density Difference Between the Experiments

As detailed in 1.3.1, two distinct experiments were performed, in which cultures were equilibrated to a 12h:12h light-dark cycle under a sinusoidal light and temperature regime (**Fig. 1.1**) by nightly dilutions. The dilutions were based on cell counts, kept consistent throughout both experiments: for Exp. 1, the cultures were diluted to  $3.1\text{-}4.2 \times 10^5 \text{ cells}\cdot\text{mL}^{-1}$ ; for Exp. 2, the post-dilution culture densities were  $2.4\text{-}4.5 \times 10^5 \text{ cells}\cdot\text{mL}^{-1}$ . This did not, however, correspond to consistency in OD750. Whereas post-dilution OD750 range for Exp. 1 was 0.5-1, the post-dilution OD750 values were twice that during Exp. 2 (**Fig. S1.1**).

### 1.4.2 Cell Cycle Synchronization

In diatoms, cell cycle progression typically consists of the following phases: G1 (growth, when the cell size increases), S (chromosomal replication), and what has been defined as a combined G2/M phase because a true pause in progression (G2) may or may not occur prior to M phase (mitosis). Additionally, chloroplasts and mitochondria must replicate prior to mitosis. In diatoms, the generation of two daughter cells via mitosis occurs, but the cells do not separate until

later, after the silica cell wall is complete. Thus, cell number in a culture increases after a peak in the population of cells in G2/M phase. It should be noted that synchronization encompasses cell-to-cell variation in the rate of cell cycle progression, and unless the cells are in a prolonged stage of the cell cycle (e. g. G1), the percentage of cells in a given phase is never 100%.

Based on evaluation of cell cycle stages, cell cycle synchronization occurred in both experiments. Better synchronization was attained during Exp. 2, with >95% of the cells in G1 at dawn and also after the majority of the cells underwent division, compared to 66% at dawn and 75-80% after the majority divided in Exp. 1 (**Fig. 1.2**). In Exp. 1, the peak percentage of cells in S phase occurred at 11:00 h, and in Exp. 2 at 11-12:00 h. The G2/M maximum was at 12-13:00 h for Exp. 1, and 13:00 h for Exp. 2. Increase in cell concentration in both experiments began after most cells in the culture entered G2/M. In both experiments, there was also a G2/M shoulder at the beginning of the dark period, and a subpopulation of cells that divided thereafter. The starting cell concentration was very similar between the experiments, but approximately 20% less at the end of Exp. 1 than Exp. 2 (**Fig. 1.2**).

#### 1.4.3 OD750 Dynamics

##### 1.4.3.1 Lack of Correspondence Between OD750 and Cell Concentration

As described in 1.3.4, OD750 can be used as proxy for AFDW, a measure of biomass, for actively growing *C. cryptica* under highly diverse conditions. In both experiments, changes in OD750 and cell concentration followed generally similar patterns throughout the intensive sampling period, but OD750, and therefore biomass, started to increase several hours before cell concentration (**Fig. 1.3A, B**). The rate of OD750 increase slowed significantly toward the end of the light period, but some increase during the dark period was observed in both experiments. The

starting OD750 for Exp. 2 was approximately twice that of Exp. 1; OD750 approximately doubled during the Exp. 2 intensive sampling period, and almost tripled for Exp. 1 (**Fig. 1.3A, B**). If cell concentration and the corresponding OD750 values are plotted sequentially, there is a clear initial period of biomass increase only, followed by increase in cell concentration along with biomass (**Fig. 1.3C, D**).

#### *1.4.3.2 OD750 Increase Rate Correlates with Light Energy Availability*

Optical density increase rate as a function of light energy availability was plotted as the change in OD750 per hour, normalized to culture density, versus average incident light intensity per hour during the light period. The data indicate a direct but non-linear correlation between optical density increase rate and incident light intensity (**Fig. 1.4**). For both experiments, the rate of optical density increase per cell relative to incident light intensity trended higher during the second half of the day (**Fig. 1.4**).

#### *1.4.3.3 Inverse Relationship Between Daily OD750 Increase and Starting OD750*

Plotting OD750 at the end relative to the beginning of the light period according to the specific growth equation  $[(\ln(\text{OD}_{\text{evening}} - \text{OD}_{\text{750 morning}})) / \text{time}]$  showed that the lower the starting OD750 (i.e., biomass) was at dawn, the more gain in OD750 occurred during the day, even at very low OD750 values (**Fig. 1.5**). The observation that starting OD750 was higher for the intensive sampling day of Exp. 2 but gain in OD750 by the end of the intensive sampling day was greater during Exp. 1 is consistent with this trend (**Fig. 1.3**).

#### *1.4.3.4 OD750 Decrease at Dawn*

A dip in OD750 within the first 2 hours of the light period was consistently observed for both experiments during the equilibration period and intensive sampling (**Fig. 1.6**). Due to the sinusoidal nature of the light regime, irradiance increased substantially immediately after dawn, and had reached half of the maximal light intensity by the time OD750 began increasing after the dip (1000  $\mu\text{mol photons m}^{-2} \text{s}^{-1}$  at 8:00 h) (**Figs. 1.1, 1.6**).

#### *1.4.3.5 OD750 Decrease at Night*

The net average decrease in OD750 at night, signifying biomass loss, was  $5.7 \pm 1.1\%$  for Exp. 1 and  $5.6 \pm 1.6\%$  for Exp. 2 during the days the cultures were diluted (**Table S1.2**). The OD750 decrease at night was higher prior to the initiation of dilutions, decreasing with each post-inoculation day in Exp. 2. No trend could be observed for Exp. 1, as only one day after inoculation was required to reach the desired cell concentration after which dilutions were initiated (**Figs. S1.1, S1.4, Table S1.2**).

#### *1.4.4 Cellular TAG Dynamics*

In both experiments, there was a slight decrease in cellular TAG levels after dawn, followed by a steep increase until the S-phase peak (**Fig. 1.7**). In Exp. 1, the increase started at 7:00 h, one hour into the light period, and peaked at 11:00 h. In Exp. 2, TAG levels increased sharply from 11:00 h to 12:00 h. A mid-day dip in cellular TAG levels followed, corresponding to the G2/M peak, a period when membrane synthesis associated with cell division is expected. As most cells completed division, the cellular TAG reserves were replenished, before declining several hours into the dark

period, after 21:00 h. Prior to the decline, a significant increase in cellular TAG after dusk was observed in Exp. 2. The decline continued until 5:00 h, the end of the intensive sampling period for Exp. 2; for Exp. 1, cellular TAG increased again after 1:00 h (**Fig. 1.7**).

#### 1.4.5 Photosynthetic Pigment Dynamics

##### 1.4.5.1 Changes in Cellular Photosynthetic Pigment Content During Intensive Sampling Period

The major *C. cryptica* photosynthetic pigments are chlorophyll a (Chl a), fucoxanthin (Fx), chlorophyll c (Chl c), beta-carotene ( $\beta$ -car), diadinoxanthin (Ddx), and diatoxanthin (Dtx), with the first three being light-harvesting and the last three photoprotective. Chl a is the major light-harvesting pigment, found in photosystem reaction centers as well as in photoantenna complexes with the accessory photopigments Fx and Chl c, of which Fx is more abundant. Ddx is converted to Dtx by de-epoxidation in response to light-induced stress, and the reaction is reversed during recovery. Because Ddx and Dtx are able to interconvert rapidly, we examined their abundance as a pool as well as separately.  $\beta$ -car also plays an important role in photoprotection, but does not participate in the aforementioned cycle [Croce and van Amerongen 2014, Kuczynska et al. 2105].

Photosynthetic pigment content per cell was measured throughout the intensive sampling period for both experiments (**Figs. 1.8, S1.5**). All of the pigments had a daytime peak, and all except for Ddx and Dtx fluctuated during dawn, dusk, and early dark period, with fluctuations in Chl a content being the highest in amplitude (**Figs. 1.8, 1.9, S1.5**). For both experiments, Chl a steadily increased after fluctuating at dawn, maximizing at noon (**Fig. 1.8A, B**). During Exp. 1, Chl a levels plateaued thereafter, prior to onset of dusk fluctuations. For Exp. 2, the Chl a peak at noon was followed by a decrease prior to fluctuations at dusk. The overall trend for Fx in Exp. 1 was an increase from dawn to dusk (**Fig. 1.8C, D**). During Exp. 2, Fx peaked at noon, with a similar

distribution on either side of the peak between dawn and dusk. The patterns of change in Chl a and Fx were similar to each other within each experiment, but with some differences (1.5.5) (**Fig. 1.9**). The Ddx+Dtx pool abundance, determined mainly by the more abundant Ddx, peaked at noon during both experiments, with a similar distribution on either side of the peak during the light period (**Fig. 1.8E, F**). Ddx followed that pattern of accumulation closely, whereas Dtx followed a different pattern (1.4.5.3) (**Fig. 1.10**). Patterns of change in Chl c and β-car content paralleled that of Fx closely for both experiments (**Fig. 1.9**). After initial fluctuation in the beginning of the dark period, there was a steady decline in Chl a, Fx, Chl c, and β-car abundance in the dark for the remainder of both experiments, whereas the Ddx+Dtx content remained relatively stable after an initial dip followed by a slight increase at the beginning of the dark period. For Exp. 1, the cellular content of all measured pigments was similar between the beginning and the end of the intensive sampling period, with Fx and Chl c slightly higher towards the end. For Exp. 2, all measured pigments were lower at the end than at the beginning of intensive sampling (**Figs. 1.8-1.10, S1.5**). The amount of each individual pigment was higher during Exp. 1 than Exp. 2, with the exception of Dtx, which was present, on average, in the same quantity during both experiments (**Table 1.1**).

The observed fluctuations in the levels of different pigments varied in both amplitude and timing, as demonstrated by co-plotting normalized pigment levels (**Figs. 1.9, S1.7**). Although only one sample per time point was taken due to sampling time limitations, these differences support the validity of the observed fluctuations, arguing against them being caused by sampling or processing error. Furthermore, sample to sample variation in photosynthetic pigments was ascertained to be too low to account for all of the observed fluctuations (1.3.8), with a SD of 0.9-4.9% of the mean of five consecutively obtained control samples for all assayed pigments (**Table S1.1**). By contrast, the SD of the mean of the first five time points taken during Exp. 1 was 6.8-8.9%

for all examined pigments, and 3.6-15.4% for the first five samples obtained during Exp. 2, with each individual pigment varying more during the experiments than the control.

#### *1.4.5.2 Photosynthetic Pigment Abundance, Cell Cycle Progression, and Changes in Light Intensity*

Examination of data in **Figs. 1.8, 1.9** and **S1.5** suggests a correlation between changes in photosynthetic pigment content per cell and changes in irradiance and/or cell cycle progression. The difference in the extent of synchrony between the two experiments allows for discernment of the potential influence of the two variables. 66% of the Exp. 1 culture and >95% of the Exp. 2 culture were similarly synchronized at dawn on the intensive sampling days (1.4.2). The daytime peaks in Chl a, Fx, Chl c, and β-car content occurred around the S phase to G2/M transition and were more protracted during Exp. 1 than in Exp. 2, along with a less complete cell cycle synchronization. This suggests that although changes in the cellular abundance of these pigments during Exp. 2 could be interpreted as following the changes in irradiance, the lower extent of synchrony in Exp. 1 reveals cell cycle as a contributing factor. By contrast, Ddx+Dtx in both experiments peaked at 12:00 h along with the light intensity and had an equal distribution on both sides of the peak during the light period, following the sinusoidal light intensity regime (**Fig. 1.8E-H**) and without observable differences due to varied extents of synchrony and therefore cell cycle progression. Additionally, the Ddx+Dtx levels remained relatively stable in the dark, whereas the other measured pigments gradually decreased. It appears that the abundance of Chl a, Fx, Chl c, and β-car may be influenced by the timing of cell cycle progression, whereas the Ddx+Dtx content may follow the changes in light intensity only (**Figs. 1.8, 1.9, S1.5**).

#### *1.4.5.3 Dtx Dynamics and Ddx+Dtx De-epoxidation State*

Dtx abundance, along with the de-epoxidation state of the Ddx+Dtx pool ( $Dtx/(Ddx+Dtx)$ ), which increased in response to light-induced stress, decreased immediately upon dawn. These parameters did not maximize along with light irradiance, unlike the Ddx+Dtx pool abundance (**Figs. 1.8, 1.10**). Rather, the daytime peak occurred before noon and was more protracted in Exp. 1 than in Exp. 2, which had a tighter peak after noon. Additionally, the de-epoxidation state increased sharply immediately following the onset of the dark period during both experiments, then returned to approximately the pre-dawn values by the end of the intensive sampling period (**Fig. 1.10**).

#### *1.4.5.4 Ratio Dynamics of Chl a to Accessory Photopigments (Fx and Chl c)*

The ratios of Chl a to the accessory photopigments Fx and Chl c paralleled each other very closely and were slightly higher for Exp. 1 (**Table 1.1**). The overall trend for the ratios was an increase during the day, with 1.6-1.9X differences between pre-dawn and maximum values (**Fig. 1.11**). After the evening fluctuations, the ratios for both experiments gradually decreased to approximately the pre-dawn levels observed at the beginning of sampling (**Fig. 1.11**).

### **1.5 DISCUSSION**

#### *1.5.1 Overview*

In this study, we strove to examine general diel trends in physiological and metabolic rhythms of the diatom *C. cryptica* in controlled simulated outdoor conditions using sinusoidal variation in light intensity and temperature. Although other environmental variables are a factor in outdoor cultivation, their transient and/or irregular occurrence can obfuscate overall larger-scale

trends, and elucidating such trends was the goal of this study. We performed two separate experiments, attempting to adapt the cultures to the same cultivation conditions prior to intensive sampling by diluting them each night for a week once they reached the desired cell density, with some differences in the timing of dilutions between the two experiments. There was variance between the cultures, potentially arising from the differences in the state and density of the inoculum and the details of pre-adaptation (1.3.1, 1.4.1), but the general observed trends were consistent. The differences found despite the cultivation conditions being carefully controlled and reproduced between the two experiments are a testament to the variability inherent to working with biological systems, and are worth documenting and appreciating as such.

### *1.5.2 Cell Cycle Synchronization*

Synchronous division has been typically assessed by tracking changes in culture density and/or division rates [Anderson and Sweeney 1977, Bonnefond et al. 2016, Chauton et al. 2013, Chisholm et al. 1980, Darley and Volcani 1971, Eppley et al. 1967, Hoogenhout 1963, Jallet et al. 2016, Kohata and Watanabe 1989, Nelson and Brand 1979, Ogbonna and Tanaka 1996, Owens et al. 1980, Post et al. 1984, Ragni and d'Alcala 2007, Sukenik and Carmeli 1990, Varum et al. 1986, Williamson 1980]. To our knowledge, this is the first study to track cell cycle progression and relate it to diel physiological and metabolic changes in light-dark synchronized microalgal cultures, allowing for a more detailed understanding of the observed phenomena. In our experiments, *C. cryptica* synchronized to predominantly divide during the light period (**Fig. 1.2**). A greater extent of cell cycle synchronization was attained in Exp. 2 than in Exp. 1; this may have been due to a difference in factors that we did not specifically investigate, such as length of the pre-adaptation period and the timing and consistency of dilutions (1.3.1). In addition to the main cell division event

in the middle of the light period (**Fig. 1.2**), there is indication that a subset of cells (approximately 20%) was dividing earlier during the light period, then amassing enough energy to divide again in the dark. This is evidenced by a G2/M shoulder at the beginning of the dark period, the timing of which is the same for both experiments despite the synchronization differences (**Fig. 1.2**). Since culture density more than doubled during the intensive sampling days for both experiments (**Fig. 1.2**), the explanation that a subpopulation of cells had divided more than once in a 24-hour period appears more likely than the notion that the late-dividing subpopulation only divided once and substantially later than the majority of the cells in the culture. Incomplete synchronies and the possibility of multiple synchronous subpopulations arising from growth regime selection have been observed in other studies and are discussed in Hoogenhout [1963].

### 1.5.3 Biomass Dynamics

OD750 is a convenient and popular method for monitoring microalgal growth, as the 750 nm wavelength is not absorbed by microalgal pigments, allowing for light scattering alone to be measured [Chioccioli et al. 2014]. Due to the susceptibility of light scattering to influence by multiple variables such as culture density, cell size, shape, and composition, it has been documented that there is not always a linear relationship between OD750 and biomass measured as AFDW [Chioccioli et al. 2014, Edmundson and Huesemann 2015]. However, we found a robust correlation between OD750 and AFDW for actively growing *C. cryptica* (1.3.4) (**Fig. S1.3**). Our ePBR experiments were carried out in the same growth medium (ASW) that was used in the raceway pond experiments from which that conclusion had been derived, using similar sinusoidal light and temperature parameters. Although the OD750 curves do not show perfectly smooth responses, they do not follow the more drastic dynamics of cell cycle changes (including cell division),

consistent with OD750 in our study predominantly being related to biomass and not the other aforementioned variables (**Fig. 1.3A, B**). This has enabled us to use OD750 to examine biomass dynamics in our cultures with a previously unreported (to our knowledge) 10-minute interval resolution.

In our study, OD750 increased for the majority of the light period, except for dawn (**Figs. 1.3, 1.6**). Culture density, however, increased only in the second half of the light period (**Fig. 1.3**), suggesting that cells initially accumulated biomass in preparation for division and continued to accumulate it throughout the light period. The rate of biomass accumulation increased with light intensity (**Fig. 1.4**), consistent with energy input correlating with biomass output, and also suggesting that there was no light saturation or substantial photoinhibition [Ho et al. 2012, Sukenik et al. 1987], despite the irradiance being high for the majority of the light period (**Fig. 1.1**). This may be attributed to the combination of high culture density and the deep and narrow shape of the ePBR [Lucker et al. 2014] resulting in the average irradiance experienced by the culture being substantially lower than the incident light, and below saturating light intensity. The rate of biomass accumulation per cell relative to incident light intensity trended higher during the second half of the day (**Fig. 1.4**). Since culture density during the second half of the day was higher than it was during the first half, the culture was more productive overall. By then, most cells would have already divided, and thus would not be expending carbon on division, which could allow for more of it to be stored. Other factors that differed between the two halves of the day were temperature (**Fig. 1.1**) and the amount of pigments and thus shading in the culture (**Fig. 1.12**), both higher during the second half. The best fit curves are not linear (**Fig. 1.4**), and suggest that the efficiency of light to biomass conversion improves with increasing light intensity, for reasons that are unclear.

We observed an inverse relationship between the starting OD750 at dawn and the subsequent OD750 increase during the day, with lower starting OD750 values corresponding to

greater OD750 increase (**Fig. 1.5**). A similar relationship had been noted previously [Grima et al. 1995, Michels et al. 2014]. Consistent with this trend, the starting OD750 for the Exp. 1 intensive sampling day was lower than that for Exp. 2, while the gain in biomass by the end of the day was greater (**Fig. 1.3**). This observation may be explained by higher OD750 values corresponding to lower light penetrance into the culture and therefore light limitation, even at low densities (**Fig. 1.5**). Less access to light would lead to less carbon fixation relative to respiration, and therefore less ability to store compounds for energy. This ties in with the observation that the rate of biomass accumulation increases with light intensity (**Fig. 1.4**).

As mentioned above, biomass did not increase during the beginning of the light period, which was also reported by Grima et al. [1995] for the diatom *Phaeodactylum tricornutum* cultivated outdoors. We observed a dip in OD750 during the first 1-1.5 hours of the light period, during which light intensity increased substantially (**Figs. 1.1, 1.6**). Biomass did not start to increase for the day until the light intensity reached nearly half of the maximum (1000  $\mu\text{mol photons m}^{-2} \text{s}^{-1}$  at 8:00 h), suggesting that lack of light availability during that time period was not accountable for the observed phenomenon. There was also a dip in TAG around then, though the timing didn't strictly correlate (**Fig. 1.7**). It is possible that energy-requiring processes began when light was sensed, but not enough energy was initially obtainable from the environment to power them and supersede respiration. Thus, stored energy, including TAG, would have needed to be mobilized, resulting in a reduction in TAG and biomass.

Biomass gains made by microalgal cultures during the day are offset by losses at night due to nighttime energy-requiring processes and the accompanying respiration [Burris 1977, Cuhel and Lean 1987, Edmundson and Huesemann 2015, Geider and Osborne 1989]. The extent of the losses depends on the species, physiological state of the culture, and environmental conditions. Generally, the higher the metabolic rate, which correlates with greater light exposure during the day, lower

culture density, exponential growth, favorable cultivation conditions, and higher temperature at night, the greater the nighttime losses will be [Bonnefond et al. 2016, Edmundson and Huesemann 2015, Geider and Osborne 1989, Grima et al. 1995, Grobbelaar and Soeder 1985, Hu et al. 1998, Le Borgne and Pruvost 2013, Michels et al. 2014, Ogbonna and Tanaka 1996]. In some cases, losses of more than 30% have been documented [Guterman et al. 1988, Hu et al. 1998, Torzillo et al. 1991]. In our study, OD750 as a proxy for biomass gained during the day was lower and the nighttime losses higher immediately post-inoculation than after the cultures had some time to adapt, with the effect being more salient for Exp. 2 (**Table S1.2, Figs. S1.1, S1.4**). This might be explained by the metabolic states of the inocula, higher initial biomass in the case of Exp. 2 resulting in less potential for gain during the day, and initial lack of synchrony resulting in more energy expended at night due to division processes. During the intensive sampling periods, nighttime losses were  $5.7 \pm 1.1\%$  and  $5.6 \pm 1.6\%$  of OD750 gained during the day for Exp. 1 and Exp. 2, respectively (**Table S1.2, Figs. S1.1, S1.4**). Since the extent of biomass loss at night has a substantial impact on the overall productivity, it is imperative in a production scenario to take it into account and minimize by strain selection and optimization of cultivation conditions. In addition to lowering the temperature at night, minimizing culture mixing at night can also lessen respiratory losses by decreasing dissolved oxygen, though this approach may negatively impact nighttime biosynthetic processes which may be important to overall productivity [Edmundson and Huesemann 2015, Ogbonna and Tanaka 1996]. Additionally, it is important to optimize biomass concentration so as to maximize the ratio of light utilization during the day to respiratory losses at night [Michels et al. 2014].

#### *1.5.4 TAG Dynamics*

TAG, of commercial interest for biofuel production, has a variety of functions in actively growing microalgal cultures and tends to hyperaccumulate in mostly cytoplasmic lipid droplets during periods of environmental stress such as nutrient limitation [Goodman 2008, Hu et al. 2008, Maeda et al. 2017, Roessler 1990, Solovchenko 2011, Thompson 1996, Zehmer et al. 2009]. In diatoms as well as other microalgae, TAG is made in smaller amounts during favorable growth conditions, typically accumulating during the day when photosynthesis occurs, and depleting at night to be used for energy and biosynthesis of other molecules [Anderson and Sweeney 1977, Bonnefond et al. 2016, Chauton et al 2013, Jallet et al. 2016, Lacour et al. 2012, Sukenik and Carmeli 1990].

Consistent with the aforementioned observations, cellular TAG levels increased toward the middle of the light period and remained high until 3 hours into the dark period during both of our experiments, suggesting that some of the carbon fixed during the day was stored as TAG, then broken down for energy and/or repartitioned into other types of molecules at night. The mid-day dip in cellular TAG levels corresponded to the time when the majority of the cells in the culture were in G2/M during both experiments (**Fig. 1.7**), likely because TAG was used for membrane lipid biosynthesis [Athenstaedt and Daum 2006, Kurat et al. 2009, Solovchenko 2011]. An alternate/additional explanation may have been that the dip occurred at the time that cell concentration began to increase (**Fig. 1.2**), and as cells divided, their TAG content was split between the daughter cells, giving a temporary appearance of decreased cellular TAG, while the total TAG, defined as the combined TAG content of all the cells in the culture, remained unchanged or continued to increase. However, the total TAG decreased at that time as well (**Fig. S1.6**), supporting the hypothesis that some of the stored TAG was used for cell division.

TAG levels increased after dark for both experiments, and more substantially during Exp. 2 (**Fig. 1.7**). Since no new carbon was being fixed at that time, the nighttime increase in TAG may be attributed to repartitioning of carbon from other molecules. The nighttime increase was followed by a decrease to approximately dawn levels, potentially due to carbon repartitioning and/or respiratory losses (**Fig. 1.7**). Consistency in TAG levels at dawn on consecutive days despite the transient daytime increase has also been observed in other actively growing microalgal cultures entrained to a light-dark regime, suggesting that such cultures transiently accumulate TAG to be actively used on a daily basis [Chauton 2013 and refs within, Jallet et al. 2016, Lacour et al. 2012, Sukenik and Carmeli 1990].

### 1.5.5 Photosynthetic Pigment Dynamics

Most previous studies documenting diel changes in microalgal photosynthetic pigment abundance have been carried out in constant temperature using a square-wave light regime [Kohata and Watanabe 1988, Kohata and Watanabe 1989, Owens et al. 1980, Post et al. 1984, Ragni and d'Alcala 2007]. Recently, two groups utilized a sinusoidal light regime, Jallet et al. [2016] examining the Chl a dynamics of the diatom *P. tricornutum* in constant temperature, and Bonnefond et al. [2016] using a sinusoidal temperature regime to examine photosynthetic pigment dynamics of the chlorophyte *Dunaliella salina*. As far as we are aware, this is the first report of photosynthetic pigment dynamics in a diatom using both sinusoidal light and temperature, with examination of diel changes in pigmentation at higher temporal resolution than previously published for any microalgal species. Specifically, whereas other groups typically sampled for pigments every few hours, we sampled as frequently as every 15 minutes during the dawn and dusk

periods when light intensity was changing rapidly (**Fig. 1.1**). This is also the first report, to our knowledge, to overlay the photosynthetic pigment dynamics data with cell cycle progression.

As seen in other studies [Jallet et al. 2016, Post et al. 1984, Ragni and d'Alcala 2007], cellular photosynthetic pigment content increased during the day and decreased by the following dawn during both of our experiments, returning to approximately pre-dawn levels of the previous day (**Figs. 1.8-1.10, S1.5**). As discussed below, Dtx followed a unique pattern relative to the other measured pigments (**Fig. 1.10**), but the abundance of the Ddx+Dtx pool exhibited the general trend of increase during the day followed by a decrease, because Ddx was the more abundant form of the two interconvertible pigments (**Figs. 1.8E-H, 1.10A, B**). There appears to be a difference between the dynamics of Ddx+Dtx and the other photosynthetic pigments (light-harvesting pigments and  $\beta$ -car), potentially indicating differences in regulation (1.4.5.2). Ddx+Dtx abundance appears to be regulated by light intensity and not affected by cell cycle progression, whereas the other photosynthetic pigments appear to be influenced by cell cycle progression and not strictly by light intensity. Ragni and d'Alcala (2007) obtained data for diel photosynthetic pigment variation in the diatom *P. tricornutum* that agree with our observations, although sampling for pigments at a lower temporal resolution and using a square-wave light regime. In their study, the light-harvesting pigments and  $\beta$ -car gradually increased throughout the light period and peaked around dusk, immediately before the majority of the culture underwent cell division, consistent with the notion that the timing of accumulation of those pigments relates to cell cycle progression. They did not observe Dtx production under their experimental conditions, however Ddx maximized much earlier than the other pigments, closer to the beginning of the light period, and remained relatively stable before decreasing in the dark. The nearly square response to the square-wave light regime, in contrast to the sinusoidal-like response to the sinusoidal light regime in our study (**Fig. 1.8G, H**), further supports the hypothesis that the Ddx+Dtx pool is regulated directly by light intensity. Owens

et al. [1980] found that the abundance of Chl a and Chl c exhibited rhythms that followed the light-dark cycle in the diatom *Skeletonema costatum* during asynchronous growth and stationary phase, with accumulation in the light and degradation in the dark. They suggested that Chl a and Chl c accumulation may be influenced by light-dark cycling as well as cell cycle progression, with synchronized division affecting the timing of photosynthetic pigment accumulation in cultures. The behavior of other pigments was not assessed. Considering the data obtained in our study and by Ragni and d'Alcala [2007], we agree with the suggestion, and extend it to potentially include Fx and β-car as well. Increase in photosynthetic pigment content per cell in preparation for division could be due to the need to populate newly divided chloroplasts. If the division takes place in daytime, increased shading may also play a role. The extent to which the shape of the light intensity curve influences timing of the accumulation of the above pigments is yet to be determined.

Sampling for photosynthetic pigment abundance with high resolution has allowed us to observe the extent to which different pigments co-varied with each other. As discussed above, the overall trends were similar for the light-harvesting pigments and β-car. However, Fx, β-car, and Chl c co-varied more closely with each other than with Chl a (**Fig. 1.9**). The observation that Chl c dynamics were more similar to Fx than to its closer chemical relative Chl a may relate to the intricacies of the molecular architecture of light-harvesting complexes and their dynamics. β-car is an earlier intermediate of the carotenoid biosynthesis pathway, which has Fx and Ddx+Dtx as the end products, thus the observed close co-variation of β-car with Fx is not surprising. Much remains to be understood about the pathway in diatoms, including the sequence of the final steps leading to the biosynthesis of Ddx and Fx and the enzymes responsible for their catalysis. One of the leading hypotheses is that Ddx serves as a precursor for both Dtx and Fx [Kuczynska et al. 2015], which makes the apparently separate regulation of the Ddx+Dtx pool from the rest of the carotenoid biosynthesis pathway, including the potentially downstream Fx, very interesting. The distinction

between Ddx+Dtx and Fx dynamics despite the possible precursor/product relationship suggests additional regulatory mechanics. This finding must be taken into consideration during further investigation of the pathway and its regulation.

Substantial fluctuations in the levels of Chl a, Fx, Chl c, and  $\beta$ -car, but not Ddx+Dtx, were observed during the dawn and dusk periods of rapid light intensity changes, providing further evidence for separate regulatory mechanisms (**Figs. 1.8-1.10, S1.5**). Photosynthetic pigment-level adjustments to abrupt and unanticipated changes in growth irradiance are known to happen on the scale of hours to days [e.g., Nymark et al. 2009, Post et al. 1984], but there are, to our knowledge, no high-resolution data available for photosynthetic pigment dynamics during anticipated gradual changes in light intensity. As described by Post et al. (1984), on longer time scales, diel rhythms in cellular Chl a abundance relative to changes in cellular Chl a content due to light intensity adaptation are kinetically distinct and can be mathematically resolved. They observed an increase or decrease in average daily Chl a content when diatom cultures grown using a square-wave light regime were shifted to lower or higher growth irradiance, respectively. At the same time, daily rhythms in Chl a abundance persisted. They posited that the fine control over cellular Chl a content may be explained by adjustments between biosynthetic and degradation rates. We suggest that the same may be the case for Chl c, Fx, and  $\beta$ -car, pending direct experimental evidence. Given what is known about the kinetics of pigmentation adjustment to irradiance changes, it is possible but unlikely that the dawn and dusk fluctuations we observed were due to dynamic adjustments of the photosynthetic apparatus to the rapidly changing light intensity during dawn and dusk, overcompensating in each direction while aiming for a moving target. Rather, we postulate that general remodeling of light-harvesting pigment-protein complexes from a daytime to a nighttime state might take place at those times. The continuation of the fluctuations into the beginning of the dark period is supportive of that hypothesis. Monitoring the abundance of relevant proteins at

those times, as well as assessing the dawn, dusk, and early dark period photosynthetic pigment and protein response at high resolution utilizing a square-wave light regime, when the change from no illumination to maximum light intensity is abrupt rather than gradual, but administered at regular intervals, would help distinguish between the contributions of entrained diel periodicity and spontaneous light intensity adaptation to the fluctuations we observed at dawn and dusk under a sinusoidal light regime.

In diatoms, there is a direct correlation between Dtx concentration and non-photochemical quenching (NPQ), a photoprotective mechanism that allows for dissipation of excess light energy as heat [Kuczynska et al. 2015, Lepetit 2012]. Although Dtx was much less abundant than Ddx during the course of both experiments (**Fig. 1.10A, B**), it exhibited reproducible patterns of accumulation, which can also be conceptualized in relation to the Ddx+Dtx pool as its de-epoxidation state, Dtx/(Ddx+Dtx) (**Fig. 1.10C, D**). There was a de-epoxidation state peak during the light period that did not correspond to the timing of maximum Ddx+ Dtx abundance, which occurred at noon for both experiments (**Fig. 1.8E-H**), perhaps due to correlation with cell cycle progression in addition to light intensity. A general trend of an increase in Dtx abundance towards the middle of the light period, followed by a decrease towards dusk was present, but not in the nearly bell-shaped curve of the Ddx+Dtx pool abundance, which the more copious Ddx paralleled more closely (**Figs. 1.8E-H, 10**). Relatively low de-epoxidation state maxima and lack of very close correlation with light intensity can be attributed to the fact that the cultures were fairly dense, so a substantial proportion of cells would not be receiving a stress-inducing amount of irradiation at any given time. What may have contributed to the timing of Ddx de-epoxidation and the presumable development of NPQ during the light period is the separation of replicated chloroplasts and/or daughter cells as the result of cell cycle progression, resulting in them losing localized shading due to the package effect (reduced *in vivo* light absorption efficiency due to the geometric organizational properties of

photosynthetic pigments in intact cells) [Geider and Osborne 1987]. The observation that the de-epoxidation state had an earlier and more protracted daytime peak in Exp. 1 is consistent with this hypothesis, as cell division started earlier than in Exp. 2 due to the lesser extent of synchronization (**Fig. 1.10C, D**). The unanticipated influence of other cell division-related processes on the de-epoxidation state cannot be ruled out, but we are not aware of studies on the subject. Epoxidation of Dtx in low light after a period of high light exposure is known to occur on the scale of minutes, as it is necessary in diatoms for resuming light harvesting activity [Goss et al. 2006, Grouneva et al. 2009], and the decrease of the de-epoxidation state by dusk is consistent with that. Another de-epoxidation state peak occurred immediately after the onset of darkness in both experiments. This can be explained by a chlororespiratory transthylakoid pH gradient that activates the Ddx de-epoxidase, leading to the accumulation of Dtx and NPQ in the dark [Jakob et al. 1999, Jakob et al. 2001]. Although the de-epoxidation state appears higher during the nighttime peak than during the day, the cellular abundance of Dtx is actually lower at that time, as is the Ddx+Dtx pool abundance; it is the proportion of the pool that is de-epoxidized that creates this appearance, not an increased absolute abundance of cellular Dtx (**Fig. 1.10**). After the initial nighttime peak, the de-epoxidation state decreased to pre-dawn levels. To our knowledge, no previous study was designed to document this phenomenon, and the exact causes for it remain to be elucidated. The observed rapid decrease in the de-epoxidation state upon dawn can be attributed to the inhibition of chlororespiration by the presence of light [Peltier et al. 1987] and the need for the system to transition from a dissipative to a light-harvesting state to take advantage of the available irradiance. Jakob et al. [1999] also observed epoxidation of night-accumulated Dtx under low irradiance at dawn in *P. tricornutum* grown using a light-dark cycle with an exponential illumination regime. It should be noted that Dtx epoxidation proceeds significantly faster in low light than in the dark, due

to the scarcity of NADPH, which is a co-factor for the Dtx epoxidase, in darkness [Goss et al. 2006, Grouneva et al. 2009].

Changes in the ratios of Chl a to the accessory photopigments Fx and Chl c may indicate changes in the composition/structure of the photosynthetic apparatus. The observed ratio fluctuations at dawn, dusk, and the beginning of the dark period (**Fig. 1.11**) indicate a dynamic adjustment of the pigments during which Chl a varied distinctly from Fx and Chl c, which varied similarly to each other (**Fig. 1.9**). Other groups have demonstrated that these ratios in diatoms remain relatively constant regardless of growth irradiance [Lepetit et al. 2012]; in accordance with those observations, and because the daytime increase in the ratios during our study did not exhibit a trend that would be consistent with them changing with light intensity, cell cycle progression, or increase in culture density, we suggest that the day-night differences may be due to diel changes in light-harvesting complex assembly, as discussed above. Ragni and d'Alcala (2007) did not observe periodic variations in the ratios during their study; we note the discrepancy, but do not attempt to explain it, due to the scarcity of this type of data obtained in controlled laboratory conditions to date. There are data from diatom-dominated field samples, however, that also indicate larger changes in Chl a content during the day in comparison to Chl c and carotenoids [Yentsch and Scagel 1958].

#### *1.5.6 Product Accumulation and Harvest Timing*

In a production scenario where microalgae experience a light-dark cycle, such as outdoors, it may be possible to take advantage of the predictable timing of various processes by deducing the best times to harvest for biomass and/or other products. For example, in our set-up with *C. cryptica*, biomass increased throughout the day, slowing around 17:00 h (**Fig. 1.3A, B**). Harvesting at

that time, after the majority of biomass gain had been completed for the day, rather than at 8:00 h (i.e., at the beginning of a typical work-day), would have approximately doubled the yield in Exp. 2, and tripled it in Exp. 1 (**Table S1.3**). Extending the harvesting time into the dark period would not have diminished the potential yield in our study, because the majority of cell division occurred during the day and nighttime respiratory losses were minimal. However, if we were working with a species that divided at night, the timing would work out differently. Biomass would likely still maximize towards the end of the light period, unless there was an external source of carbon that could be consumed heterotrophically without light energy. Cell division, however, would ensue in the dark, and the energy required for associated processes would result in a reduction of biomass available for harvest. In that scenario, it would be advantageous to harvest for biomass at the end of the light period and prior to the onset of cell division. Thus, when assessing the biomass productivity of a given strain under given conditions, it should be noted that a nocturnally dividing strain would use more energy at night than a strain synchronized to divide during the day [Grobbelaar and Soeder 1985]. Therefore, netbiomass change in a 24-hour period, rather than daytime gain or nighttime loss alone, needs to be assessed when determining a strain's overall biomass productivity in given culture conditions.

The optimal time to harvest for TAG in our study, determined by the maximal cell concentration with the highest cellular TAG levels, was 21:00 h for both experiments (**Fig. 1.12A, B**). Harvesting at that time would have improved yield approximately 4-6-fold compared to 8:00 h for both experiments (**Table S1.3**). In a culture dividing at night, TAG levels would still be maximal at the end of the light period, and it would thus be beneficial to harvest prior to onset of energy-requiring division processes.

Microalgal pigments are also of commercial interest for a variety of applications such as functional nutrition and cosmetics [Khanra et al. 2018, Matos et al. 2017]. In *Cyclotella cryptica*, Chl

a, Fx,  $\beta$ -car, and Ddx+Dtx (quantified as a pool as they may interconvert during harvesting) are the pigments that accumulate to an appreciable amount and could be harvested, perhaps along with biomass and/or TAG, to serve as high value co-products that would help offset the costs of biofuel production. In our system, the optimal time to harvest for pigments spanned from dusk through the dark period for Fx and  $\beta$ -car, a narrower time frame during the dusk to night transition for Chl a, and an even more generous time frame for Ddx+Dtx, including more of the light period, with a dip during the Chl a optimal harvesting time (**Fig. 1.12C-H**). The timing would be generally favorable for co-harvesting with either biomass or TAG, and, depending on the pigments, would improve yield approximately 1.5-3-fold (calculated as the ratio between the average pigment content for the preferred timeframe and 8:00 h) (**Table S1.3**).

The abundance of other molecules of interest, such as proteins, carbohydrates, and polyunsaturated fatty acids (PUFAs), will also exhibit diel variation in light-dark synchronized microalgal cultures. The exact details of timing for maximum yield will vary with the specifics, such as the species used, the growth regime, production system metrics, and product(s) of interest. At present, many large-scale production systems employ time-consuming harvesting methods that might not allow for taking advantage of this type of information [Barros et al. 2015, Gerardo et al. 2015]. However, the gains in productivity achieved by an informed timing of harvest may potentially help offset the costs of faster harvesting methods or inspire the development of the latter.

## 1.6 SUMMARY AND CONCLUSIONS

Diel TAG, OD750 as a proxy for biomass, and photosynthetic pigment dynamics in the diatom *Cyclotella cryptica* grown using a sinusoidal light and temperature regime simulating what

microalgae experience outdoors were examined. As is typical in microalgal cultures grown on a light-dark regime, cell cycle synchronization occurred. The main cell division event was in the middle of the light period, preceded by an increase in biomass by a few hours. This observation emphasizes the fact that the two variables, which are often used as an assessment of culture growth, do not necessarily correlate. They would be even less parallel in a nocturnally dividing culture, which would gain biomass during sunlight hours and then lose a greater proportion of it at night due to respiratory requirements associated with cell division. Cellular TAG accumulated during the day and decreased at night. The observed daytime dip corresponded to the time when the majority of the population would require lipids for division-related membrane biosynthesis, suggesting that TAG may be serving as a precursor for membrane lipids. Differences in the extent of synchrony between the two experiments and patterns of accumulation of Chl a, Fx, Chl c, and  $\beta$ -car on a per cell basis suggest that cell cycle progression influences their cellular abundance. Care must be taken when normalizing other parameters to Chl a, which is common practice, as its abundance per cell is not constant. By contrast, the Ddx+Dtx pool abundance appeared to be dictated by irradiance and independent of cell cycle progression. This suggests a separate level of regulation for these end products of the carotenoid biosynthesis pathway from Fx, the other end product, and  $\beta$ -car, a pathway intermediate, and must be taken into account in further studies of the pathway in diatoms, which still remains poorly understood. Cell cycle progression did appear to affect the proportion of the Ddx+Dtx pool present as Dtx, which correlates with NPQ and is an indicator of irradiance-induced stress. As detailed in 1.5.5, this suggests that loss of local shading due to chloroplast division and/or separation may result in stress that triggers the photoprotective mechanism. Finally, our results indicate that timing is of importance when sampling light-dark synchronized cultures for study or harvesting them for production, as it will significantly affect the abundance of various cellular components and product yields. Because of accurately mimicking

outdoor light and temperature conditions, these lab-based experiments have conceptual relevance to outdoor cultivation. The species examined, *Cyclotella cryptica*, also has relevance to outdoor production, as it has been identified as a top production candidate [Traller et al. 2016].

## **1.7 ACKNOWLEDGEMENTS**

Chapter 1, in full, has been submitted for publication. Gaidarenko, Olga; Sathoff, Corinne; Staub, Kenneth; Huesemann, Michael M.; Vernet, Maria; Hildebrand, Mark. "Timing is everything: diel metabolic and physiological changes in the diatom *Cyclotella cryptica* grown in simulated outdoor conditions." Ms. Gaidarenko was the principal author on this paper. We thank Dr. Susan Golden and her lab members for lending us the ePBR used for this work. We also thank Dr. Daniel Wangpraseurt for assistance with data interpolation. This work was supported by U.S. Dept. of Energy grant DE-SC0012556.

**Table 1.1**

Average cellular pigment content and ratios.

	Exp. 1 (pg/cell)	Exp. 2 (pg/cell)	Exp. 1:Exp. 2 Ratio
Chl a	4.34±1.15	3.58±0.66	1.21:1
Fx	1.14±0.10	1.04±0.08	1.09:1
Chl a/Fx	3.76±0.79	3.45±0.57	1.09:1
Chl c	0.17±0.02	0.15±0.01	1.13:1
Chl a/Chl c	24.95±5.35	23.38±4.13	1.07:1
β-car	0.10±0.02	0.08±0.01	1.25:1
Ddx	0.37±0.10	0.34±0.09	1.09:1
Dtx	0.05 ± 0.02	0.05 ± 0.02	1.00:1
Ddx+Dtx	0.43±0.11	0.39±0.10	1.07:1
Dtx/(Ddx+Dtx)	0.13±0.04	0.13±0.05	1.10:1
Tot Pig	6.19±1.28	5.24±0.74	1.18:1

**Table S1.1**

Sample to sample variation in photosynthetic pigment content (pg/cell).

Control Sample	Chl c	Fx	Ddx+Dtx	Chl a	$\beta$ -car
1	0.2453	1.5268	1.4614	5.9333	0.1676
2	0.2457	1.5352	1.4941	6.3008	0.1830
3	0.2335	1.5005	1.4672	6.1047	0.1779
4	0.2450	1.5107	1.4775	5.7806	0.1652
5	0.2346	1.5211	1.4967	5.6772	0.1643
Mean	0.2408	1.5188	1.4794	5.9593	0.1716
SD	0.0062	0.0136	0.0158	0.2500	0.0084
SD as % of Mean	2.57	0.89	1.07	4.20	4.88
Exp. 1 Sample	Chl c	Fx	Ddx+Dtx	Chl a	$\beta$ -car
1	0.1510	1.0122	0.3793	2.8773	0.0878
2	0.1536	1.0862	0.3960	3.0981	0.0890
3	0.1679	1.0761	0.4025	3.1216	0.0938
4	0.1382	0.9512	0.3516	2.6643	0.0771
5	0.1624	1.1361	0.4252	3.3725	0.0981
Mean	0.1546	1.0523	0.3909	3.0268	0.0892
SD	0.0114	0.0717	0.0274	0.2680	0.0079
SD as % of Mean	7.39	6.81	7.02	8.85	8.83
Exp. 2 Sample	Chl c	Fx	Ddx+Dtx	Chl a	$\beta$ -car
1	0.1396	0.9989	0.3843	3.6702	0.0760
2	0.1668	1.1247	0.4211	2.8530	0.0908
3	0.1473	1.0888	0.4062	3.7972	0.0816
4	0.1486	1.0872	0.4137	3.1542	0.0914
5	0.1699	1.0391	0.3965	2.6585	0.0709
Mean	0.1544	1.0677	0.4044	3.2266	0.0821
SD	0.0132	0.0491	0.0145	0.4975	0.0090
SD as % of Mean	8.57	4.59	3.57	15.42	10.98

**Table S1.2**  
Nightly biomass loss calculated as the percentage of OD750 gained during the day that was lost at night.

		Undiluted	Diluted	Average ± SD
Exp. 1	Date	10/20	-	-
	% Lost	10.6	-	-
Exp. 2	Date	12/16	12/17	10/21
	% Lost	67.5	32.8	4.7
				4.8
				8.0
				5.6
				6.7
				5.7
				4.7
				5.7±1.1
				-
				10/24
				12/21
				12/22
				12/23
				12/24
				12/25
				-
				5.3
				5.6±1.6

**Table S1.3**  
Yields at optimal harvesting times vs. 8:00 h.

	Time	Biomass (OD750)	Total TAG (RFU)	Chl a (µg)	Fx (µg)	β-car (µg)	Ddx+Dtx (µg)
Exp. 1	8:00 h	0.10	7.5E8	1.2	0.39	0.03	0.17
	Optimal	0.28	4.4E9	3.3	0.85	0.08	0.29
	Fold difference	2.8	5.9	2.8	2.2	2.7	1.7
Exp. 2	8:00 h	0.18	1.9E9	1.3	0.38	0.03	0.17
	Optimal	0.33	8.8E9	3.1	0.85	0.07	0.28
	Fold difference	1.8	4.6	2.4	2.2	2.3	1.6

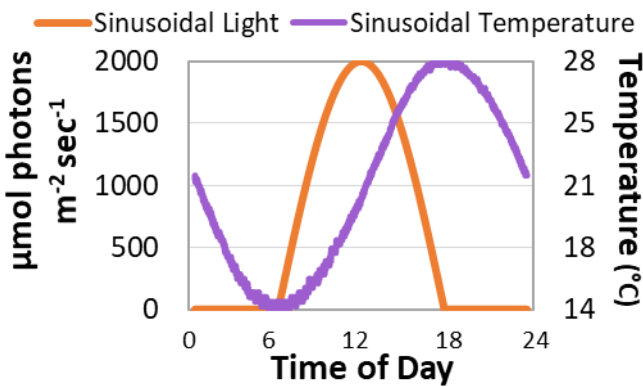


**Figure. 1.1.**  
Sinusoidal changes in light and temperature.

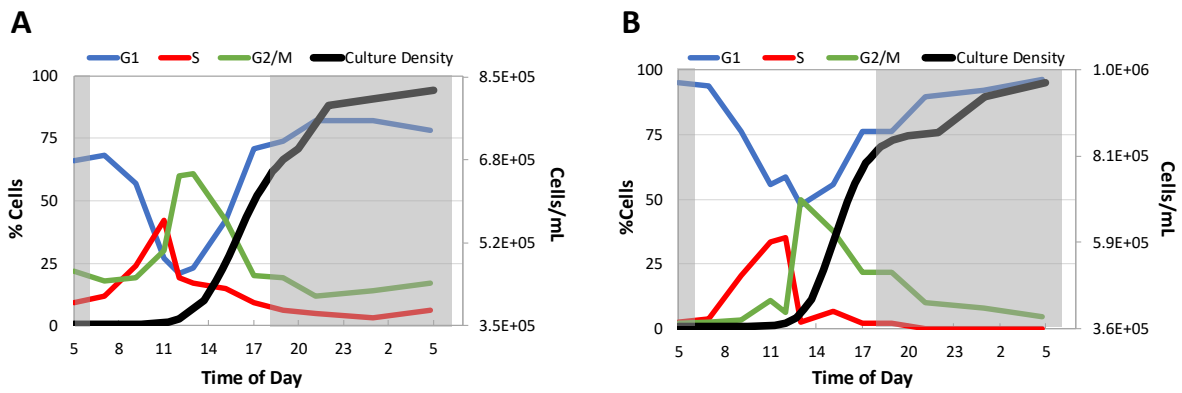


**Figure. 1.2.**  
Culture density relative to cell cycle progression. **A.** Exp. 1, **B.** Exp. 2.

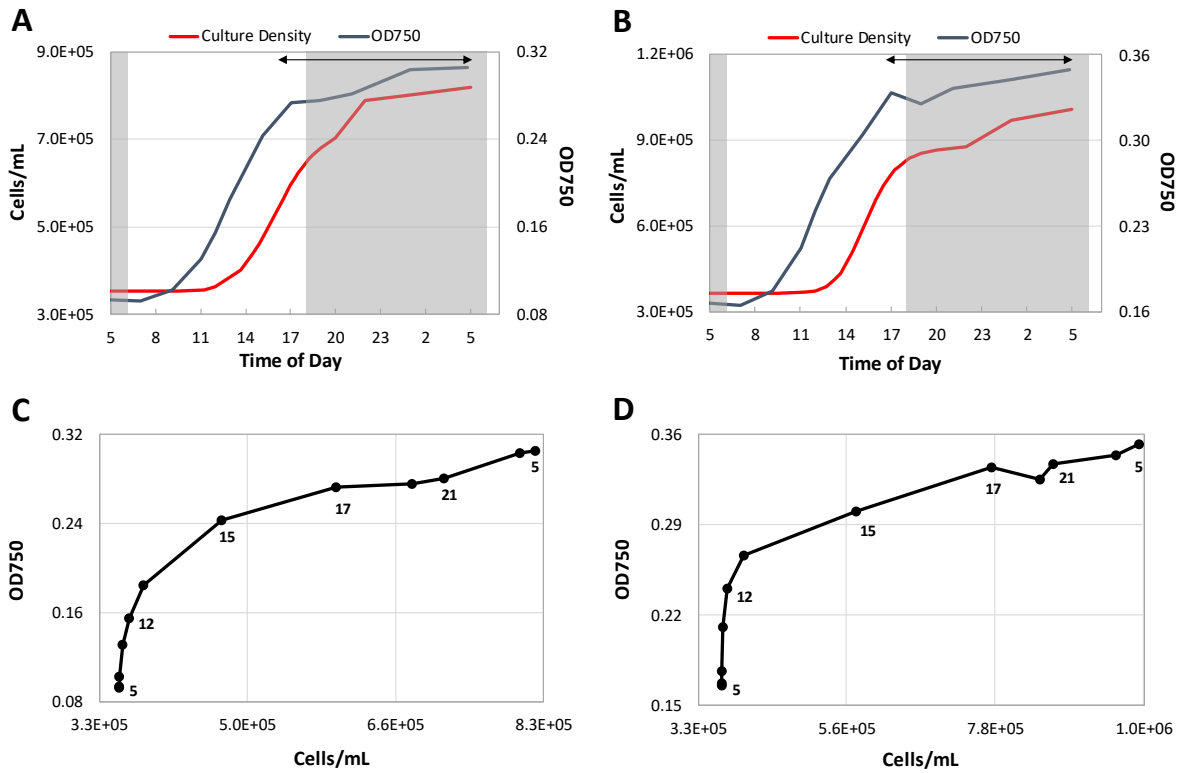


**Figure. 1.3.**

Culture density and OD<sub>750</sub>. Arrows indicate optimal biomass harvest times. **A.** Exp. 1 **B.** Exp. 2.; Culture density and corresponding OD<sub>750</sub>, plotted sequentially. Numbers on the plot correspond to time of day. **C.** Exp. 1, **D.** Exp. 2.

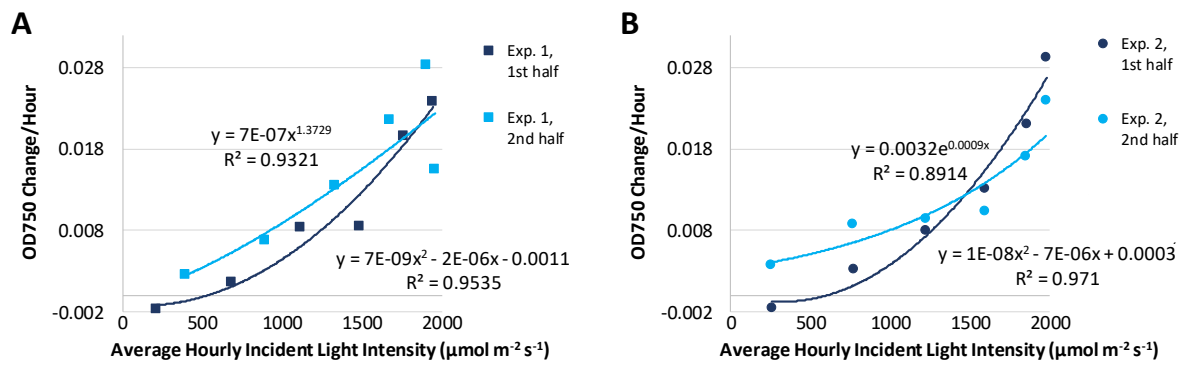


**Figure. 1.4.**

Rate of OD<sub>750</sub> increase per cell versus incident light energy intensity.

First and second halves of the day plotted separately for **A.** Exp. 1, **B.** Exp. 2.

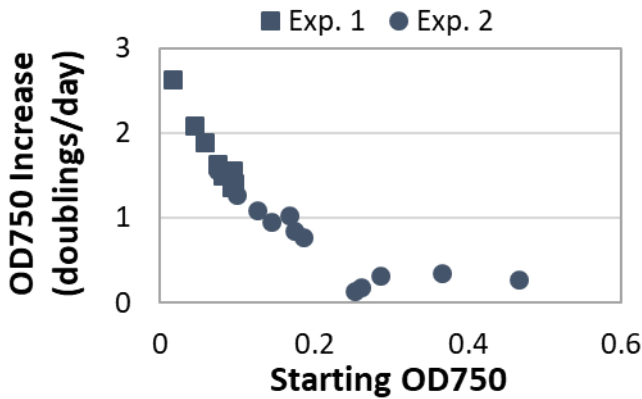


**Figure. 1.5.**

Increase in OD<sub>750</sub> per day versus OD<sub>750</sub> at dawn.

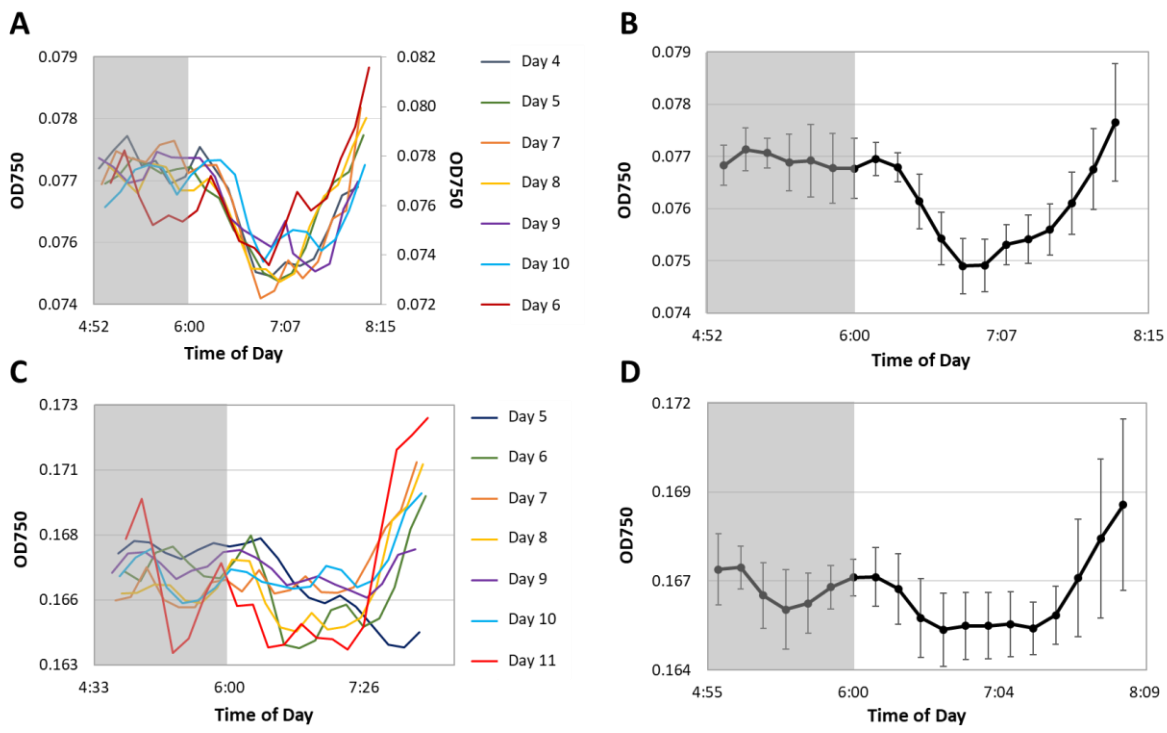


**Figure 1.6.**

Dawn dip in OD750.

**A.** Exp. 1, raw data. Oct. 24 plotted on a secondary y-axis, **B.** Exp. 1, average interpolated values,

**C.** Exp. 2, raw data, **D.** Exp. 2, average interpolated value.

Error bars represent 1 standard deviation (SD).

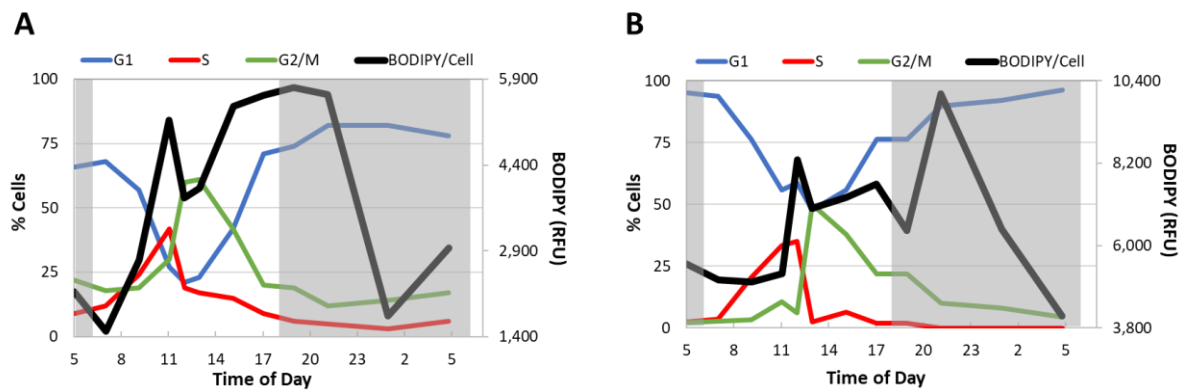


**Figure 1.7.**

Cellular TAG levels relative to cell cycle progression **A.** Exp. 1, **B.** Exp. 2.

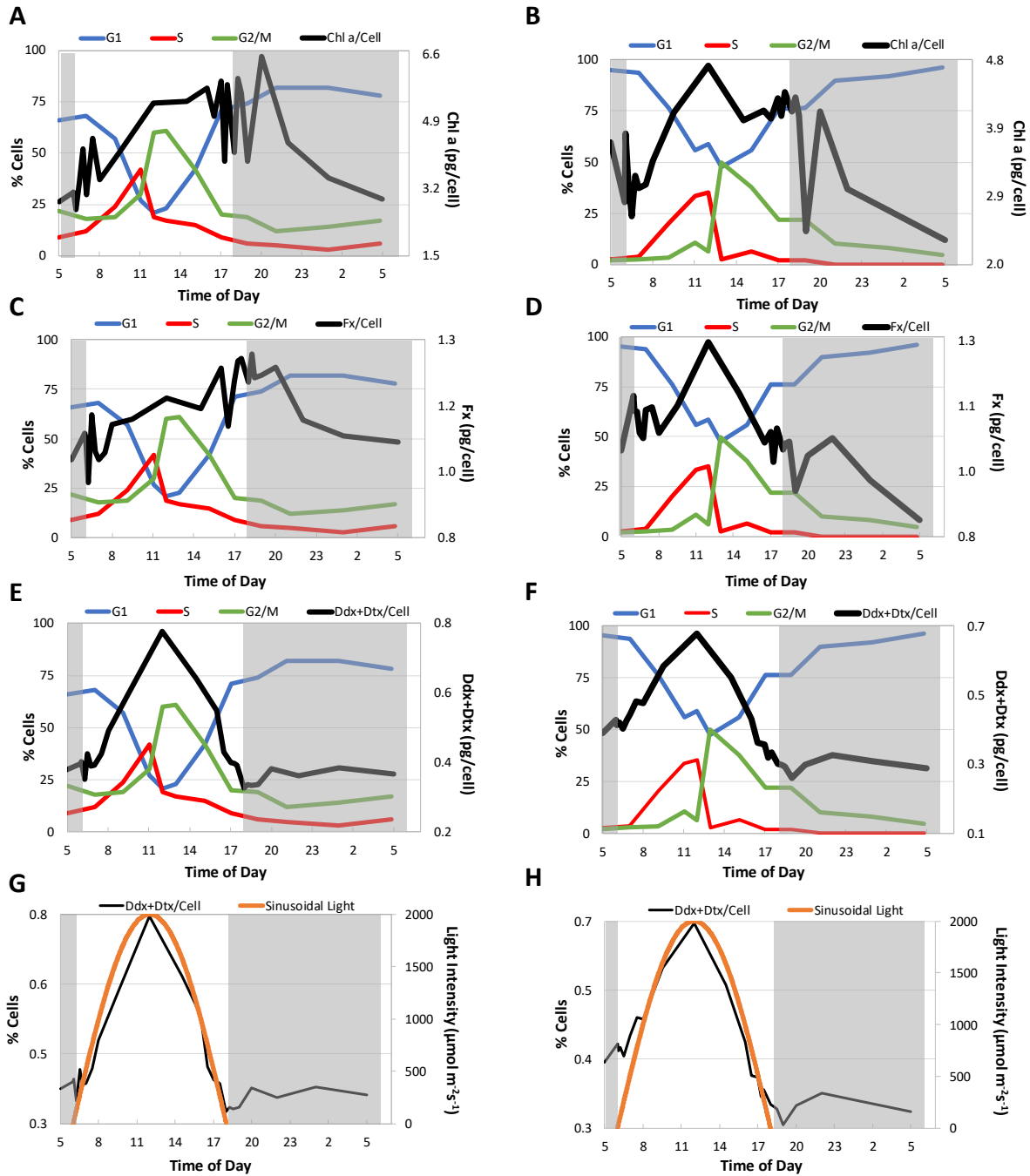


**Figure 1.8.**

Changes in cellular pigment abundance vs. cell cycle progression or light intensity.  
**Chl a** **A.** Exp. 1, **B.** Exp. 2; **Fx** **C.** Exp. 1, **D.** Exp. 2; **Ddx+Dtx** **(E, G)** Exp. 1, **(F, H)** Exp. 2.

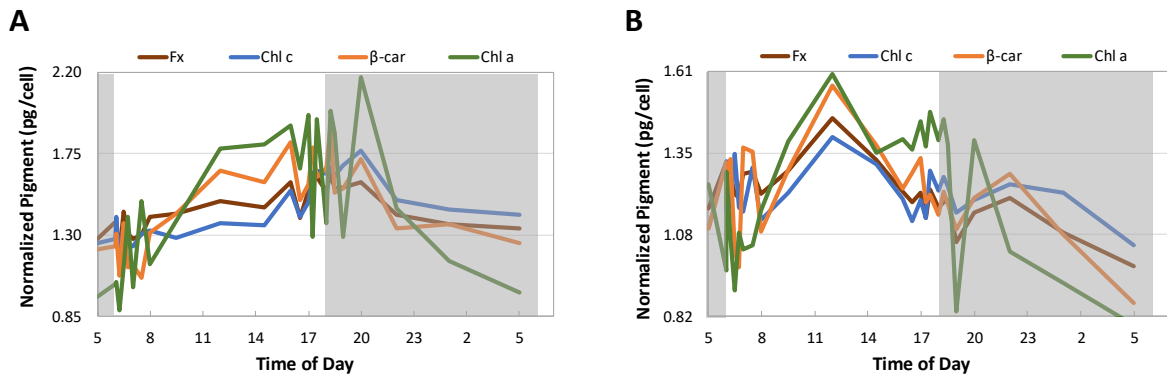


**Figure 1.9.**

Changes in cellular abundance of Fx, Chl a, Chl c, and  $\beta$ -car normalized to a common mean.

**A. Exp. 1, B. Exp. 2**

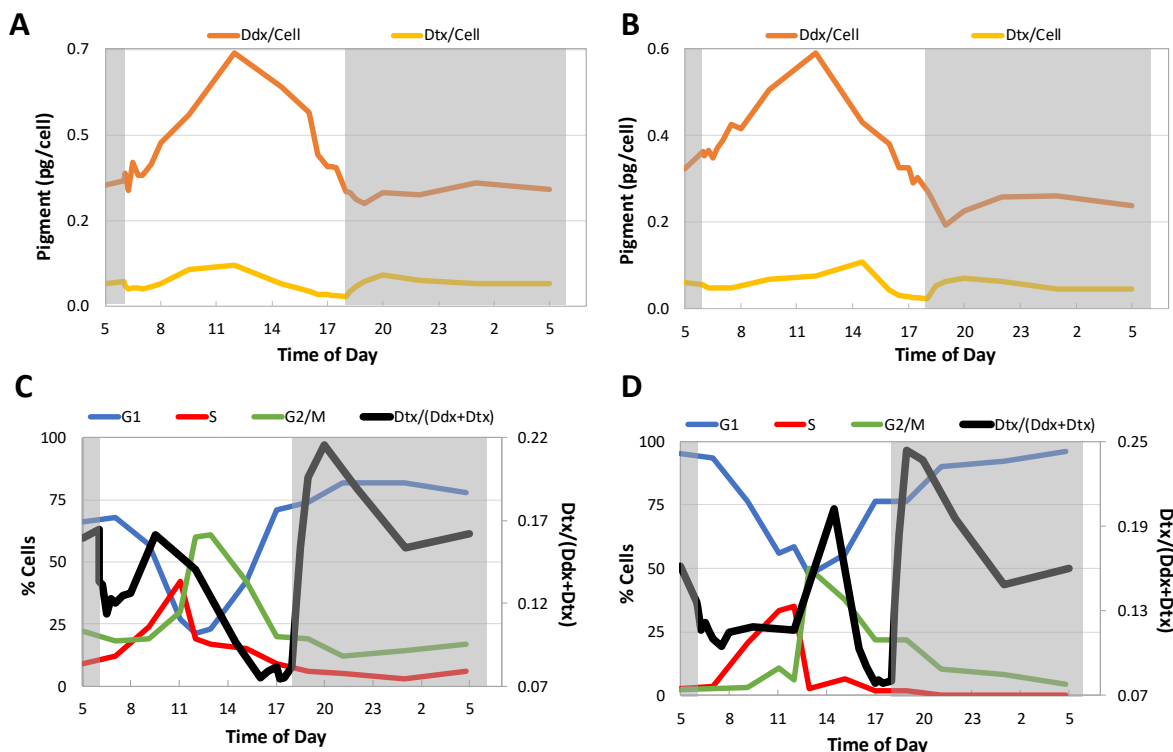


**Figure 1.10.**

Ddx and Dtx cellular abundance **A. Exp. 1, B. Exp. 2;**

Ddx+Dtx de-epoxidation state,  $Dtx/(Ddx+Dtx)$  **C. Exp. 1, D. Exp. 2.**

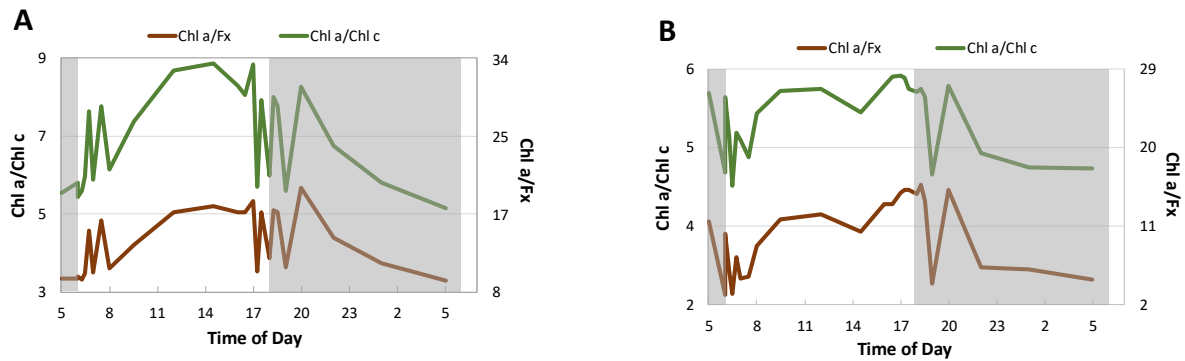


**Figure 1.11.**

Changes in the Chl a/Fx and Chl a/Chl c ratios **A.** Exp.1, **B.** Exp. 2.

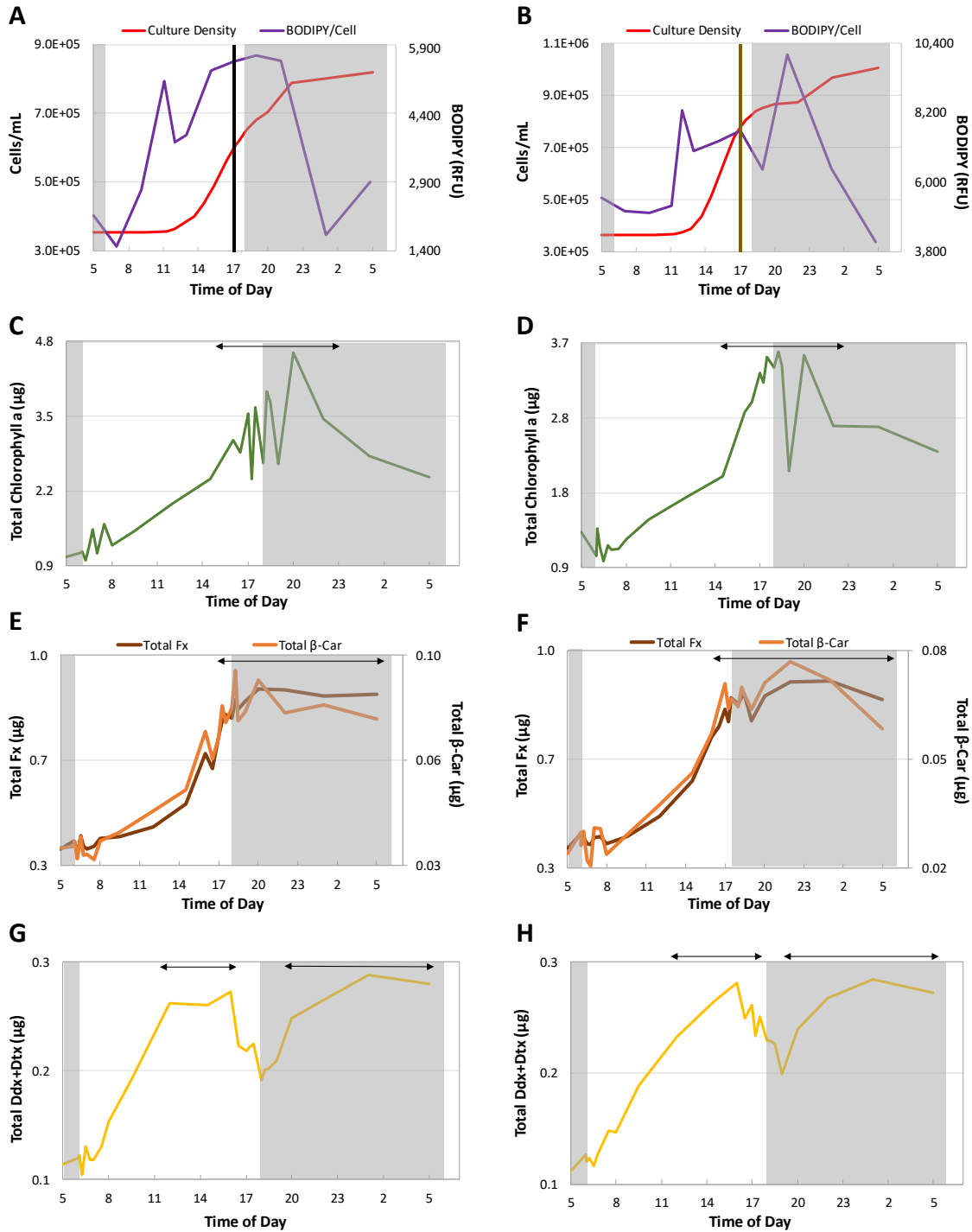


**Figure 1.12.**

Optimal harvesting times. Culture density and cellular TAG content.

**A.** Exp. 1 and **B.** Exp. 2. Black vertical bars indicate optimal harvest times;

**C.** Exp. 1 and **D.** Exp. 2; Total Fx and  $\beta$ -car, **E.** Exp. 1 and **F.** Exp. 2;

Total Ddx+Dtx. **G.** Exp. 1 and **H.** Exp. 2. Black arrows indicate optimal harvest time frames.

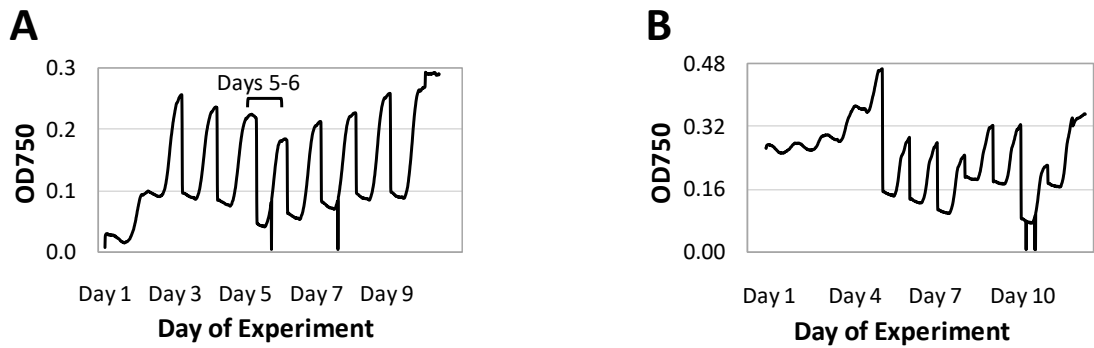


**Figure. S1.1.**  
Daily OD750 changes. **A.** Exp. 1, **B.** Exp. 2.

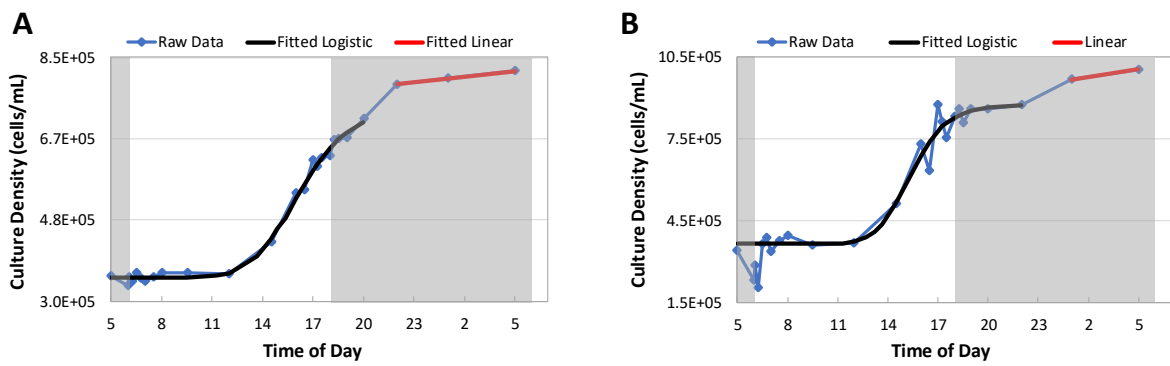


**Figure. S1.2.**  
Raw cell counts and fitted curves.  
**A.** Exp. 1. Fitted Logistic:  $y = 7.425801 + (3.528496 - 7.425801)/(1 + (x/653.6711)^{7.328171})$ ,  $R^2 = 0.99$ ; Fitted Linear:  $y = 0.0007252252*x + 7.163063$ ,  $R^2 = 0.99$ ,  
**B.** Exp. 2. Fitted logistic:  $y = 8.788881 + (3.652112 - 8.788881)/(1 + (x/604.2648)^{9.63665})$ ,  $R^2 = 0.98$ ; Linear =  $y = 0.0015x + 7.8928$ .

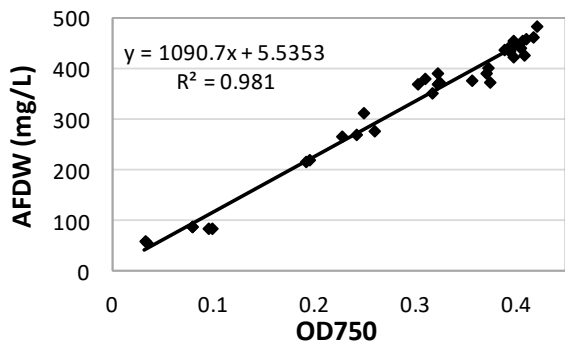


**Figure. S1.3.**

Correlation between ash-free dry weight (AFDW) and OD750.

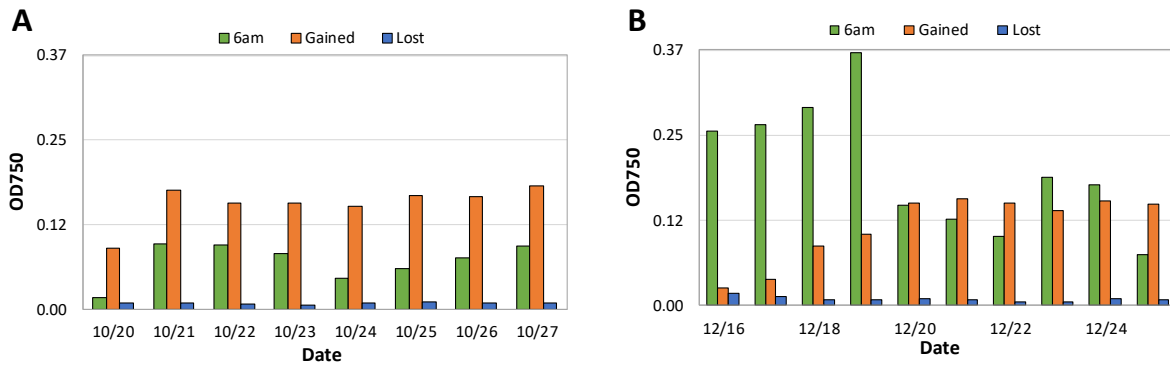


**Figure. S1.4.**

Biomass at 6am, gained by the end of the light period, and lost at night **A. Exp. 1, B. Exp. 2.**

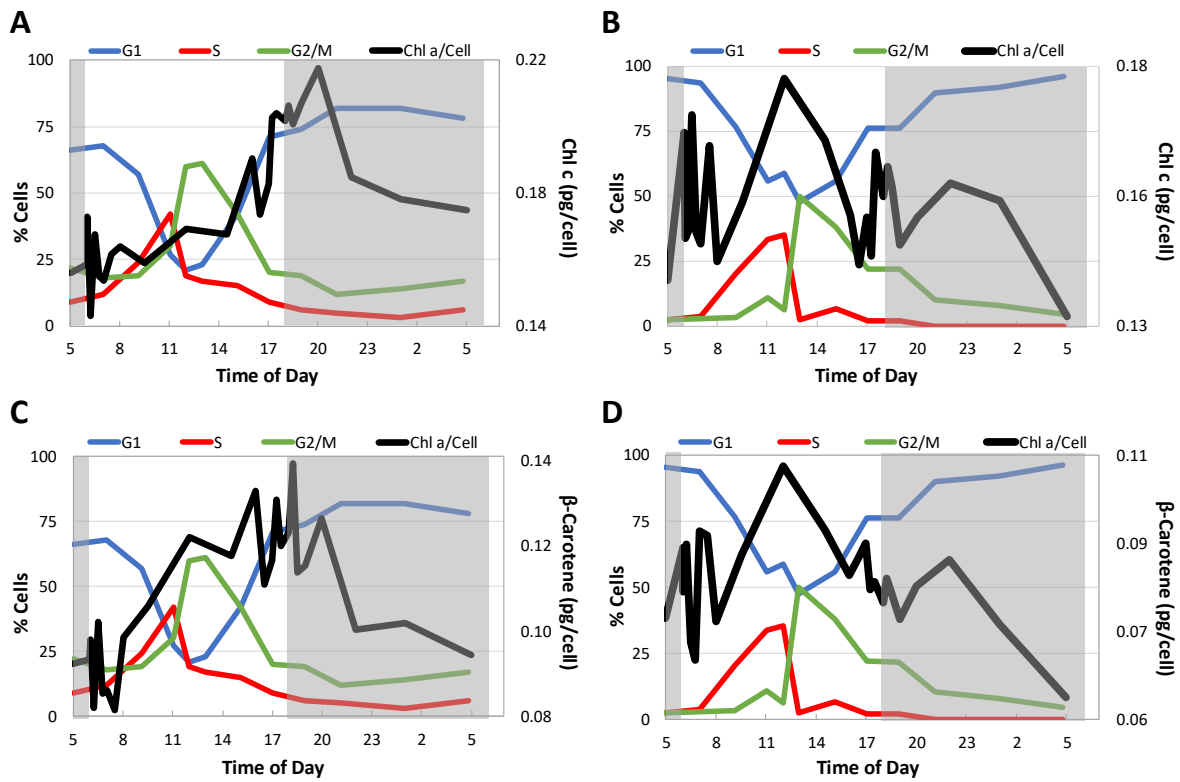


**Figure. S1.5.**  
Changes in pigment abundance vs. cell cycle progression.  
Chl c **A**. Exp. 1, **B**. Exp. 2;  $\beta$ -car **C**. Exp. 1, **D**. Exp. 2.

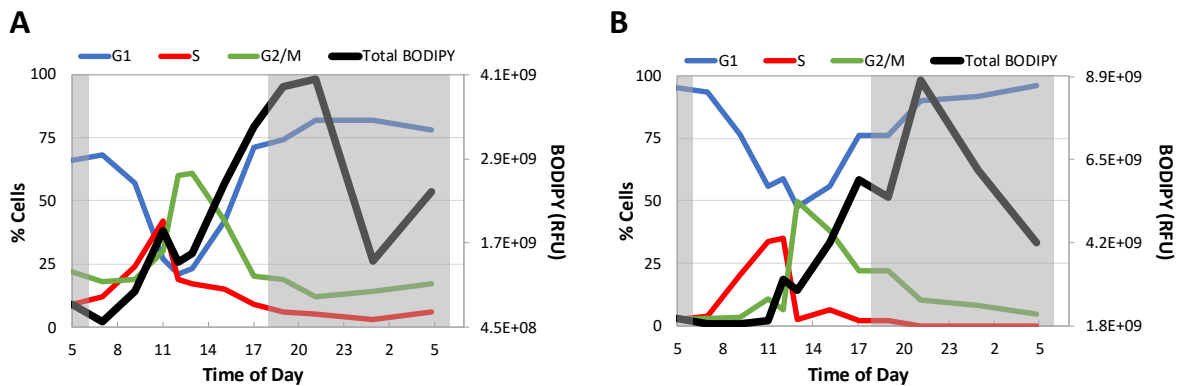


**Figure. S1.6.**  
Total TAG (combined TAG content of all the cells in the culture) versus cell cycle progression.  
**A**. Exp. 1, **B**. Exp. 2.

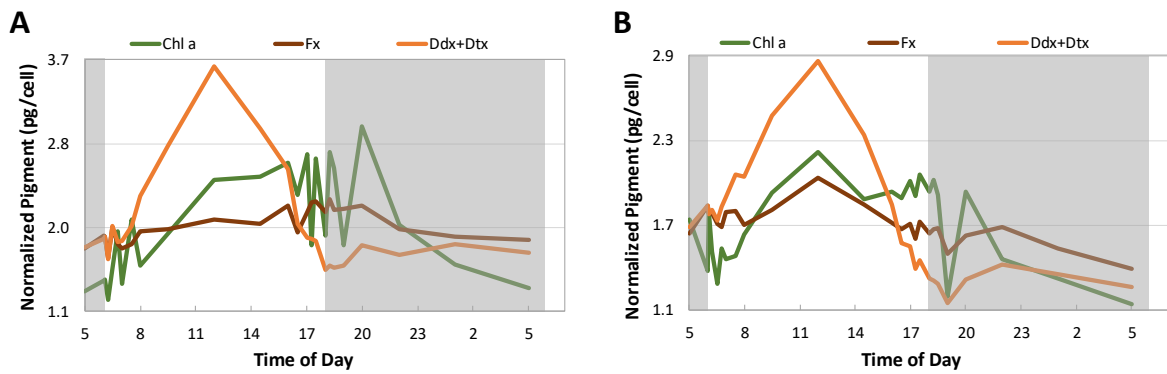


**Figure. S1.7.**

Changes in cellular Chl a, Fx, and Ddx+Dtx abundance, normalized to a common mean.

**A.** Exp. 1, **B.** Exp. 2.

## 1.8 REFERENCES

- R. Abbriano, N. Vardar, D. Yee, M. Hildebrand, Manipulation of a glycolytic regulator alters growth and carbon partitioning in the marine diatom *Thalassiosira pseudonana*. *Algal Res.* 32 (2018) 250-258.
- L. W. J. Anderson, B. M. Sweeney, Diel changes in sedimentation characteristics of *Ditylum brightwellii*: changes in cellular lipid and effects of respiratory inhibitors and ion-transport modifiers. *Limnol Oceanogr.* 22 (3) (1977) 539-552.
- K. Athenstaedt, G. Daum, The life cycle of neutral lipids: synthesis, storage and degradation. *Cel Mol Life Sci.* 63 (12) (2006) 1355-1369.
- A. I. Barros, A. L. Goncalves, M. Simoes, J. C. M. Pires, Harvesting techniques applied to microalgae: a review. *Renew Sust Energ Rev.* 41 (2015) 1489-1500.
- H. Bonnefond, N. Moelants, A. Talec, O. Bernard, A. Sciandra, Concomittant effects of light and temperature diel variations on the growth rate and lipid production of *Dunaliella salina*. *Algal Res.* 14 (2016) 72-78.
- M. S. Bono Jr., R. D. Garcia, D. V. Sri-Jayantha, B. A. Ahner, B. J. Kirby, Measurement of lipid accumulation in *Chlorella vulgaris* via flow cytometry and liquid-state <sup>1</sup>H NMR spectroscopy for development of an NMR-traceable flow cytometry protocol. *PLoS One* 10 (8) (2015) e0134846.
- C. Buchel, Fucoxanthin-chlorophyll proteins in diatoms: 18 and 19 kDa subunits assemble into different oligomeric states. *Biochem.* 42 (2003) 13027-13034.
- J. E. Burris, Photosynthesis, photorespiration, and dark respiration in eight species of algae. *Mar Biol.* 39 (1977) 371-379.
- M. S. Chauton, P. Winge, T. Brembu, O. Vadstein, A. M. Bones, Gene regulation of carbon fixation, storage, and utilization in the diatom *Phaeodactylum tricornutum* acclimated to light/dark cycles. *Plant Physiol.* 161 (2) (2013) 1034-1048.
- M. Chioccioli, B. Hankamer, I. L. Ross, Flow cytometry pulse with data enables rapid and sensitive estimation of biomass dry weight in the microalgae *Chlamydomonas reinhardtii* and *Chlorella vulgaris*. *PLoS One* 9 (5) (2014) e97269.
- S. W. Chisholm, L. E. Brand, Persistence of cell division phasing in marine phytoplankton in continuous light after entrainment to light:dark cycles. *J Exp Mar Biol Ecol.* 51 (1981) 107-118.
- S. W. Chisholm, F. M. M. Morel, W. S. Slocum, The phasing and distribution of cell division cycles in marine diatoms, in: P. G. Falkowski (Ed.), Primary productivity in the sea, Environmental Science Research Vol. 19, Springer, Boston MA, 1980.
- D. R. Clark, K. J. Flynn, N. J. P. Owens, The large capacity for dark nitrate-assimilation in diatoms may overcome nitrate limitation on growth. *New Phytol.* 155 (1) (2002) 101-108.
- R. Croce, H. van Amerongen, Natural strategies for photosynthetic light harvesting. *Nat Chem Biol.* 10 (2014) 492-501.

R. L. Cuhel, D. R. S. Lean, Influence of light intensity, light quality, temperature, and daylength on uptake and assimilation of carbon dioxide and sulfate by lake plankton. Can J Fish Aquat Sci. 44 (1987) 2118-2132.

R. L. Cuhel, P. B. Ortner, D. R. S. Lean, Night synthesis of protein by algae. Limnol Oceanogr. 29 (4) (1984) 731-744.

W. Darley, B. Volcani, Role of silicon in diatom metabolism, A silicon requirement for deoxyribonucleic acid synthesis in the diatom *Cylindrotheca fusiformis* Reimann and Lewin. Exp. Cell. Res. 58 (1969) 334-42.

W. M. Darley, B. E. Volcani, Synchronized cultures: diatoms. Methods Enzymol. 23 (1971) 85-96.

V. Ebenzer, L. K. Medlin, J. Ki, Molecular detection, quantification, and diversity evaluation of microalgae. Mar Biotechnol. 14 (2012) 129-142.

S. J. Edmundson, M. H. Huesemann, The dark side of algae cultivation: characterizing night biomass loss in three photosynthetic algae, *Chlorella sorokiniana*, *Nannochloropsis salina* and *Picochlorum* sp. Algal Res. 12 (2015) 470-476.

R. W. Eppley, R. W. Holmes, E. Paasche, Periodicity in cell division and physiological behavior of *Ditylum brightwellii*, a marine planktonic diatom, during growth in light-dark cycles. Arch Mikrobiol. 56 (1967) 305-323.

P. G. Falkowski, J. A. Raven, Aquatic photosynthesis (second edition). Princeton University Press, 2007.

M. W. Fawley, Effects of light intensity and temperature interactions on growth characteristics of *Phaeodactylum tricornutum* (Bacillariophyceae). J Phycol. 20 (1984) 67-72.

R. J. Geider, B. A. Osborne, Light absorption by a marine diatom: experimental observations and theoretical calculations of the package effect in a small *Thalassiosira* species. Mar Biol. 96 (1987) 299-308.

R. J. Geider, B. A. Osborne, Respiration and microalgal growth: a review of the quantitative relationship between dark respiration and growth. New Phytol. 112 (1989) 327-341.

M. L. Gerardo, S. V. D. Hende, H. Vervaeren, T. Coward, S. C. Skill, Harvesting of microalgae within a biorefinery approach: a review of the developments and case studies from pilot-plants. Algal Res. 11 (2015) 248-262.

J. M. Goodman, The gregarious lipid droplet J Biol Chem. 283 (42) (2008) 28005-28009.

R. Goss, E. A. Pinto, C. Wilhelm, M. Richter, The importance of highly active and ΔpH-regulated diatoxanthin epoxidase for the regulation of the PSII antenna function in diadinoxanthin cycle containing algae. J Plant Physiol. 163 (10) (2006) 1008-1021.

E. M. Grima, J. A. S. Perez, F. G. Camacho, J. M. F. Sevilla, F. G. A. Fernandez, J. U. Cardona, Biomass and icosaepentoic acid productivities from an outdoor batch culture of *Phaeodactylum tricornutum* UTEX 640 in an airlift tubular photobioreactor. Appl Microbiol Biotechnol. 42 (1995) 658-663.

J. U. Grobbelaar, C. J. Soeder, Respiration losses in planktonic green algae cultivated in raceway ponds. J Plankton Res. 7 (4) (1985) 497-506.

- I. Grouneva, T. Jakob, C. Wilhelm, R. Goss, The regulation of xanthophyll cycle activity and of non-photochemical fluorescence quenching by two alternate electron flows in the diatoms *Phaeodactylum tricornutum* and *Cyclotella meneghiniana*. *Biochim Biophys Acta.* 1787 (2009) 929-938.
- H. Guterman, S. Ben-Yakov, A. Vonshak, Automatic on-line growth estimation method for outdoor algal biomass production. *Biotechnol Bioeng.* 34 (2) (1988) 143-152.
- S. Ho, C. Chen, J. Chang, Effect of light intensity and nitrogen starvation on CO<sub>2</sub> and lipid/carbohydrate production of an indigenous microalga *Scenedesmus obliquus* CNW-N. *Bioresour Technol.* 113 (2012) 244-252.
- H. Hoogenhout, Synchronous cultures of algae. *Phycologia* 2 (4) (1963) 135-147.
- Q. Hu, N. Kurano, M. Kawachi, I. Iwasaki, S. Miyachi, Ultrahigh-cell-density culture of a marine green alga *Chlorococcum littorale* in a flat-plate photobioreactor. *Appl Microbiol Biotechnol.* 49 (1998) 655-662.
- Q. Hu, M. Sommerfield, E. Jarvis, M. Ghirardi, M. Posewitz, M. Seibert, A. Darzins, Microalgal triacylglycerols as feedstocks for biofuel production: perspectives and advances. *Plant J.* 54 (4) (2008) 621-639.
- M. Huesemann, T. Dale, A. Chavis, B. Crowe, S. Twary, A. Barry, D. Valentine, R. Yoshida, M. Wigmosta, V. Cullinan, Simulation of outdoor pond cultures using indoor LED-lighted and temperature-controlled raceway ponds and Phenometrics photobioreactors. *Algal Res.* 21 (2017) 178-190.
- M. Huesemann, A. Chavis, S. Edmundson, D. Rye, M. Wigmosta, Climate-simulated pond culturing: quantifying the maximum achievable annual biomass productivity of *Chlorella sorokiniana* (DOE 1412) in the United States, *J Appl Phycol.* 30 (2018) 287-298.
- G. F. Humphrey, Photosynthetic characteristics of algae grown under constant illumination and light-dark regimes. *J Exp Mar Biol Ecol.* 40 (1979) 63-70.
- T. Jakob, R. Goss, C. Wilhelm, Activation of diadinoxanthin de-epoxidase due to a chlororespiratory proton gradient in the dark in the diatom *Phaeodactylum tricornutum*. *Plant Biol.* 1 (1999) 76-82.
- T. Jakob, R. Goss, C. Wilhelm, Unusual pH-dependence of diadinoxanthin de-epoxidase activation causes chlororespiratory induced accumulation of diatoxanthin in the diatom *Phaeodactylum tricornutum*. *J Plant Physiol.* 158 (2001) 383-390.
- D. Jallet, M. A. Caballero, A. A. Gallina, M. Youngblood, G. Peers, Photosynthetic physiology and biomass partitioning in the model diatom *Phaeodactylum tricornutum* grown in a sinusoidal light regime. *Algal Res.* 18 (2016) 51-60.
- L. Joseph, T. A. Villareal, Nitrate reductase activity as a measure of nitrogen incorporation in *Rhizosolenia formosa* (H. Peragallo): internal nitrate and diel effects. *J Exp Mar Biol Ecol.* 229 (1998) 159-176.
- S. Khanra, M. Mondal, G. Halder, O. N. Tiwari, K. Gayen, T. K. Bhowmick, Downstream processing of microalgae for pigments, protein and carbohydrate in industrial application: a review. *Food Bioprod Process.* (2018) <https://doi.org/10.1016/j.fbp.2018.02.002>

- K. Kohata, M. Watanabe, Diel changes in the composition of photosynthetic pigments and cellular carbon and nitrogen in *Chantonella antiqua* (Raphidophyceae). J Phycol. 24 (1988) 58-66.
- K. Kohata, M. Watanabe, Diel changes in the composition of pigments and cellular carbon and nitrogen in *Pyramimonas parkeae* (Prasinophyceae). J Phycol. 25 (1989) 377-385.
- W.A. Kozlowski, D. Deutschman, I. Garibotti, C. Trees, M. Vernet, An evaluation of the application of CHEMTAX to Antarctic coastal pigment data. Deep-Sea Res. Pt I 58 (2011) 350-364.
- P. Kuczynska, M. Jemiola-Rzeminska, K. Strzalka, Photosynthetic pigments in diatoms. Mar Drugs 13 (9) (2015) 5847-5881.
- C. F. Kurat, H. Wolinski, J. Petschnigg, S. Kaluarachchi, B. Andrews, K. Natter, S. D. Kohlwein, Cdk1/Cdc28-dependent activation of the major triacylglycerol lipase Tgl4 in yeast links lipolysis to cell-cycle progression. Mol Cell 33 (1) (2009) 53-63.
- T. Lacour, A. Sciendra, A. Talec, P. Mayzaud, O. Bernard, Diel variations of carbohydrates and neutral lipids in nitrogen-sufficient and nitrogen-starved cyclostat cultures of *Isochrysis* sp. J Phycol. 48 (2012) 966-975.
- C. Lancelot, S. Mathot, Biochemical fractionation of primary production by phytoplankton in Belgian coastal waters during short- and long-term incubations with  $^{14}\text{C}$ -bicarbonate. Mar Biol. 86 (1985) 219-226.
- F. Le Borgne, J. Pruvost, Investigation and modeling of biomass decay rate in the dark and its potential influence on netproductivity of solar photobioreactors for microalga *Chlamydomonas reinhardtii* and cyanobacterium *Arthrosphaera platensis*. Bioresour. Technol. 138 (2013) 271-276.
- D. R. S. Lean, R. L. Cuhel, M. N. Charlton, Protein synthesis: a measure of growth for lake plankton. Hydrobiologia 173 (1989) 119-126.
- B. Lepetit, R. Goss, T. Jakob, C. Wilhelm, Molecular dynamics of the diatom thylakoid membrane under different light conditions. Photosynth Res. 111 (2012) 245-257.
- B. F. Lucke, C. C. Hall, R. Zegarac, D. M. Kramer, The environmental photobioreactor (ePBR): an algal culturing platform for simulating dynamic natural environments. Algal Res. 6 (2014) 242-249.
- Y. Maeda, D. Nojima, T. Yoshino, T. Tanaka, Structure and properties of oil bodies in diatoms. Phil Trans R Soc B. 372 (2017) 20160408.
- J. Matos, C. Cardoso, N. M. Bandarra, C. Afonso, Microalgae as healthy ingredients for functional food: a review. Food Funct. 8 (2017) 2672-2685.
- M. H. A. Michels, P. M. Slegers, M. H. Vermue, R. H. Wijffels, Effect of biomass concentration on the productivity of *Tetraselmis suecica* in a pilot-scale tubular photobioreactor using natural sunlight. Algal Res. 4 (2014) 12-18.
- S. Miyagishima, Regulation of cell cycle progression by circadian rhythms in *Cyanidioschyzon merolae*, in: T. Kuroiwa, S. Miyagishima, S. Matsunaga, N. Sato, H. Nozaki, K. Tanaka, O. Misumi (Eds.), *Cyanidioschyzon merolae*: a new model eukaryote for cell and organelle biology, Springer, Singapore, 2017.
- I. Morris, W. Skea, Products of photosynthesis in natural populations of marine phytoplankton from the Gulf of Maine. Mar Biol. 47 (1978) 303-312.

- S. M. Myklestad, Production, chemical structure, metabolism, and biological function of the (1-3)-linked,  $\beta$ 3-D-glucans in diatoms. *Biol Oceanogr.* 6 (1989) 313-326.
- D. M. Nelson, L. E. Brand, Cell division periodicity in 13 species of marine phytoplankton on a light:dark cycle. *J Phycol.* 15 (1979) 67-75.
- M. Nymark, K. C. Valle, T. Brembu, K. Hancke, P. Winge, K. Andersen, G. Johnsen, A. M. Bones, An integrated analysis of molecular acclimation to high light in the marine diatom *Phaeodactylum tricornutum*. *PLoS One.* 4 (11) (2009) e7743.
- J. C. Ogbonna, H. Tanaka, Night biomass loss and changes in biochemical composition of cells during light/dark cyclic culture of *Chlorella pyrenoidosa*. *J Ferment Bioeng.* 82 (6) (1996) 558-564.
- I. Orefice, R. Chandrasekaran, A. Smerilli, F. Corato, T. Caruso, A. Casillo, M. M. Corsaro, F. D. Piaz, A. V. Ruban, C. Brunet, Light-induced changes in the photosynthetic physiology and biochemistry in the diatom *Skeletonema marinoi*. *Algal Res.* 17 (2016) 1-13.
- T. G. Owens, P. G. Falkowski, T. E. Whitledge, Diel periodicity in cellular chlorophyll content in marine diatoms. *Mar Biol.* 59 (1980) 71-77.
- E. Paasche, Marine plankton algae grown with light-dark cycles. II. *Ditylum brightwellii* and *Nitzschia turgidula*. *Physiol Plant.* 21 (1968) 66-77.
- G. Peltier, J. Ravenel, A. Vermeglio, Inhibition of a respiratory activity by short saturating flashes in *Chlamydomonas*: evidence for a chlororespiration. *Biochim Biophys Acta.* 893 (1987) 83-90.
- A. F. Post, Z. Dubinsky, K. Wyman, P. G. Falkowski, Kinetics of light-intensity adaptation in a marine phytoplankton. *Mar Biol.* 83 (1984) 231-238.
- M. Ragni, M. R. d'Alcala, Circadian variability in the photobiology of *Phaeodactylum tricornutum*: pigment content. *J Plankton Res.* 29 (2) (2007) 141-156.
- P. Raimbault, M. Mingazzini, Diurnal variations of intracellular nitrate storage by diatoms: effects of nutritional state. *J Exp Mar Biol Ecol.* 112 (1987) 217-232.
- J. A. Raven, R. J. Geider, Temperature and algal growth. *New Phytol.* 110 (1988) 441-461.
- R. B. Rivkin, Carbon-14 labelling patterns of individual marine phytoplankton from natural populations. *Mar Biol.* 89 (1985) 135-142.
- P. G. Roessler, Environmental control of glycerolipid metabolism in microalgae: commercial implications and future research directions. *J Phycol.* 26 (1990) 393-399.
- R. E. H. Smith, P. Clement, E. J. Head, Night metabolism of recent photosynthate by sea ice algae in the high Arctic. *Mar Biol.* 107 (1990) 255-261.
- A. E. Solovchenko, Physiological role of neutral lipid accumulation in eukaryotic microalgae under stresses. *Russ J Plant Physiol.* 59 (2) (2012) 167-176.
- A. Sukenik, J. Bennett, P. Falkowski, Light-saturated photosynthesis – limitation by electron transport or carbon fixation. *Biochim Biophys Acta.* 891 (1987) 205-215.
- A. Sukenik, Y. Carmeli, Lipid synthesis and fatty acid composition in *Nannochloropsis* sp. (Eustigmatophyceae) grown in a light-dark cycle. *J Phycol.* 26 (1990) 463-469.

Y. Sumi, Microalgae pioneering the future-application and utilization. *Life Sci Res Unit Quart Rev.* 34 (2009) 9-21.

B. Tamburic, S. Guruprasad, D. T. Radford, M. Szabo, R. M. Lilley, A. W. D. Larkum, J. B. Franklin, D. M. Kramer, S. I. Blackburn, J. A. Raven, M. Schliep, P. J. Ralph, The effect of diel temperature and light cycles on the growth of *Nannochloropsis oculata* in a photobioreactor matrix. *PLoS One* 9 (1) (2014) e86047.

G. A. Thompson, Lipids and membrane function in green algae. *Biochim Biophys Acta.* 1302 (1996) 17-45.

G. Torzillo, A. Sacchi, P. Materassi, A. Richmond, Effect of temperature on yield and night biomass loss in *Spirulina platensis* grown outdoors in tubular photobioreactors. *J Appl Phycol.* 3 (1991) 103-109.

J. C. Traller, M. Hildebrand, High throughput imaging to the diatom *Cyclotella cryptica* demonstrates substantial cell-to-cell variability in the rate and extent of triacylglycerol accumulation. *Algal Res.* 2 (2013) 244-252.

J. C. Traller, S. J. Cokus, D. A. Lopez, O. Gaidarenko, S. R. Smith, J. P. McCrow, S. D. Gallaher, S. Podell, M. Thompson, O. Cook, M. Morselli, A. Jaroszewicz, E. E. Allen, A. E. Allen, S. S. Merchant, M. Pellegrini, M. Hildebrand, Genome and methylome of the oleaginous diatom *Cyclotella cryptica* reveal genetic flexibility toward a high lipid phenotype. *Biotechnol Biofuels.* 9 (2016) 258.

K. M. Varum, S. Mylkestad, Effects of light, salinity, and nutrient limitation on the production of  $\beta$ -1,3-D-glucan and exo-D-glucanase activity in *Skeletonema costatum* (Grev.) Cleve. *J Exp Mar Biol Ecol.* 83 (1984) 13-25.

K. M. Varum, K. Ostgaard, K. Grimsrud, Diurnal rhythms in carbohydrate metabolism of the marine diatom *Skeletonema costatum* (Grev.) Cleve. *J Exp Mar Biol Ecol.* 102 (1986) 249-256.

C. E. Williamson, Phased cell division in natural and laboratory populations of marine planktonic diatoms. *J Exp Mar Biol Ecol.* 43 (1980) 271-279.

W. Yang, S. Zou, M. He, C. Fei, W. Luo, S. Zheng, B. Chen, C. Wang, Growth and lipid accumulation in three *Chlorella* strains from different regions in response to diurnal temperature fluctuations. *Bioresour Technol.* 202 (2016) 15-24.

C. S. Yentsch, R. F. Scagel, Diurnal study of phytoplankton pigments: an *in situ* study in East Sound, Washington. *J Mar Res.* 17 (1958) 567-581.

J. K. Zehmer, Y. Huang, G. Peng, J. Pu, R. G. W. Anderson, P. Liu, A role for lipid droplets in inter-membrane lipid traffic. *Proteomics.* 9 (2009) 914-921.

## CHAPTER 2

**Novel *Thalassiosira pseudonana* violaxanthin de-epoxidase-like enzyme (VDL2) catalyzes fucoxanthin biosynthesis**

## 2.1 ABSTRACT

Despite the ubiquity and ecological importance of diatoms, much remains to be understood about their physiology and metabolism, including their carotenoid biosynthesis pathway. Early carotenoid biosynthesis steps are well-conserved. The sequence of, and enzymes that catalyze, the later steps that lead to the major accessory photopigment fucoxanthin (Fx) and main photoprotective pigment pool comprised of diadinoxanthin (Ddx) and its reversibly de-epoxidized form diatoxanthin (Dtx), remain unclear. We used sequence comparison to known carotenoid biosynthesis enzymes to identify novel candidates in the diatom *Thalassiosira pseudonana*. RNA-seq data was used to create full-length gene models, and we focused on those that encode proteins predicted to be chloroplast-localized. Based on differential transcriptional regulation of the first two biosynthetic steps, we propose that there are two ways to independently initiate carotenoid biosynthesis. Chloroplast division, which requires the population of newly divided chloroplasts with photopigments, is one proposed carotenogenic stimulus. Irradiance increase, which triggers accumulation of the Ddx+Dtx, is the other. Based on transcriptomic and physiological data, we also propose that the two predicted *T. pseudonana* zeaxanthin epoxidases have distinct roles. We identified a novel violaxanthin de-epoxidase-like enzyme (Thaps3\_11707, VDL2) that when overexpressed increases Fx abundance while stoichiometrically reducing Ddx+Dtx. Based on transcriptomics, we propose that Thaps3\_10233 may also contribute to Fx biosynthesis. Unlike other carotenoid biosynthesis genes, VDL2 and Thaps3\_10233 appear transcriptionally co-regulated with photoantenna proteins, suggesting a mechanism of diverting some precursors towards Fx rather than Ddx+Dtx when necessary to populate photoantenna proteins. Separately using antisense to target VDL2, VDL1, and both LUT1-like copies simultaneously, reduced the overall cellular photopigment content, including chlorophylls, suggesting a destabilization of light-harvesting complexes by Fx deficiency.

## 2.2 INTRODUCTION

Diatoms are incredibly diverse, environmentally flexible, and productive photosynthetic microalgae that belong to the Stramenopile or heterokont class. There are over 100,000 estimated diatom species that occupy a wide variety of habitats. Diatoms are of great ecological importance, as they are responsible for approximately 40% of primary marine productivity and play a major role in the global cycling of carbon, nitrogen, phosphorus, and silicon [Hildebrand et al. 2012, Wilhelm et al. 2006]. They have a complex evolutionary history that includes a secondary endosymbiotic event, wherein an ancient red alga was engulfed by a heterotrophic eukaryote, at least 800Ma ago. Because of this event, diatoms possess physiological and metabolic features that differ from other algal groups, such as the more extensively studied chlorophytes [Hildebrand et al. 2012, Wilhelm et al. 2006].

Photosynthetic pigments are among the distinguishing features of diatoms. Carotenoids are utilized by all known photosynthetic organisms, and the initial part of the carotenoid biosynthesis pathway from phytoene to  $\beta$ -carotene ( $\beta$ -car) is well-conserved [Bertrand 2010, Coesel et al. 2008].  $\beta$ -car is synthesized from lycopene, as is  $\alpha$ -carotene ( $\alpha$ -car) in many organisms. Both  $\beta$ - and  $\alpha$ -car have a variety of derivatives that can differ substantially depending on the taxonomic class, sometimes with further inter-species differences. Diatoms do not possess the  $\alpha$ -car branch of carotenoids, and their main photoprotective and accessory light-harvesting pigments are  $\beta$ -car derivatives. Knowledge about the sequence of the post- $\beta$ -car biosynthetic steps in diatoms, as well as the enzymes that catalyze them, is still very sparse [Bertrand 2010, Coesel et al. 2008]. One of the final products of the pathway (**Fig. 2.1**) is fucoxanthin (Fx), the main accessory light-harvesting pigment in diatoms that is responsible for their characteristic golden-brown color. It is bound to photoantenna proteins along with chlorophylls a and c (Chl a, Chl c). Most diatoms have Chl c1 and Chl c2, although Chl c3 has been found in some species as well. Unlike chlorophytes, diatoms do not

make chlorophyll b [Wilhelm et al. 2006]. Diadinoxanthin (Ddx) and diatoxanthin (Dtx) are the other final products of diatom carotenoid biosynthesis. They form a xanthophyll cycle by reversibly interconverting via epoxidation and de-epoxidation (**Fig. 2.1**), comprising the major photoprotective mechanism employed by diatoms [Goss et al. 2006, Lohr and Wilhelm 1999, Wilhelm et al. 2006]. Some Ddx molecules are bound by photoantenna proteins, while others are dissolved in the lipid shield that surrounds photoantennae [Lepetit et al. 2010]. The other xanthophyll cycle found in diatoms is the violaxanthin (Vx) cycle, in which zeaxanthin (Zx) is reversibly converted to (Vx) via antheraxanthin (Ax) by two epoxidation steps. Both cycles serve to allow the switch between light-harvesting and light-dissipative states as a rapid adjustment to irradiance changes, with the epoxide forms corresponding to the former and de-epoxides to the latter. The Vx cycle is conserved and plays a major photoprotective role in chlorophytes. While functional in diatoms, its pigments are present in small amounts compared to other photopigments, and mainly serve as precursors to the Ddx cycle pigments and Fx [Coesel et al. 2008, Lohr and Wilhelm 1999].

There are two major hypotheses regarding the biosynthesis of Ddx, Dtx, and Fx from Vx (**Fig. 2.1**). Ddx and Fx may have a common precursor, or Fx may be synthesized from Ddx. Pigment flux-based evidence supports the latter hypothesis [Goericke and Welschmeyer 1992, Lohr and Wilhelm 1999], but it is yet to be directly tested by genetic manipulation, and enzymes involved in the biosynthetic steps have not been identified. Furthermore, Phaeophyceae and chrysophytes contain Fx but not Ddx cycle pigments, and therefore Ddx is not an obligate precursor of Fx [Lohr and Wilhelm 1999]. Neoxanthin has been hypothesized as an intermediate between Vx and Ddx/Fx based on its structure. Although typically not observed in diatom pigment extracts, it was detected in an enriched fraction from the diatom *Phaeodactylum tricornutum* by Dambeck et al. [2012].

The sequencing of diatom genomes and development of genetic manipulation tools have facilitated the study of diatom carotenoid biosynthesis. Putative carotenoid biosynthesis gene

candidates have been identified in the first two available diatom genomes, *Thalassiosira pseudonana* [Armbrust et al. 2004] and *P. tricornutum* [Bowler et al. 2008], by Coesel et al. [2008] and Dambeck et al. [2012], based on sequence identity of their protein products to those of known carotenoid biosynthesis genes. Functional complementation confirming enzyme functions for the pre- $\beta$ -car part of the pathway was performed by Dambeck et al. [2012]. Lavaud et al. [2012] knocked down the *P. tricornutum* gene that encodes Vx de-epoxidase (VDE), which performs de-epoxidation in both xanthophyll cycles, resulting in a Dtx de-epoxidation deficiency (Vx de-epoxidation was not examined). Phytoene synthase (PSY), which catalyzes the first committed step of carotenoid biosynthesis, has been knocked down [Kaur and Spillane 2014] and overexpressed [Kadono et al. 2015] in *P. tricornutum*, resulting in reduced and increased cellular carotenoid content, respectively. Nevertheless, much remains to be understood about the carotenoid biosynthesis pathway in diatoms. In this study, we confirm and expand the list of putative carotenoid biosynthesis gene candidates using sequence identity-based reciprocal probing of the *T. pseudonana* and *P. tricornutum* genomes. We then focus on *T. pseudonana* and use available transcriptomic and physiological data to narrow down the carotenoid biosynthesis gene candidate list and form hypotheses about the functions of their protein products. Furthermore, we directly test the function of several enzymes hypothesized to be involved in diatom carotenoid biosynthesis through genetic manipulation.

## 2.3 RESULTS

### 2.3.1 Sequence Identity-Based Candidate Carotenoid Biosynthesis Gene Identification

The genomes of *T. pseudonana* and *P. tricornutum* were searched for genes that encode proteins with sequence similarity to those known to participate in carotenoid biosynthesis in both

organisms, in order to confirm what has been previously reported [Coesel et al. 2008, Dambeck et al. 2012] and identify new candidates. Some Basic Local Alignment Search Tool (BLAST) results indicated previously unreported gene models that overlap with previously published ones. The latter likely represent outdated models that have since been replaced. Large chromosomal pieces, sometimes encompassing genes identified as part of the carotenoid biosynthesis pathway or those found using the latter as BLAST queries, also frequently showed up in BLAST results. They may contain multiple partial sequence matches, possibly including those of domains that are present in, but not necessarily limited to, enzymes of the carotenoid biosynthesis pathway. Some open reading frames without available gene models were also found. The findings are detailed in **Appendix 2.A**, and the most current model IDs of known carotenoid biosynthesis genes and corresponding BLAST hits for which gene models are available are summarized in **Table 2.1**. The unnamed enzymes are not listed in a specific order and no relationship between those listed on the same line is implied. The diatom carotenoid biosynthesis pathway is depicted in **Fig. 2.1**.

### 2.3.2 Sequence Identity-Based Phylogenetic Analyses

Carotene cis/trans isomerase (CRTISO), LUT1-like (LTL), and zeaxanthin epoxidase (ZEP) candidate searches yielded numerous new candidates. Because many of the only publicly available Department of Energy Joint Genome Institute (DOE JGI) gene models for the LTL group are clearly incomplete, sequence identity analysis was not performed at this stage. However, it should be mentioned that the only BLAST hits for Phatr2\_34027 in the *T. pseudonana* genome were Thaps3 9541 (LTL1) and Thaps3 2703365 (LTL2). Most enzymes in this group were functionally annotated as cytochrome p450, with some exceptions. Phatr2\_47234, Phatr2\_37006, Thaps3\_4027, and Thaps3\_4026 had no functional annotation available on the DOE JGI website. Phatr2\_43563 was

functionally annotated as an iron-binding oxidoreductase, Phatr2\_50619 chitinase, Phatr2\_43537 chitinase with a diacylglycerol binding domain, Phatr2\_43469 diacylglycerol acyltransferase, Phatr2\_32833 N-acetyltransferase, and Thaps3\_14875 glycosyltransferase (UDP-N-acetylglucosamine dolichyl-phosphate N-acetylglucosamine-phosphotransferase).

Sequence identity analysis for the CRTISO group (**Fig. 2.2A, Appendix 2.B1**) revealed that Thaps3\_5221, Thaps3\_21847, Thaps3\_10233, Thaps3\_21900, and Thaps3\_7094 are more similar to the *P. tricornutum* enzymes identified by Dambeck et al. [2012] as CRTISO candidates, while Thaps3\_25361, Thaps3\_11636, Thaps3\_5859, and Thaps3\_10254 grouped closer to each other and were more dissimilar from the former group. However, both groups had members that either had Gene Ontology (GO) terms including: carotenoid biosynthetic process, oxidoreductase activity, and flavin adenine dinucleotide (FAD) binding, or did not have GO terms available. All of the proteins had the EuKaryotic Orthologous Groups Identity (KOG ID) “phytoene desaturase.”

ZEP candidate sequence identity analysis (**Fig. 2.2B, Appendix 2.B2**) showed that previously identified ZEPs [Coesel et al. 2008] form a group without additional members. Within the group, the ZEP1s and ZEP2s clustered with their counterparts, and ZEP3 was separate. No terms, predictions, or annotations were available for Phatr2\_48545 (ZEP1). All of the other proteins that had a KOG ID were designated as kynurenine 3-monooxygenase and related flavoprotein monooxygenases, and the two that did not were indicated to have a FAD-binding domain (Phatr2\_56492, ZEP3) or to be a FAD-dependent oxidoreductase (Phatr2\_56488, ZEP2) by Pfam. All of the proteins besides Phatr2\_48545 (ZEP1) had GO terms that included monooxygenase activity and cellular aromatic compound metabolic process. Most also included oxidoreductase activity, with the exception of Thaps3\_22671 and Phatr2\_43425. GO terms for Phatr2\_45936 also included small nuclear ribonucleoprotein complex, and for Thaps3\_261390 (ZEP2), xanthophyll biosynthetic process.

Sequence identity analysis was also performed on the VDE/VDL/VDR group (**Fig. 2.2C**, **Appendix 2.B3**). Four clusters resulted, with the known VDEs, VDL1s, and VDRs clustering with their counterparts, and the *P. tricornutum* VDL2 in a cluster with the two newly identified proteins, Phatr2\_bd\_1281 and Thaps3\_11707. Based on the sequence similarity, the latter is hereafter designated as the *T. pseudonana* VDL2.

### 2.3.3 Candidate Gene Expression Patterns

For all genes encoding the proteins identified in 2.3.1 (**Table 2.1**), expression patterns were obtained from the microarray dataset described in Smith et al. [2016]. Briefly, Smith et al. performed a 24-hour silicon starvation time course experiment, with cells placed in silica-free media at 0 h, sampling for a variety of physiological variables as well as the transcriptome throughout. At 4 h, the majority of cells underwent chloroplast division. There was also evidence of sustained light-induced stress throughout the duration of the experiment. Genes with similar functions appeared to be highly co-regulated, as evidenced by their sorting into clusters with similar expression patterns.

Most genes known to participate in *T. pseudonana* carotenoid biosynthesis followed a distinct expression pattern that spiked at 4 h, during chloroplast division, then decreased (**Fig. 2.3A**). Some increased expression by 4 h and remained elevated throughout, and ZEP2 was unique in having lower transcript levels throughout the experiment compared to 0 h (**Fig. 2.3B**). One half (15 out of 30) of the candidate genes identified in 2.3.1 (**Table 2.1**) based on sequence identity had expression patterns similar to those known to be in the carotenoid biosynthesis pathway (**Fig. 2.3C, D**), the other half did not (**Fig. 2.3E, F**).

Thaps3\_17707, the novel VDL2 (2.3.2), and Thaps3\_10233, found in the sequence identity-based search for CRTISO candidates (**Table 2.1**), were upregulated to a substantially higher extent than the rest of the carotenoid biosynthesis genes (**Fig. 2.3A-D**) and were previously found by Smith et al. [2016] to be in a co-regulated gene cluster with photoantenna protein-encoding genes. We examined the expression patterns of those photoantenna protein genes as well as carotenoid biosynthesis genes using an additional set of transcriptomic data [Abbriano 2017]. This RNA-seq data was obtained during a 9-hour time course experiment after re-addition of silica to silicon-starved *T. pseudonana* cultures, which typically results in a synchronous progression through the cell cycle and thus synchronous chloroplast division. VDL2 and Thaps3\_10233 had a distinct co-expression pattern in the RNA-seq silicon re-addition as well and were upregulated later and to a higher extent than the rest of the carotenoid biosynthesis genes (**Fig. 2.4A**). All but one photoantenna protein-encoding gene that clustered with VDL2 and Thaps3\_10233 in the microarray dataset [Smith et al. 2016] also clustered with them in RNA-seq dataset [Abbriano 2017] (**Fig. 2.4B**).

#### 2.3.4 Full-length Gene Models and Predicted Protein Targeting

Because gene models on the DOE JGI website are sometimes incomplete/incorrect, full-length gene models (**Appendix 2.C**) were constructed by using available RNA-seq data [Abbriano 2017, Smith et al. 2016] for all the genes known to be part of the carotenoid biosynthesis pathway, those that had similar microarray gene expression patterns [Smith et al. 2016], and Thaps3\_263437 (“ $\beta$ -carotene hydroxylase, (BCH)”), which did not (**Fig. 2.3**). Full-length gene models were translated (**Appendix 2.C**), and the likelihood of chloroplast targeting for the resultant peptides was assessed (**Appendix 2.C**), summarized in **Table 2.2**.

### 2.3.5 Additional Sequence-Based Analyses

#### 2.3.5.1 Phytoene Desaturase (PDS) and Thaps3\_bd\_1474

Thaps3\_bd\_1474, found in the PDS candidate search (**Table 2.1, Appendix 2.A**), is part of the unmapped sequence assembly of the *T. pseudonana* genome and is truncated on the 5' end due to the way those sequences were assembled. The unmapped sequence assembly is also referred to as the “bottom drawer,” and “\_bd\_” is added to the identification numbers of genes that are part of it. RNA-seq data is not available for the “bottom drawer” sequences and could not be used to construct a full-length gene model. The JGI predictions were used instead (**Appendix 2.D**). The JGI-predicted peptides for PDS1 and Thaps3\_bd\_1474 are identical where they align. The latter is approximately 200 amino acids shorter on the N-terminal side and approximately 120 amino acids longer on the C-terminal side. The PDS1 gene contains no introns, and one intron is predicted by JGI for Thaps3\_bd\_1474. If the predicted intron is disregarded and the sequence is translated as one open reading frame (**Appendix 2.D**), the resulting peptide is identical to PDS1, except for the N-terminal truncation (**Appendix 2.D**). When genomic DNA sequences that include the JGI models for PDS1 and Thaps3\_1474 and 10 kb downstream are examined, they appear identical where the gene models align and for approximately 1.8 kb downstream, with occasional single base pair differences that may be attributed to naturally occurring polymorphisms, and then abruptly become substantially different thereafter (**Appendix 2.D**). The identical region downstream PDS1 and Thaps3\_bd\_1474 includes two more genes, one predicted to encode a ribosomal protein L33 (Thaps3\_41211 and Thaps3\_bd\_1472), and the other predicted to encode a DNA methylase (Thaps3\_6523 and Thaps3\_bd\_1109). By contrast, PDS1 and PDS2 have 62.9% sequence identity (**Appendix 2.D**).

### 2.3.5.2 Thaps3\_263437 (“ $\beta$ -carotene Hydroxylase, BCH”)

Out of the two major known BCH types [Martin et al. 2008], Thaps3\_263437 was found to be more similar to the non-heme di-iron enzymes than to the cytochrome P450 monooxygenases (**Appendix 2.D**). Approximately one half of the *T. pseudonana* protein, on the N-terminal side, aligns with known BCH sequences from other organisms. The Thaps3\_263437 protein sequence was compared to 10 non-heme di-iron enzymes from diverse organisms, including two plants, one green alga, three cyanobacteria, three non-photosynthetic eubacteria, and one archaeal species, which represent four major groups of the non-heme di-iron BCHs [Tian and DellaPenna 2004]. The least similarity was found with cyanobacteria, ranging from 17-22% sequence identity. The sequence identity range for the other examined organisms is between 26-29% (**Appendix 2.D**). No known motifs or conserved domains based on sequence or predicted structure were found in the C-terminal half of Thaps3\_263437. Portions of it did exhibit limited sequence identity to unknown proteins from diverse organisms (**Table 2.3**). Neither the N-terminal (“BCH”) half nor the unknown C-terminal half of Thaps3\_263437 were found in the other currently available diatom genomes (*Phaeodactylum tricornutum*, *Cyclotella cryptica*, *Thalassiosira oceanica*, *Fragilaropsis cylindrus*, *Pseudo-nitzschia multiseries*).

### 2.3.5.3 Functional Annotation Predictions for the *T. pseudonana* Carotenoid Biosynthesis Enzymes

Sequence-based functional annotation predictions were compiled for the enzymes of the *T. pseudonana* carotenoid biosynthesis pathway (**Table 2.4**). Additionally, predicted protein structures for VDL2, Thaps3\_10233, and the C-terminal half of Thaps3\_263437 were analyzed for functional predictions. The analysis yielded no additional information.

### 2.3.6 Identification of Carotenoid Biosynthesis Genes in Additional Diatom Species

Orthologs of the carotenoid biosynthesis genes identified in *T. pseudonana* and *P. tricornutum* (2.3.1-2.3.4) were found in the four other currently available diatom genomes (**Table 2.5**). Where gene models were not available, genomic coordinates were given. Three of the *T. oceanica* genes appeared to be split into two adjacent gene models. Those were listed together, separated by a plus sign (+). The number of copies of each gene varied between species, with the most for several genes found in *C. cryptica* (**Table 2.5**).

### 2.3.7 Genetic Manipulation and Resultant Pigment Phenotypes

The following transgenic *T. pseudonana* lines were created to investigate the roles of several enzymes hypothesized to participate in carotenoid biosynthesis: overexpression (OE) of the novel VDL2, knockdown (KD) of VDL1, KD of VDL2, and a simultaneous KD of LUT1-like (LTL) 1 and LTL2, which share 48% sequence identity (**Appendix 2.D**). Four independent clones per line were then allowed to adapt to cultivation conditions, and their photosynthetic pigment content was assessed using high-performance liquid chromatography (HPLC).

For VDL2 OE, total cellular photosynthetic pigment content (Tot) varied between the four clones and two WT cultures at both low ( $30 \mu\text{mol photons m}^{-2} \text{ sec}^{-1}$ ) and high light ( $300 \mu\text{mol photons m}^{-2} \text{ sec}^{-1}$ ) without an observable trend (**Fig. 2.5A**). Nevertheless, certain pigment ratios exhibited a consistent difference between WT and VDL2 OE. Fx/Tot was increased (low light p-value = 0.02, high light p-value = 0.0008) and (Ddx+Dtx)/Tot was reduced (low light p-value = 0.0006, high light p-value = 0.0008) in VDL2 OE, but (Ddx+Dtx+Fx)/Tot was not significantly different from WT (low light p-value = 0.9, high light p-value = 0.8) (**Fig. 2.5B**). No differences were observed in  $\beta$ -car/Tot, Chl a/Tot, and Chl c/Tot (**Fig. 2.5C, D**).

For LTL KD lines, initial PCR-based screening for the presence of the full knockdown construct (promoter to terminator) revealed a selection against it, as most of the screened clones had integrated the portion allowing them to grow on selection but lost all or parts of the promoter and/or the antisense portion. Approximately 3 weeks after plating, significant pigmentation reduction became apparent in some of the clones (**Fig. 2.6A**). Four LTL KD clones were selected based on lighter pigmentation, and genomic integration of the entire KD construct was subsequently confirmed by PCR. There was a reduction in Tot in LTL KDs compared to WT, with more pronounced differences in high light than in low light (**Fig. 2.6B**). In low light, LTL KD lines had 75-93% Tot of average WT (p-value = 0.2), and 60-76% of average WT Tot in high light (p-value = 0.009). No statistically significant differences in the ratios of individual photosynthetic pigments to Tot were found (**Fig. 2.6B-D**).

Four clones each of VDL1 KD and VDL2 KD were selected based on the ability to grow on selection and PCR-assessed genomic integration of full-length knockdown constructs. Photosynthetic pigment content was assessed in high light only and Tot was found to be reduced in both lines, with the exception of the clone VLD2 KD3 (**Figs. 2.7A, 2.8A**). VDL1 KD lines contained 48-91% of the average WT Tot (p-value = 0.01), and VDL2 KD lines were at 59-87% of average WT Tot (p-value = 0.004), excluding KD3. KD3 did not significantly differ from WT in Tot. No substantial differences in the ratios of individual pigments to Tot were observed between WT and the VDL1 or VDL2 KD lines (**Figs. 2.7, 2.8**).

## 2.4 DISCUSSION

### 2.4.1 Carotenoid Biosynthesis Candidate Gene/Enzyme Identification

Building on earlier analyses [Coesel et al. 2008, Dambeck et al. 2012], we sought to identify novel gene candidates based on sequence identity of their protein products to those of previously identified carotenoid biosynthesis genes. The genomes of *T. pseudonana* [Armbrust et al. 2004] and *P. tricornutum* [Bowler et al. 2008] were chosen for reciprocal BLAST searches as the first two sequenced, and best annotated, available diatom genomes. A notable finding was that of an additional, previously unreported VDL protein in *T. pseudonana* (Thaps3\_11707), designated VDL2 in this study. It should be noted that the *T. pseudonana* VDR (Thaps3\_270211) is mis-annotated as VDL2 on the DOE JGI website.

The list of candidates for the *T. pseudonana* carotenoid biosynthesis pathway obtained by BLAST was narrowed down to those whose gene expression patterns were similar to those of genes known to participate in carotenoid biosynthesis, using available transcriptomic (microarray) data [Smith et al. 2016] (**Fig. 2.3**). The data was obtained from a 24-hour silicon starvation time course during which there was a major chloroplast division event at 4 h, and light-induced stress was sustained throughout. The latter is at least partially attributable to the culture being resuspended in silica-free media at half the density that it had grown to in regular media prior to being harvested, resulting in reduced shading [Smith et al. 2016]. Both chloroplast division and exposure to higher light are expected to result in carotenoid biosynthesis [Chapter 1, Lepetit et al. 2010], and Smith et al. [2016] did measure an overall steady increase in photopigment content throughout the time course, as well as a preferential accumulation of the photoprotective de-epoxide form (Dtx) of the interconvertible Ddx/Dtx cycle pigments. Thus, carotenoid biosynthesis activities associated with both chloroplast division and light-induced stress occurred during the experiment. Smith et al.

[2016] report substantial co-regulation of genes with related functions, as evidenced by numerous gene clusters with highly similar expression patterns. Nevertheless, it is possible that some gene candidates whose expression patterns differed from those of known carotenoid biosynthesis genes and were therefore not chosen for further study (**Fig. 2.3**), may be relevant to carotenoid biosynthesis as well, but regulated differently. Smith et al. [2016] also collected RNA-seq data alongside the microarray data, with a notable difference of the culture used for the former being resuspended in silica-free media at the same density that it had achieved in regular media prior to harvesting. Thus, unlike the culture used for the microarray data, the culture used for RNA-seq would not have been exposed to more light due to reduced shading at the beginning of the silicon starvation experiment. Even though expression patterns for many genes replicated well between the microarray and RNA-seq silicon starvation datasets, those of genes known to be involved in the light-stress response [Smith et al. 2016], as well as those of genes known to participate in carotenoid biosynthesis (**Figs. 2.3, S2.1**) did not, suggesting that the responses observed in the microarray dataset could not be attributed solely to silicon starvation but were affected by increased light exposure of the microarray culture as well. In summary, even though silicon starvation is not expected to directly affect carotenoid biosynthesis, the microarray data obtained by Smith et al. was relevant to our study. Synchronized chloroplast division and light-induced stress occurred during their experiment, requiring distinct carotenoid biosynthesis pathway responses. The silicon starvation RNA-seq dataset [Smith et al. 2016] serves as a negative control, as it was obtained from a culture treated the same way as the one used for the microarray data, except being exposed to the conditions that induced the light-induced stress response. The fact that most genes had similar expression patterns in both datasets, but light-stress response [Smith et al. 2016] and carotenoid biosynthesis genes did not (**Figs. 2.3, S2.1**), highlights the relevance of the microarray dataset to our study. No physiological data was collected from the silicon starvation

RNA-seq culture, and thus the status of light stress and pigment abundance cannot be directly referenced for that dataset [Smith et al. 2016].

Candidates were further narrowed down to those predicted to be targeted to the chloroplast by using RNA-seq-derived [Abbriano 2017, Smith et al. 2016] full-length gene models (**Appendix 2.C, Table 2.2**). Due to diatoms having evolved via secondary endosymbiosis, their chloroplasts are surrounded by the endoplasmic reticulum (ER) [Smith et al. 2012]. Thus, diatom proteins targeted to the chloroplast must also be targeted to the ER. PSY2 and LTL2 had clear ER targeting, but their predictive scores for chloroplast targeting were just below the cutoff value (**Appendix 2.C, Table 2.2**). It is likely that they are indeed targeted to the chloroplast, as chloroplast targeting predictions are not always completely accurate [Emanuelsson et al. 1999].

The majority of candidates identified by BLAST, including the numerous LTL, CRTISO, and ZEP candidates, did not meet the criteria of both having microarray gene expression patterns similar to genes known to participate in carotenoid biosynthesis and predicted chloroplast targeting. Barring potentially having excluded novel carotenoid biosynthesis genes that had different gene expression patterns, this indicates that most of the candidates were found due to containing domains that are utilized by, but not limited to, carotenoid biosynthesis enzymes. Indeed, each of the CRTISO, LTL, and ZEP candidate groups had shared functional annotation predictions.

#### 2.4.2 Stepwise Analysis of the *T. pseudonana* Carotenoid Biosynthesis Pathway

The condensation of two geranylgeranyl pyrophosphate molecules to synthesize phytoene by PSY is the first committed step of carotenoid biosynthesis and is considered rate-limiting [Bertrand 2010, Eilers et al. 2016]. It is followed by several desaturation steps catalyzed by PDS [Melendez-Martinez et al. 2015]. There are two previously reported copies of each in *T. pseudonana* [Coesel et al. 2008], and a possible additional *T. pseudonana* PDS identified in this study. Barring mis-assembly, the novel PDS candidate Thaps3\_bd\_1474 appears to have arisen as a result of a duplication event of the PDS1 locus, encompassing it, as well as two downstream genes (2.3.5.1). Because of the way “bottom drawer” sequences were processed, the N-terminus, as well as the genomic sequence upstream of Thaps3\_bd\_1474 are not available, and the size of the duplicated region is not known.

Both PSY and PDS genes exhibited two distinct gene expression patterns in the microarray data [Smith et al. 2016]. PSY1, PDS1, and Thaps3\_bd\_1474 had a spike in expression at 4 h, during the major chloroplast division event (**Fig. 2.3A, C**). By contrast, PSY2 and PDS2 had their transcript levels increase by 4 h and stay elevated throughout the time course (**Fig. 2.3B**). In vascular plants that possess more than one copy of PSY, the different genes are differentially regulated in response to developmental and environmental signals. Differential regulation based on different cellular needs may be hypothesized for microalgae that possess more than one PSY gene, but this has yet to be experimentally investigated [Melendez-Martinez et al. 2015, Tran et al. 2009]. We hypothesize that in *T. pseudonana*, PSY1 may serve to initiate carotenoid biosynthesis during chloroplast division and PSY2 may serve as an independent way to initiate carotenoid biosynthesis in response to increased irradiance, which leads to an increase in Ddx cycle pigments [Lavaud et al. 2004]. Because PDS is responsible for the next immediate steps in carotenoid biosynthesis and has also been previously suggested to be rate-limiting [Chamovitz et al. 1993], different PDS copies might be

differentially co-regulated with different copies of PSY. As detailed in Chapter 1, the cellular accumulation of all diatom photosynthetic pigments is influenced by cell cycle progression and therefore chloroplast division, with the exception of the Ddx cycle pigments, which appear to primarily respond to light intensity. The differential accumulation of Ddx+Dtx and Fx, the other end product of carotenoid biosynthesis, as well as  $\beta$ -car, a precursor for all three aforementioned pigments, suggests a differential regulation mechanism, such as independent biosynthesis induction by different copies of PSY/PDS, as proposed above. PSY1, PDS1, and Thaps3\_bd\_1474 are upregulated during chloroplast division along with the majority of carotenoid biosynthesis genes (**Fig. 2.3**) as well as chlorophyll biosynthesis genes and photoantenna protein-encoding genes [Smith et al. 2016], and thus likely respond to the cell's need to populate dividing chloroplasts with enzymes and pigments. PSY2 and PDS2 display a gene expression pattern similar to that of PsbA (**Fig. 2.3B**), a gene that encodes the photosystem II D1 protein, which is known to turn over in response to light-induced stress [Domingues et al. 2012, Wu et al. 2011]. Thus, PSY2 and PDS2 transcript levels may have been elevated throughout the time course to activate carotenoid biosynthesis in order to support the accumulation of Ddx+Dtx in response to the light-induced stress that was observed throughout the experiment, independent of the major chloroplast division event at 4 h. The transcript responses for PSY1/PDS1 and PSY2/PDS2 showed similarity in the RNA-seq data set by Smith et al. [2016] as well (**Fig. S2.1A**).

Following PDS, more desaturation is carried out by  $\alpha$ -carotene desaturase (ZDS), resulting in pro-lycopene, a lycopene stereoisomer. There is only one known copy of ZDS in *T. pseudonana*, and we present no new hypotheses or observations for this step. Pro-lycopene is isomerized to lycopene by CRTISO, and the identity of the enzyme(s) responsible for this step is not yet confirmed. Many potential CRTISO copies have been previously found in diatom genomes, including *T. pseudonana* [Bertrand 2010]. Our analysis has narrowed the list down to two candidates,

Thaps3\_21900 and Thaps3\_10233 (**Fig. 2.2A, Table 2.2**). It is possible, however, that other candidates identified by BLAST (**Table 2.1, Appendix 2.A**) might participate in this step but were excluded based on having a gene expression pattern that differed from genes known to participate in carotenoid biosynthesis (**Fig. 2.3**), or due to a false negative prediction for chloroplast targeting (**Table 2.2**).

Lycopene is converted into  $\beta$ -car by lycopene cyclase B (LCYB), for which no new candidates or hypotheses were generated by this study. The subsequent conversion of  $\beta$ -car via hydroxylation to Zx is intriguing. That reaction is typically catalyzed by one of the two known types of BCH [Martin et al. 2008], neither of which are found in any of the currently available diatom genomes, except a partial 238aa sequence in *T. pseudonana* (2.3.5.2). The latter, however, is not predicted to be targeted to the chloroplast, and has a 342aa C-terminal addition which has sequence identity to unidentified peptides from several diverse organisms (**Table 2.3**). Its gene expression pattern in the microarray dataset [Smith et al. 2016] is markedly different from any known carotenoid biosynthesis genes (**Fig. 2.3E**). Like the BCH sequence, the C-terminal peptide is not found in any other currently available diatom genomes (*C. cryptica*, *T. oceanica*, *F. cylindrus*, *P. multiseries*, *P. tricornutum*), which makes the *T. pseudonana* BCH an evolutionary curiosity. It is unlikely to participate in carotenoid biosynthesis and has possibly evolved to perform a different function by losing chloroplast targeting and gaining the C-terminal sequence.

Diatom genomes contain genes encoding LUT1-like (LTL) enzymes, which are similar to an *Arabidopsis thaliana* enzyme (LUT1) that converts  $\alpha$ -car to lutein (respective isomers of  $\beta$ -car and Zx) and has been demonstrated to have weak  $\beta$ -car hydroxylation activity. Since diatoms do not make  $\alpha$ -car, it has been hypothesized that diatom LTLs function in place of BCH, but this has not been previously experimentally assessed [Bertrand 2010]. To do so, we simultaneously knocked down both *T. pseudonana* LTL copies, which resulted in a reduction of all photosynthetic pigments

**(Fig. 2.6).** Although this does not conclusively place the LTLs in a specific carotenoid biosynthesis step, it does implicate them as being involved. Both LTLs are cytochrome P450 monooxygenases (**Table 2.4**), and the hydroxylation of  $\beta$ -car to produce Zx is the first step in the carotenoid biosynthesis pathway in which oxygen atoms are added (**Fig. 2.1**). Thus, it is unlikely that the LTLs catalyze anything upstream of  $\beta$ -car hydroxylation.

Zx, whether synthesized from  $\beta$ -car by the LTLs or another enzyme that is yet to be discovered, is part of the Vx xanthophyll cycle. The de-epoxidation reactions of both the Vx and the Ddx xanthophyll cycles are catalyzed by ZEPs [Bertrand 2010, Goss et al. 2006, Wilhelm et al. 2006]. Chlorophytes lack the Ddx cycle and typically possess one ZEP copy, while multiple ZEPs are found in all diatom genomes available to date (**Table 2.5**). It has been demonstrated that Ddx de-epoxidation is strongly inhibited by the transthylakoid proton gradient ( $\Delta\text{pH}$ ) that forms in high light. The ZEPs that operate in the chlorophyte Vx cycle, by contrast, are not inhibited by high light [Goss et al. 2006, Wilhelm et al. 2006]. Experimental evidence suggests that Zx epoxidation proceeds under high light in diatoms as well, since they perform *de novo* biosynthesis of the Ddx cycle pigments upon an increase in illumination [Lavaud et al. 2004, Lepetit et al. 2010], for which Vx is a precursor [Lohr and Wilhelm 1999]. Thus, different copies of diatom ZEPs may distinctly participate in the two xanthophyll cycles. We found that the two *T. pseudonana* ZEP copies had distinct gene expression patterns in the microarray data [Smith et al. 2006] (**Fig. 2.3A, B**). Throughout the experiment, the abundance of light-harvesting and photoprotective pigments increased, and the Ddx pool pigments continuously preferentially accumulated as Dtx, the de-epoxide [Smith et al. 2006]. Thus, we hypothesize that ZEP2, downregulated throughout the experiment, participates in the Ddx cycle, whereas ZEP1, upregulated especially during the major chloroplast division event at 4 h, participates in the Vx cycle.

De-epoxidation of the Vx cycle pigments in chlorophytes is catalyzed by VDE. Only one VDE copy is found in the available diatom genomes (**Table 2.5**), and it has been demonstrated that it participates in both diatom xanthophyll cycles [Jakob et al. 2000, Lavaud et al. 2012]. In addition to the VDE, diatom genomes encode VDE-like (VDL) and VDE-related (VDR) proteins (**Fig. 2.2C**), the function of which has not been previously determined. It has been stipulated that they may have xanthophyll cycle activity in addition to the VDE, and perhaps differ in localization from the latter [Bertrand 2010, Lavaud et al. 2012]. Because VDR appears to be present in all chlorophytes [Coesel et al. 2008], it is unlikely to catalyze any reactions that are unique to diatoms. In the present study, we identified a previously unreported VDL2 in *T. pseudonana* (Thaps3\_11707) based on sequence identity to the VDL2 in *P. tricornutum*. Overexpressing it resulted in increased cellular Fx abundance, together with a stoichiometric decrease in the cellular abundance of Ddx+Dtx. The ratio of Ddx+Dtx+Fx to total cellular pigments remained unchanged (**Fig. 2.5**). Since the abundance of Chl a did not increase along with Fx, we suggest that the excess Fx in the VDL2 OE lines was either localized in the lipid shield around the photoantennae, along with non-protein bound Ddx cycle pigments, or that it may have replaced some of the photoantenna-bound Ddx [Lepetit et al. 2010]. Eilers et al. [2015] also found that increased Fx abundance in their *P. tricornutum* PSY OE lines was not accompanied by a concomitant increase in Chl a content. While our results do not clarify whether Ddx and Fx share a common precursor or Fx is derived from Ddx, they do implicate VDL2 in Fx biosynthesis. This is the first report of an enzyme being involved in Fx biosynthesis, and the first experimental evidence for a VDL function. Our findings do not support the hypothesis that VDLs participate in xanthophyll cycling. Multiple chemical reactions must take place during Fx biosynthesis from either Ddx or the other hypothetical precursor, neoxanthin. It is possible that VDL2 is not the sole enzyme responsible for Fx biosynthesis. However, based on our findings, if other enzymes are involved in this step, they are not rate-limiting. VDL2 analysis based on sequence

as well as predicted structure revealed only a VDE-like lipocalin domain, a fold that is shared by VDEs, VDLs, and ZEPs, and allows them to bind to their pigment substrates [Coesel et al. 2008]. The chemistry necessary to synthesize Fx includes additions of one acetyl and one keto group and oxidoreductase activity. It is possible that VDL2 is able to catalyze all of the required reactions. It is capable of oxidoreductase activity (**Table 2.4**), which could catalyze everything except for the acetyl group addition. It should be noted that VDL2 is designated as part of the N-acetylglucosaminyltransferase KOG group on the DOE JGI website (**Table 2.4**), but it is unclear why the software made this prediction. No corresponding domains have been identified either by VDL2 sequence and predicted structure analyses nor by aligning VDL2 to other proteins in that group, which yielded only very sparse similarity not limited to any specific part of the sequence (data not shown). If the software designation is accurate, however, it may indicate an ability to transfer acetyl groups. Almost half of the VDL2 protein on the N-terminal side shows no similarity to other known proteins based on either sequence or predicted structure and may perform previously undescribed chemistry.

Like VDL2, Thaps3\_10233, an oxidoreductase (**Table 2.4**) initially identified by BLAST during the CRTISO candidate search, exhibited gene expression patterns in both the microarray dataset [Smith et al. 2016] and RNA-seq dataset [Abbriano 2017] that were distinct from the other carotenoid biosynthesis genes and similar to photoantenna protein genes (**Figs. 2.3, 2.4**). We suggest that Thaps3\_10233 may be involved in Fx biosynthesis along with VDL2. The co-expression of the genes encoding proteins involved in Fx biosynthesis with photoantenna protein genes may represent another layer of carotenoid biosynthesis regulation, in addition to the hypothesized separate means of inducing the pathway in response to irradiance increase and chloroplast division. Synthesizing Fx only when photoantenna proteins are also being made may be a way to ensure that pigment precursors are funneled into Fx biosynthesis only when it is needed to populate newly

synthesized photoantenna proteins, and otherwise are used to make Ddx cycle pigments. While some Ddx cycle pigments are bound to photoantenna proteins, the majority of those synthesized in response to an increase in illumination are dissolved in the lipid shield around photoantennae [Lepetit et al. 2010]. Therefore, their accumulation would not need to be coordinated with photoantenna protein production. The hypothesized mechanisms of differential carotenoid biosynthesis regulation are summarized in **Fig. 2.9**.

#### 2.4.3 Total Photopigment Reduction in Knockdown Lines

An overall reduction in cellular photopigment content was observed in LTL, VDL1, and VDL2 KD lines, without substantial differences in the ratios of individual pigments (**Figs. 2.6-2.8**). Thus,  $\beta$ -car, presumably upstream of the biosynthetic steps targeted by the KDs, as well as Chl a and Chl c, which are part of a separate biosynthetic pathway, were reduced proportionately with Fx and Ddx cycle pigments in the KD lines. Carotenoids are known to play a crucial role in the assembly and stabilization of light-harvesting complexes in photosynthetic bacteria, algae, and green plants [Moskalenko and Karapetyan 1996, Santabarbara et al. 2013]. Unlike chlorophytes that adjust the size of photoantenna complexes associated with photosynthetic reaction centers in response to changes in light intensity, diatoms co-regulate the number of reaction centers and photoantenna units. Thus, the ratio of Chl a to Fx and  $\beta$ -car does not vary substantially, while Chl c abundance appears to be more variable [Brunet et al. 2014, Lepetit et al. 2012]. In the KD lines, Chl a, Chl c, and  $\beta$ -car may have failed to accumulate due to being prevented from stable binding to light-harvesting complex proteins because of light-harvesting complex destabilization caused by a Fx deficit, especially since the pigment ratios appear to be generally maintained in diatoms. Lohr and Wilhelm [1999] monitored photopigment accumulation in *P. tricornutum* upon reducing illumination

intensity, with and without the addition of the *de novo* carotenoid biosynthesis inhibitor norflurazon, which acts upon PDS. In the norflurazon-treated sample, the abundance of Fx increased as accumulated precursor pigments were depleted. In the untreated samples, following the initial conversion of precursors to Fx, Fx abundance continued to increase, presumably via *de novo* biosynthesis. Despite the differences in final Fx content between the treated and untreated samples, final Chl a/Fx and β-car/Fx ratios did not differ substantially, demonstrating that Chl a and β-car accumulation was proportional to that of Fx. Chl c abundance was not reported [Lohr and Wilhelm 1999]. This observation provides further support for the notion that reducing the abundance of Fx will also reduce that of the other photopigments, as was observed in our KD lines (**Figs. 2.6-2.8**).

#### 2.4.4 Broader Implications of the Findings

Our results have important implications for studying diatom carotenoid biosynthesis. If knocking down most steps in the pathway will result in the same phenotype of overall pigment reduction, it will not allow the elucidation of enzyme function, as was the case with all knockdowns performed in our study. However, if it is possible to perform chemical rescue experiments by feeding various pigments in the pathway to knockdown lines, that may be a viable approach to further pathway elucidation. There are some exceptions, however, for which the knockdown approach alone may be helpful. VDE, for example, does not participate in forward *de novo* carotenoid biosynthesis. It has been knocked down in *P. tricornutum* without reducing pigment content, resulting only in impaired Ddx de-epoxidation (and likely that of Vx as well, which was not measured) [Lavaud et al. 2012]. Knocking down the two *T. pseudonana* ZEPs may help confirm our hypotheses about them as well. If, as we expect, ZEP1 participates in the Vx cycle, knocking it down

should result in overall pigmentation reduction, as forward biosynthesis through that pathway is necessary for Vx biosynthesis, and therefore that of Fx and Ddx cycle pigments. However, if the hypothesis put forth by Lohr and Wilhelm [2001] that Vx is synthesized via  $\beta$ -cryptoxanthin from  $\beta$ -car is correct, the ZEP1 knockdown may not have as much of an effect on the downstream pigments, but may result in Zx accumulation under certain conditions [Lohr and Wilhelm 1999]. Knocking down ZEP2 on the other hand should not affect total cellular pigment content but rather result in a Dtx epoxidation defect upon a shift from high light to low light, if our hypothesis that it participates in the Ddx cycle is correct. Our hypothesis about there being two ways to independently induce carotenoid biosynthesis in response to either chloroplast division or an increase in illumination may be tested by knocking down PSY1 and PSY2 separately as well. If PSY1 indeed serves to initiate carotenoid biosynthesis during chloroplast division in order to populate newly divided chloroplasts with pigments, knocking it down should result in an overall pigment reduction. If PSY2 initiates carotenoid biosynthesis in order to make more Ddx cycle pigments in response to increased illumination, knocking it down should not affect cellular pigmentation at low light intensities, but should result in impaired Ddx cycle pigment pool accumulation upon being transferred to higher light. The aforementioned experiments were out of the scope of this study.

Overexpression, as a different approach to assessing enzyme function, may be limited by substrate availability and not usable for all the pathway steps. Heterologous complementation, such as performed by Dambeck et al. [2012] for the earlier carotenoid biosynthesis steps in *P. tricornutum*, may help in the study of the function of enzymes involved in the later steps as well.

Finally, our findings must be taken into consideration if altering diatom pigment content by genetically manipulating carotenoid biosynthesis is of interest. It does not appear possible to reduce the amount of the main accessory photopigment Fx without affecting the abundance of other photopigments, in order to accumulate  $\beta$ -car for commercial purposes or obtain a

photoantenna reduction phenotype that has been achieved in chlorophytes [e.g., Kirst et al. 2012], for example. On the other hand, it is possible to increase cellular Fx content, which may be of interest due to its various health-promoting activities [Peng et al. 2011].

The *T. pseudonana* genes identified and discussed in this study are also found in all other currently available diatom genomes (**Table 2.5**). Thus, our findings are relevant to diatom carotenoid biosynthesis in general, and not limited to our model species. There may exist, however, interspecies differences in certain aspects of the pathway. For example, *P. tricornutum* has only one copy of PSY, unlike *T. pseudonana* and other diatoms with sequenced genomes available that have at least two (**Table 2.5**). Therefore, the step that PSY catalyzes could not be used by *P. tricornutum* to differentially initiate carotenoid biosynthesis in response to chloroplast division and higher illumination. However, *P. tricornutum* does have two copies of PDS, which we hypothesize are differentially used by *T. pseudonana* along with the two PSY copies (**Fig. 2.9**). Consequently, *P. tricornutum* might use PDS, but not PSY, to differentiate between the two possible carotenogenic needs of the cell. Another observation is that some carotenoid biosynthesis genes in *P. tricornutum* are adjacent and appear to be divergently transcribed [Coesel et al. 2008], whereas no such relationships exist between the carotenoid biosynthesis genes in *T. pseudonana*. Interestingly, two such pairs in *P. tricornutum* are VDE with ZEP3 and VDL2 with ZEP1. Since de-epoxidation and epoxidation of xanthophyll cycle pigments are in opposition of each other, it is possible that ZEP3 functions in a process other than xanthophyll cycling. *P. tricornutum* has three copies of ZEP (**Table 2.5**), and it is possible that ZEP1 and ZEP2 differentially participate in the two xanthophyll cycles as we propose they do in *T. pseudonana* (**Figs. 2.1, 2.9**), while the third copy has evolved to perform a different role. Xanthophyll epoxidation and Fx biosynthesis on the other hand are likely to co-occur, and thus the co-regulation of ZEP1 and VDL2 is not surprising. ZEP1 in *P. tricornutum* may participate in the Vx cycle as we suggest the *T. pseudonana* ZEP1 does, and upregulating ZEP1

together with VDL2 when Fx biosynthesis is necessary would be logical. Diatoms are incredibly diverse and adapted to a wide variety of environmental conditions over the course of evolution, and many strategies employed by different species may vary [Hildebrand et al. 2012], including those related to photosynthesis and photoprotection [Lavaud and Lepetit 2013]. However, increasing what is known about a process in one diatom species ultimately facilitates future efforts for studying it in others, and improves our overall understanding of these environmentally important and commercially promising organisms.

## 2.5 METHODS

### 2.5.1 Sequence Identity-Based Carotenoid Biosynthesis Gene Candidate Search

*P. tricornutum* and *T. pseudonana* genome sequence data was accessed on the Department of Energy Joint Genome Institute (DOE JGI) website at <https://genome.jgi.doe.gov/Phatr2/Phatr2.home.html> and <https://genome.jgi.doe.gov/Thaps3/Thaps3.home.html>, respectively. Database searches were performed using the tBLASTn function available on the website, comparing protein queries to translated nucleotide sequences. Redundant gene models, and those representing pieces of more complete models, were not listed. Sequence identity analyses were performed on protein sequences predicted by the DOE JGI website. Multiple sequence alignment, percent identity matrix generation, and phylogenetic tree construction were completed using Clustal Omega (<https://www.ebi.ac.uk/Tools/msa/clustalo/>) [Sievers et al. 2011]. Trees were visualized using Interactive Tree of Life (iTOL) (<https://itol.embl.de/>) [Letunic and Bork 2016]. Gene Ontology (GO) terms, EuKaryotic Orthologous Groups Identity (KOG ID), and Protein Family (Pfam) information were provided by the DOE JGI website.

### *2.5.2 Full-length Gene Model Construction*

RNA-seq data [Abbriano 2017, Smith et al. 2016] was visualized using the Integrated Genomics Viewer (IGV) [Robinson et al. 2011, Thorvaldsdottir et al. 2013]. Exon boundary coordinates were used to obtain genomic sequences on the DOE JGI website.

### *2.5.3 Predicted Protein Targeting Analysis*

Open reading frames for the full-length gene models were obtained using the online ExPASy Translate tool (<https://web.expasy.org/translate/>). Because chloroplast-targeted diatom proteins must cross the ER membrane first, online programs SignalP 3.0 [Bendtsen et al. 2004] and SignalP 4.1 [Petersen et al. 2011] were used to predict ER targeting, and ChloroP 1.1 [Emanuelsson et al. 1999] was used to predict the presence of chloroplast transit domains, as previously discussed in Smith et al. [2012].

### *2.5.4 Additional Sequence-Based Analyses*

Alignments and sequence identity analyses were performed with Clustal Omega (2.5.1). BCH sequences were obtained from the National Center for Biotechnology Information (NCBI) website (<https://www.ncbi.nlm.nih.gov/>) using GenBank accession numbers published by Tian and DellaPenna [2004]. BLASTp and tBLASTn programs on the NCBI website were used to search for proteins and translated nucleotide sequences with sequence identity to the C-terminal portion of Thaps3\_263437 (“BCH”). Conserved protein domain and motif analyses were performed using the NCBI Conserved Domains Search (<https://www.ncbi.nlm.nih.gov/Structure/cdd/wrpsb.cgi>) [Marchler-Bauer et al. 2017], the ScanProsite tool (<https://prosite.expasy.org/scanprosite/>) [De

Castro et al. 2006], and InterPro (<https://www.ebi.ac.uk/interpro/>) [Finn et al. 2017]. Functional annotation predictions for the *T. pseudonana* carotenoid biosynthesis enzymes were obtained from the DOE JGI website as well as by protein sequence analysis using InterPro and Pfam (<https://pfam.xfam.org/search/sequence>). Structure-based functional annotation predictions were performed with Phyre2 [Kelley et al. 2015] (<http://www.sbg.bio.ic.ac.uk/phyre2/html/page.cgi?id=index>).

Additional diatom genomes were accessed at:

<http://genomes3.mcdb.ucla.edu/cgibin/hgGateway?hgSID=23003&clade=plant&org=Ahi+simulation+02&db=0> for *Cyclotella cryptica* (2011 Assembly),  
<https://genome.jgi.doe.gov/Fracy1/Fracy1.home.html> for *Fragilariaopsis cylindrus*,  
<https://genome.jgi.doe.gov/Psemu1/Psemu1.home.html> for *Pseudonitzschia multiseries*, and  
<https://genome.jgi.doe.gov/Thaoce1/Thaoce1.home.html> for *Thalassiosira oceanica*.

Carotenoid biosynthesis genes in those genomes were found by using BLAT for *C. cryptica* and tBLASTn for the others, with predicted *T. pseudonana* protein sequences (2.3.4) and Phatr2\_56492 (*P. tricornutum* ZEP3) as queries.

### 2.5.5 Genetic Manipulation

Cloning was carried out using MultiSite Gateway technology (Thermo Fisher Scientific, Waltham, MA, USA) as previously described [Shrestha and Hildebrand 2015]. VDL2 OE was driven by the *T. pseudonana* nitrate reductase (NR) promoter, LTL KD by the *T. pseudonana* ribosomal protein L41 promoter, and VDL1 and VDL2 KDs by the *T. pseudonana* acetyl CoA carboxylase (ACCase) promoter, with the corresponding terminators used respectively. As demonstrated previously [Shrestha et al. 2013], the rpL41 is the strongest promoter out of the three, and NR is the

weakest. The KD constructs comprised a nourseothricin resistance gene encoding nourseothricin N-acetyltransferase (NAT1) upstream 500-600 bp of antisense per gene of interest on the same transcript. Plasmid and primer details are available in **Appendix 2.E**. The constructs were transformed into WT *T. pseudonana* using tungsten microparticle bombardment with Bio-Rad PDS-1000/He, following procedures described by Davis et al. [2017], with the modification of incubating cells in dim light overnight following the bombardment. VDL2 OE was co-transformed with another plasmid carrying the NAT1 gene under the *T. pseudonana* ACCase promoter (received from N. Kroger, Germany). Genomic integration of the constructs was confirmed by PCR [Shrestha and Hildebrand 2015]. For VDL2 OE, RNA extraction, reverse transcription, qRT-PCR primer design, and qRT-PCR with normalization to the TATA box binding protein (Thaps3\_264095) were performed as in Shrestha and Hildebrand [2015]. Four clones were chosen for further analysis (**Fig. S2.2**).

#### 2.5.6 Cultivation Conditions and Photopigment Analysis

*T. pseudonana* WT and transgenic cultures were cultivated at either 30 or 300  $\mu\text{mol}$  photons  $\text{m}^{-2} \text{sec}^{-1}$  (natural white LED lighting, superbrightleds.com, NFLS-NW300X3-WHT-LC2), using a 12:12 h light:dark regime, at 18°C. 50 mL cultures in Erlenmeyer flasks were maintained in Artificial Sea Water (ASW) medium [Darley and Volcani 1969] with rapid stirring. Each experimental set included 2 WT and 4 transgenic cultures. After inoculation, the cultures were grown to  $1-3 \times 10^6$  cells/mL, then allowed to adapt to the cultivation conditions by daily dilutions that maintained exponential growth with culture density under  $2.5 \times 10^6$  cells/mL for a minimum of 2 weeks prior to sampling for photopigments. Cultures were rotated between stir plates each day to minimize any position-specific differences. Sampling was performed within the first two hours of the light period. Immediately prior to sampling, cultures were allowed to adapt to the light environment of the

biosafety cabinet for 45-90 min. 10-20 mL of  $1 \times 10^6$ - $2.5 \times 10^6$  cells/mL cultures were harvested, processed, and analyzed by HPLC as previously described [Kozlowski et al. 2011]. HPLC analysis employed an internal control of including the same sample in two different quantities to ensure precision in pigment quantification, which scaled accordingly. An online one-way ANOVA calculator accessed at <https://www.socscistatistics.com/tests/anova/default2.aspx> was used for statistical analysis of pigmentation differences between WT and transgenic lines.

## 2.6 ACKNOWLEDGEMENTS

Chapter 2, in full, is material currently being prepared for submission for publication. Gaidarenko, Olga; Mills, Dylan W.; Vernet, Maria; Hildebrand, Mark. "Novel *Thalassiosira pseudonana* violaxanthin de-epoxidase-like enzyme (VDL2) catalyzes fucoxanthin biosynthesis." Olga Gaidarenko was the principal researcher and author of this work. We thank Dr. Sarah R. Smith and Dr. Raffaela M. Abriano for helpful discussions and data that made this work possible, as well as Dr. Roshan P. Shrestha for helpful discussions and providing genetic manipulation tools. Additionally, we thank Dr. Bradley Moore and Dr. Jonathan Chekan for providing valuable perspective and insights. We also thank Dr. James Golden for critically reading the chapter and providing helpful input. This work was supported by U.S. Dept. of Energy grant DE-FOA-0001471.

**Table 2.1.**

Model IDs of known carotenoid biosynthesis genes/enzymes and corresponding BLAST results.

Sequence Identity BLAST Results For:	Enzyme Name	<i>T. pseudonana</i>	<i>P. tricornutum</i>
Phytoene Synthase (PSY)	PSY1	Thaps3_268908	Phatr2_56481
	PSY2	Thaps3_263269	-----
Phytoene Desaturase (PDS)	PDS1	Thaps3_23291	Phatr2_45735
	PDS2	Thaps3_1383	Phatr2_55102
	-----	Thaps3_bd_1474	-----
$\zeta$ -Carotene Desaturase (ZDS)	ZDS	Thaps3_24832	Phatr2_53974
Carotene Cis-Trans Isomerase (Prolycopene Isomerase) (CRTISO)	-----	Thaps3_7094	Phatr2_45243
	-----	Thaps3_21900	Phatr2_9210
	-----	Thaps3_21847	Phatr2_54842
	-----	Thaps3_5221	Phatr2_51868
	-----	Thaps3_10233	Phatr2_54826
	-----	Thaps3_11636	Phatr2_54800
	-----	Thaps3_5859	Phatr2_42980
	-----	Thaps3_25361	-----
	-----	Thaps3_10254	-----
Lycopene $\beta$ -cyclase (LCYB)	LCYB	Thaps3_270357	Phatr2_56484
$\beta$ -Carotene Hydroxylase (BCH)	BCH	Thaps3_263437	-----
LUT-Like (Lutein Deficient-Like) (LTL)	LTL1	Thaps3_9541	Phatr2_50101
	LTL2	Thaps3_270336	Phatr2_26422
	-----	Thaps3_33926	Phatr2_34027
	-----	Thaps3_32491	Phatr2_33568
	-----	Thaps3_1549	Phatr2_6940
	-----	Thaps3_264647	Phatr2_46438
	-----	Thaps3_25944	Phatr2_31339
	-----	Thaps3_14875	Phatr2_47234
	-----	Thaps3_4027	Phatr2_37006
	-----	Thaps3_4026	Phatr2_43466
	-----	Thaps3_bd_518	Phatr2_43467
	-----	Thaps3_269400	Phatr2_43562
	-----	Thaps3_264325	Phatr2_50619
	-----	Thaps3_263399	Phatr2_43469
	-----	-----	Phatr2_32833
	-----	-----	Phatr2_43537

**Table 2.1, continued.**

Model IDs of known carotenoid biosynthesis genes/enzymes and corresponding BLAST results.

Zeaxanthin Epoxidase (ZEP)	ZEP1	Thaps3_270370	Phatr2_45845
	ZEP2	Thaps3_261390	Phatr2_56488
	ZEP3	-----	Phatr2_56492
	-----	Thaps3_1961	Phatr2_43425
	-----	Thaps3_6395	Phatr2_47925
	-----	Thaps3_20663	Phatr2_45936
	-----	Thaps3_22671	-----
Violaxanthin De- Epoxidase (VDE), Like (VDL), VDE-Related (VDR)	VDE	Thaps3_7677	Phatr2_44635
	VDL1	Thaps3_22076	Phatr2_46155
	VDL2	Thaps3_11707	Phatr2_45846
	VDR	Thaps3_270211	Phatr2_56450
	-----	-----	Phatr2_bd_1281

**Table 2.2.**

Targeting predictions for known carotenoid biosynthesis enzymes and candidates.

\*ChloroP score very close to the cutoff (0.500), chloroplast targeting possible.

Predicted Targeting	Gene/Protein ID	Name	Notes
Chloroplast	Thaps3_268908	PSY1	
	Thaps3_23291	PDS1	
	Thaps3_1383	PDS2	
	Thaps3_24832	ZDS	
	Thaps3_270357	LCY-B	
	Thaps3_9541	LTL1	
	Thaps3_270370	ZEP1	
	Thaps3_261390	ZEP2	
	Thaps3_7677	VDE	
	Thaps3_22076	VDL1	
	Thaps3_11707	VDL2	
	Thaps3_270211	VDR	
	Thaps3_21900		Found in CRTISO BLAST search.
	Thaps3_10233		Found in CRTISO BLAST search.
Endoplasmic	Thaps3_263269	PSY2*	ChloroP Score = 0.499, close to the 0.500 cutoff.
Reticulum (ER)	Thaps3_270336	LTL2*	ChloroP Score = 0.497, close to the 0.500 cutoff.
	Thaps3_14875		Clear ER targeting, possible signal anchor. Clear lack of predicted chloroplast targeting.
	Thaps3_264647		Clear ER targeting, possible signal anchor. Clear lack of predicted chloroplast targeting.
	Thaps3_5221		Clear ER targeting, possible signal anchor. Clear lack of predicted chloroplast targeting.
Other	Thaps3_bd_1474	PDS3	Missing N-terminus, prediction unavailable. Appears identical to PDS1 (2.5.1).
	Thaps3_263437	BCH	Clear lack of ER or chloroplast.
	Thaps3_4026		Clear lack of ER or chloroplast.
	Thaps3_25361		Clear chloroplast, but not ER.
	Thaps3_33926		Clear chloroplast, but not ER.
	Thaps3_1549		Clear chloroplast, but not ER.
	Thaps3_6395		Clear chloroplast, but not ER.
	Thaps3_bd_518		Unclear, RNA-seq data unavailable to confirm gene model.

**Table 2.3.**

Partial sequence identity matches for the Thaps3\_263437 C-terminal, non-BCH-like peptide.

Portion of C-terminal part	BLAST Result Type	Sequence Identity	Organism
81-88%	Unidentified or hypothetical proteins	28-39%	<i>Chrysochromulina</i> sp. CCMP291 (haptophyte) <i>Aurantiochytrium</i> sp. FCC1311 (labyrinthulomycete) <i>Oikopleura dioica</i> (tunicate)
26-37%, C-terminal	Translated nucleotide sequences	41-43%	<i>Oikopleura dioica</i> (tunicate) <i>Homo sapiens</i> (primate) <i>Pan troglodytes</i> (primate)
17%, middle	Translated nucleotide sequence	38%	<i>Arachis hypogaea</i> (green plant)

**Table 2.4.**  
Sequence-based functional annotation of *T. pseudonana* carotenoid biosynthesis enzymes.

Name/ID	Gene Ontology (GO)	Eukaryotic Orthologous Group (KOG)	Protein Family (Pfam)	InterPro Family
PSY1 Thaps3_268908	GO:0009058 biosynthetic process  GO:0016740 transferase activity	KOG1459 Squalene synthetase	PF00494 Squalene/phytoene synthase	IPR002060 Squalene/phytoene synthase
PSY2 Thaps3_263269	GO:0003824 catalytic activity  GO:0008299 isoprenoid biosynthetic process GO:0009058 biosynthetic process GO:0009507 chloroplast GO:0016117 carotenoid biosynthetic process GO:0016740 transferase activity	KOG1459 Squalene synthetase	PF00494 Squalene/phytoene synthase	IPR002060 Squalene/phytoene synthase
PDS1 Thaps3_23291	GO:0004497 monooxygenase activity  GO:0009507 chloroplast GO:0016117 carotenoid biosynthetic process GO:0016491 oxidoreductase activity	KOG0029 Amine oxidase	PF01593 Flavin-containing amine oxidase	IPR014102 Phytoene desaturase

**Table 2.4, continued.**Sequence-based functional annotation of *T. pseudonana* carotenoid biosynthesis enzymes.

Thaps3_bd_1474	GO:0016491 oxidoreductase activity	KOG0029 Amine oxidase	PF01593 Flavin- containing amine oxidase	IPR036188 FAD/NAD(P)-binding domain superfamily
PDS2	GO:0009507 chloroplast	KOG0029 Amine oxidase	PF01593 Flavin- containing amine oxidase	IPR02937 Amine oxidase
Thaps3_1383	GO:0016117 carotenoid biosynthetic process			IPR014102 Phytoene desaturase
	GO:0016120 carotene biosynthetic process			IPR036188 FAD/NAD(P)-binding domain superfamily
	GO:0016166 phytoene dehydrogenase activity			IPR002937 Amine oxidase
	GO:0016491 oxidoreductase activity			
ZDS	GO:0016117 carotenoid biosynthetic process	KOG0029 Amine oxidase	PF01593 Flavin- containing amine oxidase	IPR014103 Zeta-carotene desaturase
Thaps3_24832	GO:0016491 oxidoreductase activity			IPR036188 FAD/NAD(P)-binding domain superfamily
	GO:0016719 carotene 7,8- desaturase activity			IPR002937 Amine oxidase
CRTISO	GO:0016117 carotenoid biosynthetic process	KOG4254 Phytoene desaturase	PF13450 NAD(P)- binding Rossmann- like domain	IPR036188 FAD/NAD(P)-binding domain superfamily
Thaps3_21900	GO:0016705 oxidoreductase activity, acting on paired donors, with incorporation or reduction of molecular oxygen			
	GO:0050660 flavin adenine dinucleotide binding			
Thaps3_10233	GO:0015036 disulfide oxidoreductase activity	KOG4254 Phytoene desaturase	PF13450 NAD(P)- binding Rossmann- like domain	IPR036188 FAD/NAD(P)-binding domain superfamily

**Table 2.4, continued.**Sequence-based functional annotation of *T. pseudonana* carotenoid biosynthesis enzymes.

LCY-B Thaps3_270357	GO:0016117 carotenoid biosynthetic process GO:0016491 oxidoreductase activity GO:0016705 oxidoreductase activity, acting on paired donors, with incorporation or reduction of molecular oxygen GO:0050660 flavin adenine dinucleotide binding	PF01593 Flavin-containing amine oxidase N/A	IPR002937 Amine oxidase IPR010108 Lycopene cyclase, beta/epsilon IPR036188 FAD/NAD(P)-binding domain superfamily
LTL1 Thaps3_9541	GO:0008152 metabolic process GO:0009507 chloroplast	PF05834 Lycopene cyclase N/A	IPR010108 Lycopene cyclase, beta/epsilon IPR036188 FAD/NAD(P)-binding domain superfamily
LTL2 Thaps3_270336	GO:0004497 monooxygenase activity GO:0005506 iron ion binding	PF00067 Cytochrome P450 N/A	IPR001128 Cytochrome P450 IPR02401 Cytochrome P450, E-class, group I IPR001128 Cytochrome P450 IPR02401 Cytochrome P450 IPR001128 Cytochrome P450, E-class, group I

**Table 2.4, continued.**Sequence-based functional annotation of *T. pseudonana* carotenoid biosynthesis enzymes.

ZEP1	GO:0020037 heme binding	KOG2614 Kynurenine 3-monoxygenase and related flavoprotein monooxygenases	PF01494 FAD binding domain	IPR036396 Cytochrome P450 superfamily
Thaps3_270370	GO:0004497 monooxygenase activity	GO:0006725 cellular aromatic compound metabolic process	GO:0008152 metabolic process	IPR036188 FAD/NAD(P)-binding domain superfamily
	GO:0006118 obsolete electron transport	GO:0009507 chloroplast	GO:0016491 oxidoreductase activity	IPR002938 FAD-binding domain
ZEP2	GO:0004497 monooxygenase activity	KOG2614 Kynurenine 3-monoxygenase and related flavoprotein monooxygenases	PF01494 FAD binding domain	IPR036188 FAD/NAD(P)-binding domain superfamily
Thaps3_261390	GO:0006725 cellular aromatic compound metabolic process	GO:0008152 metabolic process	GO:0016123 xanthophyll biosynthetic process	IPR002938 FAD-binding domain
VDE	GO:0055114 oxidation- activity	N/A	PF07137 VDE	IPR010788 VDE lipocalin domain

**Table 2.4, continued.**

Sequence-based functional annotation of *T. pseudonana* carotenoid biosynthesis enzymes.

				IPR012674 Calycin
	GO:0046422 violaxanthin de-epoxidase activity			
	GO:0009507 chloroplast			
VDI1	GO:0055114 oxidation-reduction process	N/A	PF07137 VDE lipocalin domain	IPR010788 VDE lipocalin domain
Thaps3_22076	GO:0046422 violaxanthin de-epoxidase activity			IPR012674 Calycin
	GO:0009507 chloroplast			
VDI2	GO:0055114 oxidation-reduction process	KOG4157 β-1,6-N-acetylglucosaminyltransferase, contains WSC domain	PF07137 VDE lipocalin domain	IPR010788 VDE lipocalin domain
Thaps3_11707	GO:0046422 violaxanthin de-epoxidase activity			IPR012674 Calycin
	GO:0009507 chloroplast			
VDR	N/A	N/A	N/A	IPR012674 Calycin
Thaps3_270211				

**Table 2.5.**

Carotenoid biosynthesis genes in currently available diatom genomes.

	<i>T. pseudonana</i>	<i>T. oceanica</i>	<i>C. cryptica</i>	<i>P. tricornutum</i>	<i>F. cylindrus</i>	<i>P. multiseries</i>
PSY1	Thaps3_268908	scaffold_1529: 4644-6041	g3020512_08749	Phatr2_56481	Fracy1_264173	Psemu1_284362
PSY2	Thaps3_263269	Thaoce1_76633	g1711422_03357	-----	Fracy1_233859 scaffold_81: 89953-89306	Psemu1_21973 Psemu1_252566
PDS1	Thaps3_23291	Thaoce1_74122	g3033530_08435	Phatr2_45735	scaffold_15: 196010-194589	Psemu1_296799
	Thaps3_bd_1474?	-----	g3033529_10333	-----	-----	-----
	-----	-----	g2978166_08271	-----	-----	-----
PDS2	Thaps3_1383	Thaoce1_69579	g3041196_11323	Phatr2_55102	scaffold_41: 345681-344246 Fracy1_260963	Psemu1_184015
	-----	-----	-----	-----	-----	-----
ZDS	Thaps3_24832	Thaoce1_79521	g3029884_03203	Phatr2_53974	Fracy1_291551 scaffold_28: 522744-521104 Fracy1_231297	Psemu1_201585
	-----	-----	-----	-----	-----	-----
CRTISO	Thaps3_21900	scaffold_8852: 1169-2900	g3031469_09996	Phatr2_45243	scaffold_15: 1032105-1030436 Fracy1_225509	Psemu1_296898
	-----	-----	-----	-----	-----	-----
CRTISO	Thaps3_10233	Thaoce1_83016+83017	g3032342_19300	Phatr2_9210	Fracy1_274697	Psemu1_238122
or Fx Synth.	LCY-B	Thaps3_270357	Thaoce1_81190	g2984704_14008	Phatr2_56484	Fracy1_183412 Psemu1_181616
	-----	-----	-----	-----	-----	-----
LTI1	Thaps3_9541	Thaoce1_93110+93111	g3003680_30430	Phatr2_50101	Fracy1_261383	Psemu1_242952
LTI2	Thaps3_270336	Thaoce1_94290	g3010342_02309	Phatr2_26422	scaffold_46: 478885-477109	Psemu1_249715

**Table 2.5, continued.**

Carotenoid biosynthesis genes in currently available diatom genomes.

ZEP1	Thaps3_270370	scaffold_194192-1117	g3029177_02308	-----	-----	-----	-----
	Thaoce1_86217	-----	g2969398_36291	Phatr2_45845	Fracv1_232148	Psemu1_318239	-----
ZEP2	Thaps3_261390	Thaoce1_91593	g3012830_03620	Phatr2_56488	Fracv1_208380	Psemu1_249822	-----
ZEP3	-----	-----	g3012829_03620	Phatr2_56492	Fracv1_260743	Psemu1_321577	-----
VDE	Thaps3_7677	scaffold_16: 15273-16483	g3000467_15552	Phatr2_44635	Fracv1_267113	Psemu1_282298	-----
VDL1	Thaps3_22076	Thaoce1_92196	g3024877_16840	Phatr2_46155	Fracv1_212709	Psemu1_312307	-----
VDL2	Thaps3_11707	Thaoce1_75745	g2981206_02202	Phatr2_45846	Fracv1_291552	Psemu1_252938	-----
	-----	-----	g2981205_02344	Phatr2_bd_1281	-----	-----	-----
	-----	-----	g2981208_01259	-----	-----	-----	-----
	-----	-----	g2981207_01260	-----	-----	-----	-----
VDR	Thaps3_270211	Thaoce1_72825+72826	g2981650_01688	Phatr2_56450	scaffold_62: 310847-309744	Psemu1_170800	-----
	-----	-----	g3028784_03450	-----	Fracv1_269417	-----	-----
	-----	-----	g2990797_01166	-----	-----	-----	-----
	-----	-----	g3022545_01165	-----	-----	-----	-----

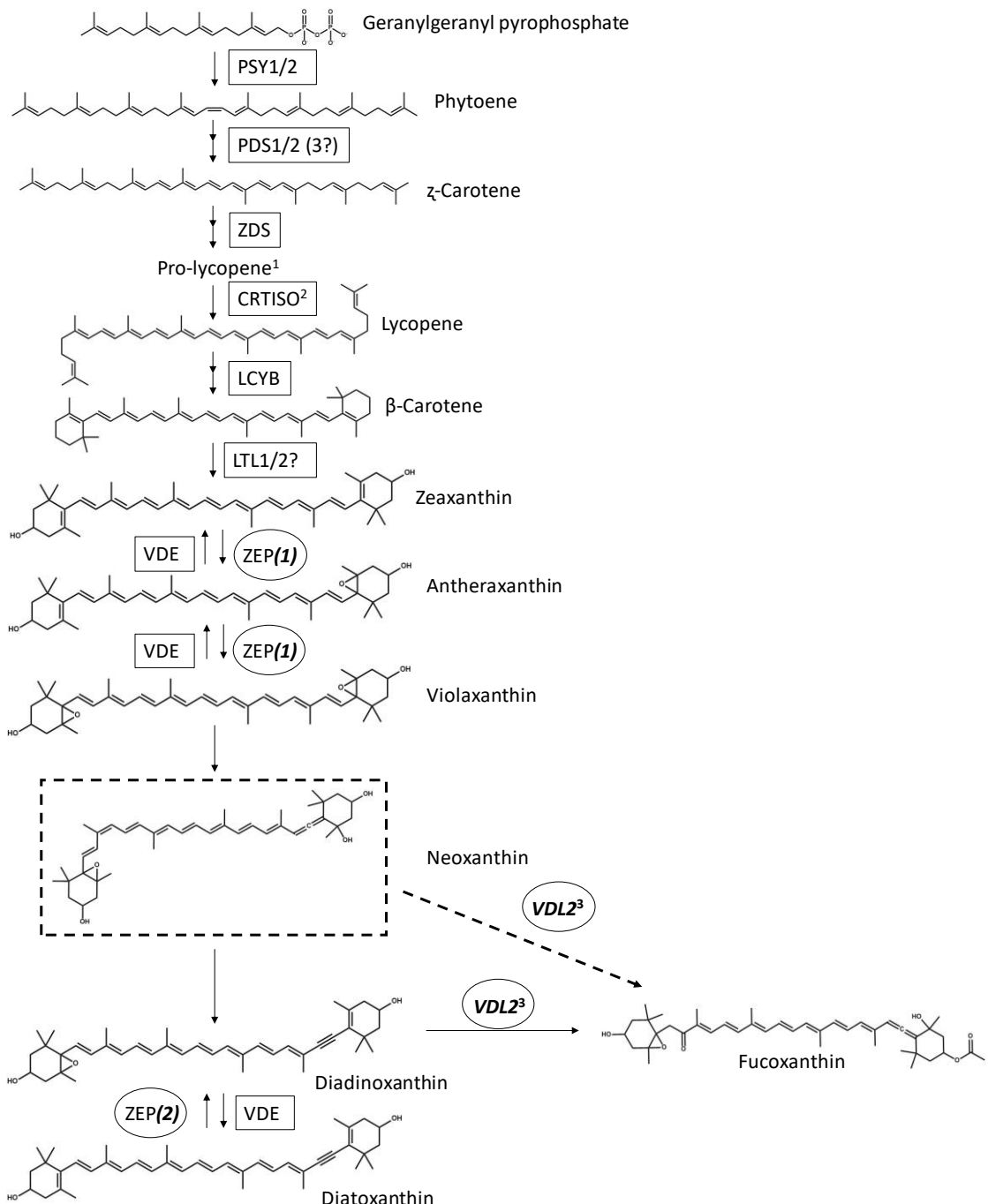


**Figure 2.1.**

Putative carotenoid biosynthesis pathway in *T. pseudonana*. Enzymes assigned to steps based on this study are depicted in ovals in bold italics. <sup>1</sup>Pro-lycopene is a stereoisomer of lycopene. <sup>2</sup>Thaps3\_21900 is hypothesized to catalyze this step. Thaps3\_10233 might also be involved. <sup>3</sup>Thaps3\_10233 might also be involved. PSY = phytoene synthase, PDS = phytoene desaturase, ZDS =  $\alpha$ -carotene desaturase, CRTISO = carotene cis/trans isomerase, prolycopene isomerase, LCYB = lycopene cyclase b, LTL = LUT-like, ZEP = zeaxanthin epoxidase, VDE = violaxanthin de-epoxidase, VDL = VDE-like.

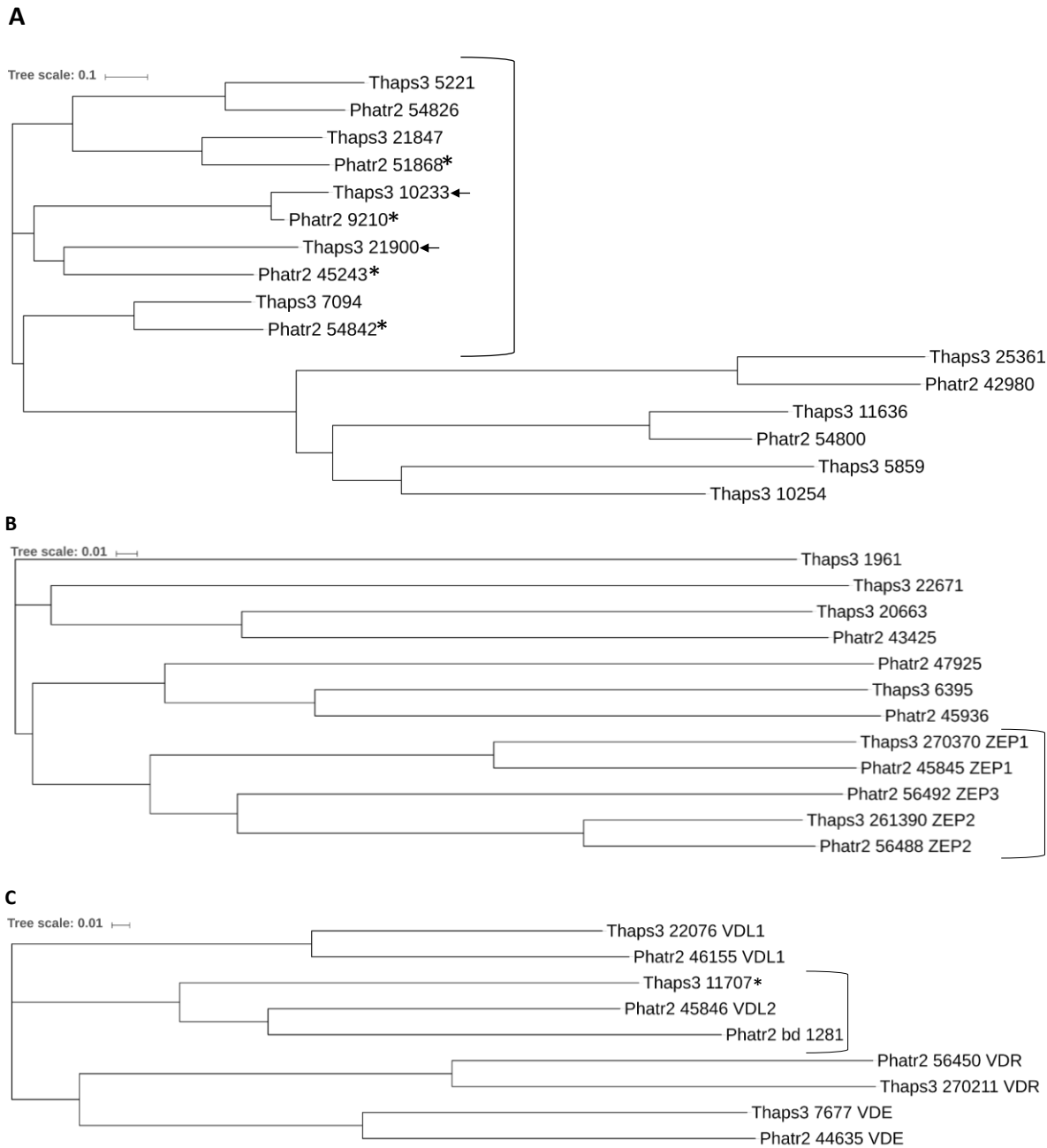


**Figure. 2.2.**

Sequence identity-based phylogenetic trees. **A.** CRTISO candidates and related proteins. The bracketed group includes those previously identified as CRTISO candidates by Dambeck et al. [2012], indicated with an asterisk (\*). Candidates hypothesized to be involved in carotenoid biosynthesis based on transcriptomic analysis and predicted chloroplast targeting are indicated with an arrow (←). **B.** ZEPs (bracketed) and related proteins. **C.** Known VDEs, VDLs, VDRs, and related proteins. Group including the *P. tricornutum* VDL2 is bracketed. The novel *T. pseudonana* protein Thaps3\_11707, hereafter designated VDL2, is indicated with an asterisk (\*).

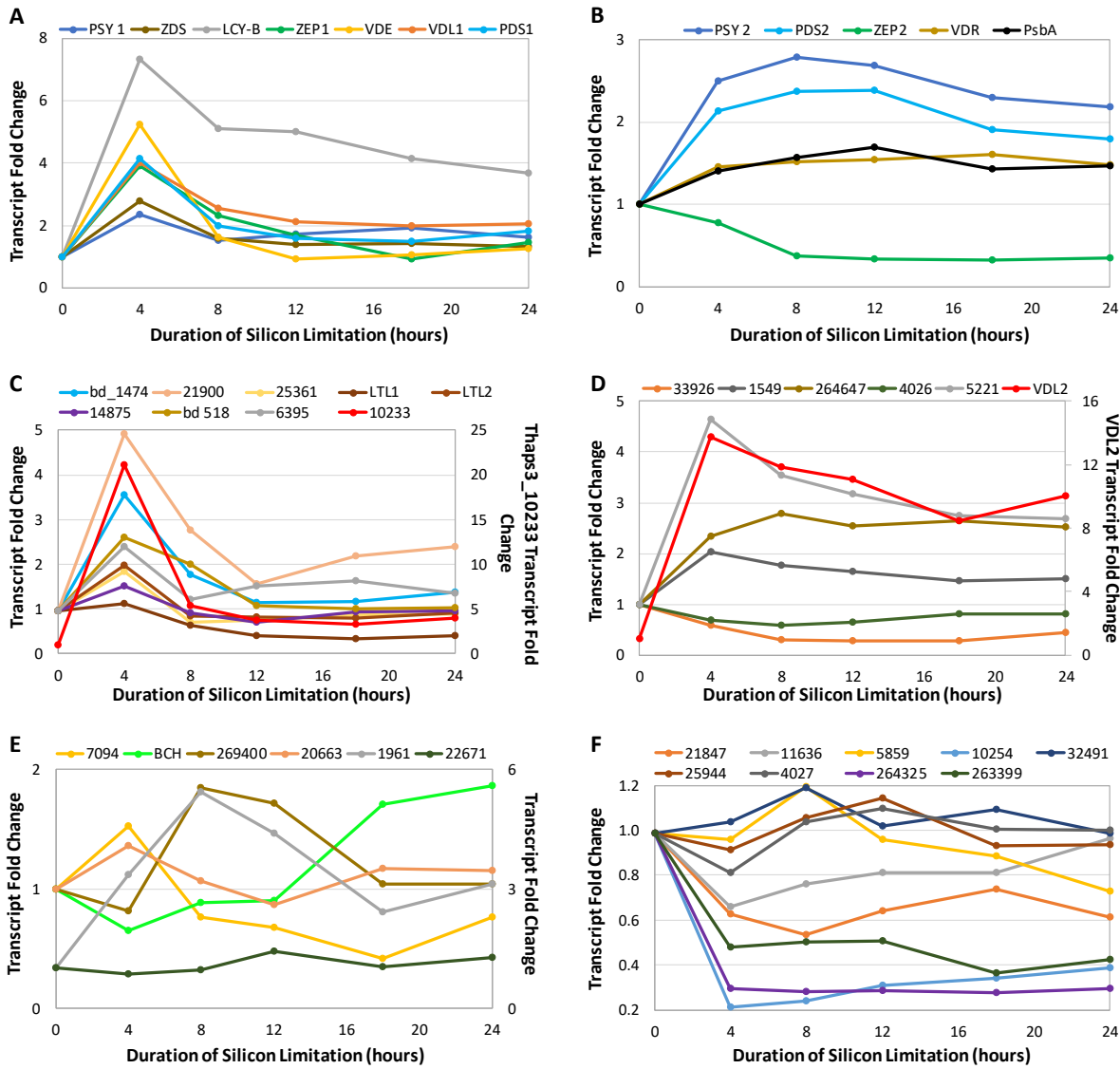


**Figure. 2.3.**

Candidate gene silicon starvation microarray expression patterns [Smith et al. 2016].

**A, B.** Genes known to be involved in carotenoid biosynthesis (except PsbA, which encodes the photosystem II D1 protein);

**C, D.** Genes with expression patterns similar to those in A and B, chosen for further study.

**E, F.** Genes with expression patterns different from those in A and B, not chosen for further study.

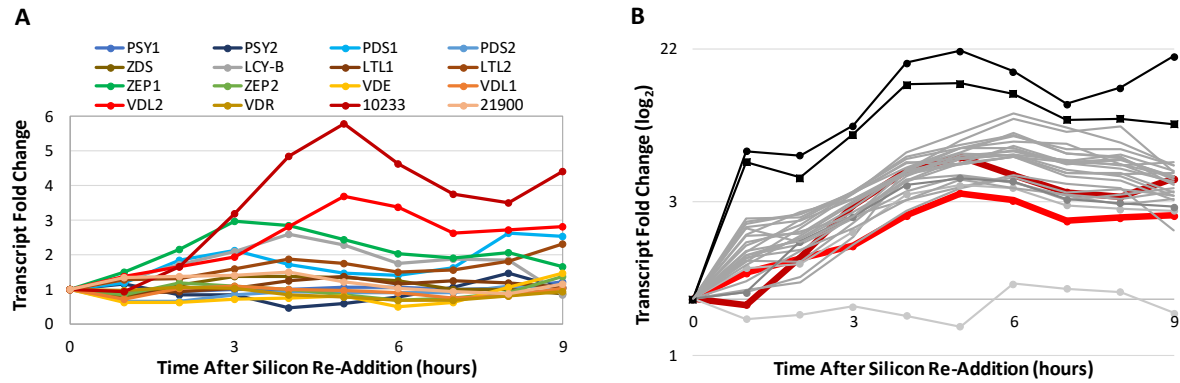


**Figure 2.4.**

RNA-seq gene expression patterns [Abbrriano 2017].

**A.** Carotenoid biosynthesis genes; **B.** VDL2 (bright red), Thaps3\_12033 (dark red), and photoantenna protein genes: Thaps3\_32723 (light grey, circles), Thaps3\_38667 (black, circles), Thaps3\_42962 (black, squares), Thaps3\_2601, 2845, 3815, 5174, 6139, 7916, 10219, 29375, 30385, 31749, 31983, 33018, 33131, 33606, 34276, 36081, 38122, 39813, 40747, 262313, 262332, 268127, 270092 (dark grey).

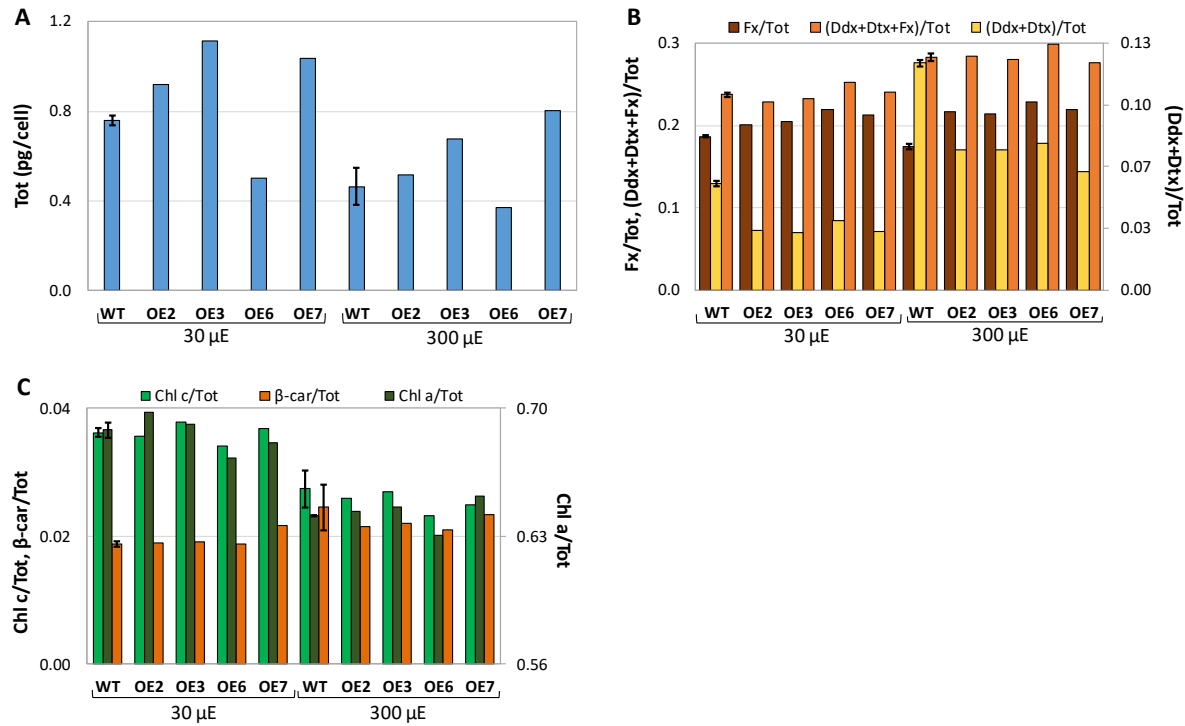


**Figure. 2.5.**

HPLC-based pigment analysis of wild-type (WT) vs. VDL2 overexpression (OE) lines cultured at 30  $\mu$ mol photons  $m^{-2} sec^{-1}$  ( $\mu$ E) and 300  $\mu$ E. WT data is an average of two independent cultures. **A.** Total cellular photopigments (Tot); **B.** Fx/Tot, (Ddx+Dtx)/Tot, (Ddx+Dtx+Fx)/Tot; **C.** Chl a/Tot, Chl c/Tot,  $\beta$ -car/Tot.

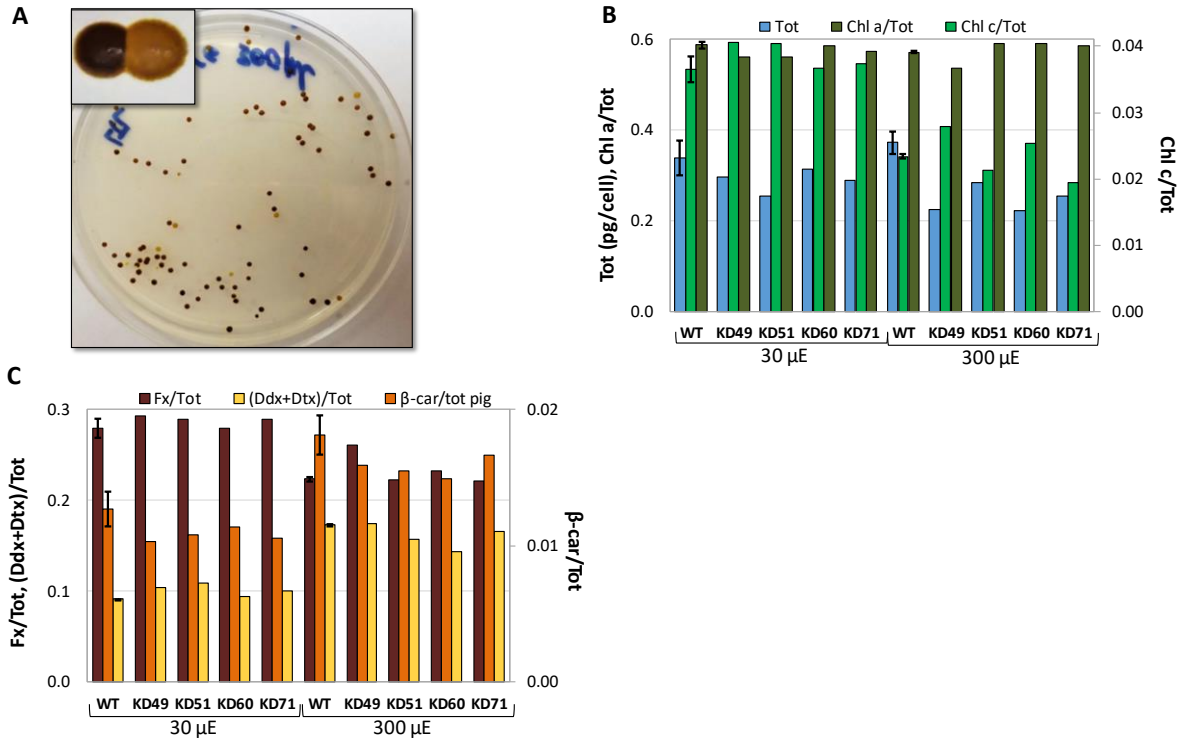


**Figure. 2.6.**

**A.** Lighter-pigmented LTL knockdown (KD) colonies among those with wild-type (WT)-equivalent pigmentation; HPLC-based pigment analysis of LTL KD clones cultured at 30  $\mu$ mol photons  $m^{-2}$  sec $^{-1}$  ( $\mu$ E) and 300  $\mu$ E. WT data is an average of two independent cultures. **B.** Tot, Chl a/Tot, Chl c/Tot; **C.** Fx/Tot, (Ddx+Dtx)/Tot,  $\beta$ -car/Tot.

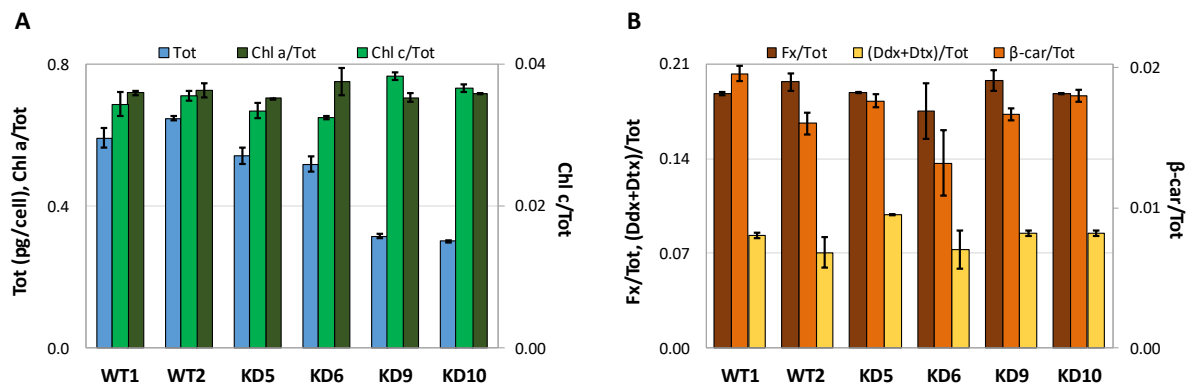


**Figure. 2.7.**  
HPLC-based pigment analysis of wild-type (WT) vs. VDL1 knockdown (KD) clones cultured at  $300 \mu\text{mol photons m}^{-2} \text{ sec}^{-1}$ . Each data point is an average of two samples taken from the same culture. **A.** Tot, Chl a/Tot, Chl c/Tot; **B.** Fx/Tot, (Ddx+Dtx)/Tot,  $\beta$ -car/Tot.

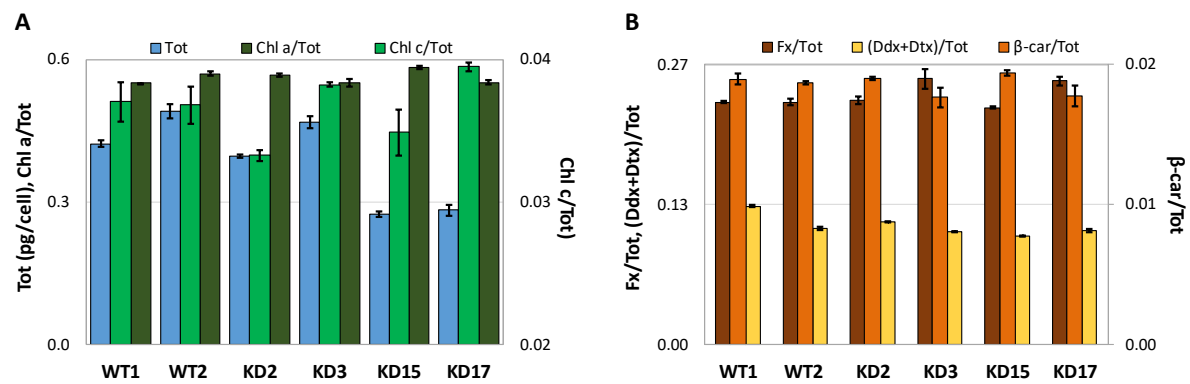


**Figure. 2.8.**  
HPLC-based pigment analysis of wild-type (WT) vs. VDL2 knockdown (KD) clones cultured at  $300 \mu\text{mol m}^{-2} \text{ sec}^{-1}$ . Each data point is an average of two samples taken from the same culture. **A.** Tot, Chl a/Tot, Chl c/Tot; **B.** Fx/Tot, (Ddx+Dtx)/Tot,  $\beta$ -car/Tot.

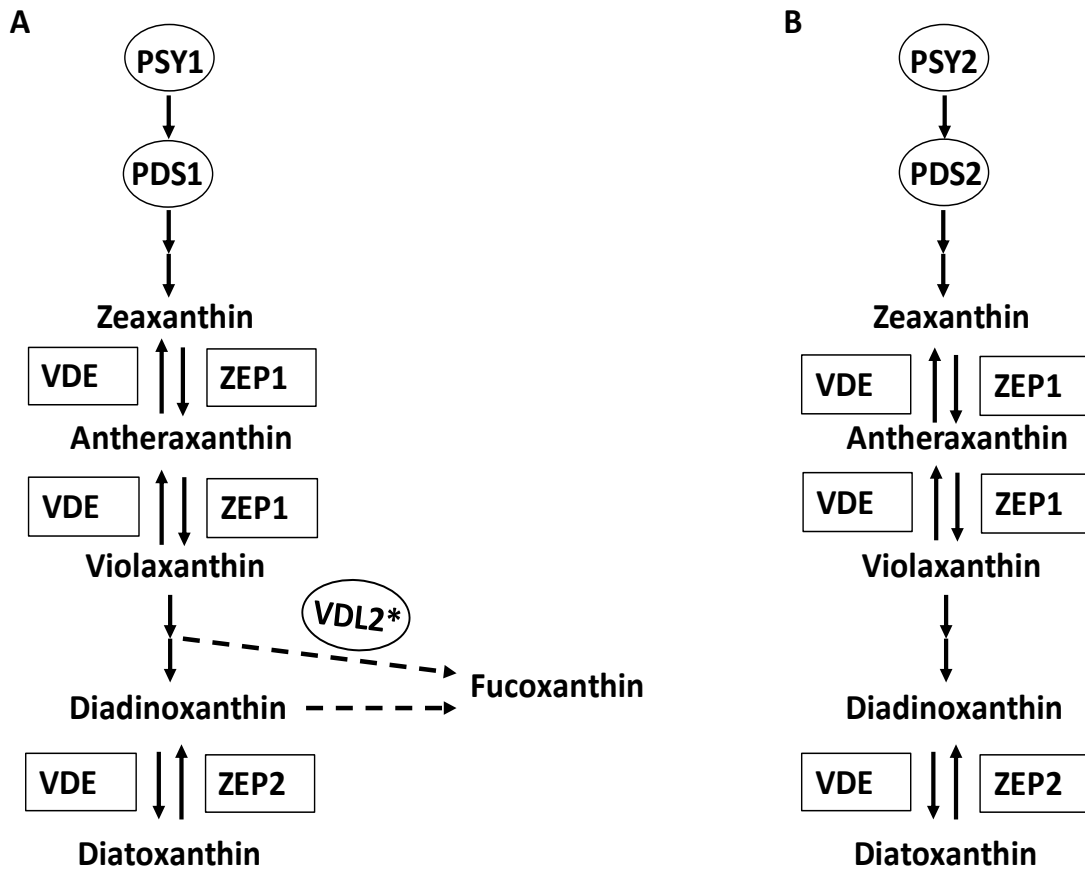


**Figure 2.9.**

Model of differential carotenoid biosynthesis regulation in *T. pseudonana*. Differentially utilized enzymes are designated by ovals. **A.** During chloroplast replication: some flux is directed towards Fx biosynthesis to populate photoantenna proteins. \*Thaps3\_10233 might also be involved. **B.** During an increase in illumination: Ddx+Dtx accumulate, mostly in the lipid shield around photoantennae.

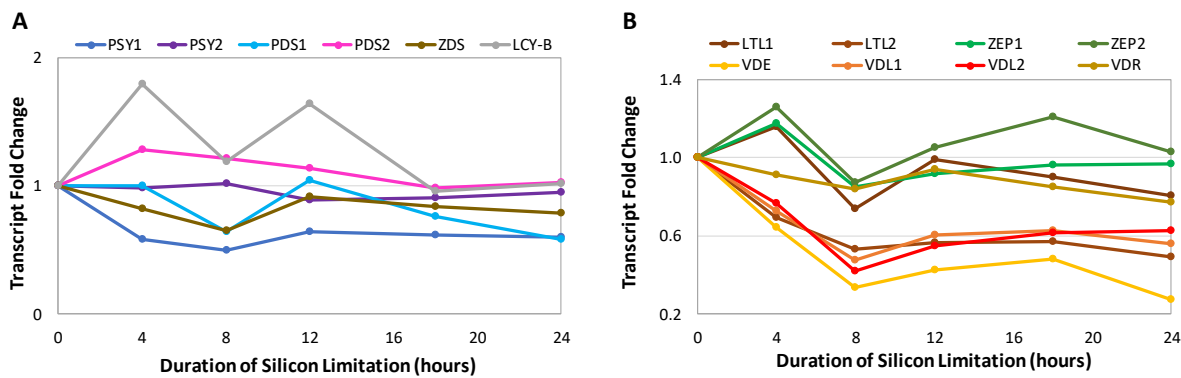


**Figure. S2.1.**

RNA-seq carotenoid biosynthesis gene expression patterns during silicon starvation

[Smith et al. 2016]. **A.** Pre- $\beta$ -car part of the carotenoid biosynthesis pathway;

**B.** Post- $\beta$ -car part of the carotenoid biosynthesis pathway.

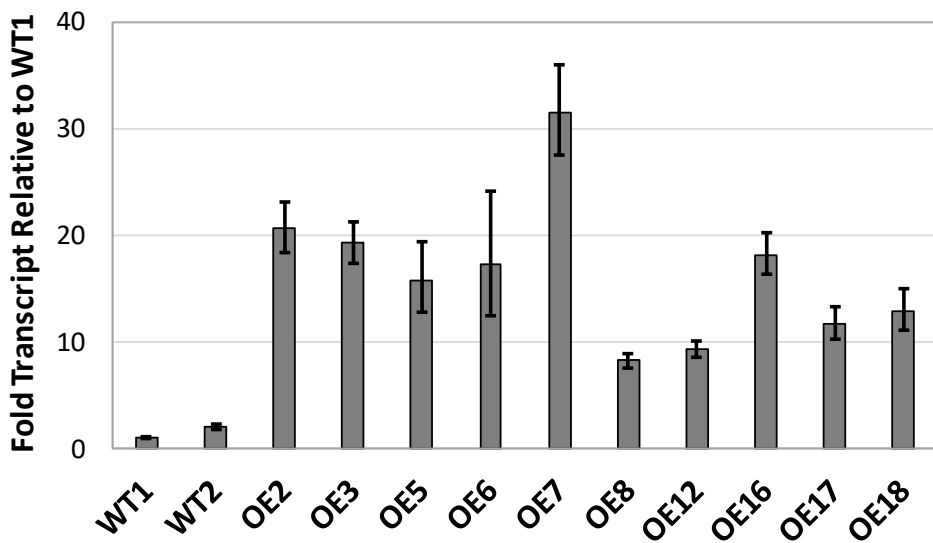


**Figure. S2.2.**

qRT-PCR screen for VDL2 overexpression (OE) compared to wild-type (WT) transcript

levels. Clones 2, 3, 6, 7 were chosen for analysis. Each data point represents an average of two wells.

## 2.7 REFERENCES

- Abriano, R. (2017) Insights into the molecular regulation of growth and carbon flux in marine diatoms. Diss. University of California, San Diego.
- Armbrust E. V., Berhes J. A., Bowler C., Green B. R., Martinez D., Putnam N. H., Zhou S., Allen A. E., Apt K. E., Bechner M., Brzezinski M. A., Chaal B. K., Ciovitti A., Davis A. K., Demarest M. S., Detter J. C., Glavina T., Goodstein D., Hazi M. Z., Hellsten U., Hildebrand M., Jenkins B. D., Jurka J., Kapitonov V. V., Kroger N., Lau W. W., Lane T. W., Larimer F. W., Lippmeier J. C., Lucas S., Medina M., Montsat A., Obornik M., Parker M. S., Palenik B., Pazour J. G., Richardson P. M., Rynearson T. A., Saito M. A., Schwartz D. C., Thamatrakoln K., Valentin K., Vardi A., Wilkerson F. P., Rokhsar D. S. (2004) The genome of the diatom *Thalassiosira pseudonana*: ecology, evolution, and metabolism. *Science* 306(5693): 79-86.
- Bendtsen J. D., Nielsen H., von Heijne G., Brunak S. (2004) Improved prediction of signal peptides: SignalP 3.0. *J Mol Biol* 340: 783-795.
- Bertrand M. (2010) Carotenoid biosynthesis in diatoms. *Photosynth Res* 106: 89-102.
- Bowler C., Allen A. E., Badger J. H., Grimwood J., Jabbari K., Kuo A., Maheswari U., Martens C., Maumus F., Ollilar R. P., Rayko E., Salamov A., Vandepoele K., Beszteri B., Gruber A., Heijde M., Katinka M., Mock T., Valentin K., VerretF., Berges J. A., Brownlee C., CadoretJ., Chiovitti A., Choi C. J., Coesel S., De Martino A., Detter J. C., Durkin C., Falciatore A., FournetJ., Haruta M., Huysman M. J. J., Jenkins B. D., Jiroutova K., Jorgensen R. E., Joubert Y., Kaplan A., Kroger N., Kroth P. G., La Rouche J., Lindquist E., Lommer M., Martin-Jezequel V., Lopez P. J., Lucas S., Mangogna M., McGinnis K., Medlin L. K., Montsant A., Oudot-Le Secq M., Napoli C., Obornik M., Parker M. S., Petit J., Porcel B. M., Poulsen N., Robison M., Rychlewski L., Rynearson T. A., Schmutz J., Shapiro H., Siaut M., Stanley M., Sussman M. R., Taylor A. R., Vardi A., von Dassow P., Vyverman W., Willis A., Wyrwicz L. S., Roksar D. S., Weissenbach J., Armbrust E. V., Green B. R., Van de Peer Y., Grigoriev I. V. (2008) The *Phaeodactylum* genome reveals the evolutionary history of diatom genomes. *Nature* 456: 239-244.
- BrunetC., Chandrasekaran R., Barra L., Giovagnetti V., Corato F., Ruban A. V. (2014) Spectral radiation dependent photoprotective mechanism in the diatom *Pseudo-nitzschia multiseries*. *PLoS One* 9(1): e87015.
- Chamovitz D., Sandmann G., Hirschberg J. (1993) Molecular and biochemical characterization of herbicide-resistant mutants of cyanobacteria reveals that phytoene desaturation is a rate-limiting step in carotenoid biosynthesis. *J Biol Chem* 268(23): 17348-17353.
- Coesel S., Obornik M., Varela J., Falciatore A., Bowler C. (2008) Evolutionary origins and functions of the carotenoid biosynthetic pathway in marine diatoms. *PLoS One* 3(8): e2896.
- Dambek M., Eilers U., Breitenbach J., Steiger S., Buchel C., Sandmann G. (2012) Biosynthesis of fucoxanthin and diadinoxanthin and function of initial pathway genes in *Phaeodactylum tricornutum*. *J Exp Bot* 63(15): 5607-5612.

Darley W., Volcani B. (1969) Role of silicon in diatom metabolism: a silicon requirement for deoxyribonucleic acid synthesis in the diatom *Cylindrotheca fusiformis* Reimann and Lewin. *Exp Cell Res* 58: 334–42.

Davis A., Abbriano R., Smith S. R., Hildebrand M. (2017) Clarification of photorespiratory processes and the role of malic enzyme in diatoms. *Protist* 168(1): 134-153.

De Castro E., Sigrist C. J. A., Gattiker A., Bulliard V., Langendijk-Genevaux P. S., Gasteiger E., Bairoch A., Hulo N. (2006) ScanProsite: detection of PROSITE signature matches and ProRule-associated functional and structural residues in proteins. *Nucleic Acids Res* 34(Web Server Issue): W362-W365.

Domingues N., Matos A. R., da Silva J. M., Cartaxana P. (2012) Response of the diatom *Phaeodactylum tricornutum* to photooxidative stress resulting from high light exposure. *PLoS One* 7(6): e38162.

Eilers U., Bikoulis A., Breitenbach J., Buchel C., Sandmann G. (2016) Limitations in the biosynthesis of fucoxanthin as targets for genetic engineering in *Phaeodactylum tricornutum*. *J Appl Phycol* 28(1): 123-129.

Emanuelsson O., Nielsen H., von Heijne G. (1999) ChloroP, a neural network-based method for predicting chloroplast transit peptides and their cleavage sites. *Protein Sci* 8(5): 978-984.

Finn R. D., Attwood T. K., Babbitt P. C., Bateman A., Bork P., Bridge A. J., Chang H., Dosztányi Z., El-Gebali S., Fraser M., Gough J., Haft D., Holliday G. L., Huang H., Huang X., Letunic I., Lopez R., Lu S., Marchler-Bauer A., Mi H., Mistry J., Natale D. A., Necci M., Nuka G., Orengo G. A., Park Y., Pesseat S., Piovesan D., Potter S. C., Rawlings N. D., Redaschi N., Richardson L., Rivoire C., Sangrador-Vegas A., Sigrist C., Sillitoe I., Smithers B., Squizzato S., Sutton G., Thanki N., Thomas P. D., Tosatto S. C. E., Wu C. H., Xenarios I., Yeh L., Young S., Mitchell A. L. (2017) InterPro in 2017 – beyond protein family and domain annotations. *Nucleic Acids Res* 45(Database Issue): D190-D199.

Goericke R., Welschmeyer N. A. (1992) Pigment turnover in the marine diatom *Thalassiosira weissflogii*. II The  $^{14}\text{CO}_2$ -labeling kinetics of carotenoids. *J Phycol* 28: 507-517.

Goss R., Pinto E. A., Wilhelm C., Richter M. (2006) The importance of a highly active and ΔpH-regulated diatoxanthin epoxidase for the regulation of the PSII antenna function in diadinoxanthin cycle containing algae. *J Plant Physiol* 163(10): 1008-1021.

Hildebrand M., Davis A. K., Smith S. R., Traller J. C., Abbriano R. (2012) The place of diatoms in the biofuels industry. *Biofuels* 3(2): 221-240.

Jakob T., Goss R., Wilhelm C. (2001) Unusual pH-dependence of diadinoxanthin de-epoxidase activation causes chlororespiratory induced accumulation of diatoxanthin in the diatom *Phaeodactylum tricornutum*. *J Plant Physiol* 158: 383-390.

Kadono T., Kira N., Suzuki K., Iwata O., Ohama T., Okada S., Nishimura T., Akakabe M., Tsuda M., Adachi M. (2015) Effect of an introduced phytoene synthase gene expression on carotenoid biosynthesis in the marine diatom *Phaeodactylum tricornutum*. *Mar Drugs* 13(8): 5334-5357.

Kaur S., Spillane C. (2015) Reduction in carotenoid levels in the marine diatom *Phaeodactylum tricornutum* by artificial microRNAs targeted against the endogenous *phytoene synthase* gene. Mar Biotechnol 17(1): 1-7.

Kelley L. A., Mezulis S., Yates C. M., Wass M. N., Sternberg M. J. E. (2015) The Phyre2 web portal for protein modeling, prediction and analysis. Nat Protoc 10: 845-858.

Kirst H., Garcia-Cerdan J. G., Zurbiggen A., Ruehle T., Melis A. (2012) Truncated photosystem chlorophyll antenna size in the green microalga *Chlamydomonas reinhardtii* upon deletion of the *TLA3-CpSRP43* gene. Plant Physiol 160(4): 2251-2260.

Kozlowski W. A., Deutschman D., Garibotti I., Trees C., Vernet M., An evaluation of the application of CHEMTAX to Antarctic coastal pigment data. Deep-Sea Res. Pt I 58 (2011) 350-364.

Lavaud J., Lepetit B. (2012) An explanation for the inter-species variability of the photoprotective non-photochemical chlorophyll fluorescence quenching in diatoms. Biochim Biophys Acta 1827(3): 294-302.

Lavaud J., Materna A. C., Sturm S., Vugrinec S., Kroth P. G. (2012) Silencing of the violaxanthin de-epoxidase gene in the diatom *Phaeodactylum tricornutum* reduces diatoxanthin synthesis and non-photochemical quenching. PLoS One 7(5): e36806.

Lavaud J., Rousseau B., Etienne A. (2004) General features of photoprotection by energy dissipation in planktonic diatoms. J Phycol 40: 130-137.

Lepetit B., Goss R., Jakob T., Wilhelm C. (2012) Molecular dynamics of the diatom thylakoid membrane under different light conditions. Photosynth Res 111(1-2): 245-257.

Lepetit B., Volke D., Gilbert M., Wilhelm C., Goss R. (2010) Evidence for existence of one antenna-associated, lipid-dissolved and two protein-bound pools of diadinoxanthin cycle pigments in diatoms. Plant Physiol 154: 1906-1920.

Letunic I., Bork P. (2016) Interactive tree of life (iTOL) v3: an online tool for the display and annotation of phylogenetic and other trees. Nucleic Acids Res 44(Web Server Issue): W242-W245.

Lohr M., Wilhelm C. (1999) Algae displaying the diadinoxanthin cycle also possess the violaxanthin cycle. PNAS 96(15): 8784-8789.

Lohr, M., Wilhelm C. (2001) Xanthophyll synthesis in diatoms: quantification of putative intermediates and comparison of pigment conversion kinetics with rate constants derived from a model. Planta 212(3): 382-391.

Marchler-Bauer A., Bo Y., Han L., He J., Lanczycki C. J., Lu S., Chitsaz F., Derbyshire M. K., Geer R. C., Gonzales N. R., Gwadz M., Hurwitz D. I., Lu F., Marchler G., Song J. S., Thanki N., Wang Z., Yamashita R. A., Zhang D., Zheng C., Geer L. Y., Bryant S. H. (2017) CDD/SPARCLE: functional classification of proteins via subfamily domain architectures. Nucleic Acids Res 45(Database Issue): D200-D203.

Martin J. F., Gudina E., Barredo J. L. (2008) Conversion of β-carotene into astaxanthin: two separate enzymes or a bifunctional hydroxylase-ketolase protein? Microb Cell Fact 7:3.

Melendez-Martinez A. J., Mapelli-Brahm P., Benitez-Gonzalez A., Stinco C. M. (2015) A comprehensive review on the colorless carotenoids phytoene and phytofluene. *Arch Biochem Biophys* 572: 188-200.

Moskalenko A. A., Karapetyan N. V. (1996) Structural role of carotenoids in photosynthetic membranes. *Z Naturforsch* 51c: 763-771.

Peng J., Yuan J., Wu C., Wang J. (2011) Fucoxanthin, a marine carotenoid present in brown seaweeds and diatoms: metabolism and bioactivities relevant to human health. *Mar Drugs* 9: 1806-1828.

Petersen T. N., Brunak S., von Heijne G., Nielsen H. (2011) SignalP 4.0: discriminating signal peptides from transmembrane regions. *Nat Methods* 8: 785-786.

Robinson J. T., Thorvaldsdottir H., Winckler W., Guttman M., Lander E. S., Getz G., Mesirov J. P. (2011) Integrative Genomics Viewer. *Nature Biotechnol* 29: 24-26.

Santabarbara S., Casazza A. P., Ali K., Economou C. K., Wannathong T., Zito F., Redding K. E., Rappaport F., Purton S. (2013) The requirement for carotenoids in the assembly and function of photosynthetic complexes in *Chlamydomonas reinhardtii*. *Plant Physiol* 161: 535-546.

Shrestha R. P., Haerizadeh F., Hildebrand M. (2013) Molecular genetic manipulation of microalgae: principles and applications. In: Richmond A., Hu X. (Eds), *Handbook of microalgal culture: applied phycology and biotechnology*, 2<sup>nd</sup> edn. John Wiley & Sons, Ltd., Oxford UK, pp. 146-167.

Shrestha, R. P., Hildebrand M. (2015) Evidence for a regulatory role of diatom silicon transporters in cellular silicon responses. *Eukaryot Cell* 14(1): 29-40.

Sievers F., Wilm A., Dineen D., Gibson T. J., Karplus K., Li W., Lopez R., McWilliam H., Remmert M., Soding J., Thompson J. D., Higgins D. G. (2011) Fast, scalable generation of high-quality protein multiple sequence alignments using Clustal Omega. *Mol Syst Biol* 7: 539.

Smith S. R., Abbriano R. M., Hildebrand M. (2012) Comparative analysis of diatom genomes reveals substantial differences in the organization of carbon partitioning pathways. *Algal Res* 1(1): 2-16.

Smith S. R., Gle C., Abbriano R. M., Traller J. C., Davis A., Trentacoste E., Vernet M., Allen A. E., Hildebrand M. (2016) Transcript level coordination of carbon pathways during silicon starvation-induced lipid accumulation in the diatom *Thalassiosira pseudonana*. *New Phytol* 210(3): 890-904.

Thorvaldsdottir H., Robinson J. T., Mesirov J. P. (2013) Integrative Genomics Viewer (IGV): high-performance genomics data visualization and exploration. *Brief Bioinform* 14: 178-192.

Tian L., DellaPanna D. (2004) Progress in understanding the origin and functions of carotenoid hydroxylases in plants. *Arch Biochem Biophys* 430(1): 22-29.

Tran D., Haven J., Qiu W., Polle J. E. W. (2009) An update on carotenoid biosynthesis in algae: phylogenetic evidence for the existence of two classes of phytoene synthase. *Planta* 229(3): 723-729.

Wilhelm C., Buchel C., Fisahn J., Goss R., Jakob T., LaRoche J., Lavaud J., Lohr M., Riebesell U., Stehfest K., Valentin K., Kroth P. G. (2006) The regulation and nutrient assimilation in diatoms is significantly different from green algae. *Protist* 157(2): 91-124.

Wu H., Cockshutt A. M., McCarthy A., Campbell D. A. (2011) Distinctive photosystem II photoinactivation and protein dynamics in marine diatoms. *Plant Physiol* 156(4): 2184-2195.

## APPENDIX 2.A BLAST RESULTS

### 1. Phytoene Synthase (PSY)

Previously reported single-copy PSY in *P. tricornutum* (Phatr2\_56481) [Coesel et al. 2008], was confirmed to have no other BLAST hits in the *P. tricornutum* genome. A BLAST search against the *T. pseudonana* genome yielded two hits, one previously published as PSY1 (Thaps3\_268908) [Coesel et al. 2008], and previously unpublished Thaps3\_263269, which overlaps with previously published PSY2 (Thaps3\_258309) [Coesel et al. 2008].

### 2. Phytoene Desaturase (PDS)

BLAST queries of the previously published *P. tricornutum* PDS1 (Phatr2\_45735) and PDS2 (Phatr2\_55102) [Coesel et al. 2008] against the *P. tricornutum* genome yielded each other, as well as a large chromosomal region (chr\_1:926023-1979107) that includes Phatr2\_53974, the  $\zeta$ -carotene desaturase (ZDS) (3). In *T. pseudonana*, BLAST searches with the aforementioned *P. tricornutum* gene products yielded Thaps3\_23291, which overlaps with the previously published PDS1 (Thaps3\_6524) [Coesel et al. 2008], Thaps3\_1383, previously published as PDS2 [Coesel et al. 2008], Thaps3\_bd\_1474 (not previously published), as well as the *T. pseudonana* ZDS (3), Thaps3\_28432.

### 3. $\zeta$ -Carotene Desaturase (ZDS)

No candidates besides Phatr2\_53974 and Thaps3\_24832 (2) were found. The former had been reported by Coesel et. al. [2008], and the latter overlaps with the previously published gene model, Thaps3\_37288 [Coesel et al. 2008].

#### *4. Carotene Cis-Trans Isomerase (Prolycopene Isomerase) (CRTISO)*

Exhaustive reciprocal BLAST searches between the *P. tricornutum* and *T. pseudonana* genomes starting with the products of four genes identified by Dambeck et al. [2012] as *P. tricornutum* CRTISO candidates (Phatr2\_45243, Phatr2\_9210, Phatr2\_54842, Phatr2\_51868) as queries yielded numerous hits in both organisms.

For *P. tricornutum*, the findings (in addition to the aforementioned genes) were Phatr2\_54826, Phatr2\_54800, Phatr2\_42980. Three large chromosomal regions were repeatedly found as well: chr\_1:1011072-1894441 (containing Phatr2\_42890, Phatr2\_9210, and Phatr2\_53974, the ZDS), chr\_6:586147-620230 (containing Phatr2\_45243), and chr\_15:52824-647530 (containing Phatr2\_54826 and Phatr2\_54800).

The findings for *T. pseudonana* were Thaps3\_7094, Thaps3\_21900, Thaps3\_21847, Thaps3\_5221, Thaps3\_10233, Thaps3\_11636, Thaps3\_5859, Thaps3\_25361, and Thaps3\_10254. Two large chromosomal pieces were also found: chr\_6:68923-1558412 (containing Thaps3\_5859) and chr\_15:676997-739441 (containing Thaps3\_10233 and Thaps3\_10254).

#### *5. Lycopene $\beta$ -cyclase (LCYB)*

Phatr2\_56484 [Coesel et al. 2008] generated no additional BLAST hits in the *P. tricornutum* genome, and only Thaps3\_270357 in the *T. pseudonana* genome. The latter generated no additional BLAST hits in either of the genomes, and overlapped with the previously reported gene model, Thaps3\_261407 [Coesel et al. 2008].

## *6. $\beta$ -Carotene Hydroxylase (BCH)*

As reported in Coesel et al. [2008], no BCH was found in the *P. tricornutum* genome, and only Thaps3\_263437, previously reported as a partial sequence [Coesel et al. 2008], was found in the *T. pseudonana* genome.

## *7. LUT-Like (Lutein Deficient-Like) (LTL)*

Exhaustive reciprocal BLAST searches between the *P. tricornutum* and *T. pseudonana* genomes, starting with Phatr2\_50101 and Phatr2\_26422 reported as LTL1 and LTL2, respectively, by Coesel et al. [2008], yielded many hits in both genomes.

For *P. tricornutum*, the findings were Phatr2\_34027, Phatr2\_33568, Phatr2\_6940, Phatr2\_46438, Phatr2\_31339, Phatr2\_47234, Phatr2\_37006, Phatr2\_43466, Phatr2\_43467, Phatr2\_43562, Phatr2\_50619, Phatr2\_43469, Phatr2\_32833, Phatr2\_43537. Several regions without available gene models also appeared in the BLAST results: chr\_2:488287-489217, chr\_4:1314546-1315166, chr\_8:134705-134894, chr\_8:983359-983442, chr\_15:149534-149668, and chr\_15:494943-495059. Where open reading frames were readily apparent, the hypothetical protein products were included as BLAST search queries. Additionally, there were several larger regions: chr\_2:487571-543110, chr\_2: 540661-973489, chr\_4:48892-1315175 (contains Phatr2\_34027), chr\_8:134708-983593, and chr\_11:518522-869181 (includes Phatr2\_37006).

For *T. pseudonana*, Thaps3\_9541 was confirmed to be LTL1, and a more complete model for LTL2 (Thaps3\_270336) compared to the previously reported one that was missing the N-terminus (Thaps3\_36235), was found [Coesel et al. 2008]. Additional results were Thaps3\_33926, Thaps3\_32491, Thaps3\_1549, Thaps3\_264647, Thaps3\_25944, Thaps3\_14875, Thaps3\_4027,

Thaps3\_4026, Thaps3\_bd\_518, Thaps3\_269400, Thaps3\_264325, Thaps3\_263399. Two large chromosomal regions were also found: chr\_9:88966-685832 (includes Thaps3\_270336) and chr\_3:2376984-2382496 (includes Thaps3\_14875, Thaps3\_4026, Thaps3\_4027, and Thaps3\_25944, which appear immediately adjacent to each other, in the order listed).

#### *8. Zeaxanthin Epoxidase (ZEP)*

For *P. tricornutum*, previously published [Coesel et al. 2008] ZEP1 (Phatr2\_45845), ZEP2 (Phatr2\_56488), and ZEP3 (Phatr2\_56492) were confirmed. Additionally, Phatr2\_43425, Phatr2\_47925, Phatr2\_45936, and chr\_21:64775 – 64879 (no gene model) were found.

For *T. pseudonana*, Thaps3\_270370 was identified as ZEP1, overlapping with the previously reported Thaps3\_269147, and Thaps3\_261390 was confirmed as ZEP2 [Coesel et al. 2008]. Additional findings were Thaps3\_1961, Thaps3\_6395, Thaps3\_20663, Thaps3\_22671, and chr\_9:932102-933624 (no gene model).

#### *9. Violaxanthin De-Epoxidase (VDE), VDE-Like (VDL), VDE-Related (VDR)*

In *P. tricornutum*, previously published VDE (Phatr2\_44635), VDL1 (Phatr2\_46155), and VDL2 (Phatr2\_45846) were confirmed [Coesel et al. 2008], and Phatr2\_bd\_1281 was found. Additional found sequences without available gene models were bd\_29x34:989-1110, chr\_2:9199-9410, and chr\_1:974981-975118.

In *T. pseudonana*, previously reported VDE (Thaps3\_7677) and VDL1 (Thaps3\_22076) were confirmed [Coesel et al 2008], and Thaps3\_11707 as well as chr8: 84698 – 842033 were found.

Only previously reported Phatr2\_56450 and Thaps3\_270211 [Coesel et al. 2008] were found in the VDR search.

## APPENDIX 2.B ALIGNMENTS AND PERCENT IDENTITY MATRICES

### 1) CRTISO Percent Identity Matrix

```

1: Thaps3_25361 100.00 47.05 16.73 16.24 16.79 18.23 19.17 18.06 16.46 17.20 15.98 19.00 18.10 18.94 17.98 19.76
2: Phatr2_42980 47.05 100.00 16.61 16.85 16.60 16.04 16.96 18.22 16.96 17.09 19.25 18.32 19.62 19.64 17.65 19.75
3: Thaps3_5221 16.73 16.61 100.00 57.64 35.21 36.94 32.19 32.73 30.20 31.70 32.04 32.56 18.32 18.30 17.49 19.42
4: Phatr2_54826 16.24 16.85 57.64 100.00 36.55 35.94 34.01 32.73 31.65 33.06 32.34 34.94 17.92 20.03 18.49 19.77
5: Thaps3_21847 16.79 16.60 35.21 36.55 100.00 58.92 36.35 37.59 32.29 33.98 32.16 35.21 17.42 18.71 18.18 22.05
6: Phatr2_51868 18.23 16.04 36.94 35.94 58.92 100.00 35.51 34.78 31.49 33.59 31.83 34.95 20.00 19.75 18.37 20.99
7: Thaps3_7094 19.17 16.96 32.19 34.01 36.35 35.51 100.00 59.07 34.94 38.37 37.07 38.36 22.20 22.60 20.13 22.95
8: Phatr2_54842 18.06 18.22 32.73 32.73 37.59 34.78 59.07 100.00 33.74 37.45 35.55 38.13 21.05 20.56 20.48 21.98
9: Thaps3_10233 16.46 16.96 30.20 31.65 32.29 31.49 34.94 33.74 100.00 85.09 36.67 36.57 18.40 20.49 17.93 20.19
10: Phatr2_9210 17.20 17.09 31.70 33.06 33.98 33.59 38.37 37.45 85.09 100.00 37.65 38.39 19.05 21.46 20.10 22.53
11: Thaps3_21900 15.98 19.25 32.04 32.34 32.16 31.83 37.07 35.55 36.67 37.65 100.00 43.01 18.59 19.59 19.51 19.76
12: Phatr2_45243 19.00 18.32 32.56 34.94 35.21 34.95 38.36 38.13 36.57 38.39 43.01 100.00 20.35 22.35 20.78 21.30
13: Thaps3_11636 18.10 19.62 18.32 17.92 17.42 20.00 22.20 21.05 18.40 19.05 18.59 20.35 100.00 59.69 22.22 27.49
14: Phatr2_54800 18.94 19.64 18.30 20.03 18.71 19.75 22.60 20.56 20.49 21.46 19.59 22.35 59.69 100.00 21.68 24.68
15: Thaps3_5859 17.98 17.65 17.49 18.49 18.18 18.37 20.13 20.48 17.93 20.10 19.51 20.78 22.22 21.68 100.00 28.43
16: Thaps3_10254 19.76 19.75 19.42 19.77 22.05 20.99 22.95 21.98 20.19 22.53 19.76 21.30 27.49 24.68 28.43 100.00

```

### CRTISO Alignment

Thaps3_25361	MRMGRPNKKLRLSTSQTTNPNNPKYSSPTLVVGQVSSNVIHSIYGPALTKLAVESV---	56
Phatr2_42980	MRIGKPLRKSRRAWKKV-GVNNGTPKYVSPESVVGRINSDIISSVLAPKIAALASAL---	55
Thaps3_5221	-----	0
Phatr2_54826	-----	0
Thaps3_21847	-----	0
Phatr2_51868	-----	0
Thaps3_7094	-----	0
Phatr2_54842	-----	0
Thaps3_10233	-----	0
Phatr2_9210	-----	0
Thaps3_21900	-----	0
Phatr2_45243	-----	0
Thaps3_11636	-----	0
Phatr2_54800	-----MTPVTQSPPVELSTD-PPVALSLALPPLSPTADGTLQHHH	39
Thaps3_5859	-----	0
Thaps3_10254	-----	0
Thaps3_25361	-----EEYADAV-LRWEASLPEVLVK-----	76
Phatr2_42980	-----ERYAGEL-LVYEDIMKKVNSN-----	75
Thaps3_5221	-----	0
Phatr2_54826	-----	0
Thaps3_21847	-----	0
Phatr2_51868	-----	0
Thaps3_7094	-----	0
Phatr2_54842	-----	0
Thaps3_10233	-----	0
Phatr2_9210	-----	0
Thaps3_21900	-----	0
Phatr2_45243	-----	0
Thaps3_11636	-----	0
Phatr2_54800	LTTTDDESSSPWPVIRSVFRGQNNFSDPLNRGWNPWRPGISSLQDKCGVEYVKMHGQYFP	99
Thaps3_5859	-----	0
Thaps3_10254	-----	0
Thaps3_25361	-----P-----SQLDDAEDIDVDADGTFEKGEEVEVDLDGSILPSHDNDDKTSS	121
Phatr2_42980	-----E-----S-----IDGLLESDS-----SIIIQ---DG---I	94
Thaps3_5221	-----	0
Phatr2_54826	-----	0
Thaps3_21847	-----	0
Phatr2_51868	-----	0
Thaps3_7094	-----	0
Phatr2_54842	-----	0
Thaps3_10233	-----	0
Phatr2_9210	-----	0

Thaps3_21900	-----	0
Phatr2_45243	-----	0
Thaps3_11636	-----	0
Phatr2_54800	TSGSGFSTGPVGQHDGHELEQRCDTERQGGGVNKGNHVEANVATSVLCATE-----CCL	154
Thaps3_5859	-----	0
Thaps3_10254	-----MGFIVRGTRARSVS-----SR-----LAV	20
Thaps3_25361	PTMPTSNNRL--FTTQSSIDNLTALLTDSQH-FSTTNAWKIHANAAKFERLLDEKYGRFR	178
Phatr2_42980	PQQ-PQRPV--FHSQFSVDEAASIFSETSEHFFAKAGKWKAHANAAKFERILDEKYGILR	151
Thaps3_5221	-----	0
Phatr2_54826	-----MLV-----ESKKSRDG---SRTSS---RS---	18
Thaps3_21847	-----	0
Phatr2_51868	-----	0
Thaps3_7094	-----	0
Phatr2_54842	-----	0
Thaps3_10233	-----	0
Phatr2_9210	-----	0
Thaps3_21900	-----	0
Phatr2_45243	-----	0
Thaps3_11636	-----	0
Phatr2_54800	PHREPEPKTVCVVVLRLSQLRDPTFQQDEVSALGAFRGWIGNEVDRLFEW---AA---	206
Thaps3_5859	-----	0
Thaps3_10254	KGQSPNPL-----ESQLTNW---RE---	37
Thaps3_25361	PFIESHPELEVFIKKVQRKYAMGQFSPLRKGECPMSTSSIMLLFMMHRNGVRKELVALV	238
Phatr2_42980	PFITNHPEIEHFIRGVQRKYAMGYFSPRQGDPIPRTAVIILFMMQRGQMRWEIMLLT	211
Thaps3_5221	-----	0
Phatr2_54826	-----LDTKTHCVCSTS-----KQ-----	32
Thaps3_21847	-----	0
Phatr2_51868	-----	0
Thaps3_7094	-----	0
Phatr2_54842	-----	0
Thaps3_10233	-----	0
Phatr2_9210	-----	0
Thaps3_21900	-----	0
Phatr2_45243	-----	0
Thaps3_11636	-----	0
Phatr2_54800	-----TAAKALCMANWQ-----GKSRLLK---K---FGATVRRLD	235
Thaps3_5859	-----	1
Thaps3_10254	-----PPRRPFSKVQTH-----ASNQL-----QSEVM	59
Thaps3_25361	ALFTLVGLEPWALVGLVCVGKYSVDQRRRKRIGGMP-----KKVKV---V	280
Phatr2_42980	TLFFFLIGLQPWALVAVVGVLQGLLMRRKAKPLGKMK-----RFIPA---V	253
Thaps3_5221	-----	22
Phatr2_54826	-----NSVRPANTLLRSR-----ARHTLIWLFYVWEWNTTTAFAPSRIA	75
Thaps3_21847	-----MK-----VSTTAT-FALLQIGTAAVSAFTSP-----	25
Phatr2_51868	-----MANISKD-R--L-TGRFLA-FLLLVLANKETSSFCVQSGYRS	37
Thaps3_7094	-----MLPHT-----TVHGVVALATLLLNAFVLVDSFAPS-----	30
Phatr2_54842	-----MFAISSQLT--LTLVGHILLHHMM-ENSAICSAFPASQRTT	39
Thaps3_10233	-----MIGRKY---S-LAASA---LAIIA-SLTSTTAFAAPPSSLL	33
Phatr2_9210	-----	0
Thaps3_21900	-----MIR-----SISA---LALLAACCPSVFSFAPLSVF--	27
Phatr2_45243	-----MR-----FSER---SLIACAICSISSAFVPIIHTPO	28
Thaps3_11636	-----MNT-----ITDLLFQNPSFTIV-L-----LPLLFTASFIFYIT-----	32
Phatr2_54800	KACGPFGWTAWILFPCQTLQMQRDRHYTR-YAIGRS-R-TLGDAESCFLVWL-----	284
Thaps3_5859	ELFSSINYDPWTLPAS-----FY-Y-PTIITA-C-IPLLFIATAYWLLIRR-----	45
Thaps3_10254	DSLSKISS---SLLGDGKHT---KVTTV-ATVAGL-T-LGTLFIARRIYL-----	101
Thaps3_25361	ESYYAHGVG-----EEESEEVERSK---KYAILEKPVGT-----IFNPA	319
Phatr2_42980	ESYYTDAKTDT-----EK-----HELLLHPVGE-----PL-PS	280
Thaps3_5221	T-D-----	40
Phatr2_54826	AFRA-----SRGR-----KLTTSVSSLVSGDKRD	99
Thaps3_21847	---SI-----NSVIRSPSTHLRS-----SPSATAST-----	48
Phatr2_51868	RHYFSA-----NFLSVQPSDVARG-----SSTAPAAAI---ADAPT	70
Thaps3_7094	-PRCSH-----R-----YH-----I---SSAA---STTLH	48
Phatr2_54842	FSNCRR-----S-KN-----RVGRHGCF---LLASQ	61
Thaps3_10233	RSTRHLHSTVEETTNGEAATNTNVEQIKDTSRDKVMTFSYDMSIEPKYEKPTY---PGTGN	90

Phatr2_9210	-----		0
Thaps3_21900	-----RANAP-----SSL		35
Phatr2_45243	-----H-----QSPRTTRH---QFT-----RIYAAV-----SSV		49
Thaps3_11636	-----RWPQARP-VQFRR-----AD--RFRPEKV		53
Phatr2_54800	-----HWPARRVKLHPRR-----AS--RFRPELV		306
Thaps3_5859	---QLH-----REKGKLPKYDAIP-----SSVLKHIASKQ		72
Thaps3_10254	-----WMKEFPSSDSLP-----STNPVKQ-GFS		123
Thaps3_25361	DLSLRDEEYDVILLGCGPEVLYTASLL-SRAGKKTIVLSPREDASGCLTLQNG-----		371
Phatr2_42980	KEEIDASLFDALILGSGPASLYIASLL-SRAGRKVLVLSRNADSGCLSIKHAE-----		333
Thaps3_5221	DGGDEVHEVDIAVVAGAGIGGLCAGAIALNTLYDKKVGVYESHYLAGGCAHSFSRSVK-----		96
Phatr2_54826	CASPADDLVDAVIAGAGLGGLCAGAIALNTLYGKKVGIYEAHYLAGGCAHAFDRRAA-----		155
Thaps3_21847	ITDADEEEWDVVVVGSGVGGLSAAAMC-ARYGLKTICVEAHADAPGVAHSFERRAS-----		103
Phatr2_51868	GSIYREETVDVVVIGAGVGGLSCAALS-SKYGMDTLCLEAHDTAGGCAHSFERYSA-----		125
Thaps3_7094	ATTPPHSEYDAIIVGSGIGGLSAAALL-SHYGYSVAVFAEHSTPGAAHGYTVNA-----		102
Phatr2_54842	SATPGTTSPVVVGSGIGGLCAAAML-AKYGYTVALSHNVPGGAAHGFTRDP-----		116
Thaps3_10233	GMSGDSGEYDIVIGSGMGGLACSAALS-AKYGSRVLCLESIHVKCGGAHTFSRMHN-----		145
Phatr2_9210	-----DVIVIGSGMGGLACGALS-AKYGDKVLVLESHIKCGGAHTFSRMHN-----		46
Thaps3_21900	ASTTYQDEVDCIVIGSGIGGLSACALL-AATGRTVRVLEQHYEIGGCAGAHFYMDMNGKTV		94
Phatr2_45243	PSNSIPDEADVVVIGSGLAGLSCAALL-AHCGKRVVVLRESHDAPGAAHGW-----		100
Thaps3_11636	P----SNIDIVIGSGSGGTVANLL-AQSGQRLVLEQHSVITGGCTHSFR-----		99
Phatr2_54800	LENGKQRRFDTIVIGSGSGGCACANLL-AQSGQRLVILEQHTKTGGCTHSFR-----		357
Thaps3_5859	VLRDLSGKIDVAIVGSGIAALNASAL-AHQGYKIAVFQEINVGGCTHTFE-----		123
Thaps3_10254	IKSVSSTNWDVIVIGSGAGGLTTAALL-SKEGKKVLVLEQHDIAGGNLHTFS-----		174
	: : * . * . : . . . . *		
Thaps3_25361	-----KTNVPFDIDGSNIAHLARQ-----QSLLAPA-----LCTTTDT		404
Phatr2_42980	-----YSNVPFDVEASNVAKISRQ-----QQILAPA-----LCTETDT		366
Thaps3_5221	-----IGDDEQPTTFTFDSCPTIVLGCSK-----EPYNPLQQVLRAGVDDQIEWLPYDG		146
Phatr2_54826	-----D-----GVNFTFDSCPTILLGCSS-----PPFNALQVQLDAVGQK-----		190
Thaps3_21847	-----SSPNRPVFDSCPSLLSGMSS-----KGTNPLRQVLDAVGTAEEVQWKTYDG		150
Phatr2_51868	-----ASKTTPFRCDFDSCPSLVSGLSE-----KGTNPLRQVLDAVGTAEEVQWKTYDG		172
Thaps3_7094	-----KDVGPLTFDTGPSFFSGLNSNPYPAKSSNPLRSILDIID--EKVECIPYTT		150
Phatr2_54842	-----KIEGEFRFDGPSFFSGINSDTPAKASNPLRTVLDIAID--ERVECIPYTT		164
Thaps3_10233	-----GGKYSFEVGPSSIFEGLDR-----PSLNPLRMIFDILE--ETMPVKTYKG		187
Phatr2_9210	-----GEKYSFEVGPSSIFEGLDR-----PSLNPLRMIFDVL--EEMPVKTYTG		88
Thaps3_21900	PSSALKDDPTKKKGELFHFEAGPSLYSGLSEE--RTPNPLKHIYQMIE--EEPEWLTYDQ		149
Phatr2_45243	-----RRGFHFESGPSSLYSGFAME--RSPNPLKNIFOITG--EDCEWITYDR		143
Thaps3_11636	-----EEGCEWDTGLHYVSKAMA---TPTKRAGAIMSFMS-RGKQSFTPFP		142
Phatr2_54800	-----DRGCEWDTGLHYTSAGMG---RSTCRPGAIMHFMT-QGLQKWTPL--		398
Thaps3_5859	-----KQGFEEFDVGVHVYVGGFG-----TVVKHMYDELS-DGQLKWTKL--		160
Thaps3_10254	-----EKGYEFDTGLHYVGGKVG-----DKSSSVRKQLDYVM-DTDVEWEKM--		215
	: :		
Thaps3_25361	QGGIRFA-----RIG-SEVDGYAHISLSPGLGTDISNECIPIVLT-----AEGEV		450
Phatr2_42980	QGGVRFA-----QIG-SNEDAHAFEIILSIPGMGTDSYDEELPFILNA-----DGGTA		412
Thaps3_5221	WGMIEHPMQ-----PKEKRWKF--KV---G---PNHFEDGPLQVF--ASNLN		183
Phatr2_54826	-----NPGK-----DNELRWKV--IL---G---RDEFQRGPLTRF--GG-PK		221
Thaps3_21847	WMVHDTAfp-----MDDSRSSFRLT-----G---SDGTWEDAIEAKAG--VDSRR		191
Phatr2_51868	WLVHDT-----DDKVFKVTT-----G---DSGAFEDALEKKAG--INAKR		208
Thaps3_7094	FGLMFPE-----GVFVHSSNF-----G---KEG-STVEA-----VSGSN		180
Phatr2_54842	FGLQFPE-----GNFEHSCFF-----G---AQG--GLLEQ-----LQGTT		194
Thaps3_10233	LGWTPS-----GYWRFPPIGS-----REGFQELLMEQCG--EDGEK		221
Phatr2_9210	LGWTPPT-----GYWRFPPIGS-----QSKFEDLLMEQA--EDGPK		121
Thaps3_21900	WGAFLPE-----APEGYQMSI-----G---AENFCKILET-----YGEG		181
Phatr2_45243	WGTVMMPD-----GT-KFAAKI-----G---PEEFQDVLES-----QGGPG		174
Thaps3_11636	STPYDEIVFPKDANVKDGAPNEFSHKF--YD---G---VNRTVSSVIGSIDPSNELKH		193
Phatr2_54800	QDPYDEVIFPPDDFVKLGVPNESSYRF--VS---G---ADETIQSVLASIDPEHRELEK		449
Thaps3_5859	DRVYDVMYNGRTG-----ERYEI-TD---D---HDK-----NRRLTK		191
Thaps3_10254	DIYDVAICDEEQ-----F--NF--CS---S---WKT-----LKVELKK		244
Thaps3_25361	ALAEYCSTYLGDAFPGTLDGNDNGNSTSLSYLKACGQINAGSGDFYL-----AKLFP		503
Phatr2_42980	GLIDDAAKYLNDGWPDAE--GGNGNSVTGAYAAACEAINSTANEFYI-----SKILS		462
Thaps3_5221	ALEEF-----NQLREITKPLVTGAATI PAMAMRPGQSAVL		218
Phatr2_54826	ALEEF-----EALREATKDLLAG-AKIPAMAMRPGPSALV-		255
Thaps3_21847	EFTKF-----KKKMMSSGLSESSALLPPMALRGDFGALF-		226
Phatr2_51868	EFIEF-----KRKVLEEGGLAEASAYIIPPFA RGCGITALA-		243
Thaps3_7094	GVQEWF-----ASLMKSMDPLA QAVDAMPTLALRADLGLLA-		215
Phatr2_54842	AQKEW-----QALMQSMGPLEKAVAALPTAALRGDIGLL-		229

Thaps3_10233	AIGEW-----	KALRERLRTLGGSTQAVALLNLRQAGFLA-	256
Phatr2_9210	AVEEW-----	NMLRKRLKTLGGSTTAVSLLNLRQDPGFLA-	156
Thaps3_21900	AVEDW-----	EKLAEQIIRPMAGGIKGIPHAAIRGDWGIFL-	216
Phatr2_45243	AREEF-----	AALMERMKPLSDAAQALTSLALREDPAVVV-	209
Thaps3_11636	RVDTF-----	MDI---CLDVHNG---F-VAL--GIYRLLP	219
Phatr2_54800	RARLY-----	MDL---CTDINSG---F-TAL--GISRVL	475
Thaps3_5859	DFGID-----	EQSW-RKFDRKKAYAKFWAMVV--FSLKLFH	224
Thaps3_10254	KFPEE-----	SDAIDKHFQLVQSTVKLFPVFM--GIKNLPT	278
.			
Thaps3_25361	KAAES-----	FKSSDSNV----YQQ-ASIRPASTFL----N-KCLPLNTHVRAL	542
Phatr2_42980	EKVNS-----	LRS--SPT----YQD-SGIRYAOQSL----N-KTFTINPHTRSL	499
Thaps3_5221	PLLRY-----	LPSLISI---ISNGVEASTGPFPAPYM---NGPIFTVKDPWLRSW	261
Phatr2_54826	PLIRY-----	FSTLVTL---LSQGSK-ATGTFASFI---DGPNFTVTDPWLRSW	297
Thaps3_21847	T-MGS-----	YVFKFLT---IGLOQTLLTGPFTECM----N-LYGLNDRFNRQW	266
Phatr2_51868	S-LAN-----	YMFKLLS---IGSKGALLTGPFSKVM----D-LHGLKDPFVRKW	283
Thaps3_7094	STSQF-----	LPNFAKL---NPLQNLKLTKPFNSII---N-EAGVKDTFIRNW	256
Phatr2_54842	TAAPF-----	LPNFTTL---NPLENLKLTPQFSAIV---N-P-SVSNVFTRNW	269
Thaps3_10233	TTAGS-----	LPFVVTB---PDVFG-DLSLTFFDLS---KTVDEFVTVPFLRN	298
Phatr2_9210	TTAGS-----	LPFVATH---PDVFL-DLSLTFDLSH---KTVDKIVTVPFLRN	198
Thaps3_21900	TLILK-----	YPLSFNMN--VLKYAPAFATAPFD--L---D-KLGVTNKFLRN	255
Phatr2_45243	-TLLK-----	YPRDLIA---TQAQGQALNEPFKNM----D-EMKIEKFKVKNW	249
Thaps3_11636	SYLKFLMKDKVERLYKYGSMTVKDAQHAVLKLGYSKEELLK-NCPTAP-EMEDDP SIRR	277	
Phatr2_54800	SWMHFLVRSRIDRLMKFAAMTVRDVQYGMNLNLGTIEELLKDGCPPAPAGSEPDPSIR	535	
Thaps3_5859	PMVRLA-----	WPFVC---IPYRRCALRSTIDVL-----NDCGFSQEA	261
Thaps3_10254	PLFRLVM-----	WLFDS---K---LGVYRKTTKEVL-----ESITSNRKL	312
:			
Thaps3_25361	MAAI--GMANE NLSPDKTSMAAHVTNVCAMTSTEGYA-----	YPVGGPRA LCHALTS	592
Phatr2_42980	MAGI--GMKGENIRPGAT SMAAHVTNI SAALS GEGMH-----	YPIGGPRA LCR ALAN	549
Thaps3_5221	LNALAFSLSG---LPADRTSAGAMAYVLFDMHREGAA-----	LDYPRGGLGEVV KALVN	312
Phatr2_54826	LDALAFSLSG---LPASRTAAA MAF TLSDMHRGAA-----	LDYPKGGMGAIAEALVR	348
Thaps3_21847	FDYLA FALSG---LDAAH TQAAPVAYTMIDLHKDGA V-----	LDYPKGGMDSM IQALVN	317
Phatr2_51868	FDYLA FALSG---V DASH TQAAA VAYMMMDLHKKDA V-----	LDYPMGGMDSL VQALVS	334
Thaps3_7094	LDVLCFC LSG---VPSDTGITAEMAMM MG EFYDE DAI-----	MDCPVG GASA IV DALVR	307
Phatr2_54842	LDLLCFCLSG---LPAKGTITAEMAMM MG EFYAPG AV-----	MDCPKGGQAQSIVKALVR	320
Thaps3_10233	IDTMCI-FCG---FPAK GAMTA HLLY I LERFFEE TAA-----	FSVPIGGTCE LGNTLQR	348
Phatr2_9210	IDTMCI-FCG---FPAK GAMTA HMLY I LERFFEE SAC-----	YSVPIGGTCE MGNTLVR	248
Thaps3_21900	LEMLAFLLQG---LPADQTLTVV MAYMVEDFFRENA V-----	MDFPKGGSGELMGALAR	306
Phatr2_45243	LDMLCFLLQG---LPASDTMNAV MAYMLADWYRPGV T-----	LDFFPKGGSSSI VSALVR	300
Thaps3_11636	TAVLTHPIGDYAVQPRDATF--AAHGV TMAHYVN GSPNHN LVI TKG V ATQNISTR LTS	335	
Phatr2_54800	KAVLTHPIGDYAVQPRDATM--AAHGV TMAHYQDGAC-----	YCVGPTQQIS VRSSS	585
Thaps3_5859	AGALTYHWGDHV VPPPHRCF-----FMT ALLD THYKG GGY-----	FPRGG SRSIA KCLVS	311
Thaps3_10254	QGVLSYHYGDYGEHPSRGAF--VMHSMICVHYRG GAY-----	YPVGGPLSIAKSIAT	362
* : :			
Thaps3_25361	VIEQ-----	NGGRVVSGVLLQELLFEKLEKKEETKDGE S-KEPKPRCKGIRLEN GL-	645
Phatr2_42980	VVLR-----	SGGRV L TSVDVAELIFGE PREQASKG KQKE GDNDG PPP PRCVG KV L SDGR-	603
Thaps3_5221	GVEQK---SIGSKVHL SRH VES IDTNEE-----	G-DR--VIGLTV RKN GG	351
Phatr2_54826	GVQQG---SNGSQVHL RQP VKE IDFSED-----	G-TI--ATGLT L RNR G-	386
Thaps3_21847	GLEMK RDN VES GE LRLK SVER FV LNEV-----	K-NKAT CTGV L EN-G-	359
Phatr2_51868	GIKT----NGGE LRLN SRS VERMILEDN-----	N-GRVE CKGV VL TD-G-	371
Thaps3_7094	GIEK----KGK VFC NSR DEI CIE NG-----	K----AVGV RLAK NY-	341
Phatr2_54842	GIEK----YGGEV VCNT HV QEV VENE-----	K----AVGV VIK QGK-	354
Thaps3_10233	GLEK----YGGKLQLNAHV D EIL VENG-----	R----AVGV RL MN-G-	381
Phatr2_9210	GLEK----FGG KIQLNAHV D EIL VENG-----	R----AVGV RL KN-G-	281
Thaps3_21900	GVTKR----EGCS VEV STS VDEV I VENG-----	R----AVGV RL AK SG-	341
Phatr2_45243	AVQK----NGSSVC VN SH D EIL VENG-----	K----TVGV RL TD-G-	333
Thaps3_11636	MVRS----F GG EALI DAT VRG II I ENG-----	RAVG KV VS NT D-	369
Phatr2_54800	MVRE----F GG EVL TDAT VR E I LEH G-----	RAVG V RV SNT S-	619
Thaps3_5859	AITR----RG GHV FAL SPV D EIL TKKN-----	MFGK FIAT GV SV RG ID-	350
Thaps3_10254	TIEK----HGG KV L VR APV SSV LV DEK-----	N---RAYGV VV KG K E-	397
* : :			
Thaps3_25361	--ELSVS-D-----	-KGAVV SFM GM IPTFLQLVSPDVR TAEGV-----PAGL	683
Phatr2_42980	--EIKFA-SDRFDE--	-KNGS CLP A VI SMEGFIWT FINMLPDD IRM KYV-----PRGL	651
Thaps3_5221	KKVIVKA-----	-KEGV VCN PMW SLR KLI KRN NAL S VL GG DKAT SSS GGL	396
Phatr2_54826	--RILA-----	-REGV ICNAP VWS LKSL RPTR-----	410
Thaps3_21847	--TILKA-----	-RRGV ICNAP LWN MKA LLED SITN PL DL-----	391
Phatr2_51868	--TVVNA-----	-RKG VV SNA PI WNL MARILED S VP GEV ND-----	403
Thaps3_7094	--SRIKA-----	-TKGV ISN LS VWD LMNS GIV---D-----	366

Phatr2_54842	--QRVAA-----SKAVISNLSVWDLFGSIL---D-----	379
Thaps3_10233	--NVVKA-----RKAVVSNATPFDTVKLMPKAEPEKG-----	412
Phatr2_9210	--NVVKA-----NKAVVSNATPFDTVKMLGEKQALPEG-----	312
Thaps3_21900	--RIIKA-----KEAVISNADLYNTYKFVPEGKHGGFD-KER-----	375
Phatr2_45243	--RKVHA-----TQAVVSNADPYISNKLNNARKSGQLNKA-----	368
Thaps3_11636	--ELEECTSEEDLAKVPAV-----EYNKFLPQDLPVV-----	399
Phatr2_54800	--ALAECKSDAERAQVPVTTELRAKAVVCATSVYNLYNNLLPQDIAQV-----	664
Thaps3_5859	--IVVKKC-----VVS DAGFLNTFGIDSEG NKP ALV D SNA ASQR-----	388
Thaps3_10254	--VLAK-T-----IVSSIGAPATFGKLLPESHRHLV-----	425
Thaps3_25361	PALEERRPLMRVMISLKGKDDLNLTGADWYRLPNATLPRDELDPMTGQVKFGTIGVDDD	743
Phatr2_42980	PALSSRRPVFKVLFALKGSADQLNVTGADYYRLPNAAVARDEFQDQSSQIKHGEIGWSDS	711
Thaps3_5221	KAKQSWMTSFDTD-PSTGRGSVLRPKPAEDTTIEKSLEKCDSAEMTGSFLHLHLALNAT	455
Phatr2_54826	-----S-GEADETLLRGACDTEAKTGSFLHLHLALESS	441
Thaps3_21847	-----SVAAAVNDVRSQANE MEMTGSFMHLLHGIPND	423
Phatr2_51868	-----ARRSIVKAIQKQADDMSMTGSFMHLLHGIPKA	435
Thaps3_7094	-----TDLF--PEDFVKERKATPACPSFMHLHVGFQIT	397
Phatr2_54842	-----TTLL--PNSLVQQKLSTPLGKSF MHLHVGF R M S	410
Thaps3_10233	-----LTKWREELGKLP RHGAISHLFLAIDAE	439
Phatr2_9210	-----VAKWKEELGKLP RHGAIMHLFLAIDAK	339
Thaps3_21900	-----IEYL--GLTAKPKDG SVE FCKS FMHLLAVKAE	406
Phatr2_45243	-----TDHLDALINTDKTEGGIADLKSF HIIHAGIDAA	401
Thaps3_11636	-----KKFKDE--ATIRQSNGHVF LFC KLRGN	424
Phatr2_54800	-----KEF QDP EKRTI IQS NGHIF LFC KIKGD	691
Thaps3_5859	-----ALLHNAGFPTLDSVIPCISNL SFIG LDRT	419
Thaps3_10254	-----SKQLES MKDNM IASNL TLM S MFVG IS DP	453
Thaps3_25361	NTGASEELI LG EATDE TEATT----SHTRGKRKNKAATSKAPRSKFTSGV SWMKV SFPSAK	799
Phatr2_42980	DTG DNG DAY ADGGK NLMD V IN QDP GSIS DEH IVN SSKR KAR KTF EAG SS WLH VSFP SAK	771
Thaps3_5221	GLDLQS---LE-PH-YTVM DRGL---EGDG-KV--IDG--VKD DSS GEL NMIAV SNPC VL	502
Phatr2_54826	GLN LDN---LE-AH-YTVM DRSL---GGDG-SS--VNG--VLDG PCG I L NMIAV SNPC KI	488
Thaps3_21847	GLPA---DLD-CH-HS VL N LEH-----DVTAAQNL VIV SI PT IF	457
Phatr2_51868	GLPE---HLE-CH-HS VL N MQD-----DVTAEQNM VI SI PT VF	469
Thaps3_7094	KEEL SK---LQ-AH-YI F M ND W-----R-----GV PAEE NCAL V S IPS VH	433
Phatr2_54842	KGE LQT---LQ-AH-YM HME DWG---R-----GV QD E D N A V L V S IPS VH	446
Thaps3_10233	G LD L SHI---QD-PA-HL VV QD W D W-----R-----S L QD S QN L C SFF I P S IL	476
Phatr2_9210	D LD L SHI---QD-PA-HL VV QD W D W-----R-----S L QD S QN L C SFF I P S LL	376
Thaps3_21900	L IPE---DAP-PQ-WT VV QD W D W-----K-----G ID AT GN V V V V SG SKL	441
Phatr2_45243	GLPDQPSADFP-AQ-WAV VR D W D W-----A-----PEG VES PRN I VLC S MP SLI	442
Thaps3_11636	A D E I G---LP-DHNLWYFNGYD---LDDA-FDKYFAN-----PTEVR PPT VYIGFPCTK	470
Phatr2_54800	PTE LK---LP-AH NLWYFNS YD---IDDA-FEAYFTD-----PV QOR PPT VYIGFPCTK	737
Thaps3_5859	DEE LE---LP-AQ NVW HVHD W D W-----H DAA-WK NM MNA I SPY QSL AD QTPFL FIS NE SA K	470
Thaps3_10254	ENSLA---LP-KRN YWI HD SW D W-----H DKN-IE-----AFKKNP KPPV FFV SFSS AK	497
Thaps3_25361	-----DPSWQDRHGDV STC VVT VEA- DDDF VQM FD TKPKI Y SV-----LK	838
Phatr2_42980	-----DPSFEERHGKTT C VVT IE A- DDDF VTYF DT KPKI Y V I-----KN	810
Thaps3_5221	-----DNTL API EGFI IM HAY G---AGNE PFEI WK PPT ASK GNAS PNTAGE GEI I GGER C	553
Phatr2_54826	-----DNSI LAP DGT I VV HAY S---AGNE PYE I WE GLD R-----	518
Thaps3_21847	-----DPSI LAP EGY HII HAY T---AASEDFA DWER MLIG ELD GG K-----PEFT DY K	501
Phatr2_51868	-----DPSI LAP EGY H VV HAY T---AACDGFDQWT PYL DSG KET G-----K	506
Thaps3_7094	-----DNTL API DPN HAVL HI Y T---PATE LYER WEN V K R N T-----	465
Phatr2_54842	-----D DTL API EG YAVL HI Y T---PATE DFT R WEN V QSK-----	477
Thaps3_10233	-----DKTLC PEG KH V I H V Y S---SG GEPY E PWE K L K P G T-----	508
Phatr2_9210	-----DKTLC PEG KH V I H V Y S---SG GEPY E PWE K L K P G T-----	408
Thaps3_21900	-----DQS I LAP P G YHV H I H A Y T---AGNE SYE DWE QF EH LM D D A A-----VR D	480
Phatr2_45243	-----DPSI LAP E G K H V L H A Y T---PATE PYA DW G MDR K S-----	474
Thaps3_11636	FGL IR QD IT W Q K R F P V N SNC I L I S D G L W E W F E K W Q D K P V-----RN	511
Phatr2_54800	-----DTSW Q R F P G V SNC I L I S D G L W E W F E K W Q D K P V-----HN	772
Thaps3_5859	-----DPDF GT KHPG KAT SEV F A V C K Y D L F E K W A D T A H-----NS	505
Thaps3_10254	-----DPT YSS R N P G K Q V A L V V G P G F D H V A V F Q N E R V-----KH	532
	* :	
Thaps3_25361	A---GNGERERL R D R V L K D L L E T F P Q L Q G Q L E ---TV QICGPVR-----	876
Phatr2_42980	A-SAT KG D L D R L L E R V K K D V Y H I F P Q L R D K V D ---HCEICGP F Q-----	850
Thaps3_5221	S P S T Y Q A L K D S R S K V L W R A V E S V I P D A R E R T V---L A L I G S P R T---H E R F L R R P C G - S	605
Phatr2_54826	R S D G Y M C L K D R A E V L W R A V E S I I P D A R N R V V---I S E I G S P I T---H E R F L N R P R G - T	570
Thaps3_21847	R T K A Y K D L K Q E K A E A L W L A L E R I I P D V R E R A K R E G S V V E V G T P L T---H R R Y N R R Y R G - T	557
Phatr2_51868	V V D G Y N E L K D E K A D V L W R A V E R V I P D V R L R A K Q K G S I I L V G T P L T---H R R Y N Q R Y R G - T	562

Thaps3_7094	--PEYNQLKEERSAFLWKVLEKIIPDIRQRAV	--HSDKVGTPLT--	HQRFLNRYRG-S	515
Phatr2_54842	--EAYEKLKEERSQYLWKLTRIVPDIRERAR	--IVRVGTPLT--	HQRFLRKYKG-S	527
Thaps3_10233	--EEYEAYKNERAEVLWRAVERCIPDVRDRVE	--FSIVGSPLA--	HEAFLRRDRG-T	558
Phatr2_9210	--QEYDDYKNERAKVLWEAVERCIPDVRDRLE	--FSIVGSPLA--	HEAFLRRDRG-T	458
Thaps3_21900	KDAAYQTFKDERAQPIWDAIQKRAPAVVKGA-C-	VIEKVATPLT--	HARFLNRHRG-N	533
Phatr2_45243	--EEYTKKKEQAADFLWSAIEEYIPNARDRAVP	--GTVQIGTPLT--	HERFLRRTRG-T	526
Thaps3_11636	RGEYEYLEFKDKLTHHLLDLQEFVPQVKGR	--YHHLGTPLS--	EETFLASYRGGS	564
Phatr2_54800	RGSDYEEFKEKLSKHLLLEIFEFVPEVKDKIE	--FSFLGTPLS--	EQTYLNSFCAGS	825
Thaps3_5859	RGDYTELKEKIIIESYLNVFYLHF	PCKHGEG---NLAKCTVLTMSADSMA*	554	
Thaps3_10254	RGKEYTDMKKEWEIVYMEAFLKQFPELKDKVD	--YVEFGTALS--	NDFYLGTNRGAV	585
	*	.	.	.
Thaps3_25361	SGLTHNGPRF-----	AIKGNRPETPYPGLYIGGADLTVGDSFSGAIVGGWLAAN	925	
Phatr2_42980	KGLSHNPERF-----	AAKGIRADTPYPGLFVGGSDLTVGESFSGDIVGAWLAAN	899	
Thaps3_5221	YGAFAED-----	CLKDGSTPISNLVLSGDGVF--PGIG-----IPAV	640	
Phatr2_54826	YGSATED-----	YLAGDSTSIGNLLLAGDGIF--PGIG-----LPAV	605	
Thaps3_21847	YGPAPSNGND-----	VWELPGPKTPIEGLLACGDCCF--PGIG-----LPGV	597	
Phatr2_51868	YGPAPGPGKD-----	VWELAGATTKIKGLLACGDSTF--PGIG-----LPGV	602	
Thaps3_7094	YGPPAIRAGDA-----	SFPFPNTPIQGLLCGDSCF--PGIG-----VPAV	553	
Phatr2_54842	YGPQAIQAGVG-----	SFPFAGTPIRQLLTCGDSCF--PGIG-----VPAV	565	
Thaps3_10233	YGMAMAAGSSAPQSGILGSVLPPFPNLKTPV	DGLLRCGDSCF--PGIG-----TPSA	609	
Phatr2_9210	YGMAMAAGTSAPQAGLQNILLFFFPFPNLKTPV	DGLLRCGDSCF--PGIG-----TPSA	509	
Thaps3_21900	YGLAIAPDNA-----	EGWKFPDVKTPLEGYYRCGDSTT--SGIG-----VPAT	574	
Phatr2_45243	YGPRVEV--G-----	AGQTLPGHKTPLPGFYMVGDFTF--PGIG-----VPAT	565	
Thaps3_11636	YGTQCVCTEMF-----	APINRNWTTTPFTEVPGLYLAGSDAFL-PSVTGAMYGGCLAS	616	
Phatr2_54800	YGTKLPSMF-----	AKSNRRWTTSPHTSIPGLYLAGSDAFL-PAVCGAMYGGCFGAI	877	
Thaps3_5859	-----	-----	554	
Thaps3_10254	YGLSHTPERF-----	N---LQWL-KPKTPIQNFYLTGQDVCS-CGITGALVGGYLSAY	633	
Thaps3_25361	AIMGYSFM-----	DHMY--L-GKN-ITS	QQFIEEPIL	955
Phatr2_42980	AVEQYGPL-----	DHLF--L-QKN-ITTDI-----	EQFLEEPGW	929
Thaps3_5221	ALNGASAANGF-----	VGIFDQWR-CM-DYLLKAKGIIA*	-----	671
Phatr2_54826	AISGASAANAM-----	VSVFKQWE-CL-DELGKSQKL*	-----	635
Thaps3_21847	AASGTIAANTL--	VDSSVQLD-LM-SELKDSGALQ*	-----	628
Phatr2_51868	AASGTIAANTM--	TTIANQRN-LM-KELKAKGALQ*	-----	633
Thaps3_7094	AGSGMIAANSVSLDSIGAQUE-VL-SKIKQQ*	-----	-----	582
Phatr2_54842	AGSGLLAAHSVSWDSIGPQD-LL-KTLQKRK*	-----	-----	595
Thaps3_10233	AASGAIAANTM--	THVDNHLK-ML-SEASKLDPMYKFLDAGIMQVYKPLVQGFTPSPEL	665	
Phatr2_9210	AASGAIAANTM--NPVGKHLD-LL-----	-----	-----	530
Thaps3_21900	ASSGAVCANAI--	MSVWDQLS-LN-QKIKMP*	-----	601
Phatr2_45243	AASGAIAANTL--	VSVFDHLA-ML-DKVRLEPEKEQKS*	-----	598
Thaps3_11636	AVLGLTGTMRIGH-AILT	HLAMRLREENPKLKSIE-----AYMLAVKKFTE*---	661	
Phatr2_54800	AVLGLHLRALKLT	-AFIAHFACCTDEDPKIGWIQ-----AYILAWKKFMND*--	923	
Thaps3_5859	-----	-----	554	
Thaps3_10254	AISPRCFRL--TA-SLLN*	-----	648	
Thaps3_25361	ATERNGVIVDDVAVPFKEVVVDMQGITDADRSTAESSKEE*	-----	997	
Phatr2_42980	VDEE-----	DVAIPYKSADAKKKD	950	
Thaps3_5221	-----	-----	671	
Phatr2_54826	-----	-----	635	
Thaps3_21847	-----	-----	628	
Phatr2_51868	-----	-----	633	
Thaps3_7094	-----	-----	582	
Phatr2_54842	-----	-----	595	
Thaps3_10233	RTDQYVSGAGVAPVDYTATDPSVSERIDL*	-----	694	
Phatr2_9210	-----	-----	530	
Thaps3_21900	-----	-----	601	
Phatr2_45243	-----	-----	598	
Thaps3_11636	-----	-----	661	
Phatr2_54800	-----	-----	923	
Thaps3_5859	-----	-----	554	
Thaps3_10254	-----	-----	648	

## 2) ZEP Percent Identity Matrix

1: Phatr2_47925	100.00	31.88	32.79	20.94	21.18	19.89	21.58	21.35	23.27	20.05	22.40	19.67
2: Thaps3_6395	31.88	100.00	46.63	22.93	18.67	18.94	21.71	26.03	24.36	20.46	21.14	19.61
3: Phatr2_45936	32.79	46.63	100.00	21.19	22.89	19.45	19.89	25.15	22.67	19.10	19.40	19.32
4: Thaps3_1961	20.94	22.93	21.19	100.00	22.54	22.92	24.21	25.13	24.02	22.81	26.11	22.77
5: Thaps3_270370_ZEP1_	21.18	18.67	22.89	22.54	100.00	65.42	33.85	33.48	33.67	20.00	20.93	21.04
6: Phatr2_45845_ZEP1_	19.89	18.94	19.45	22.92	65.42	100.00	33.41	35.44	35.52	19.56	22.22	22.65
7: Phatr2_56492_ZEP3_	21.58	21.71	19.89	24.21	33.85	33.41	100.00	44.88	42.80	20.00	21.03	22.19
8: Thaps3_261390_ZEP2_	21.35	26.03	25.15	25.13	33.48	35.44	44.88	100.00	78.51	21.62	23.16	25.08
9: Phatr2_56488_ZEP2_	23.27	24.36	22.67	24.02	33.67	35.52	42.80	78.51	100.00	21.76	23.33	23.84
10: Thaps3_22671	20.05	20.46	19.10	22.81	20.00	19.56	20.00	21.62	21.76	100.00	25.82	24.67
11: Thaps3_20663	22.40	21.14	19.40	26.11	20.93	22.22	21.03	23.16	23.33	25.82	100.00	44.80
12: Phatr2_43425	19.67	19.61	19.32	22.77	21.04	22.65	22.19	25.08	23.84	24.67	44.80	100.00

## ZEP Alignment

Phatr2_47925	-----	-----	-----	-----	-----	-----	-----	-----	-----	-----	-----	-----	0
Thaps3_6395	-----	-----	-----	-----	-----	-----	-----	-----	-----	-----	-----	-----	0
Phatr2_45936	MADQSAARKTLPSLLRHFEGTELTVELKTGRPLYRGTLSSADQAMNLTLLEDASLLQLRLIVN	-----	-----	-----	-----	-----	-----	-----	-----	-----	-----	-----	60
Thaps3_1961	-----	-----	-----	-----	-----	-----	-----	-----	-----	-----	-----	-----	0
Thaps3_270370 (ZEP1)	-----MTV-----RRIASLAIGISLSTLCAFTVIS---	-----	-----	-----	-----	-----	-----	-----	-----	-----	-----	-----	26
Phatr2_45845 (ZEP1)	-----	-----MKFSTTVSSALFLIASV--	-----	-----	-----	-----	-----	-----	-----	-----	-----	-----	17
Phatr2_56492 (ZEP3)	-----	-----MK-RSCSIVTILY--	-----	-----	-----	-----	-----	-----	-----	-----	-----	-----	12
Thaps3_261390 (ZEP2)	-----	-----	-----	-----	-----	-----	-----	-----	-----	-----	-----	-----	0
Phatr2_56488 (ZEP2)	-----MGLSFL-SLCAVLTASS--	-----	-----	-----	-----	-----	-----	-----	-----	-----	-----	-----	16
Thaps3_22671	-----	-----	-----	-----	-----	-----	-----	-----	-----	-----	-----	-----	0
Thaps3_20663	-----MVSTILIFILVACLLLQST--	-----	-----	-----	-----	-----	-----	-----	-----	-----	-----	-----	19
Phatr2_43425	-----	-----	-----	-----	-----	-----	-----	-----	-----	-----	-----	-----	0
Phatr2_47925	-----	-----	-----	-----	-----	-----	-----	-----	-----	-----	-----	-----	0
Thaps3_6395	-----	-----	-----	-----	-----	-----	-----	-----	-----	-----	-----	-----	33
Phatr2_45936	-----MSSSDRHSSQLNQPKRPRHEEPSHSI-----MAFDL--KN-	-----	-----	-----	-----	-----	-----	-----	-----	-----	-----	-----	120
Thaps3_1961	-----QQHKGAFRRGSSSAAVPSTLSLVHIRGSTIRFIHFDPQLDLTLTIKQGIDRSWRMEHNSE	-----	-----	-----	-----	-----	-----	-----	-----	-----	-----	-----	0
Thaps3_270370 (ZEP1)	-----SSRTTIKPLNVGEQASSSIGPATLLRNLKQNL-----PQIDWLAEKGKS	-----	-----	-----	-----	-----	-----	-----	-----	-----	-----	-----	70
Phatr2_45845 (ZEP1)	-----STTSFTPVQSFGVHR-----	-----	-----	-----	-----	-----	-----	-----	-----	-----	-----	-----	33
Phatr2_56492 (ZEP3)	-----VATT-----	-----	-----	-----	-----	-----	-----	-----	-----	-----	-----	-----	16
Thaps3_261390 (ZEP2)	-----	-----	-----	-----	-----	-----	-----	-----	-----	-----	-----	-----	0
Phatr2_56488 (ZEP2)	-----AMAF-----	-----	-----	-----	-----	-----	-----	-----	-----	-----	-----	-----	20
Thaps3_22671	-----	-----	-----	-----	-----	-----	-----	-----	-----	-----	-----	-----	0
Thaps3_20663	-----CDAFTF-----	-----	-----	-----	-----	-----	-----	-----	-----	-----	-----	-----	25
Phatr2_43425	-----	-----	-----	-----	-----	-----	-----	-----	-----	-----	-----	-----	0
Phatr2_47925	-----	-----	-----	-----	-----	-----	-----	-----	-----	-----	-----	-----	0
Thaps3_6395	-----RSPYEKKMERVITACPKCNGEGKVRAP-----LSKKARAQRKRMQQSQTGDTTN	-----	-----	-----	-----	-----	-----	-----	-----	-----	-----	-----	82
Phatr2_45936	-----PGWDETTIHEGPFTVCPKCHGDGHIVHQ-----ASKKQKLRHKRART--NGDYTD	-----	-----	-----	-----	-----	-----	-----	-----	-----	-----	-----	169
Thaps3_1961	-----MPCSQLLSTAFNNNDYNHLI-----	-----	-----	-----	-----	-----	-----	-----	-----	-----	-----	-----	23
Thaps3_270370 (ZEP1)	-----PSNK--IDIPDHVATVLAQPNAPKRAESEERTHKIRSRAKQASEDA--MALRGMLIG-D	-----	-----	-----	-----	-----	-----	-----	-----	-----	-----	-----	125
Phatr2_45845 (ZEP1)	-----RT--LL---VTPRHATVEPPVREPETSDRVQRDRFRKASQDA--ANAKGCVAQDD	-----	-----	-----	-----	-----	-----	-----	-----	-----	-----	-----	83
Phatr2_56492 (ZEP3)	-----VRAFAPAP--LVQ-----SScffQRQPTT--TAR--FVSGTA	-----	-----	-----	-----	-----	-----	-----	-----	-----	-----	-----	47
Thaps3_261390 (ZEP2)	-----	-----	-----	-----	-----	-----	-----	-----	-----	-----	-----	-----	0
Phatr2_56488 (ZEP2)	-----VTTRSPACNDVTRSLH-RINTRHMTPFYPASSLR--IST--RVASTA	-----	-----	-----	-----	-----	-----	-----	-----	-----	-----	-----	63
Thaps3_22671	-----	-----	-----	-----	-----	-----	-----	-----	-----	-----	-----	-----	11
Thaps3_20663	-----PSSGVLRDVRVSINGSVERRCSLPASEHVQHVAASSTSSSS	-----	-----	-----	-----	-----	-----	-----	-----	-----	-----	-----	67
Phatr2_43425	-----	-----	-----	-----	-----	-----	-----	-----	-----	-----	-----	-----	0
Phatr2_47925	-----	-----	-----	-----	-----	-----	-----	-----	-----	-----	-----	-----	34
Thaps3_6395	-----MGKKRQSRRPLDGAHIAIIGSGLAGLSTALSLE	-----	-----	-----	-----	-----	-----	-----	-----	-----	-----	-----	142
Phatr2_45936	-----APNLAILKKPCKECDGSGLIAINPLDTTERKQTTPQIQPNFSVAIVGGGIGGGIALAAALQ	-----	-----	-----	-----	-----	-----	-----	-----	-----	-----	-----	220
Thaps3_1961	-----TPAP-QRLETCRECDSSGLVQSDT-----DPPVDTLPEIAVVGGGLAGLALAAACR	-----	-----	-----	-----	-----	-----	-----	-----	-----	-----	-----	60

Thaps3_270370 (ZEP1)	DDAN-----	AWWR-EQRS-IPEGGRVVTTDDPLTVLVAGGGLAGLVAAACH	170
Phatr2_45845 (ZEP1)	GDES-----	SWWR-K--P-LPEDNDVISNQRPLRVVIAGGGVAGLVAAACH	126
Phatr2_56492 (ZEP3)	PPS-----	SNVA-SEEKVAISEAHLRKVLIAGAGVGGSLAKVLT	87
Thaps3_261390 (ZEP2)	ADF-----	NSSD-YELLGRPARPGRPLKVAIAGGGVGGLTAALCML	47
Phatr2_56488 (ZEP2)	VPP-----	EDVA-FDKLSPAREGRPLKIAIAAGGGVGGLTACML	103
Thaps3_22671	VPS-----	APPH-TTV--DDISNLEHHPLVIIIGGGIGGLVLALCLD	49
Thaps3_20663	TRS-----	RSST-TTLQAATAPHQPVQKVAIIGSGIAGLALAHAF	107
Phatr2_43425			0
Phatr2_47925	QG-----	GFTNVHIIYERDGSHDARKEGYGLTLTNPTGVILHQLNV	74
Thaps3_6395	HR-----	NIP-CIVYERDLSFEERKQGYGLTMQQGARALR-SLGF	180
Phatr2_45936	HR-----	GMK-YTVYERDLDHFQRSQGLD-----	243
Thaps3_1961	NK-----	NPNLIER-LTVYEQAKEYPT-AGAGFGFSPNGQICLSSIGI	102
Thaps3_270370 (ZEP1)	S-----	K---GMK-VALFEQASSYAPY-GGP-IQIQSNALRALQQINP	207
Phatr2_45845 (ZEP1)	A-----	K---GMQ-VAIFEQASQYAPY-GGP-IQIQSNALRALERINP	163
Phatr2_56492 (ZEP3)	KM-----	P---TMD-VTVLEQTSEFKR-GGP-IQIASNAMEILKHMDK	125
Thaps3_261390 (ZEP2)	K-----	K---GFD-VTVYEKTAAFARF-GGP-IQFASNALSVIKEIDE	84
Phatr2_56488 (ZEP2)	K-----	K---GFD-VTVYEKTAAFARF-GGP-IQFASNALSVIKEIDE	140
Thaps3_22671	QVYNHSITTDANGEPITSSSVKFP-IHVYESTAEYSAN-AGGAIGLYPNGLRLVRNLSR	107	
Thaps3_20663	S-----	NNPSSNNNKIQ-IDIFDSRTNLDEK-AGSGIQLT-GGLVALNEISN	152
Phatr2_43425			0
Phatr2_47925	LE-----	EIA-----QSDCPRSRSHYM--FNA-NGEIQGYFG	102
Thaps3_6395	FSFSDGEDD---	NNNCGKKA-VDENTSNTKQKFGIHSTRHVV--HHP-DGTVVGEWG	232
Phatr2_45936		-----SDGIMSTKHVV--HEP-DGAIVGEWG	266
Thaps3_1961	YGYKKFILPFNSM-----	KR-LNKEGNL-----VNQSDV-----	130
Thaps3_270370 (ZEP1)	EIQFELVTAGCTADRVSGLKIGYKKGNK--LA-----	GL--YDAGDW-----	246
Phatr2_45845 (ZEP1)	VICEEIRKAGTVTADRVSG-LKIGYKKGNK-----	KQ--YEKGDW-----	204
Phatr2_56492 (ZEP3)	PVFDKVMEMKFTFTGTRACG-IKDGLRADGSFRMTNDSDLYLWNP-----	EW-----	153
Thaps3_261390 (ZEP2)	ELFERVMDKFTFTGTRACG-IKDGLRADGSFRMTEDRDLYLWNP-----	EAPADW-----	133
Phatr2_56488 (ZEP2)	TLFERVMDKFTFTGTRACG-IKDGLRADGSFRMTEDRDLYLWNP-----	DAPADW-----	189
Thaps3_22671	GSSPSYLDSEHVKFGANCNPNLLQNVR-----	TAGCDIYRWRMRHDGLQAVAREDE	159
Thaps3_20663	NLYNEVVESS-----	ERLVSKCRPWFGGNKDDAGVEQGWQ	190
Phatr2_43425	MDAG-----	TGVRSRCKPWNPAFPDT-----	25
Phatr2_47925	NA-----	F-----A--	106
Thaps3_6395	MK-----	V-----WGGRFE--	241
Phatr2_45936	LR-----	K-----WGRSER--	275
Thaps3_1961	LR-----	EL-----	134
Thaps3_270370 (ZEP1)	LV-----	RFDTIGP-----	255
Phatr2_45845 (ZEP1)	LV-----	RFDTLQP-----	213
Phatr2_56492 (ZEP3)	YA-----	KFDLKTP-----	162
Thaps3_261390 (ZEP2)	FV-----	KFPLRQC-----	142
Phatr2_56488 (ZEP2)	FV-----	KFPLKQC-----	198
Thaps3_22671	LLPDIKVDESEMAMLEVLDSEKGTGSRSSAVSRADSTSQDV	GERANRRPHGGSFANA	219
Thaps3_20663	LL-----	ELDIQNA-----	199
Phatr2_43425	LL-----	DLDLLKT-----	34
Phatr2_47925		R-----NRGWGQRGNLRVPRQ	122
Thaps3_6395		KN---GRKHAKRQNNAHISRQ	258
Phatr2_45936		-----AKKPKRQNIIHIARQ	289
Thaps3_1961		-----SNRHGFGIAGC-LRS	148
Thaps3_270370 (ZEP1)		-----ALEAGLPATVVVDRP	270
Phatr2_45845 (ZEP1)		-----ALDAGLYPTVVVDRP	228
Phatr2_56492 (ZEP3)		-----AENRNMPYTGVIERP	177
Thaps3_261390 (ZEP2)		-----ADLFGLPYTGVIDRP	157
Phatr2_56488 (ZEP2)		-----ADLFGLPYTGVIDRP	213
Thaps3_22671	MGALEAMKDMSONLSQLSRLSRI	SFTGSDATTSAGGSDKSTPRASRVVDTTELLSLGIRRW	279
Thaps3_20663	IRENA-----	AADASKQHGAEEGDSNKQY--SLVREDGEVVAYTILRG	240
Phatr2_43425	VQNA-----	-GSDV-S-NALIREGKLWTSIMRG	60
 			*
Phatr2_47925	RVRQILASRL---	KITETHWDHKLVGVSGCENG-----NICALFQLEGA-AEEKLLV	171
Thaps3_6395	NLRQLLMEML--	HPGTIQWGQKFVGYSQGSSDDDSQDQPSLQVFRRRSNDCEEVAT	315
Phatr2_45936	SLRWQLYKAA--	GGRTANIAWNHRLLQYKQRV-----DAPGWEKFQV----DDQIIAH	337
Thaps3_1961	DLVNLVQL---	DTQHGGKGALKYSEKLVGINPIH--DKVELEF-----ESGRQD-	194
Thaps3_270370 (ZEP1)	VIQQILVKYG--	FPEGTVRIKSRIQSIEDL---GKG--RGVSRTL-----EDGTKA-	314

Phatr2_45845 (ZEP1)	VIQQILLEHG--IPEKTVRIKSRIANYEEL----GPG--KGVRILL-----EDGTVA-	272
Phatr2_56492 (ZEP3)	DLQQIFLDSLPK---GTVKNGDGVARYEKL----PDG--GVKAIV-----KSGKEV-	219
Thaps3_261390 (ZEP2)	DLQEILLDECRKIKPDIQNGNPVNGYVSK----GKG--NGVTVNLD-----ADGTTA-	203
Phatr2_56488 (ZEP2)	DLQEILIDECKRLKPDFLINGNPVVGYEDL----GKG--QGVTINL-----NDQTTA-	259
Thaps3_22671	KYQQVLYDQC-KEVGIQFHMGKRLQSVTSIPASGEDGD--AKSLLF-----KDGSR-	329
Thaps3_20663	TLQRILREQLAQEHGVDVQFDKRLCGMAY--SNEENG--VKCQF-----NDGTTG	287
Phatr2_43425	ALQEALYGALPSNVRQNQFGKVLVDL---SVREGG---IECLF-----SDGSVAG	106
:		
Phatr2_47925	GADLVVAADGIRSAVLQHAYP-QAPPI-----	197
Thaps3_6395	TASLVLVGCDFGIRSSVRSAKLGEDGTPL-----	342
Phatr2_45936	KADLIVGADGLRSQVRSLIGEDRTPL-----	364
Thaps3_1961	LVLVLIGADGINSSVSKLLNIDDEIA-----	P 221
Thaps3_270370 (ZEP1)	YADVLVGADGIWSQVRKNLHGLDDGAGGAFAASGAAGGALDDAEARKLARDTVAIAAKADR	374
Phatr2_45845 (ZEP1)	YADVLIGSDGIWSSVRIMHGGLDQGADGFASGAAGGALNEAEARRMAKDSVLMANNANR	332
Phatr2_56492 (ZEP3)	YGDVLIGADGIWSAVERATMRDS-----PAKGDGSGA	250
Thaps3_261390 (ZEP2)	EADVLVGSDFGIWSAIRAQMYGEEI-KKS-----SNNALKRQGC	240
Phatr2_56488 (ZEP2)	SADVLVGSDFGIWSAVRDQMYKEGGVKST-----SANKKKRQGC	297
Thaps3_22671	TASLVLIGADGINSKVRNYVTNPKPATA-----TKQQEYVP	366
Thaps3_20663	PYDLVVVGCDGIQSFKVQVNTGSQLPNA-----DSSSA	320
Phatr2_43425	PFDDVVVGCDGIKSACKYVENGRILPKD-----AKREGDSVA	143
::: * :		
Phatr2_47925	QSLGIRLILGISSSF-----THVHLKER--GFYTLDSGKRLFVMPFART	239
Thaps3_6395	RYLDCIVILGIAPSP-----TSALTDGET--VFQTADGITRLYVMPFAEA	385
Phatr2_45936	RFLDCIVILGICPIAGISL-----EGQQSDLLDGET--VFQTADGVTRIYIMPFTTT	414
Thaps3_1961	IYSGANIFYGKIPNPDGHE-----YLRGHPIFTEG----SVTNGPGTGEFI---	263
Thaps3_270370 (ZEP1)	RFSGFTCYAALAPHRASN-----ENVSYQILLGEK-KYFVSTDGGDRQQWF--	421
Phatr2_45845 (ZEP1)	RYSKFTCYAALTEHRASN-----EEVSYQILLGKD-KYFVSTDGGERQQWF--	379
Phatr2_56492 (ZEP3)	TYSGYTVFAGELAYDSFDN-----GOVGYKVYIGPQ-QYFVITDIGNGNYQWY---	297
Thaps3_261390 (ZEP2)	TYSGYTVFAGETVLFKTEDY-----YETGYKVYIGPQ-RYFVTSVDGDRVQWY---	287
Phatr2_56488 (ZEP2)	DYSGYTVFAGETILKTPDY-----YATGYKVYIGPQ-RYFVTSVDGDRGRIQWY--	344
Thaps3_22671	AYTGVTCMLMGCASVPRIRGICFPSSAT-TKCHACYYPTRAPKEVDEGNADDTPRVPSGD	425
Thaps3_20663	IYSGIRITFAIQEGDADDN--PVQAKGAQFTQFFGNG-AYALTSSYAGKGVPAAKG-	375
Phatr2_43425	VYSLRIRYAVKDGNSEEK---QA---ETATLSQYFGEQ-AYGLDGIYAGPGQPHTKC-	195
.		
Phatr2_47925	AEWAVIDDNATSCSQPTGEQYMWQLSFASSDDKTY----SSTE-----LQQALFHC RDW	290
Thaps3_6395	GD-----DSSGLSTDNTKGLSMWQLSPFMDETDATRLSQLGSSA-----KEEALKRCGAW	436
Phatr2_45936	-----AYMWQLSPFMAEQALSLSKGP SAL---KKEAIRRCQSW	451
Thaps3_1961	---AF---HTGAEDN--KTFIWANTY--ASNSPPPK-----REDW	293
Thaps3_270370 (ZEP1)	--AL---IREPAGGVDP EPT-----PEDPHPKLTRLRKEFACNGS-GDADGNVW	464
Phatr2_45845 (ZEP1)	--AL---IREPAGGVDP EPT-----PENPTPKLTRLQEFNHEEP-GDQNGDVW	422
Phatr2_56492 (ZEP3)	--AF---LARPADSASST-----DMPDGQSKYLQE-----FAGW	327
Thaps3_261390 (ZEP2)	--AF---FALPPGTKKAPSGWG-----DYIKSL-----HQGW	314
Phatr2_56488 (ZEP2)	--AF---FALPPGTKKAPSGWGSTRDGQTDPEENLVDYVKGL-----HEGW	386
Thaps3_22671	YEQVF---QIYFPSPIERPDTWRTLT P-----TEAKEECRELA-----KKLREDGW	468
Thaps3_20663	--AF---LIYTDDYYGP-----FPK-----SVFKRDESEVAVKPSVEAAAENADW	416
Phatr2_43425	--AF---LVYLDPDYVGP-----FKK-----KRAR---LESKPS---VDENADW	228
*		
Phatr2_47925	HEPVQE-----LMLS-TSQESIWGTLLYDRNP--EILHKH--	322
Thaps3_6395	HDPILK-----LLRS-TPEDFITGYPCYDRLVERKELRDG--	471
Phatr2_45936	HTPVFD-----ILYS-TPIELVSGYPVYDRALLTPELLQE--	485
Thaps3_1961	SEGNFH EKL DILL KYPTS---HPIHKFAEL-TGESDLLHFGLYR-----HHK	337
Thaps3_270370 (ZEP1)	DPFALE-----LINA-ASEEDIKRRLDLYDGAPLLTLDPQRLL	501
Phatr2_45845 (ZEP1)	DDFAYE-----LFKA-TPEDFIKRRDLYDGSPPLL-----M	451
Phatr2_56492 (ZEP3)	SEEVHH-----ILRA-TQEHEIEQRDLYDRPPSA-----M	356
Thaps3_261390 (ZEP2)	SDEVM T-----VLDS-TPPDSVEQRDLYDRPPEL-----L	343
Phatr2_56488 (ZEP2)	SDEVM M-----VLDS-TSPDSVEQRDLYDRAPEL-----F	415
Thaps3_22671	DEQFLAPLESETL-TGVL-RVGLRSRE-----ALDV-WHVGG-----S	503
Thaps3_20663	TQDNRVPREHVAE-CIKVLKTAAPGNDVADIVSNSNRFFDLGVYFHN PFS-----W	467
Phatr2_43425	TQDVRKSIEVARETMLDQTKSLGVPTDLSPTISAADRFFELGVYFHN PFS-----T	280
.		
Phatr2_47925	-----LQINDTLP RR LIV GDACHAMS PFKQGANQALQDGRVLVKH L TSARVE-----	371
Thaps3_6395	-----CDKSQSANA FVTLLGDACHHPMS PFKQGANQ ALLDAVLLSQKLFDISRIHNGKTNV	527
Phatr2_45936	-----TASVTLVGDACHHPMS PFKQGANQ ALLDALALVRSIYKHCKTAGSY--	531
Thaps3_1961	NTWS-----KDRV VLLGDACHATLPYVGQGANQ AIE DAI YLA VCLNR-----	379
Thaps3_270370 (ZEP1)	SPWA-----KGPVALCGDAAHPMMPLNLQGGCQATEDGYRLVEELAKVQH-----	546
Phatr2_45845 (ZEP1)	QGWS-----KGQVAICGDAAHPMMPNLQGGCQATEDGYRLAEELATVRT-----	496

Phatr2_56492 (ZEP3)	KPWT-----DGPVALLGDGVHAMMPNLQGGGCQAIEDAFVIGQELGSATK-----	401
Thaps3_261390 (ZEP2)	RSPA-----DGNVVLIGDAVHPMPNLLQGGCQAIEDAFVLSSETLEACES-----	388
Phatr2_56488 (ZEP2)	RSPA-----NGNVVLIGDAVHAMMPNLQGGCQAIEDAYVLTETLANTRT-----	460
Thaps3_22671	IGVASGEDNDDVGRAVLLGDAAHPPVPIGQGAMMAMEDAGTLALLIARYCPLDTNSPT	563
Thaps3_20663	NGWVREFDKSA-KYAVLAGDAAHAMPPFLGQGANQALQDAYLLAEKVFEYNDQVEQYSPV	526
Phatr2_43425	QGWSREMDSKGGSVVLCGDAAHALPPFLGQGSNQAIQDAYCLAKQLYAYNAEIEQG--	337
	: * * . * * ***. * *. : :	
Phatr2_47925	-----IAVSNTQREIVQRTASVVAASRQASVYWHFQQLVMPKDQDTQKFA	417
Thaps3_6395	NEQQPTISLNESTPQALAEFENDMLQRCEVKVKSADAALKLHSDVA-----	574
Phatr2_45936	-----DSNSLERAVKEFEVEMILRSAVKVEASEAARFLHTEIA-----	570
Thaps3_1961	-----HDNYSDAFADYYDKRFPRTKRIVQFAGIMHKLYHT-----	414
Thaps3_270370 (ZEP1)	-----SRDVPGLGRYSRVRVIRTAAIQGFAQLGS DLLVD-----	583
Phatr2_45845 (ZEP1)	-----TKDIEGALQEYRKRIPRTTIIQALAQLGS DLLVD-----	533
Phatr2_56492 (ZEP3)	-----RSQIVDVKLREYQORRLIRSAVQGLS RFA S D II IR-----	GFD 439
Thaps3_261390 (ZEP2)	-----TQKLEDALQDFYKKRIVRVSVIQF QFLSKLASDLIIN-----	AFD 426
Phatr2_56488 (ZEP2)	-----TEKLQDALQEYRKRI RVS T QFLSKLASDLIIN-----	AFD 498
Thaps3_22671	VD-----FSLFKKAMHAYESLRVSRTKTILGSSVELGKTQQKRAE-----S-----KLY	607
Thaps3_20663	VRGGE-STAEPNLKALLNEYEKRRWLPTTSITAKAAGLGYLETG-S-----GFF	573
Phatr2_43425	-----RDANLNAMLKD YEN TRWPSTFGIFWKSTFLGYLETG-GE-----D-----GLY	379
	:	
Phatr2_47925	GVCSQDIPALLHALQKKNIKANSANDLDKSVQCTI---DELQLIGPPEVRRKAES ELKEA	474
Thaps3_6395	-----IQEGNITRGAAA-LD-----AKG*-----	591
Phatr2_45936	-----IQKGNVTRGAAS-RS-----ILIKSNEEDTATTE*-----	598
Thaps3_1961	DS-----WLVHKA-----LDVLIGSIINGGAALKQLEREIINECPVKDYQQY	456
Thaps3_270370 (ZEP1)	LM-----MTI-----	588
Phatr2_45845 (ZEP1)	KM-----MTI-----	538
Phatr2_56492 (ZEP3)	TP-----AKIYRD---ENGK-----FQ-----FENCNYAGIVTK	465
Thaps3_261390 (ZEP2)	TP-----WSPHDD---LGKS-----WK-----S-----YLTF	445
Phatr2_56488 (ZEP2)	TP-----WSPHDN---LGKS-----WK-----S-----YLTF	517
Thaps3_22671	NA-----WREWSIKA-----QVWAYGTLPMRPG AAS D YM TK	639
Thaps3_20663	GN-----FR*-----	577
Phatr2_43425	AR-----FRDVF F K T-----MGAV-----GIAEWVLI--SAAKPKI*-----	408
Phatr2_47925	HFDLARQAILSSEMNNLAFLRKLSWEYPNLIR-----NV-DVDDMTCLQKA AK	522
Thaps3_6395	-----591	
Phatr2_45936	-----598	
Thaps3_1961	AFNRQ*-----	461
Thaps3_270370 (ZEP1)	-----PLLGPFLLMTQLSMPFILR LYTPSF*	615
Phatr2_45845 (ZEP1)	-----PLVGPFFLFMTQVSM P F V L R F L Y T P E F *	565
Phatr2_56492 (ZEP3)	ILQP-----ILPI---FFSVQFAFLYDG-----WKNDKQIDFK AFL GFS VL	503
Thaps3_261390 (ZEP2)	FWKVRGVAPFYGN ECQHIS Y S L L F S T Q Q P S-----	475
Phatr2_56488 (ZEP2)	FWKPILOQFAIFPM-----QFAYLYSY Y PTGNM GDLP A K L E I W K E K H K T D A E A V F E Q A S K	572
Thaps3_22671	VEEVVLE*-----	646
Thaps3_20663	-----577	
Phatr2_43425	-----408	
Phatr2_47925	SGHIRIA---HWLITEAGCL---VDA-RLL---NDLSIKSYM K ALL KM YM*-----	562
Thaps3_6395	-----591	
Phatr2_45936	-----598	
Thaps3_1961	-----461	
Thaps3_270370 (ZEP1)	-----615	
Phatr2_45845 (ZEP1)	-----565	
Phatr2_56492 (ZEP3)	GGLIVSL---VLFELAEAGLGIGLGA E ALL GA E GLL DF G G IS A A I Q D F F L G G G A A G L *	557
Thaps3_261390 (ZEP2)	-----475	
Phatr2_56488 (ZEP2)	EGFVMEHEASF KKAEVE---LSPTALAATKEELS*-----	604
Thaps3_22671	-----646	
Thaps3_20663	-----577	
Phatr2_43425	-----408	

### 3) VDE/VDL/VDR Percent Identity Matrix

1: Phatr2_56450_VDR_	100.00	52.25	17.27	17.45	14.40	17.05	16.82	16.67	13.54
2: Thaps3_270211_VDR_	52.25	100.00	16.24	17.33	16.25	16.05	18.10	16.75	11.46
3: Thaps3_7677_VDE_	17.27	16.24	100.00	56.04	26.69	23.60	21.62	22.31	18.89
4: Phatr2_44635_VDE_	17.45	17.33	56.04	100.00	26.49	24.01	21.93	21.65	15.56
5: Thaps3_22076_VDL1_	14.40	16.25	26.69	26.49	100.00	65.61	30.81	30.30	30.21
6: Phatr2_46155_VDL1_	17.05	16.05	23.60	24.01	65.61	100.00	28.57	28.30	28.42
7: Thaps3_11707	16.82	18.10	21.62	21.93	30.81	28.57	100.00	53.25	39.29
8: Phatr2_45846_VDL2_	16.67	16.75	22.31	21.65	30.30	28.30	53.25	100.00	54.46
9: Phatr2_bd_1281	13.54	11.46	18.89	15.56	30.21	28.42	39.29	54.46	100.00

### VDE/VDL/VDR Alignment

Phatr2_56450 (VDR)	MKLHRKGRYRLLVTAVLLGTVCFSVPENLRGSVRIPRKNANAGSVPGBTHTVSKQPSASA	60
Thaps3_270211 (VDR)	-----MAMVLLIRTA-----IASYSLTL-----TSAFSSSIRPTCRT	33
Thaps3_7677 (VDE)	-----	0
Phatr2_44635 (VDE)	-----	0
Thaps3_22076 (VDL1)	-----	0
Phatr2_46155 (VDL1)	-----	0
Thaps3_11707	-----MSASSSS-----	7
Phatr2_45846 (VDL2)	-----MK-----	2
Phatr2_bd_1281	-----	0
Phatr2_56450 (VDR)	TRHKVSQTSDANALPIKNDLIQGPVSANKSIGSITFLLPSSGADEIKTNFGSSSPVGNP	120
Thaps3_270211 (VDR)	FRQS-----TPHHATASNVDIIGTVALLVPPSSSTE--LSKYGSKSPAPRP	76
Thaps3_7677 (VDE)	-----MK-----LFL-----SLVLAAP	13
Phatr2_44635 (VDE)	-----MKFLGVTSLCLW-----SVVNRENV	21
Thaps3_22076 (VDL1)	-----MRP-----STSAL-----TVVLGT--	14
Phatr2_46155 (VDL1)	-----MRFAWVAAGVVL-----TTTQA--	19
Thaps3_11707	-----TTTTNAGKRARSWPSSASTS-----SMPTRS--	35
Phatr2_45846 (VDL2)	-----RATRKRTLAATLWIAMSSVTG-----SGPGRT--	29
Phatr2_bd_1281	-----	0
Phatr2_56450 (VDR)	SLDEAVRHANKSQYFSQDGRVETRIVYVPIEEQDESWKDLLETDVLLAMGLQYEADLAF	180
Thaps3_270211 (VDR)	SYQEEAAELHARKISHFSDGRIEATVVTPTSTNQDDT--DDVCLTSNALIALGITDPAEVQY	134
Thaps3_7677 (VDE)	VSSFAPSNPVVS---THSSVHSQQHN-H-----VLEAHND-----	45
Phatr2_44635 (VDE)	SEAFAPRHQLSLR---PSSRTSAFSRAP-----ILSLRK-----	53
Thaps3_22076 (VDL1)	-IAIV-----SCSQ-LN-----NNVS-AF	30
Phatr2_46155 (VDL1)	-LVPL-----DCTG-MGETRTSGI--RP-----IRGLESNMA-RY	49
Thaps3_11707	-ILILATFLSLTSSS-SSTSVEAAFGVGSP-----AVGLRSHTAAST	74
Phatr2_45846 (VDL2)	-AAFAP-----SGNNNNNGCHGLS-----RVALHTTELQAH	59
Phatr2_bd_1281	-----	0
Phatr2_56450 (VDR)	A--RKLFFQQRH-DRDAEHRFRQCHFAIDCAQ-SFPTMVGPYDSENPSFRAKLLPWTKHAS	236
Thaps3_270211 (VDR)	L---STTFRKRRTSHQETSSYNTCQFALDCGSNNYAPLVGPWDEANPSILAEIAPWTGVAS	192
Thaps3_7677 (VDE)	-----NMDDITFSLSARNINNE-----IVE-R-----IGKV-----	70
Phatr2_44635 (VDE)	-----YDSDSEVEND-----LLS-K-----LNPFQNW--QTA	77
Thaps3_22076 (VDL1)	STRSSSLTQRHKTCTITTS-SSSLVYNP-----N-NDD-----DNSNRSQHKPNP	73
Phatr2_46155 (VDL1)	ATVRHGTDQ--TNHGITSS-SERQWPFP-----R-GG-----SSPRA	82
Thaps3_11707	SKQQSSLYAQ-KKNNIDSSDNPLSYLF-----LSSDP-----ETKRLQKQTAT	118
Phatr2_45846 (VDL2)	SKPPHQSQSPQ-T-----RYTPSAMNIQ-----F-PEP-----DESLHVWDHVRN	97
Phatr2_bd_1281	-----	0
Phatr2_56450 (VDR)	GKRISQQMVALLQRGNNSDDF---VFAIMLF---LNQFSGSSVDWVKHSIDATWEKGPLR	289
Thaps3_270211 (VDR)	GKRlteQMNGLFEKQTSDEF---ALAVMLF---FNRFSGAAIPWVQHSIDVTWEKGGLVQ	245
Thaps3_7677 (VDE)	T----TSALLALTLSFSAI-----TSPISGPNGDVLSIIPSAN---AAD	107
Phatr2_44635 (VDE)	L----QSTALALTIGVASW-----TSL-----PTIVPPFAA---TTD	108
Thaps3_22076 (VDL1)	F----LSAALTAAVTSLFLSSLPS---A-----TFASTPASTTQKYDGFAEYAKENKM	120
Phatr2_46155 (VDL1)	V----ARSVATFGLGFSIALASVFGVA-----APVGADTPAVKYDGFAEYAQDNQM	131
Thaps3_11707	-----LFSTLGFSALFLTNPPLIPHLPFSPSLSSANAEDELYAKYGGK----GLDT	164
Phatr2_45846 (VDL2)	-----IGKVCTGFAL---AGLLSALVSF---TSPVWAENELSAKYGG----GLDT	137
Phatr2_bd_1281	-----	0

Phatr2_56450 (VDR)	NAQEVVSMVSCKGDCVVKCV-QDDNCRECLEVLTAldTR--DQVASYRTIVSYESDLLKD	346
Thaps3_270211 (VDR)	NAKEIIFSMITKCGPCITKCL-NDENCSQCINALDKIDTR--DQVTSYRTVVSFESELLRD	302
Thaps3_7677 (VDE)	GAKIGLCLVKKCRVPLAKCI-TNPNCANVICINSNGKEDETGCQINCNGVFENDVVGE	166
Phatr2_44635 (VDE)	SKSIVSCLFQKCPPLAKCI-ANPKCLANVVCINTCTGRPDEIECQIECGNLFENEVVGE	167
Thaps3_22076 (VDL1)	EQSDVGCFINKCGDQTQLF-SNPRGIKGVSCLGRCKGE---QSCATRCFAEGSELDN	176
Phatr2_46155 (VDL1)	EQSDVGCFINKCGDQTQLF-SNPRGIKGVSCLGRCKGE---QSCATRCFAEGSESINA	187
Thaps3_11707	SLVDKDCLVNQCQVQAKACLQDDPDCRKGLTCAKCLGD--NACITGCFARYGNENLDE	221
Phatr2_45846 (VDL2)	SLVDQNCLVSACSLQTKACLQDDPSCRKGLTCAKCLGD--NACITGCMARYGNANLDN	194
Phatr2_bd_1281	-----MERYSNDKLNN	11
	: : :	
Phatr2_56450 (VDR)	FSFCILQKNNIFNCDAASLPTLPNVQPVATWREQPLTEIASLLVGHILNDEA-APESSLR	405
Thaps3_270211 (VDR)	FSLCILQKNNIFECASAEIPELPVVKPMSTWRGKDVTWARGIMIGHLEGAGGSLEGNLQ	362
Thaps3_7677 (VDE)	FNKCAVTDMTCVPQKKDDGSYP-----VPSKDVLVQSF-----DTKL	203
Phatr2_44635 (VDE)	FNKCVLTDMKCVPKQGDDGSYP-----VPAPEIVVPKF-----DTKF	204
Thaps3_22076 (VDL1)	WLSCТИEDYECVKVPKNIIDN---S-----AENVGYDTTVKKF-----DPST	214
Phatr2_46155 (VDL1)	WLSCTIEENECVKVPKVNVDN---S-----AEDIGYSTTLRSF-----DPQS	225
Thaps3_11707	LLKCTIEDHECIKVAILEGGGDVLG-----REPKSPAPTVQGF-----DLAS	263
Phatr2_45846 (VDL2)	LLKCTIEDHECIKVAILEGGADVFG-----QEPRAPAPTVTAF-----DPKS	236
Phatr2_bd_1281	LLKGTIEDHECTKVAILEGGIEVFG-----QELRASDSTVTAF-----DPKS	53
	: : :	
Phatr2_56450 (VDR)	TDISWKVACGANEAAYDKFPSQNQLFYPAARGRD-----LW-----	440
Thaps3_270211 (VDR)	LGWSWKVACGANVAYDQFFPSQNQLFYPSAKGKD-----LW-----	397
Thaps3_7677 (VDE)	WNGRWFITAGQNKLFDTFFPCQVHFFTETAPGKF-----VGK-----	239
Phatr2_44635 (VDE)	FDGRLYIISAGQNKLFDVFFCQVHFFTETEKGKF-----FGK-----	240
Thaps3_22076 (VDL1)	LVGNWYKTDGLNPNYDLFDCQSNTFDFSDDTK-----KELD	250
Phatr2_46155 (VDL1)	LVGTWYKTDGLNPNYDLFDCQKNTFTP--TSD-----KELD	259
Thaps3_11707	MEGTWYKVAGYNPNYDCYACQRNTFSPEGGLSDLSLQLPTGGILGSLNAVGSIGADRLQ	323
Phatr2_45846 (VDL2)	LQGSWFKVVGYNPNYDCYACQRNTFSAPDSANGRNNN---LLWSVASGNTNPATVNQLR	293
Phatr2_bd_1281	LQSSWFGKVAHNPNYDCYACRGIQSMDV-----LIVFHCGETK---DRDR	95
	* : * : :	
Phatr2_56450 (VDR)	YDPVFRVETL--DGR-----NVWCKRH-----YKVRPA	466
Thaps3_270211 (VDR)	YDPVFRVETI--DGR-----NVWCKRH-----YKVRNG	423
Thaps3_7677 (VDE)	--LNWRIE--EPDGE-----FFTRD--AVQEFVQDP	264
Phatr2_44635 (VDE)	--LNWRVE--QPDPN-----FFTRD--ALQEFVQDP	265
Thaps3_22076 (VDL1)	MGIFFRVRPRPEEYGG-----GFWEINSLEHMHIVDAVSP-	283
Phatr2_46155 (VDL1)	MGIFFRVRQRPESGG-----GYWENALTEHMIVDVPVQP	293
Thaps3_11707	VDVEFSMPRYLPDGSPQPPSGVRESFISSADSMEGSGLQSVGYNQYSTHETMVFDTVKSN	383
Phatr2_45846 (VDL2)	MDVEFSMPHLLPDGSPPPSNVRESILVSGEDGSVFGSKSIALNDYRTRBTMVFQVSTG	353
Phatr2_bd_1281	KGINFFLTHFFDADTVQ*-----	112
	: : :	
Phatr2_56450 (VDR)	DIPG-TFRF-----SVLDNGITSNEFWTIVGVADD----LSW	498
Thaps3_270211 (VDR)	ETPG-TFKF-----SVLDNGVTNSNEFWTIVGAADD----LSW	455
Thaps3_7677 (VDE)	NNPA-----HL--INH-----DNEYLHYQDDWYIVDYAADDNKEGVPP	300
Phatr2_44635 (VDE)	NQPG-----HL--INH-----DNEYLHYEDDWVVIDYEYDGNKDGVP	301
Thaps3_22076 (VDL1)	-----ELDNPTGRTMHTAGKMYGLKFTENWYILGE--SNGDNDIPP	322
Phatr2_46155 (VDL1)	PTAGTQLVASANAATGDLNDELNPTGRTMHTAGKMYGLETFENWYILGE--SDGKGSVPP	351
Thaps3_11707	GVGE-AVKL----ALGKRGEEKLRSRTAHSEGEMFGLKFENWYIIQG--NNP--GQDE	433
Phatr2_45846 (VDL2)	N----NMVF----H-KGTTQEVSYSRTAHSEGEMFGLKFENWYIIIGE--NDP--GQPE	399
Phatr2_bd_1281	-----	112
	: : :	
Phatr2_56450 (VDR)	IVFHYAGAASAVGQRYLGGLLCTADGSLPDESQRPEIWVRLRSAGIQPWDLYT-VNNDLT	557
Thaps3_270211 (VDR)	VVFHYAGAAGAVGQRYLGGLLCTPTGELPPEEDLGHYINFLRSAEIEPWELFV-VDNDDQ	514
Thaps3_7677 (VDE)	FAFVYYRGENDAWIGGGAVVYTRDSKLPE-SLLPRLREAACKVNFDKDFDLDLTDNSCK	359
Phatr2_44635 (VDE)	FAFVYYRGNNDAEWGGGGVVYTRAQLP-E-SLLPRLRVAEEAKIGDFDKDFVITDNTCP	360
Thaps3_22076 (VDL1)	FKLVAYKGHTL-QGNYEEAFVYAKESVLPK-EAVGAVREAAKAGLDFDK-FTRIDNTCP	379
Phatr2_46155 (VDL1)	FKLVAYKGHTL-QGNYEEAFVYAKESVLPK-EAVGAVREAAKAGLDFDK-FTRIDNTCS	408
Thaps3_11707	FKFVYYNGKTR-QNTYDGAIFIYSRSRTLSP-ASMEKVKIAKDAGMNPDQ-FCKIQNSCF	490
Phatr2_45846 (VDL2)	FKFVYYNGKTR-QNTYEGAFVYRSKELAP-ESMAKVYSIAKEAGMKVDQ-FCRIRNGCF	456
Phatr2_bd_1281	-----	112
	: : :	
Phatr2_56450 (VDR)	SPG-----AQEAGPPPLDYFRREVLAKR-----AASSPHP*--	587
Thaps3_270211 (VDR)	SPG-----ALAAGAPPLDYFRKTASVIG-----*	537
Thaps3_7677 (VDE)	ALEKG-EEVVLR-EKFAGKMAIQTEK-----QLQQQAVLARTAASNTVKGEV	404

Phatr2_44635 (VDE)	TDLSGKEKQILR-EKFAGKVALQTEQ-----	406
Thaps3_22076 (VDL1)	QLQAQVTRLRGNAVNSIKAQK	
Phatr2_46155 (VDL1)	TTTKS-----LNDASAGTG-TSTTDWVDLVVGEGGVIDWV---VPGWRGEYKN*-----	423
Thaps3_11707	V-GDS-----LNDAQAGTG-TSTTDWINLVVGEGGVIDWI---SPGWRGEYKAKR*-----	453
Phatr2_45846 (VDL2)	DGEDDKQEMMMNPQREGLG-SPSNPFRGILASTK-VSQFLGVESVAETTYNEPKSTIS	548
Phatr2_bd_1281	SEDET-----VVKAPSSGLG-SQSNPFRGILASTR-ISQLLGVEPVAARDTVRRNAPT--	506
	-----	112
Phatr2_56450 (VDR)	-----	587
Thaps3_270211 (VDR)	-----	537
Thaps3_7677 (VDE)	TAVEKSLQK-----IEEKALAFEKELMKDVVSVEKEIVKEVEEVEKEIVQEEQKIFGG	457
Phatr2_44635 (VDE)	LFFEQGLEAQKAYDALEETEKQFERETSQQ*-----	437
Thaps3_22076 (VDL1)	-----	423
Phatr2_46155 (VDL1)	-----	453
Thaps3_11707	SNFLQGSQATNRKADAVQERPWPKEMGDY-----LEDP-----RRHFRLMDS	590
Phatr2_45846 (VDL2)	-----SPTLQPAVGTIASRPWWYEIGDY-----LENP-----HRHFQVMDS	542
Phatr2_bd_1281	-----	112
Phatr2_56450 (VDR)	-----	587
Thaps3_270211 (VDR)	-----	537
Thaps3_7677 (VDE)	IR*-----	459
Phatr2_44635 (VDE)	-----	437
Thaps3_22076 (VDL1)	-----	423
Phatr2_46155 (VDL1)	-----	453
Thaps3_11707	LRTDMDWPDYIKEKNW*	606
Phatr2_45846 (VDL2)	LRLPMTWAEDVKN*---	555
Phatr2_bd_1281	-----	112

## APPENDIX 2.C FULL-LENGTH GENE MODELS, PROTEIN TARGETING PREDICTIONS

### 1) *Thaps3\_268908 (PSY1)*

Exon 1:

>Thaps3 chr\_5:1332233-1330996

```
TACTTTGAAGCCTTCCCTACTACTTCTCAATACGTTTGCAATCTTGCTGCATAAA  
CATTAAAGATTGATTTGCCGGTTGATACACAACGATACGGAAGAAGTGAAAATCAATT  
GCAAAACGGAACAGTACCTCTGCCGTAGAGGAACACAACATGAGGATATCATCCATTGTA  
GCAGCCACCCTGATCACGTGCGATGTTGCTTCAGCATGGTCATCGTCTGCATTACATCA  
CGTTATCTATCAAGACACAGCATCGGTCTCAGGCATCAACCAAAGAAGAGACGGATCA  
ATCTTGATGTCGTGTCACAAAAAGAAAGTAGTAGTAGTAGCAGCAGCGGCCAAGGA  
CGCACCAACAAAGAGATTCAAACGAATTAGCATTAGGTGTTACTCTGATGGAGGTCCG  
GTGATTGATTTGCCCGTCAAAGATACCACATCTGTCAGAAATAGCACTTGCCGAC  
TCACGAAAGAAGTACGAAGCCAGTGGTCTACAATTAGCCTAATCCGGGAGGAAGATTA  
ATGGGTATCAACGATGAGGTTGTCAGAGGTTGGCTATGAGATTGGGAGTTGCCGAA  
GAATATTGGACAAGGAGTCTGGAGAGACTGTAGATGAATTGGTCAAAAGGTTGCTCGA  
TACCTCGTTCAAAGTCAAATACGGATACGTTCCCTGAAATGGAAGAGGAGGAAGCACCG  
TTTACTAACAGGAGAAGATTAGGTTCAATCGTCTCTTATCCGAGCCTACGAAGAACATCA  
GGGATTGTCACATCAGCATTGCCAAACCTTTACCTCGGTACACAAGTTCCGGAA  
CCATCCATGAAGGCCATTGGCAATTACGTTGGTCCGTAGAACAGATGAAATCGTC  
GATGCCCTCGTCTGCCGTACGATCTAACGAAATGTTGACAGATTGTCGGAG  
TGGGAGATTGTCGTGAGAGACTGTTGATCGAGGGGGAGGTTGATGCTGGACTTG  
CCACTGTTGGACTGTAAGGTCAAGTATCCTACGTTGCCATTACACCATTTCAGATATG  
ATACGTGGTATGTTGATGGACATCCCTGGGCTGGGACAAGAGAGATCGATACTGGGAT  
GAGTTGCACCTATATTGTTATCGCGTGGCCGGACTGTGGGGTTGATGTCCATGCCAGTG  
TTGGATGTGCCAGGTTACACCGATGAAGTTGCAAA
```

Exon 2:

>Thaps3 chr\_5:1330907-1330265

```
GGAGCCTGCTTTCGCTTGGTGCATTCCAATTACCAATTCTCCGTGATGTA  
AGAGGATGCTGAGAAACGCGAACGTGTATACCTCCCAACGAGACATGGAGAGGTTGG  
AGTTACTGAACGACAAATTGGACAAAGTAGTGGATGAGAACTACATTAATCTCATGAA  
GTTTGAGATTGCTCGTCCCAGATGTACTACGCTCGTCTGAGAGGTTGCCATGCT  
TCGCCAGAGTCACGTCTGCCAGTGCAACTCTCGTGGATGCTACGGGAAGATATTGGA  
CAAATTGAGGAGAATGGATATGATTGCTGACAAAACGAGCATATGTTGTAAGTGGGA  
GAAGTTGGCAGGAATCCAGCGTCTGGTACCGTACTCTGATATTGCAAAGGCAATGCC  
ACTCCCTGGGATTGGGAGCGTCCGTCGTTAGAAGAATATGAAAAAGTTGGAACAAAT  
GTTGGAGAATAATGGTAGAACAAAGGGGGAGCTCAGCGACAAGTATTGCAAAG  
CCTCAACAAATAAGTCAACTCGCAAACCTCAACGAAAGCATTGCTGCATCGCAGGC  
AGCGTTGAATAAAACAATAATGTAGACAATGATGACGCAGTT
```

*Translated:*

MRISSIVAATLITCDVASAWSAFTSPLSIKTQHRSQASTKRRDGSILMSAVSQKESSSSSGQG  
RTTKEISNELALGVTLDDGPVIDFASVKDTSRAEIALADSRKKYEASGATISPNGGRL

MGINDEVVAEVGYEIGEFAEEYLDKESGETVDELVQKVARYLRSKSNTDTFPEMEEEAP  
FTNQEKFIRNFNRLSRAYEESGIVTSFAKTFYLTQVLPEPSMKAIWAIYVWCRRTDEIV  
DAPRPAAHDPNAEMLTDLSEWEIRLERLFDRGEVDVLDPLLDCKVKYPTLPITPFSDM  
IRGMLMDIPGLGQERYDTWDELHLYCYRAGTVGLMSMPVFGCAEGYTDEAKEPALS  
VAFQITNILRDVGEDAERVYLPQRDMERFGVTERQIFDKVVDENYINLMKFEIARAR  
MYYARALRGVPMLRPESRLPVQLSDAYGKILDKIEENGYDSLTKRAYVGKWEKLAGIPA  
SWYRTLDIAKAMPLPGDWERPSLEEYEKSLEQMLENKWVEQRGSSATSDYLQLSNK-

*Targeting:*

SignalP 3.0 - NN = Yes, Cleavage Site ASA-WS

SignalP - HMM = Yes, Cleavage Site ASA-WS, Signal Peptide Probability = 0.993

SignalP 4.1: Yes, Cleavage Site ASA-WS, D = 0.554 (D-cutoff = 0.450)

ChloroP: Yes, Score = 0.558

## 2) *Thaps3\_263269 (PSY2)*

No introns.

>Thaps3 chr\_7:1643508-1642761  
AAAAAAAGTCGGATTGATAACAACCAGAAGCGAAGTACACCGACCCAAACAACCAACAC  
CCCAACACCTCGGTCTGATCTGCTCTGCACACTCCAATGATGCTCTACTATTATCAATA  
TCGGCGTTATGCAACATCTCACTTGCTCGAGCGTTGGAACCTCTACCAACGAACCGC  
ATCAACCACCCACCTCGACCTCTCCCTTGTCCACCTATCTGAACCTCGTCTATATAGC  
AGCCCACATTAGCCAACCAACAATATCCAATGAAATTATACAACCTATGTCAAACAC  
GATCCCATTCTATTATTGATCGCGACTGTTACCGTATCAAACCTCGGGTCGACGCGTCG  
GCTTATACGCATGGTGTCAAGATTGGATGAAATCACAGATGATCCATCAGCTAATGTG  
CACTCTATACAACAACACTGATTGATTGGGAGGATCGATTGTATCAATGCTTACAACGAAACTCAAAC  
CAGCCTGTGGATGAAATGGACGATGCATTGTATCAATGCTTACAACGAAACTCAAAC  
CTAAATGAGCGACCTTCAAGACATGATTGTGGGTATGAAGAGTGATGCTGTTCAACT  
ATTGTACAATAAGCAGTATGGAGGAGTTGGAAGAATATGCCATCAAGTCGCTGGAAC  
GTGGGATTAATGCTGCTTCCGGAATCGTGTGGAGAAGGCACGTCAGCCTGCCATTGCTCT  
TGGAAAGGCCATTCAACTGATTAACATA

*Translated:*

MMLLLLSISALCNISLARAFCGNLSPTNR  
INHHLDLSSFVHLSRTRLYSSPHSANPTISNEIIQL MSKHDPIILFASRLLPYQTAVDAS  
ALYAWCRLFDEITDDPSANVHSIQQQLIDWEDRFKKLCTGQPVDEMDDALYQCLQRNSNS  
LNERPFQDMIVGMKSDAVPTIRTISMEELYYAYQVAGTVGLMLLPESCSEGTSACHCS  
WKGHSTD-

*Targeting:*

SignalP 3.0 - NN: Yes, Cleavage Site ARA-FG

SignalP 3.0 – HMM: Yes, Cleavage Site ARA-FG, Signal Peptide Probability = 1.000

SignalP 4.1: Yes, Cleavage Site ARA-FG, D = 0.826 (D-cutoff = 0.450)

ChloroP: No, Score = 0.489

If the first methionine is omitted, the ChloroP score becomes 0.499.

### 3) *Thaps3\_23291 (PDS1)*

No introns.

```
>Thaps3 chr_6:1795938-1794225
AACGAAAGCGTCTCTCGGCGTCAGCCTCCTCTTCACTGTCAGTCAGTTGT
GTTGAACACTCTGCTCTTCATTCACTCCTCATTACTACCACTGCTATTGCAACTGGC
TGCGTATCTGACTCTCCTCAATTGTCACTCCCATAGGCCACGTTACCACATCATT
TCACCATGATCATTACAATTCATCCTCTCCACCGTCTAGCGACATCAATGCCCTTC
AACCACACACACCCATCCTCTCAAACCATCCTCTCCAACCCTGTCATCGCTCCCCA
AAATCGGCCTTCCAACCTCGTTATGAAGGACTTCCGAAACCAAATGTCGAAGATAACAG
ACAACATCGCTACGCAGAGGCCATGTCCACTAGCTCAAGACGTCTCCGAGTGACGA
ATGATTCACAGAAGAAGAAGGTGGCTATCATTGGAGGAGGATTATCAGGTCTGTCTTG
CCAAGTACCTCTCCGATGCCGGCATGAACCCACCGTATACGAAGCACGTGATGTACTCG
GAGGAAAGGTGTCAGCGTGGCAAGATGAAGATGGAGACTGGATCGAAACAGGTCTTCACA
TCTCTCGGAGCATACCCAACGTTATGAACATGTTGCTGAGCTTGGCATCCACGATA
GGCTCAGTGAAGATTACCAAATGATTTGCAATGCAGGAACCTCCGGAGAGTTCA
CTACCTTGATTCATCCCTGGTATTCCAGCTCCGTTCAACTTGGATTGCCATTCTTA
TGAATCAAAGATGTTGACGTTGGTAAAAAAATTCAGACCGCTCCTCTTCTCCTA
TGCTTATTGAGGGACAGTCATTGATGCTCAGGATGAGTTGAGTGTGACGCAAGTTCA
TGAGGAAGTACGGTATGCCTGAGAGAATCAACGAGGAGGTGTTATTGCGATGCCAAGG
CGTGGACTTATTGATCCTGATAAGTTGAGTATGACTGTGGTCTACGGCTATGAACA
GGTTCTGAATGAGAGTAATGGACTTCAGATGGCATTGGATGAAACATGCCGTGATA
GGTGGTGCACCCACGAAGGAGTATGTGGAAGCACGCCGGAGGAAAGGTCAAATTGAAC
CTCCCATTAAAGGAGATTGTGACCAACGACGATGGAACATCAATCACCTCTCCTCGAT
CTGGCGAGAAGATTGTGCCGATGAATACGTCCTGCCATGCCGTGGACATCGTCAAAC
GTATGCTTCCCACACGTGGCAGACTATGCCCTACTCCGTCAGCTGACGAACCTGAGG
GCATCCCTGTTATCAACTGACATGTGGTCATCGTAAGTTGAAAGCAGTCGACCATC
TTGCTTCAGTCGCTCCCCACTCCTTCCGTCACGCCGACATGTCGTCACATGCAAGG
AGTACGAAGATCCAAACAAGTCCATGTTGAAATTGGTCTTGCTCCCTGCTCCTATTG
CCGGAGGAAATGTCAACTGGATTGAAAGTCAGATGAGGAATCATTGATGCTACCATGG
GTGAGCTTGCTGCCCTTCCCTACCGAGATTGCGAATGATGATAAGTGGCCTGCTACGA
```

AGATGCAGGGACCTAATGGACAGGCAAAGCTTGAGAAGTATGCTGTTGAAGGTGCCAA  
GGAGTGTATGCTGCCATTCTGGTGAGTGAAA

*Translated:*

MIITNFILSTVLATSMAFQPHTPILSKPSFSNRVHRSPKIGSSNLVMKDFPKPNVEDTD  
NYRYAEAMSTSFKTSRVTNDSQKKVAIIGGLSGLCAKYLSAGHEPTVYEARDVLG  
GKVSAYQDEDGDWIETGLHIFFGAYPNVMNMFAELGIHDRLQWKIHQMIFAMQELPGEFT  
TFDFIPGIPAPFNFGLAIMQNQKMLTLGEKIQTAPPPLPMLIEGQSFIDAQDELSVTQFM  
RKYGMPERINEEVFIAMAKALDFIDPDKLSMTVVLAMNRFLNESNGLQMAFLDGNQPDR  
WCTPTKEYVEARGGKVKNSPIKEVTNDDGTINHLLRSGEKIVADEYVSAMPVDIVKR  
MLPTTWQTMPYFRQLDELEGIPVINLHMWFDRKLKAVDHLCFSRSPLSVYADMSVTCKE  
YEDPNKSMLELVFAPCSIAGGNVNWIGKSDEIIDATMGELARLFPTEIANDDKWPATK  
MQGPNGQAKLEYAVVKVPRSVYAAIPGE-

*Targeting:*

SignalP 3.0 - NN: Yes, Cleavage Site SMA-FQ

SignalP 3.0 - HMM: Yes, Cleavage Site SMA-FQ, Signal Peptide Probability = 0.864

SignalP 4.1: Yes, Cleavage Site SMA-FQ, D = 0.603 (D-cutoff = 0.450)

ChloroP: Yes, Score = 0.550

#### 4) *Thaps3\_1383 (PDS2)*

Exon 1:

>Thaps3 chr\_1:1373161-1372917  
CGGGGAACAGACCTCAGACGTCCTTAAGTTGGATCCTCTCATCCCTACTAACCAATC  
ATGAAGTTCTTCTACCGCTGCTACCAGCAGTCGCTGGGGCCTCTCCATAACGCACCTC  
TCACAACACCCATCGTACGCATGCATCAATCTTGTCACATCGCTGACTCTTCCCTCC  
TCCTCCACATCGCAACGTCCAAGACGTCCAACCTCTGATCGTATTGCAATACACAAAC  
TTTAA

Exon 2:

>Thaps3 chr\_1:1372807-1372145  
AGAAGCGAAAGAGTTGAGTCAGAAATTATAACAGACTTCAACAACTACAAAGGTTGG  
TAGTGGCGAACCGAAGCGAGTTGCCATTCTGGAGGTGGTCTTCTGGTCTTCGTGTGC  
AAAGTATCTCTCAGATGCTGGTCACATCCCAACCTGTACGAGGCTGTGGTCTCGG  
GGGCAAGGTCTCGGCATGGCAAGATGAAGACGGAGATACTCGAGACCGGACTACACAT  
TTCTTGGTCTTATCCAAACATCCACAATCTTTGATGGGCTGAAATACAAGACAG  
ATTGCAATGGGCTCCTCACAGAAATGACATTGCCATGCAAGAGCTTCCGGCAATTAC  
CACCTTGAGTTCCCTGCTGGCGTTCCATTGAATATGGCTGCTGCGATTCTGGG

GAATACTGAAATGCTTACGTTGGAAGAAAAGATTAAAATGGTCCAGGGCTATTACCAAT  
GCTATTGGAAGGGCAATCTTCATTGACGAGCAAGATGAGCTTCTGTTTCAATTGAT  
GCAGAAGTATGGTATGCCGAACGTATCAATGAAGAGATATTATTGCAATGGAAAAGC  
ACTGGACTTCATCGACCCTGATCTACTGTCCATGACGGTTGTTCTCACGGCAATGAATCG  
TTT

Exon 3:

>Thaps3 chr\_1:1372066-1371065

CATCAACGAAGCAGACGGAAGCCAAACAGCTTCCTGATGGGAATCCCCAGAGCGACT  
ATGTCAACCTATGAAAGAGTCCATCGAAAAGAAGGGAGGAGAAGTAGTTGCAACAGTCC  
TGTAGTTGAGATTCAACTGAACGAAGAGAGTAACGTCAGTCTCTCAAACTTGCAAATGG  
AACTGAAATCACAGCAGATTATTACGTGCGCAGTGCCTGTTGATGTCTCAAACGTCT  
CGTCCCACGCAGTGGTCAACAATGCCTACTTCGTCAACTTGATGAACATTGAAGGAAT  
ACCTGTCATCAACATTAGATTGGTTGACCGAAAGCTCAACTCGGTGGATGGATTGTG  
CTTAGTGGTCTCCACTGTTGAGTGTCTATGCGGATATGCAACGTGTTGCGAAGAATA  
TGCAAGTAACGATAAAATCCATGTTGGAGTTGGTGTGACCGTGTCTCCTGAGGCAGG  
ATCTCCATTGAATTGGATTGCGAAGCCAGACTCTGATATCATTGACGCAACAATGAAGGA  
GTTGGAGCGCCTTTCCCTGGAGATCGTCCGATGCTCCGAGGAGAACCGCAGG  
TGTTGTAAGTCTACGGTGGTCCGTACCTCGAAGTGTATGCGGCTTCTGGCAG  
AAACAAATATAGACCTAGTCAGGAATACCAATCGAAAACCTCATTATGGCTGGAGATTA  
TGCAACACAGAAGTACCTGGTAGCATGGAGGGGCTGTACTCTCAGGGAAACTGCAGC  
TGAGGTCATTGCGACAAGTTCATGGCAGAGCGGGAGAGGAAAGGGTCAAAGAGGTACA  
CTCATCGGTGCTACGAAGCAAATCGAAGAGAGAACCCAGCGGTATTGCAATGGAAAA  
AGGCAGAGTGTGCGCAACATCGTATGGAGGTGGTCAACAAGGTGGCTTGAAAATCCCTA  
AAAGTTAGACTAATGCACTGTACAATCTGCTCAGGATGTTT

*Translated:*

MKFLLPLPAVAGAFSITHLSQHPSLRMHQSLSTSLYSSS  
SSTSQRPRRPTPDRIRNTQNFKEAKELSQKFITDFQQLQKVGSGEPKRVAIFGGGLSGLS  
CAKYLDAGHIPTLYEARGVGGKVSQWQDEDGDTVETGLHIFFGAYPNIHNLFDGLKIQ  
DRLQWAPHRMTFAMQELPGQFTTFEPAGVPAPLNMAAAILGNTEMLTLEEKIKMVPGLL  
PMLLEGQSFIDEQDELSVLQFMRKYGMPERINEEIFIAMGKALDFIDPDLLSMTVLTAM  
NRFINEADGSQTAFLDGNPPERLCQPMKESIEKKGGEVVCNSPVVEIQLNEESNVKSLKL  
ANGTEITADYYVSAVPVDVFKRLVPTQWSTMPYFRQLDELEGIPVINIQIWFDRLNSVD  
GLCFSRSPLLSVYADMSTCCEYASNDKSMLELVFAPCSPEAGSPLNWIAKPDSIIDAT  
MKELERLFPLEIGPDAPEEKRANVKSTVRVPRSVYAVPGRNKYRPSQESPIENFIMA  
GDYATQKYLGSMEGAVLSGKLAEEVICDKFMGRAERKGVKEVHSSVLTKQIEERTPAGIA  
MEKGRVSPSYGGQQGGFENP-

*Targeting:*

SignalP 3.0 - NN: Yes, Cleavage Site AGA-FS

SignalP 3.0 - HMM: Yes, Cleavage Site AFS-IT, Signal Peptide Probability = 0.994

SignalP 4.1: Yes, Cleavage Site AFS-IT, D = 0.465

ChloroP: Yes, Score = 0.569

5) *Thaps3\_24832 (ZDS)*

No introns.

>Thaps3 chr\_14:437250-439255

```
CTCAACCAACGAAGAACGCTTTTTTCACTTGTGTCAGCTCTCATTCTCTGCGACCC  
AACCCATAGAGACTGCCGAAAACAATTCACATCCATGCACCTCACATAGCCACTCCGAA  
ACACCTGCCATGCGTCTCTCCACAGCCTCCTCGTCGGATGTGCTCTCCAGCAACACAC  
TCGTTCCACCTTCCCTCCGCCAGCACCTCTCCGTCGTCCCGTACCGTCGCCACCACA  
TCATCCCTCTCCATGTCCGCCGCCACCTCTGAAGGGAGAATTACCTCCGAATCCGCCAAA  
CAACAAATCGGAAACGACTCCTCCTCAACGAAAACCTCATGGCGCGTGCCAAAACGGA  
CCTGGCAAAGTCAACGACGAAAAGCTCAAGATTGGAGTAGTCGGCGCTGGTTGGCGGGT  
ATGGTCGCCCGATGGACTTGGCCGATGCAGGTATGACGTGGAGATGTTGAGTTGAGG  
CCTTTGTGGGGGGAAAGGTTGCGTGGAGATAAGGGAGGGATCATATTGAGATG  
GGGTTGCATGTGTTCTTGGGTGTTATTATAACTGTTGGATTATGAAGAGAACGGGA  
TCGTTTGATACCGAGTTGAGGATTAAAGAGCATATTACACTTTGTGAATGAGGGTGGG  
ATTGGGGTGCGTTGGACTTCAAATTCCATTGGGGCTCTATTCCGGGACTTCAAGCC  
TTGCTCGTACGGAGCAGTTGGATGGATGACAAGTCCACAATGCACTGAGGTTGGGT  
ACTTCCCTATTGTGAGGGCGCTGTTGACTTGATGGTGTATGGATATGGTGCAGAC  
TTGGATGATATCACGTTACTGAGTGGTTACTCAGTTGGAGGATCAGGAGGAGTTG  
GATAGGATGTGGGATCCCAGCGTATGCGCTGGTTCATGGATTGCGATCACATCTG  
GCAAGGTGCATGCTGACAATCTTATGCTTTCGCCATCAGAACTGAAGCGAGTGTGTT  
AGAATGCTGGAAGGAAGTCCTCAGACGTGCTGCACGATCCTATTCTCAAGTATTGGG  
GATCGTGGGGTCAAGATCAATACCTCCATGGGATGCAAGAGAGATCGTCACGATGTGG  
GAGAATGGCAAGCCTATTAGAGTGAUTGGAATCAAGGTTGGACCCAAGGGAGGAGTTG  
GAGTTGATGCCGTGGTTGTGCATTGGATGTTCTGGAATAAAAAGGTCTGCCTCAA  
TCATTCAAGGGATCACTACCCAAATGTTGACAACATTACAACCTGACACTGTTCTATT  
GCTACCGTTCAAGTCGATTGATGGATGGGTGACTGAAATGAATGACGACGTTCGCATG  
ATGGATATTCTGGAGATCAATCCGACGGACGTGGCGGTGGAATTGACAACCTCTAC  
TCTGCCGATGCTGAGTTCTCATGCTTCGCTGATCTGCCCATCACTCTCCGGAGAGTAC  
TACAAAGAAGGGAGGGAGTCTCATCCAAGCAGTGTGTTGACGAACGTGCCTTGATCGT  
TCCAATGACCAAATTGTCAGATTGCATCAGTCAATTGAACTCACTGTTCCCTCCAGT  
AAGAAGCTCAATTGACCCCTGGTCAAGTGTGGTCAAGTTGGGACAATCACTGTACAGAGAG  
AAGCCAGGACAGGACAAGTCCGTCGAAGCAGGCTACTCCCATCTCAATTGGATTCTG  
GCTGGAAGTTACACTTACCAAGATTACTGGATTCCATGGAGGGTGTACCGTAGTGGT
```

TTGATGGTGGCGGATGAGATTATTGCAAGAGCTGACGGACCTAATGGATTGAAGGCACAG  
ACTGCCAAGCGATGGCCAATGGGAGTGGAAAGAAGGCTATTAGTGAGGAAAAGGTTCCA  
TTCTTGATCAGCGTCGGCATAATGGGGTACAGCAGGCGGAGGATAATGTTCTTAATG  
ATATTAGTTGAAATACTAAGGCAGG

*Translated:*

MRLSTAFLVGCVL PATH  
SFHLPSASTSLRPPVTATTSSLSMSAATSEGEFTSESAKQQIGNDNSFLNENLMARAQNG  
PGKVNEDEKLKIGVVGAGLAGMVAAMDLADAGHDVEMFELRPFVGGKVSSWKDKEGNHIEM  
GLHVFFGCYNYLFGIMKRTGSFDTELRIKEHIFTVNNEGGILGALDFKFPIGAPISGLQA  
FARTEQLGWDDKFHNALRLGTSPIVRALFDGGMMDVRDLDDITFTEWFTQLGGSRGSL  
DRMWDPPIAYALGFIDCDHISARCMLTIFMLFAIRTEASVLRMLEGSPQTCLHDPILKYLG  
DRGVKINTSMGCREIVHDVDENGKPIRVGKVGPKEELEFDVAVCALDVPGIKKVLPQ  
SFRDHYPMFNDNIYNLDTVPIATQVRFDGWTEMNDDVRMMDISGDQSDRGGGIDNLLY  
SADAEGSCFADLAITSPEYYKEGEGSLIQAVFDERAFDRSNDQIVQDCISQLNSLFPSS  
KKLNCTWSSVVKLGQSLYREKPGQDKFRPKQATPISNFFLAGSYQDYLDSMEGATRSG  
LMVADEIIARADGPNGLKAQTAKAMANGSGKKAISEEKVPFFASASA-

*Targeting:*

SignalP 3.0 - NN: Yes, Cleavage Site THS-FH

SignalP 3.0 - HMM: Yes, Cleavage Site THS-FH, Signal Peptide Probability = 0.999

SignalP 4.1: Yes, Cleavage Site THS-FH, D = 0.543 (D-cutoff = 0.450)

ChloroP: Yes, Score = 0.572

### 6) *Thaps3\_270357 (LCYB)*

No introns.

```
>Thaps3 chr_2:1232356-1230385
CGGGTTGACACGTCATCACCTTCTATCACTCGCTCGCTGGCATTCTCCTCATGG
TGGCCGTCAATCCTCTCCACGCTGTGGCATTAGCAGTGTCTCATCGGCGGCATATGCCT
TTGTATCTCCTACACCAGTCGTCCTCTCCCCGTGTCGGCTAGAGTGACACCCCTGTCTG
GTGCACCTTACTGCACCTCATATCGCGTTCGTATTCCACTCCTCCGACAACGTCCA
TCCAATCTCGTACCAACCTCCTCTACAATCTTGATCCCGTCCAACCCAACACTCTCACTC
CAAACCTCTCAAGATACTCGATGTTCTCGTCTCGGAAGCGGACCTGCAGCACGATCCA
TCGCCACCCCTCTCCCAAAGCAAACGACAAAGCATACTCGTACTCTAGCAGACT
CAAATTACGATCGCAGATGGGCTCTAACTACGGTGTGGCAAGATGAATGGCAATCTA
TTTGCAAACATATGAATCATTCAATCAGCCCATTGTAATGAAGTTATTGATCGGTTGT
GGATGTCGACGGATTGTTCTCGGTGGCTTTGACATCGCTCGCGAGCAACGGATGA
GATTGGATAGGCCATTGAGGATTGAGAGGGATGTGCTGAGAAGAGTGTGAGTCCAG
CGAGTGAAGTGAAGACACAGAACGATGGAGAGGGACAGCAAACATCGTGTACACGTG
```

CCAATCACATGTCAAAGTGCACGTCTGTGAACATTATTCTCCCTCTGGATCAATGGTAC  
ACGATGAATCTGGAACCAGTGTGTTGATTCAATCAAAGGATGGTATATTCTCAAGTAC  
GTGCAAAGCTAGTTGTGGATTGTACGGGACATGAATCCAAATCGTGTGAAGGATGATC  
GTATGAAATCCATTCCCTCAGGCTTCAGATTGCCTACGGTATTCTAGCAGAAGTTGACG  
AGACGAGCATACAAACAATGATTCTCGGGTCCGTACTCAAAGAGGCAATGACTTGT  
TTGATTACAGAACCGATCACTTCCGGAAGGTTCTAATGAGTTGGCTAAAGCAGAAAAGG  
CACCGACGTTCATGTACGCCATGCCACTCAATGGGAATCGTATCTTTTCAAGAGACAT  
CGTTAGTGGCTAGACCAGCATTATCATTCAAAGAATGCAAAGATCGATGCATGACACGTC  
TCGAGCACTGGGGATTACTGTTACAAAGGTTGAGGAAGAGGAGTTTGCTACATTCAA  
TGGGAGGACCGTGGCCAGCCAAAGACCAAAGAGTTATTGGATTGGAGGTGCGGCTGCGA  
TGGTTCATCCTAGTACTGGGTACCAACCTGTGAGCAATGATGGAGCAGGAGAAGTAG  
CCAAAGTATTGTGAAGAGTTGGAAGAGAAGAACTGGAACCCAGATAGGGCAGCTGCAC  
GTGCTTACAATGCAATTGGTACCAACGACCATTGCCAACGAAACTTGCAGTCTTG  
GAGGTGAATTCTTGATGAAGCAAACGTAGTAGGGCTGCGAGGCTTCTTGATGGCTTCT  
TCAAGCTTCCCTTGCTGTGGGGAGGGTCTCGCTGGATGGCTGGACTGCCAAACA  
ATGAGAATCAGGAGACGTGGTGGCACGGTAGTGTGTTGGTTGACGTTGTTCAAAGC  
TACCCGTCTGTGGCGGTAGATATGCTGGATCGATAGCAACATACTCCATTCAAGG  
GAGTACCACTGCCTCAGTCGGTACACCGTTATTGGGATTGCTGATGGATATGAGTACA  
GGGAAAAGAAGAGTTCTAGGTGATGTCAGCGAAGCATGAGGAAGGAGAATGATTA  
TGGAGTCGACTGTTGAGGAAGTAGTTCTGAGACTTGAAGAAAAGACAGCGGCGTGAT  
TGGATTGATAACTCTATTGAAATGTAGTGTAGATAACACAACAGATT

*Translated:*

MVAVNPLHAVALAVLPSAAYAFSPTPVVSPSSARVTPLSG  
APYCTSRYRHSHSFPTTSIQSRTTSSTIFASASNPTLPTSQDTCDVLVLGSGPAARSI  
ATLLSSKANDKAYDVLLADSNYDRRWAPNYGVWQDEWQSICKYESFNQPIGNEVIDRLW  
MSTDCCFFGSFDIAAEQRMRLDRPYCRIERDVLRVLPASEVKTQNDGEGTANYRVTRA  
NHMSKCTSVNIYSPSGSMVHDESGTSVLIQSKDGDISQVRALKVVDCGHESKIVLKDDR  
MKSIPPGFQIAYGILAEVDETSIPNNDFCGPYFKEAMTLFDYRTDHFPEGSNELAKAEKA  
PTFMYAMPLNGNRIFFEETSLVARPALSFOECKDRCMTRLEHLGITVTKVEEEFCYIPM  
GGPLPAKDQRVIGFGAAAMVHPSTGYHLCRMMGAGEVAKVIREELEEKNWNPDRAAAR  
AYNAIWSPPTIAQRNFAVFGGEFLMKQNvvGLRGFFDKPLGLWGGFLAGWPGLPNN  
ENHETWWARLVFGLTFSKLPVSADVMLGSIATYSISEGVPLPQSVPPLLGLPDGYEYR  
EKKSSIGDVAAKHEARRMIMESTVEEVVPVDFEEKTA-

*Targeting:*

SignalP 3.0 - NN: Yes, Cleavage Site AYA-FV

SignalP 3.0 - HMM: Yes, Cleavage Site AYA-FV, Signal Peptide Probability = 0.996

SignalP 4.1: Yes, Cleavage Site AYA-FV, D = 0.670 (D-cutoff = 0.450)

ChloroP: Yes, Score = 0.570

7) *Thaps3\_263437 (BCH)*

No introns.

>Thaps3 chr\_8:927506-925618

```
CGTCATCAGTCACCTTCTTCTCACCTCATCCACCCGCCATCCATCATCCACCC  
TCTACCACCTATCATCTACATACATTCAACCATGCATCAGCTATCCAGACTGCTTCCA  
AACTCTTCCCAGTCATCGCTACCTACATCATTGCGAAGTATGCTCTCCCTCACATCAATA  
CGATCCTTCACTGTTCAAACACCTTGAGCAACTTGTGAGAATAACATACACCGTCCTCT  
TTGCAATAGCGATGGAGTACATTCAAGATATAGTCAGTACTGCTACTGTGGCATGGAAAGT  
TCCCTTGGGATTAAATGGCTCACATCATCAGTATCCAGCTGTTGGAAGCACACCTG  
TGTATGGACACAACAATCCGTACGTCTCCAGCCATTGAGTTGAACGATGCATTGCCG  
TTTCTTGCAACGATTGCCACATTGCAATGTGGATAGGGTCAGAGCCTCCATCAACCT  
TGACAAAAGATTGTTCTATTGGTATTGGATTGGAGTGAATCTCTATGGCCTTCATACT  
TTGTCGGTCACGACATTGTTGTCACGAACGTTGGCAAGGGAGTAGCAAACGCTTGA  
GACGAGCATTCCGTATATGGAGCAATGTGCTTCTGTTCATATCCGGTATCATCACAAGT  
TGACGAAACGTAGTAATGATTGATCCATATGGAGCGCCTACGGCTTGGTGGTC  
CGTCGGAAGTAGAGTGTGAAACAGAGGTCAATGGTATGCACCGATGCCTATGCGTTGA  
AAGCTATTCTGGATAGCAACATTGATCTTCTCGCATCGACAATTACAGCTCGTTGT  
CTCCGGCAGCTCAAGCAATTGTCCTCGGATGTGAGGATGGTGTGGCTCCGGCACAT  
TGTCAGACAATACAACAACATCTCGTGTACGGCAAGCTGCTCTATTGAACTGGCAAT  
CAACTCCATCGAGACTGATGCCACGGACTTCTGGGCTATTCAAGTGGCATTGGTT  
CATACCTCATCTTGCCACAGTCGCTAGGCGATCTGAAACACATACAAATGCAACAAAC  
CACCATATCTCATCTTCTATGCAACAGGCCACATCATGGAATGCTCTGGAGGATATA  
TGATTGTCAACTGCTCTCAAATACAAGAATGCTGTTAGGAGATGTGCAAAACTTC  
AGGTTTGTGCTGCTACTTCATTGTTAGGTTCTCCGACTCGTCGGTGTGCTGATAC  
GTCTCGAGAGCAACACAATTACAACATCGCTGAGATGTCTGACTTAATGTTACGATAT  
CAGCAGTGGTGTGACTCTATCGTCTTGATGCAGTCGTTGACATGTCAAAGCAGAGCG  
TTGTCCTCGGACAATCAATCGCATTGGTATCATGGGATATTGCTCTTCCGTGTATC  
CAATCCAACGTGGAAATGATTGCTTATTTACGTTCCAGCTACAGTGCAGTTAGTTGT  
TGCAAGCCAGTGGAAATGATTGCTTATTTACGTTCCAGCTACAGTGCAGTTAGTTGT  
TTCTCTCGGAGCAACGCTGTATCAAAGAAAGATAATGTCATCAGAGTATGGGATTA  
TATCATTGATGGTGTACTTGATGCCTATTGGCAACTGTGCTCAGCCAAGAGATAACATA  
TCCCAGACGTTCGACGCAGAGAATCTTACCATGCGAAGATCCAGCAATGGATTG  
TGGAAAGAGAAAGTACTGAAGCGTTGGACTTTCTCGTTATGCACGTTCCATCTTGACCA  
CAGTCCTGGGTATTAAATTGAGTCACCCCGTAGCATGATGGAAATCTCCAATTAACT  
AATTGCACATTAATCATTGTTGATTATC
```

*Translated:*

MHQLSRLLSKLFPVIATYIIAKYALPHINT  
ILHCSNTLSNFVRITYTVLFAIAMEYISRYSHCYLWHGKFLWWINGSHHHQYPAVGSTPV  
YGHNNPYVSPAIELNDAFAVFFATIATLAMWIGSEPPSTLTKDCSIGIGLGVLYGLSYF  
VGHDIVAHERLGKVANALRRAFPYMEQCASVHIRYHHKLTKRSNDSDPYGAPYGFWLGP  
SEVECLNRGQWYAPMPMSLKAISWIATLIFFASTIHSSLSPAQAQAIVLLGCVGWCGSGTL

SDNTTSRRIGKLLSLNWQSTPSRLMPHGLSGLISVGIGSYLIFGHSLVGLKPYTMQQP  
PYLIILYATATSWNALGGYMIVNTAPPNTRMLFRCAILQVCLSYFIVRFLPHSSVLLIR  
LESNTITTSRCLDLIVTISAVVCTLSFFDAVVDMSKQSVLGQSIAGIIGILLSVYP  
IQLSLQGEWWSCIQNRYPMQASGMIAVYVPATVTSLFLFGATLYQRKIMSASEYGII  
SLMVILVCLLATVLSQEIHIPDVSTQRIYLPCEDPAMDSLEEKVLEALDFSRYARSILTT  
VLGIKFESPA-

The underlined portion aligns with BCHs from plants and green algae (**Appendix D**).

*Targeting:*

SignalP 3.0 - NN: Yes, Cleavage Site VIA-TY

SignalP 3.0 - HMM: No, Signal Peptide Probability = 0.299

SignalP 4.1: No, D = 0.285 (D-cutoff = 0.500)

ChloroP: No, Score = 0.458

### 8) *Thaps3\_9541 (LTL1)*

No introns.

>Thaps3 chr\_13:695539-693528  
CTCCAACTCGCATCGGTCAACACAACACTGCAAGAGCGAAGGAAAAGCCAAACCTAAC  
ATGAAGTTCACACAGCTCGCCGTCTGCTGGACGTCGGTACAATGCCTCGTT  
CCATCGTCCTCACCTCTCCAGCGTTGAAGAATGAGCAGCAGCAAGTACGTGCATCATCT  
CCACTGTACGCACTTGATACCAAGAAAAGGAAGAAACCACCGGCCACCTCTGCTTCC  
TCTACCGACACATCTCCACACCAGCAGCAGCAGCCACTGAAGAATCCGAAGGACTCCA  
TGGTGGTGGGAATACATCTGGAAGCTCCCCTGAATGCAACCAGCGAACCGAGGACCGAC  
ATCATCTTCGCCGACAGTGCTCGCGTCTCGCACGAACATTGAACAAATCTACGGAGGA  
TTCCCCCTCCCTCGATCAATGTCCATTGGCCGAAGGAGAAATTACCGATATTGCCATGGGA  
ACAATGTTCATCGGTTGCAGAGGTATCAACAAACAGTATGGAAGTCCGTACAAACTGTGC  
TTTGGTCAAAGAGCTTCTGGTATTGGATCCAGTTCAAGCCAAACACGTTCTACGC  
GATGCCAACACTCTACGATAAAGGAATCTTGGCTGAGATTCTTAAACCGATCATGGGG  
AAGGGGTTGATTCCAGCAGACCCAGAAACGTGGTGGTACGACGTAGGGCGATTGTTCT  
GCCTTCACAAGGCGTGGTGAATCATATGGTGGATTGGTATTGCAATGAAGGA  
TTGATTGCTTCGTTGGAGGAGGCAGAAGAAAAATGATGCTCCTAACGGACAACAGGGT  
GGAAAGATTGAGATGGAAGAAAAGTTTGCACTGTCAGTGGCACTGGACATCATTGGTTGTCG  
GTGTTCAACTATGAATTGGATCAGTGAGCGAAGAATCACCAGTGTACAGGCAAGTGTAC  
TCTGCATTGGTGGAGGCAGAACATCGTAGCATGACTCCGCTCTACTGGGATTGCCA  
TTGCCAACGAGGTGGTACCGTCTACGCAAGTCAATAGCGATCTCAAGGTCTGGAT  
GATGTGTTGACTGATTGATCGTGGCAAGAACCTACGTCAGTGGAGGACATTGAA  
GAGTTGGAGAAGCGTGATTATGCCAATGTGAAGGATCCATCGTGTGCGATTCTGGTG  
GATATGAGAGGTGCTGATATTGATAATAAGCAATTGAGGGATGATTGATGACGATGCTT

ATTGCAGGGCACGAGACGACTGCGCTGTGTTGACTTGGCGTTGAGCTAACAAAG  
CATCCGGAACAGATGCCAAGGTTCTGCCGAGATTGATTCTGTGTTGGAGATCGTACA  
CCGACATATGACGATATCAAAGAGATGCAGTATTGAGGTTGGTGGTGCAGAGACTTG  
AGGTTGTATCCTGAGCCTCCGCTGTGATTCTGCTGTTGAGAACGAAAACAAGTTGCC  
AAGGGAGGTGGAAGGGAGGCTACTGTGATTCTGCTGTTGAGGATATCTTCTATCATTGTAC  
AATCTTACCATGATGAGAGGTTCTGCCGGAGCCTAATGAGTTCAAGCCCAGAGAGATGG  
GAGAGCAAGTATATCAATCTGAGGTACCAAGAATGGGCTGGATATGATCCTGCAAAGTGG  
ATAAATACCAACTGTACCCAAACGAGGTCGCGTCCGACTTGCCACTTGCCATTCGGA  
GGAGGAGCACGAAAGTGTGTCGGAGACGAGCTCGCCACGTTGGAGGCAACTGTGACTTTG  
GCAATGTTACTCCGTCGCTTGAGTTGACTCTGCCAGCTTGCTGCTTCGAAG  
ATTGACATTATGGATCATCCAGAGGATTGGAGCATGCGGTTGGTATGAGGACCGGAGCT  
ACTATTCTACTAGGAAGGGATTGCATATGGTGATTAGGAAGCGTGAGTTGAGTTCTATT  
AGAGCCTAGTCTAACAAACTATGGTCATT

*Translated:*

MKF TTALAVLCWTSVTNAFVPSSFTSPALKNEQQQVRASS  
PLY ALDTKEKEETTTATSASSTDSTS TPAAAATEESEGLPWWWEYIWKL PVMQPAEPGTD  
IIFADSARVLRTNIEQIYGGFPSDLQCPLAEGEITDIADGTMFIGLQRYQQQYQSPYKLC  
FGPKSFLVISDPVQAKHVLRDANTLYDKGILAEILKPI MGKGLIPADPETWSVRRRAIVP  
AFHKAWLNHMVGLFGYCNEGLIASLEEAKKNDAPNGQQGGKIEMEEKFCVALDIIGLS  
VFNYEFGSVSEESPVIKAVYSALVEAEHRSMTPAPYWDLPFANEVVPRLRKFNSDLKVLD  
DVLTDLIDRAKNSRQVEDIEELEKRDYANVKDPSLLRFVDMRGADIDNKQLRDDLMTML  
IAGHETTAAVLTWALFELTKHPEQMAKVRAEIDSVLGDRPTYDDIKEMQYRLVVAETL  
RLY PEPPLLIRRCR TENKLPGGGREATVIRGMDFL SLYNLHDERFWPEPNEFKPERW  
ESKYINPEVPEWAGYDPAKWINTNLYPNEVASDFAYLPFGGGARKCVGDEFATLEATVTL  
AMLLRRFEFEDSAKLAASKIDIMDH PEDLEHAVGMRTGATIHKGLH MVIRKREL-

*Targeting:*

SignalP 3.0 - NN: Yes, Cleavage Site TNA-FV

SignalP 3.0 - HMM: Yes, Cleavage Site TNA-FV, Signal Peptide Probability = 0.999

SignalP 4.1: Yes, Cleavage Site TNA-FV, D = 0.797 (D-cutoff = 0.450)

ChloroP: Yes, Score = 0.548

### 9) *Thaps3* 270336 (LTL2)

Exon 1:

>Thaps3 chr\_9:683521-684549  
CGCCCTCCCTCAACCACTTCCACGCTTTGGCTCTGGTTAGCTGCTGATAAAAGTTG  
AGAGTAGTCCAACAATACAGCAATACGACTCTTCTGCTGCTAGTAGTAGACTGTGTAT  
CATCGTGGAGGAAGCTGAGTTGATTGGATAGAATTGGGCTGATACAACGGATAGAAAG  
AACATCAAGATGTGCACCAACTATCCAGCCGTCGGACGCTGTTGGCGTTGACTTCGCC

TTTACTGGATGCACTGCCTTCAACTACCACCGGCCACACCATCACGTGCGTCATAACA  
AAAGCATACAGTACCCACCTGATAAAGAGATCAAAGAAAAGCAACGCTCTCGTAACCCA  
AGCAAGATCTACACACAAGCAGACATAGATACTCTCGATCTCCTCGTACGAAAACGAA  
CTCCTAGCAGCATGGGATACAGACTCATCCCTAACGTGGATTGACTGGGAGATTGAA  
AAGCTACGACGAAATTTGCAGGCCCTGCCAAAGAGAAGATGGACAGTGGTTGTAAA  
CCAAGTCTATTGATTCCTCGTACCAACACACCATCGAACGTAGTTGGTGAGCAAT  
ACTGGTGAACGATATGAAAGTCTCCAAAACCGGTGAATATGCTTGATGTAGGATTGCTG  
ATCACCAAGAATCTATTGAACACTCTGGATTGGCGAGTCGGTATGGCAGCCGTG  
CCGGATGCAGTGATTCAAAAGTATGAAGGAAGTTCTCCTCATCAAGGGTGTGCTC  
GGTGGTGAATCTCAAACACTCGCAGGAGGACCACTATTCTACTCCTGCAAAGTATTAT  
CAGGACTATGGACCCATCTTAATTGAGCTTGGCCGAAGAGAGTTCTGGTCATCTCC  
GATCCTGTTATGGCGAGGCATATCTGAGGGATAGTAGTCCAGAGCAGTATTGCAAGGGA  
ATGTTGGCGGAGATTGGAGCCAATCATGGCGATGGTCTTATCCCTGCTGATCCAAAAA  
ATTGGAAAG

Exon 2:

>Thaps3 chr\_9:684641-685198

GTACGACGACGAGCAGTCGCTCCGGCTTCCACAAAAAGTGGCTAACAAATATGGTACT  
CTCTTGGTACTGTGGTGAACGTCTCGTTAACGATCTCGATGCACGGCTACTGCTAAG  
ACTCCAGTGGATATGGAAGAACGATTCTGCTCCGTAACGCTGGATATCATTGGAAAAGCA  
GTCTCAACTATGACTTGGTCAGTTACGAAGGAGTCTCAAATTGTCAAAGCAGTGTAC  
CGCGTGCTCGTGAGGCAGAACATCGATCATCTTCAATTCCGACTGGGATTGCC  
TATGCTGATAAGTGGATGGAGGTCAAGTTGAATTCCGAAAAGATATGGGATGTTGGAT  
GATATCTAACAAAACAATCAATCGCGCTATTGAGACTAGGGACGAGGCAAGCGTAGAA  
GAGTTGGAGGATAGAGATGTTGGAGATGATCCAAGTTGTTGAGGGATGATTGATGACAATGCTTATTGCA  
GGACACGAGACAACGGCT

Exon 3:

>Thaps3 chr\_9:685302-685832

GCAATGCTTACTTGGACAGTGTGGACTTGTGAGCAATGATTCTGGTTGATGAAGGAG  
ATTCAAGGCCGAAGTACGAACAGTCATGGGTGACAAATTGCGCTCAGATTACGATGACATT  
GCCAAAATGAAGAACGATGAGATATGCTTGATAGAACGACTTCGTTGTATCCAGAACCA  
CCTGTTCTCATCGTGGCAAGGTCTGAGGACAACCTCCAGCGGGTGGTCTGGTTG  
TCGGGTGGTGTCAAAGTATTGCGAGGAACAGACATCTTCATTCTACATGGAATCTTCAT  
CGTGCTCCAGAGTATTGGAGAACGAGTATGATCCCACGCGATGGAACGACGA  
TTCAAAAACCCGGAGTGAAGGGCTGGAATGGATACGACCCAGAGAAACAATCAGAGTCG  
TCGCTGTATCCGAATGAGATCACTGCGGACTATGCATTCCCTCGTTGGTGCAGGGAG  
CGAAAGTGCATTGGGGATCAATTGCAATGCTGAAGCATCAGTCACTCTG

Exon 4:

>Thaps3 chr\_9:685927-686236

GCCATGATCATAAACAAAGTTGACTTACATTAGTTGGCAGTCCAAAAGATGTCGGCATG  
AAAAGTGGGCAACCATTACACCATGAATGGACTCAACTTGGTGGTGAGTCGTCGGTCG  
GAAGATAATCCGATTCCGGAGACCAATGATTACTGGATACAGCAGCATTGTCGAGAGGT  
CTCAATGTCAATGGACGACCATATTCAACCAATGAAGATGCTGCCTGGACGGCATCTTCT

CGAGATAAGAATGAGGGAGTTGTCTCGGTTAGTTAATTAAAGTTATCTAGGATATAAG  
AGGATTCTGT

*Translated:*

MCTKLSSRRTLLALYFAFTGCTAFQLPSATPSRASITKAYSTHLDKEIKSKTPLVNP  
SKIYTQADIDTLDLSSYENELLAAWDTDSLQRGFDWEIEKLRRNFAGLRQREDGQWVRK  
PSLFDFLVTNTPSNVVGVSNTGERYESPPKPVNMLDVGLLTKNLLNTLGFGPSLGMAAV  
PDAVIQKYEGSFFSIKGVLGGDLQTLAGGPLFLLLAKYYQDYGPINLSFGPKSFLVIS  
DPVMARHILRDSSPEQYCKGMLAEILEPIMGDGLIPADPKIWVRRRAVPGFHKWLNN  
MVTLFGDCGERLVNDLNDARATAKTPVDMERFCSTLDIIGKAVFNYDFGSVTKESPIVK  
AVYRLVLRREAHRSSSFIPYWDLPYADKWMGGQVEFRKDMGMILDDILTKLINRAIETRDEA  
SVEELEDRDVGDDPSLLRFLADMRGEDLTSKVLRDDLMTMLIAGHETTAAMLTWTVFGLV  
SNDSGLMKEIQAEVRTVMGDKLRPDYDDIAKMKKMRYALIEALRLYPEPPVLIRRARED  
NLPAGGSGLSGGVKVLRGTDIFISTWNLHRAPEYWNPEKYDPTRWERRFKNPGVKGWNG  
YDPEKQSESSLYPNEITADY AFLPFGAGKRKCIGDQFAMLEASVTLAMIINKFDFTLVGS  
PKDVGGMKTGATIHTMNGLNLVSSRRSEDNPIPETNDYWIQQHLSRGLNVNGRPYSTNEDA  
AWTASSRDKNEGVVSLVN-

*Targeting:*

SignalP 3.0 - NN: Yes, Cleavage Site CTA-FQ

SignalP 3.0 - HMM: Yes, Cleavage Site CTA-FQ, Signal Peptide Probability = 0.990

SignalP 4.1: Yes, Cleavage Site CTA-FQ, D = 0.724 (D-cutoff = 0.450)

ChloroP: No, Score = 0.497

#### 10) Thaps3\_270370 (ZEP1)

No introns.

```
>Thaps3 chr_6:1420465-1418423
CTCCGTTCTCATTTCCTTTCTTCCAAACTTCTTCCGCTGCTGGAGCACCAACGGGT
AAACAGTGGCAGCAGAGGACAAATCAACTAGTACAGTACAACGAATCATGACGGTTAGAA
GAATGCCCTCGCTGCCATTGGTATCTCGCTGTCCACCTGACATGTGCATTGTCACGA
TCTCCTCGTCTCGTACTACCATAAACCTCTCAATGTCGTTGGCGAACAGGCCTCTCCA
TCGGACCAGCAACTCTCCTCCGTAATCTCAAACAAAACCTACCAACAAATAGATTGGCTAG
CGGAAGGTAAAGGCTGCCATCCAACAAGATTGACATTCTGATCATGTAGCTACAGTGC
TTGCTCAACCAAATGCTCAAAGCGCGAAGCTGAGAGTGAGAACGTACGCATAAGATCC
GCAGTAGAGCAAAGCAGGCTAGCGAAGATGCAATGGCATTGCGTGGTAGTTGATTGGAG
ATGATGACGCCATGCATGGTGGCGTGAACAACGTTCTATTCCAGAGGGAGGACGAGTAG
TTACAACGGATGATCCATTGACTGTTCTTGCTGGCGGTGGATTGGCTGGTTGGTT
TCGCTGCAGCATGCCATTCAAAGGCATGAAAGTTGCATTGTTGAGCAGGCTCGTCTT
ATGCTCCTACGGAGGCCAATTCAATGCATTGAGGGCTTGCAGCAA
```

TCAATCCTGAGATCTTCAGGAGTTGGTTACTGCTGGAACATGCACTGCGGATCGTGTGT  
CTGGATTGAAGATTGGATATAAGAAGGGAAACAAACTTGCTGGACTGTACGATGCAGGAG  
ATTGGTTGGTGAGGTTGACACTATCGGACCAGCGTTGGAAGCTGGATTGCCAGCAACTG  
TGGTTGTGGATAGGCCAGTCATTAGCAGATTCTGGTGAATATGGCTTCCTGAGGGCA  
CCGTGCGTATCAAATCACGTATCCAATCGTATGAGGATCTGGGAAGGGACGTGGAGTGA  
GTGTCACCTTGGAAAGACGGGACGAAAGCGTACGCAGATGTATTGGTAGGAGCTGATGGCA  
TCTGGTCTCAAGTTAGAAAAGAATCTCACGGATTGGACGATGGAGCTGGAGGGTCGCTG  
CATCGGGCGCAGCAGGAGGTGCATTGGACGATGCCAAGCACGCAAATTGGCACGTGATA  
CAGTCGCAATTGCAGCCAAGGCCGATCGCTGTTCTGGTTCACATGTTACGCTGCAC  
TGGCTCCTCATCGGGCATCCAACATCGAAAATGTGCGTATCAAATCTGTTGGAGAGA  
AGAAGTACTTGTATCTACCGATGGAGGAGGAGACAGGCAACAGTGGTTGCACTCATTC  
GCGAACCTGCCGGGGAGTGGATCCTGAGCCCACCTCCGAGGGATCCTCACCTAAGCTCA  
CTCGTCTAGGAAGGAATTGCGTCAATGGAAGTGGTATGCTGATGGCAATGTTGG  
ATCCATTGCAATTGGAGTTGATCAATGCAAGCCTCGGAAGAAGACATCAAGCGTCGTGATT  
TATACGACGGAGCTCCTCTTGAECTACCCCTGACCCACAACGTTGTTGAGTCCATGGG  
CAAAGGGACCTGTGGCACTTGGGAGATGCAGCACATCCAATGATGCTAACCTCGGAC  
AAGGAGGATGCCAACAGAACGAGACGATACCGTCTCGTCAAGAGAGTTGCAAGGTGC  
AGCATTCAAGAGATGTTCCAGGAGCACTCGGGAGATACTCTCGCGTGTGATTAGGA  
CAGCCATTATCCAAGGTTTGCTCAGCTTGAAGTGTCTGTTGTTGACTTGTGATT  
TGATGACTATTCCACTCTGGGTCCTCTTGACTACACACCTCTTTAAGAGAGATGCTGATG  
TCATTTGAGATAACCTCTACACACCTCTTTAAGAGAGATGCTGATGATTGAG  
AAGCAGATGTTAATGGTAATATTCTGATAAGGTTAAACTTATGATGGAGTTGCTGT  
CCA

*Translated:*

MTVRRIASLAIGISLSTLTCAFVTI  
SSSRТИKPLNVVGEQASSIGPATLLRNЛKQNLПQIDWLAEGKGSPSNKIDIPDHVATVL  
AQPNAPKREAЕSEERTHKIRSRAKQASEDAMALRGMLIGDDDANAWWREQRСIPEGGRVV  
TTDDPLTVLAGGLAGLVAAACHSKGMKVALFEQASSYAPYGGPIQIQSNALRALQQI  
NPEIFQELVTAGTCTADRSGLKIGYKKGNKLAGLYDAGDWLVRFDTIGPALEAGLPATV  
VVDRPVIQQILVKYGFPEGTVRIKSRIQSYEDLGKGRGVSVTLEDGTKAYADVLVGADGI  
WSQVRKNLHGLDDGAGGFAASGAAGGAADDAEARKLARDTVAIAAKADRRFSGFTCYAAL  
APHRASNIEVSQILLGEKKYFVSTDGGGDRQQWFALIREPAGGVDPPEPTPEDPHPKLT  
RLRKEFACNGSDADGNVWDPFALELINAASEEDIKRRDLYDGAPLLTLDPQRLLSPWA  
KGПVALCGDAAHPMMPNLGQGGCQATEDGYRLVEELAKVQHSRDVPGALGRYSRVRVIRT  
AIIQGFAQQLGSDLLVDFDLMMTIPLLGPFFLMTQLSMPFILRYLYTPSF-

*Targeting:*

SignalP 3.0 - NN: Yes, Cleavage Site TCA-FV

SignalP 3.0 - HMM: Yes, Cleavage Site TCA-FV, Signal Peptide Probability = 0.960

SignalP 4.1: No, Cleavage Site TCA-FV predicted, D = 0.436 (D-cutoff = 0.500)

ChloroP: Yes, Score = 0.526

11) *Thaps3\_261390 (ZEP2)*

Exon 1:

>Thaps3 chr\_2:1117778-1118447

```
TCCCCCTCTCGGGTTGTGTCAGACGCAGACGTCCCTCGCATTGTAGTCAGTCCA  
AGCAACACCAATCAATTAAACAGAACATGAAGCTCTCCATCGTGTGCTTATTATTAACG  
TCGGCGACGTCAAGCCTCATCGCTCCATCAACCACACGCACATCAGTGGCGTCACAACG  
TCATCATTGCAAATGTGCGAGGAAGTGCCCTCAAATGGCGATGACGAAGCCGACGCC  
GACTTCAATTCTCGGATTATGAACCTCTCGGAAGACCCAGCTGCCCTGGCGTCCTCTC  
AAAGTAGCCATTGCTGGTGGTGTGCGTGGTCTCACAGCTCGCTATGTATGTTGAAG  
AAGGGATTGACGTGACGGTGACAAAAGACTGCTGCCCTGCTCGTTGGACCC  
ATTCAAGTTGCCCTAAATGCTCTTCTGTCTACAGGAGATTGACGAGGAGTTGTTGAA  
CGTGTAAATGGATAAGTTCACCTCACTGGTACAAGAGCTTGTGGTATCAAAGACGGTTG  
AGAGCGGATGGATCGTCCGTATGACGAATGATTCCCTGGACTACTTGTGGAATCCCGAG  
GCTCCTGCTGATTGGTTGTCAAGTCCCTTGAGGCAGTGTGCTGATTGTTGGACTT  
CCCTACACTG
```

Exon 2:

>Thaps3 chr\_2:1118548-1119207

```
GCGTCATTGACAGACCCGATTGCAGGAAATTCTTCTGATGAGTCAGAAAGATCAAGC  
CCGATTTCATTCAAATGGCAACCCAGTGAACGGATACGTTAGCAAAGGAAAAGGCAACG  
GAGTGAAGTGAACCTGCCGATGGAACAACTGCAGAGGCTGACGTCCCTGTTGGTCGG  
ATGGTATTGGTCTGCTATTGCTCAGATGTATGGGGAGGAGATAAAAAGAGTTCAA  
ACAATGCACTCAAACGTCAAGGCTGCACGTACAGTGGATATACCGTCTTGCTGGAGAGA  
CTGTGCTCAAGACGGAGGATTACTACGAGACTGGATACAAAGTGTACATTGGCCTCAAC  
GCTACTTGTGACTTCAGATGTAGGAGACGGAAGAGTGCACTGGTACGCTTCTTGCT  
TGCGCCGGGTACGAAGAAAGCACCAAGTGGATGGGAGGTACCGAGCGAACAGCGCAGG  
ACGACCCAGAGGAGAATCTGTAGATTACATCAAATGTTGCATCAGGGATGGTCGGATG  
AAGTCATGACTGTTCTGATTCTACCCCTCTGATAGTGTGAGCAACGTGACTTGTACG  
ATAGGCCACCTGAGCTATTGAGAAGTTGGCTGATGGAAACGTCGTCTCATTGGTGATG
```

Exon 3:

>Thaps3 chr\_2:1119282-1119556

```
CTGTCCACCCGATGCCCCAAACCTGGACAAGGAGGATGCCAAGCAATTGAAGATGCAT  
TTGTTCTTCTGAAACGCTGGAGGCATGCGAATCTACTCAAAGTGGAGGATGCTTGC  
AGGACTTTACAAAAGCGTATCGTCTGTTAGTATTGTGCACTGCCCTCAGTCGGTAG  
CGAGTGAAGTGTGATCATCAATGCGTTGATACACCCTGGAGTCCTCATGACGACCTCGGAA  
AGTCGTGGAAGAGTTATTGACTTCTTCTGGAG
```

Exon 4:

>Thaps3 chr\_2:1119650-1119989

```
CCCATTCTCAGTATGCCATCTCCCTGCACAGTTGCTTATCTTACTCATACCACCA  
ACGGAAACATGGGAGGTTGCCTCTGCTCTGAAGCAAAGTGAAGAAACAGCACGAA  
GAGGACGCTGAGATGGCATTCAATAGGGTAGAGGAAGAGGGGCAATCAACTAGAGGACCG  
AGTTTCTCAAAATAGCAGAGTCAGAGACGGTGTGGCTGCAAAGAAGATGTAATGACTA  
AGAAGGAAGGAAGAGGGATATGATGCGTGTACTCAGGCTACAAGGGTTGTTAGTGGG  
TGAAGAGTGCAACTATTTAGTACAAAAGTACAGAATGCA
```

*Translated:*

```
MKLSIVCFIILTSATSIFIAPSTTRTSVAVTT  
SSFANVRGSALQMADDEADADFNSSDYELLGRPARPGRPLKVAIAGGGVGLTAALCMLK  
KGFDVTYEKTAAFARFGGPIQFASNALSVIKEIDEELERVMDKFTFTGTRACGIKDGL  
RADGSFRMTNDSLDYLWNPEAPADWFVKFPLRQCADLFGLPYGVIDRPDLQEILLDEC  
KIKPDFIQNGNPVNGYVSKGKGNGVTVNLDGTTAEADVLVGSDGIWSAIRAQMYGEEIK  
KSSNNALKRQGCTSGYTVFAGETVLKTEDYYETGYKVYIGPQRYFVTSDVGDGRVQWYA  
FFALPPGTTKAPSGWGGERTAQDDPEENLVVDYIKSLHQGWSDEVMTVLDSTPPDSVEQR  
DLYDRPPELLRSWADGNVVLIGDAVHPMMPNLQGGCQAIEDAFVLEACESTQKLE  
DALQDFYKKRIVRVSVQFLSRLASDLIINAFDTPWSPHDDLGSWKSYLTFFWKPILO  
AIFPAQFAYLYSYHPTGNMGLPSALEAKWKKQHEEDAEMAFNRVEEGQSTRGPSFFKI  
AESETVLAAKM-
```

*Targeting:*

SignalP 3.0 - NN: Yes, Cleavage Site TSA-FI

SignalP 3.0 - HMM: Yes, Cleavage Site TSA-FI, Signal Peptide Probability = 0.998

SignalP 4.1: Yes, Cleavage Site TSA-FI, D = 0.793 (D-cutoff = 0.450)

ChloroP: Yes, Score = 0.551

## 12) Thaps3\_7677 (VDE)

No Introns.

>Thaps3 chr\_8:842679-841117

```
AGGACAACAACCAACACCCTGCCATTGAACACTCTGTTGCTGCTCTACCCAATAGACGC  
CATGAAGCTGTTCTTCTCTCGTCTGGCGCTGCACCAAGTGTCTCCTCGCACCATC  
AAACCCAGTTGATCTCGTACTCATTCATCGGTACACTCCAACAAACATAATCACGTGCT  
CGAAGCTACAACGACAACATGGATGACATTACCTCTCCCTATCCGCCAGGAATATCAA  
CAACGAGATCGTAGAGCGAATTGGCAAAGTAACCACCTCAGCTCTCGCATTGACGCT  
CAGTTCTGCCCCATCACATCGCCATCTCCGGTCCAACGGCGACGTACTATCGTCCAT  
CCCATCTGCCAACGCTGCCATGGTCAAAGATCGGTCTATGCCCTGTCAAGAAGTGCAG  
AGTTCCCTGGCCAAGTGTATCACCAACCCAAACTGCCTGCTAATGTGATTGCATCAA
```

TTCTTGCAACGGAAAGGAAGATGAGACTGGATGTCAGATTAATTGTGGAAACGTCTTGA  
GAATGACGTTGTTGGGGAGTTCAACAAATGTGCCGTACCGATATGACGTGCGTCCCTCA  
AAAGAAAGACGATGGAAGTTATCCCGTCCCACCAAGATGTATTGGTCCAATCGTTGA  
TACCAAACATGGAACGGAAGATGGTTCATCACCAGGGCAGAACAGCTCTTGATAC  
GTTCCCATGTCAAGTCCACTTCTCACCGAGACTGCTCAGGCAAGTCTCGGGAAATT  
GAATTGGCGTATCGAAGAGCCTGATGGAGAATTCTTCACTCGTATGCTGTGCAAGAGTT  
TGTTCAAGGATCCAAACAATCCTGCTACTGATCAACCACGACAATGAATATTGCATTA  
CCAAGATGATTGGTACATTGGATTATGCCCGGATGATAACAAGGAGGGTGTCCCTCC  
CTTGCAATTGTGATTACCGTGGTGGAGAATGATGATGCATGGATTGGATACGGTGGAGCTGT  
GGTGTACACTCGTGAATTCAAAGTTGCCAGAGTCTCTCCTACCGTCTCGTGAGGCTGC  
TAAGAAGGTAAACTTGACTTCGACAAAGACTTGATCTCACGGACAACACTCGTGAAGGC  
ACTTGAGAAGGGAGAGGAGGTGTTGAGGGAGAAGTTGCTGGTAAGATGGCATTCA  
GACGGAGAACAGTGCACACAGCAGGCTGTGTCAGAACACTGCGCTAGTAATACTGT  
AAAGGGTGAAGTGAUTGCTGTTGAGAAATCGCTCAGAAGATTGAAGAGAAGGCTTGGC  
GTTTGAGAAGGAATTGATGAAGGATGTTGTTCACTGGAAAAGGAGATCGTAAAGGAAGT  
TGAAGAGGTAGAGAAGGAGATTGTTCAAGAGGAACAAAGATCTTGGTGGTATTAGATA  
GAUTGGTTGAGTTAGTGGAGTAAATGCTACTCATTGACTTATCTTGGAAATGATATTG  
AGAAGACGTCTAAATGCACTGCGAGTAAGAAGATCTTATGTGAATGGAAAAGTATGAA  
TGG

*Translated:*

MKLFLSLVLAAPVSS  
FAPSNPVVSRTHSSVHSQQHNHVLEAHNDNMDDITFLSARNINNEIVERIGKVTSALL  
ALTLSFSAITSPISGPNGDVLSIPSANAADGAKIGLCLVKKCRVPLAKCITNPNCLANV  
ICINSNGKEDETGCQINCNVFENDVGEFNKCAVTDMTCVPQKKDDGSYPVPSKDV  
QSFDTKLWNGRWFITAGQNKLFDTPCQVHFFTETAPGKFVGKLNWRIEEPDGEFFRDA  
VQEJVQDPNNPAHLINHDNEYLHYQDDWYIVDYAADDNKEGVPPFAFVYRGENDAWIGY  
GGAVVYTRDSKLPESSLRPLREAACKVNFDKDFTDNLNSCKALEKGEEVLREKFAGK  
MAIQTEKQLQQQAVLARTAASNTVKGEVTAVEKSLQKIEEKALAFEKELMKDVSVEKEI  
VKEVEEVEKEIVQEEQKIFGGIR-

*Targeting:*

SignalP 3.0 - NN: Yes, Cleavage Site VSS-FA

SignalP 3.0 - HMM: Yes, Cleavage Site VSS-FA, Signal Peptide Probability = 1.000

SignalP 4.1: Yes, Cleavage Site VSS-FA, D = 0.682 (D-cutoff = 0.450)

ChloroP: Yes, Score = 0.529

13) *Thaps3\_22076 (VDL1)*

Exon 1:

>Thaps3 chr\_4:141771-142931

```
CCCATAACAGCGCTTCCAACACCGCAACATGAGACCGTCAACCTCTGCCTTGACAGTCGT  
CTAGGCACCATTGCGCTTGTCACTGCAGCCAGCTAACAAACAATGTATCCGCCTCTC  
TACAAGATCATCGTCGTTGACGCAAAGACACAAGACATGCACCATCACAAACATCATCATC  
ATCTCTCTACGTGAACCCCCAACACGATGATGACAACACTCCAACAGATCCAACACAAACC  
CAATCCCTCCTCTCAGCGGCACTAACGCCGCAGTCACCACATCCCTCTCCTCATC  
TCTCCCCAGTGCCACCTCGCCTCCACACCGGCCTCCACAACGCAAAAGTACGACGGCTT  
CGCCGAGTACGCCAAGGAAAACAAATGGAACAATCGGACGTAGGATGCTTCTTAACAA  
GTGTGGCGATCAGACGAAACAACGTGTTAGTAATCCCCGTGGTATCAAGGGGGTGTG  
TTTGGGACGGTGAAGGGGGAAACAATCGTGTGCTACGCGGTGTTGCTGAGTTGGAG  
CGAGGATTGGACAACGGTTATCGTCACTATTGAAGATTATGAATGTGTGAAAGTTCC  
AAAGAATATTGACAACACTGCCGAGAATGTGGGGTATGATACTACCGTGAAGAAGTTGA  
TCCGTCAACGTTGGGGAAAGTGGTACAAGACGGATGGACTGAATCCAATTACGATCT  
GTTCGATTGTCATCTAACGTTGACTTTCACTGATGATACGAAAAAGGAGTTGGATAT  
GGGTATCTCTTAGAGTGCCGCGTCCAGAAGAATACGGAGGTGGATTCTGGAGAACAG  
TCTTACAGAGCACATGATTGTTGATGCCGTATCACCGAGTTAGACAACCTACTGGAAG  
AACGATGCATACCGCTGGTAAGATGTATGGGCTCAAATTCACTGAGAACTGGTACACT  
CGGAGAATCCAATGGTGATAATGATATCCCTCGTTAAGTTGGTGGCGTATAAGGGGCA  
TACGTTGCAAGGGATTATGAGGGAGGCCTTGTATGCGAAGGAGAGTGTGTTGCCGAA  
GGAGGCTGTGGGGCGGTGAGGGAGGCTCGGGCAAGGCTGGACTGGACTTCGACAAGTT  
CACGAGGATTGATAATACTTG
```

Exon 2:

>Thaps3 chr\_4:143069-143272

```
TCCAACCACAACAAAACACTGAATGATGATGCATCGGCTGGAACCTGGAACGTCTACCACAGA  
CTGGGTTGATCTGTAGTTGGTAAGGAGGAGTTATTGATTGGGTTGTTCTGGATGGAG  
AGGAGAGTACAAAACAGGTTAGAGCGTCGAAGAAGAAGATGCTTTCTAACCT  
AAAATCTGGGTATTGTCGTCCCGA
```

*Translated:*

```
MRPSTSALTIVLGTIALVSCSQLNNNVSFSTRSSLTQRHKTCTITSSS  
SLYVNPNNDNSNRSQHKPNPFLSAALTAAVTSLFLSSLPSATFASTPASTTQKYDGF  
AEYAKENKMEQSDVGCFINKCGDQTQLFSNPRGIKGVSCLRCKGEQSCATRCFAEFGS  
EDLDNWLSCTIEDYECVKVPKNIDNSAENVGYDTTVKKFDPLSTLVGKWYTDGLNPNYDL  
FDCQSNTFDFSDDTKKELDMGIFFRVPRPEEYGGGFWENSLEHMIVDAVSPELDNPTGR  
TMHTAGKMYGLKFTENWYILGESNGNDIIPPFKLVAYKGHTLQGNYEEAFVYAKESVLPK  
EAVGAVREAAKAGLDFDKFTRIDNTCPPTKSLNDASAGTGTSTTDWVDLVGEGGVID  
WVPGWRGEYKN-
```

*Targeting:*

SignalP 3.0 - NN: Yes, Cleavage Site VSC-SQ

SignalP 3.0 - HMM: Yes, Cleavage Site VSC-SQ, Signal Peptide Probability = 0.970

SignalP 4.1: Yes, Cleavage Site VSC-SQ, D = 0.694 (D-cutoff = 0.450)

ChloroP: Yes, Score = 0.568

**14)Thaps3\_11707 (VDL2)**

Exon 1:

>Thaps3 chr\_22:194840-195897

```
ATTCCTTCACTTTACTTGATTCAAATCTTAATAGACATAGCCTTTACGTGGCAAA  
GGTCGCGTCATTGCCAGGAGGTTGAAGCAAAACAGTGGACGACGTCGCTCGTAGGGACG  
GACAGCGAGAGAGGCCACCCCAGCTGTTGCATCCAAACAACCATCCATCGTAGACTCAA  
TACACATCAACTGATAACAGAGTGGTGTGATACTGTCAGTTAGAGTTCATGGATTAGA  
AAGACTGCAAGTGAGATACACCACAGTCCAGATGCCCTGAGTTGAATAGTCAAAGTTT  
TGCTCCCTCAATACAAAACAAATGTCGGCATCATCATCATCAACAAACAACAACAAA  
CGCTGGAAAGAGGGCACGATCGTGGCCGTCTCATCCGCATCAACATCATCAATGCCCTAC  
TCGGTCGATACTGATACTGGCAACCTTCTCTCATTCAGTGCCTCGTCGTCAACATC  
GGTGGAAAGCTGCCCTGCGCAGCCCTGCCGTTGACTAGATCTCACACTGCTGCC  
AACATCAAAGCAGCAGTCGCTCTACGCTCAAAGAAGAACATCGACTCATCCGA  
CAACCCGCTATCATATCTATTGATCTATCCTCCGATCCAGAAACCAACGTCGCC  
AAAACAAACAGCCACCCCTTCTCCACCCCTCGGCTTCTCCGCCCTTCCCTACCAATCC  
ACTCATCCCCACCTCCCTCTCCCCCTCCCTCAGCAGTGCACGCCAACGCC  
CTATGCTAAATATGGTGGCAAAGGCCCTCGATACATCCTAGTCGACAAAGACTGTCTCGT  
CAATCAATGTCAAGTCAAGGCCAAAGCGTGTCTCAGGATGATCCGATTGAGAAAGGG  
ATTAACGTGTACTGCCAAGTGTGGGGGATAATGCGTGCATTACGGGGTGTGTTGCTAG  
GTATGGGAATGAGAATTGGATGAGTTGAAGTGTACTATTGAGGATCATGAGTGTAT  
TAAGGTGGCTATTTGGAGGGTGGGGCGATGTGCTTG
```

Exon 2:

>Thaps3 chr\_22:195996-196062

```
GGCGAGAGCCAAAGTCGCTGCTCCTACTGTTCAAGGGTTGATCTAGCCAGTATGGAAG  
GGACTTG
```

Exon 3:

>Thaps3 chr\_22:196169-196611

```
GTATAAAGTAGCAGGCTACAACCCCAACTACGATTGCTACGCCCTGCCAACGAAACACCTT  
CTCCTCACCGAAGGCCGCTCTCCGACTCACTCCAACCAACAGGAGGAATACTCGG  
CTCTCTATCCAACGCTGTAGGTTCCATCGGTGCAGATCGCTACAAGTCGATGTGGAATT  
CAGTATGCCGAGGTATTGCCAGATGGTAGTCCTCAGCCACCGAGTGGAGTGC  
ATTCAATTAGTAGTGTGATTCAATGGAAGGGAGTGGGGTGCAGAGTGTGGGGTACAATCA  
GTACTCGACTCATGAGACAATGGTGTGTTGATCGGTCAAGAGTAATGGTGTGGGGGAAGC
```

TGTGAAATTGGCTTGGTAAGAGGGGAGAGGAAGTTGTATCGAGGACGGCTCATTC  
GGAAGGAGAGATGTTGGACTGA

Exon 4:

>Thaps3 chr\_22:196740-197411

```
AATTCTGGGAGAACCTGGTACATCATTGGCCAAAACAACCCGGCCAAGACGAGTTCAAAT
TCGTCTACTACAACGGCAAGACACGTCAAAATACCTACGACGGTGCCTCATCTACTCCC
GATCACGCACCCTCTACCCCGCTCCATGGAGAAAGTCTACAAGATTGCAAGGATGCGG
GTATGAATCCTGATCAGTTTGTAAGATTAGACACTCTGCTTGACGGTGAGGATGATA
AGCAAGAGATGATGATGATGAATCCTCAGAGAGAAGGACTGGTAGTCCTCCAATCCAT
TTAGGGGTATTTGGCATCTACGAAAGTATCTCAATTCTGGGAGTTGAATCTGTGGCGG
CCGAGACTACGTACAACGAACCAAAGAGTACGATATCGTCCAACTTCTCAAGGGAGTC
AGGCTACCAACCGCAAAGCGGATGCCGTTCAGGAGAGGCCGTGGTGGAAAGGAAATGGGAG
ATTATTGGAAGATCCTAGACGGCATTCGTTGATGGATAGTCTGAGAACAGATATGG
ATTGGCCGGATTATATCAAAGAGAAGAATTGGTGAAGGAGTCGGCATGCTGAGTAGTTA
CGAAACTACTTTGTTGGAGTATGTACTATTCTATGATCAAAGATGTAAGGGTA
ACTTAAAGAAC
```

*Translated:*

MSASSSSTTTTN  
AGKRARSWPSSASTSSMPTRSILILATFLSLTSSSTSVEAAFVGSPA VGLRSHTAAS  
TSKQQSSLYAQKKNNIDSSDNPLSYLFDLSSDPETKRLQKQTATLFGSALFLTNP  
LIPHLPSPLSSANAEDELYAKYGGKGLDTSLVKDCLVNQCQVQAKACLQDDPDCRKG  
LTCTAKCLGDNACTGCFARYGNENLDELLKCTIEDHECIKVAILEGGDVLGREPSPA  
PTVQGFDLASMEGTWYKVAGYNPNYDCYACQRNTFSSPEGGLSDSLQLPTGGILGSNA  
VGSIGADRLQVDVEFSMPRYLPDGSPQPPSGVRRESFISSADSMEGSGLQSVGYNQYSTHE  
TMVFDTVKNSGVGEAVKLALGKRGEEKLYSRTAHSEGEMGLKFWEWYIIGQNNPGQDE  
FKFVYYNGKTRQNTYDGAFIYSRSRTLSPASMEKVYKIAKDAGMNPDQFCIQNSCFDGE  
DDKQEMMMMMNPQREGLGSPSNPFRGILASTKVSQFLGVESVAAETTYNEPKSTISSNFLQ  
GSQATNRKADAVQERPWKEMGDYLEDPRRHFRIMDSLRTMDWPDYIKEKNW-

Based on the targeting analysis of the above peptide (a delayed signal sequence and clear chloroplast targeting), it appears that the protein starts at the second in-frame methionine. The following analysis pertains to the latter.

*Targeting:*

SignalP 3.0 - NN: Yes, Cleavage Site SSS-TS

SignalP 3.0 - HMM: Yes, Cleavage Site VEA-AF, Signal Peptide Probability = 1.000

SignalP 4.1: Yes, Cleavage Site SSS-TS, D = 0.799 (D-cutoff = 0.450)

ChloroP: Yes, Score = 0.554

15) *Thaps3\_270211 (VDR)*

Exon 1:

>Thaps3 chr\_2:1186955-1187856  
GGGGGTGATGAGGAGCCGAGGGCGCCGAGCAACGACGCGAGCAACTACACAACGAGCAA  
CCCCACAACAAGAACAAATGGCAATGGTCTGCTGATACGGACAGCAGTGATAGCTTCATA  
TAGCCTAACATTGACATCGGCATTTCTCATCAATAAGGCCACTGCCGGACATTCTG  
TCAGAGTACACCACATCATGCAACCGCTTCAACGTCGACATCATCGGTACAGTGGCACT  
TCTCGTGCCTCTCGTCCACTGAGCTGCAAAGTATGGATCCAATCTCCAGCACCTCG  
ACCATCCTATCAAGAACAGCTGAACACTTGGCTCGAAAATAAGTCACCTCTGACGG  
TCGAATAGAACAGTAGTAACACCATCAACTAATCAAGATGACACGGACGACGTCTG  
CCTTACATCTAATGCACTGATTGCTTGGAAACTGACCCAGCGGAAGTCCAATACCT  
TTCCACGACGTTCGTAAACGTCGCACATCTCATCAAGAACAGTCCTCTTATAACACGTG  
TCAATTGCAATTAGACTGCGGCAGCAACAACTATGCACCTCTCGTGGACCATGGATGA  
AGCCAATCCATCCATTCTCGCCGAAATTGCTCCGTGGACAGGTGTGGCATCTGGCAAACG  
TCTGACAGAACAAATGAATGGCTGTTGAAAAGCAAACATCTGATGAGTTGCCTTGGC  
AGTTATGCTTTCAATCGGTTCTGGCGCTGCTATTCTGGGTGCAACACTCAAT  
TGATGTAATTGGAGAACGGATTGGTCCAGATGCAAAGGAGATCTCTATGATTAC  
AAAGTGTGGACCTGCATTACCAAGTGTGAACGATGAGAATTGTTCTAGTGTATCAA  
CG

Exon 2:

>Thaps3 chr\_2:1187934-1188181  
CACTTGACAAGATCGACACACAGAGACCAAGTCACAAGTTAGAACAGTCGTGTCGTTG  
AAAGTGAAGTCTAGGGATTTCAGCTGTGTATTTGCAAAGAACATCTCGAGT  
GCTCAGCTGAGATCCCAGAGTGTGCCAGTTGCAAACCGATGAGCACATGGAGAGGGAAAGG  
ATGTTACGACGGACGTCGCGAGAGGCATTATGATTGGCACTAGAAGGAGCGGGGGGAT  
CGCTAGAG

Exon 3:

>Thaps3 chr\_2:1188256-1188336  
GGGAATTGCAACTGGTCTCTGGAAAGGTGGCTGCGGAGCAAACGTTGCCTATGAT  
CAGTTCCCTCTCAAATCAG

Exon 4:

>Thaps3 chr\_2:1188422-1189161  
TTGTTTACCCATCTGCAAAGGGGAAGGATCTTGGTACGACCTGTATTCCGAGTAGAA  
ACAATTGACGGTAGAAATGTCTGGTCAAACGTCACTACAAAGTCAGGAATGGAGAAACT  
CCTGGTACGTTCAAATTCTCGGTATTGGACAATGGCGTAACGAGCAACGAGTTCTGGACG  
ATTGTCGGGGCTGCTGACACTGTCGTGGTTGTATTCATTACGCTGGAGCTGCTGGC  
GCTGTAGGCCAGAGGTATTGGGAGGACTGCTGTGCACACCAACGGGAGAGCTGCCACCA  
GAAGAAGACCTGGACACATCTACAATTCTCGATGGCGAAATTGAACCGTGGAG  
TTATTGTTGTGGACAATGATGATCAGTCGCCTGGTGCCTAGCAGCAGGCCTCCACCG  
CTGGATTACTTCAGAAAAGACTGCATGGTCATTGGCTGAGCATTGCGCTGTACTATGTT  
AATCCTTAAGCCAAGATACTCTCAAGCAACGGCGAATGCTCCGTTGCGAAAGTTATGC

ATTACACCCAGTGCTATCGTCGAACCGAAATATCACCGCAACGTCAAGAGGCAAGTCG  
CTAATAAAAGATGCAGAACGGCAACTGACAAAGCAGCTTGATCCTGGAACGTCGCC  
TTTGTAAACACTTGCCAAGCTTGTATTCTGCCGACACGTCCGTTGAGGAATGGTAACAAA  
GGAACCTCATTGACTCGTA

*Translated:*

MRSRGAPSNDASNYTTSNPTTRTMAMVLLIRTAVIASYSLTLSAFSSSIRPTCRTFR  
QSTPHHATASNVDIIGTVALLVPSSSTELSKYGSKSPAPRPSYQEAAEHLARKISHFSDG  
RIEATVTPSTNQDDDDVCLTSNALIALGITDPAEVQYLSTTFRKRRTSHQETSSYNTC  
QFALDCGSNNYAPLVGPWDEANPSILAEIAPWTGVASGKRLTEQMNGLFKEKQTDEFALA  
VMLFFNRFSGAAIPWVQHSIDVTWEKGLVQNAKEIFSMITKCGPCITKCLNDENCSQCIN  
ALDKIDTRDQVTSYRTVVSFESELLRDFSLCILQKNNIFECSAEIPELPVVKPMSTWRGK  
DVTTDVARGIMIGHLEGAGGSLEGNLQLGVSWKVACGANVAYDQFPSQNQLFYPSAKGKD  
LWYDPVFRVETIDGRNVWCKRHYKVRNGETPGTFKFSVLDNGVTSNEFWTIVGAADDLSW  
VVFHYAGAAGAVGQRQLGGLLCTPTGELPPEEDLGHYINFLRSAIEPWEFLFVVDNDDQS  
PGALAAGAPPDYFRKTASVIG-

*Targeting:*

SignalP 3.0 - NN: No

SignalP 3.0 - HMM: No, Signal Peptide Probability = 0.163

SignalP 4.1: No, D = 0.173 (D-cutoff = 0.500)

ChloroP: Yes, Score = 0.579

Based on the clear predicted chloroplast targeting, the analysis was repeated with the peptide starting with the second in-frame methionine, with the following results:

SignalP 3.0 - NN: Yes, Cleavage Site TSA-FS

SignalP 3.0 - HMM: Yes, Cleavage Site TSA-FS, Signal Peptide Probability = 0.975

SignalP 4.1: Yes, D = 0.654 (D-cutoff = 0.450)

ChloroP: Yes, Score = 0.561

Based on the clear ER and chloroplast predicted targeting, it is likely that the peptide begins at the second in-frame methionine.

16) *Thaps3\_bd\_1474*

No available RNA-seq data for the unmapped “bottom drawer” sequences.

Gene model predicted by JGI (below) cuts off abruptly on the N-terminal side due to the way the unmapped sequences were assembled. Some N-terminal sequence is likely missing.

JGI-Predicted Exon 1:

>Thaps3 bd\_37x91:13831-12903

```
CTTATGAATCAAAAGATGTTGACGTTGGGTGAAAAAATT CAGACCGCTCCTCCTCTTCCTATGCT  
TATTGAGGGACAGTCATT CATTGATGCTCAGGATGAGTTGAGTGTGACGCAGTCATGAGGAAGTACGGT  
ATGCCTGAGAGAATCAACGAGGGAGGTGTTATT GCGATGCCAAGGC GTGGACTTATT GATCCTGATA  
AGTTGAGTATGACTGTGGTGCTTACGGCTATGAACAGGTTCTGAATGAGAGTAATGGACTTCAGATGGC  
ATTCTGGATGGAATCAGCCTGATAGGTGGTGCACTCCCACCAAGGAGTATGTGGAAAGCACCGCGGAGGA  
AAGGTCAAATTGAAC TCTCCATTAGGAGATTG TACCAACGACATGGAAC TATCAATCACCTCTCC  
TTCGATCTGGCGAGAAGATTG TGGCCGATGAATACGTCTCTGCCATGCCGTGGACATCGTCAAACGTAT  
GCTTCCCACAACGTGGCAGACTATGCCCTACTCCGTCAGCTGACGAAC TTGAGGGCATCCCTGTTATC  
AACTTGACATGTGGTCATCGTAAGTTGAAAGCAGTCGACC ATTTGCTTCAGTCGCTCCCCACTCC  
TTTCCGTCACGCTGACATGTCCGTACATGCAAGGAGTACGAAGA TCCAACAAGTCCATGTTGGAAATT  
GGTCTTGCTCCCTGCTCTCTATTGCCGGAGGAATG TCAACTGGATTGGAAAGTCAGATGAGGAAATC  
ATTGATGCTACCATGGGTGAGCTTGCTGCCCTTCCCTACCGAGATTGCGAATGATGATAAGGGCTG  
CTACGAAGATGCAGGGACCTAATGGACAGGCAAAGCTTGAGAAGTATGCTGTTGAAGGTGCCAAGGAG  
TGTGTATGCTGCCATTCTG
```

JGI-Predicted Exon 2:

>Thaps3 bd\_37x91:12821-12475

```
GACGTAACAAATACCGCCCCAGTCAGACCTCCCCATC  
CCACACTTCACCATGGCTGGATGCTACCTCACAAAGTCCCTCGGATCCATGGAGGGTGCACCCCTCG  
CCGGGAAGCTT GCTGCCGAGGT CATTGCCAACCGTGCCTCGGAAATGCGGATAAGCCAGTCAGGAGAT  
TCAGCAACACATTATCGACTCGGCTAGTAAGCATGTTGTAAGGAGGCCAGTGGGTGTGAAGGGAGAGGGA  
GCGATTGCAATTGGAGGGGGGTACTGTTGAAAGAAGGAGGAGGATTGTTGAGGGAGTCGGATCCTG  
CTCAGTATGAGTTGGCAGTAGCCAAGTAA
```

*Translated:*

```
MNQKMLTLGEKIQTAPPLPMLIEGQS FIDAQDELSVTQFMRKYGM PERINEEVFIAMA  
KALDFIDPKLSMTVLTAMNRLNESNGLQMAFLDGNQPDRWCTPTKEYVEARGGVKL  
NSPIKEIVTNDDGTINHLLRSGEKIVADEYVSAMPDIVKRMLPTTWQTMPYFRQLDEL  
EGIPVINLHMWFDRKLKAVDHLCFSRSPLLSVYADMSVTCKEYEDPNKSMLELVFAPCSP  
IAGGNVNWIGKSDEEIIDATMGELARLFTEIANDDKWPATKMQGPNGQA KLEKYAVVKV  
PRSVYAAIPGRNKYRPSQTSPIPHFTMAGCYTSQKFLGSMEGATLAGK LAAEVIANRALG  
NADKPVKEIQQHIIDSASKHVVKEPVGVKGEGAI AFGGGYTVGKKEEDLLRESDPAQYEL  
AVAK-
```

Genomic sequence disregarding the predicted intron:

```
>Thaps3 bd_37x91:13831-12475
CTTATGAATCAAAGATGTTGACGTTGGGTGAAAAAATTCAAGACCGCTCCTCTTCTTCTATGCT
TATTGAGGGACAGTCATTGATGCTCAGGATGAGTGAGTGTGACGCAGTCATGAGGAAGTACGGT
ATGCCTGAGAGAATCAACGAGGGAGGTGTTATTGCGATGGCCAAGGCCTGGACTTATTGATCCTGATA
AGTTGAGTATGACTGTGGTCTACGGCTATGAACAGGTTCTGAATGAGAGTAATGGACTTCAGATGGC
ATTCTGGATGAAATCAGCCTGATAGGTGGTGCACCTCCACCAAGGAGTATGTGAAAGCACGGAGGA
AAGGTCAAATTGAACCTCCCATTAGGAGATTGTGACCAACGACATGGAACATCAATCACCTCTCC
TTCGATCTGGCAGAGAAGATTGTGGCGATGAATACGTCTGCCATGCCGTGGACATCGTCAAACGTAT
GCTTCCCACAACGTGGCAGACTATGCCCTACTCCGTCAGCTGACGAACATTGAGGGCATCCCTGTTATC
AACTTGCACATGTGGTCATCGTAAGTTGAAAGCAGTCGACCACCTTGCTTCAGTCGCTCCCCACTCC
TTTCCGTCACGCTGACATGTCGTACATGCAAGGAGTACGAAGAGATCCAACAAGTCATGTTGAAATT
GGTCTTGCTCCCTGCTCTCTATTGCCGGAGGAAATGTCAACTGGATTGAAAGTCAGATGAGGAAATC
ATTGATGCTACCATGGGTGAGCTGCTGCCCTTCCCTACCGAGATTGCGAATGATGATAAGTGGCCTG
CTACGAAGATGCAGGGACCTAATGGACAGGCAAAGCTTGAGAAGTATGCTGTTGAAGGTGCCAAGGAG
TGTGTATGCTGCCATTCTGGTGAAGTGAAGGAGTGTGCGGTGAATCTCGTCGTACCTGGCCAAC
TACTGACTCTGTTCTTTAAATCATATCAGGACGTAACAAATACCGCCCCAGTCAGACCTCCCCATC
CCACACTTACCATGGCTGGATGCTACCTCACAAAAGTCCTCGGATCCATGGAGGGTGCCACCCCTCG
CCGGGAAGCTTGTGCCGGAGGTCAATTGCCAACCGTGCCTCGGAAATGCGGATAAGCCAGTCAGGAGAT
TCAGCAACACATTATCGACTCGGCTAGTAAGCATGTTGTAAGGAGGCCAGTGGGTGTAAGGGAGAGGGA
CGATTGCATTGGAGGGGGGTATACTGTTGAAAGAAGGAGGAGGATTGTTGAGGGAGTCGGATCTG
CTCAGTATGAGTTGGCAGTAGCCAAGTAA
```

Peptide sequence disregarding the predicted intron:

```
MNQKMLTLGEKIQTAPPLPMLIEQSFIDAQDELSVTQFMRKYGMPERINEEVFIAMA
KALDFIDPKLSMTVLTAMNRLFNESNGLQMAFLDGNQPDRWCTPTKEYVEARGGVKL
NSPIKEIVTNDDGTINHLLRSGEKIVADEYVSAMPDIVKRMLPTTWQTMPYFRQLDEL
EGIPVINLHMWFDRKLKAVDHLCFSRSPLLSVYADMSVTKEYEDPNKSMLELVFAPCSP
IAGGNVNWIGKSDEIIDATMGELARLFPEIANDDKWPATKMQGPNGQAKLEYAVVKV
PRSVYAAIPGE-
```

No predicted targeting to the ER or chloroplast for either peptide, however due to the high likelihood of a missing N-terminus, such analysis is inconclusive.

### 17) Thaps3\_21900

No introns.

```
>Thaps3 chr_3:1688852-1690753
CAACGACCGACGGCACACAACCCAACACCAAAATGATCCGTTCAATATCAGCGTTGGCA
CTCCTGGCAGCCTGCTGCCATCCGTTTTCTCGCTCCCTATCAGTATTAGAGCA
AATGCACCATCTTCACTGGCATCGACCACCTATCAAGATGAAGTAGACTGCATCGTTATC
GGCAGTGGCATCGGTGGTCTCGTGTGCAGCCCTTAGCAGCCACAGGTCGTACCGTA
```

CGCGTCCTAGAGCAACATTATGAAATAGGAGGATGCGCACATGCATTTACATGGATATG  
AATGGCAAGACGGTACCTCGTCTCGCCTGAAGGATGACCCTACAAAGAAAGGAGAGTTG  
TTTCATTCGAAGCAGGGCTAGTTGTACAGTGGACTATCGGAGGAGAGAACACCGAAC  
CCGCTTAAGCACATCTCAAATGATCGAGGAAGAGCCAGAGTGGTAACGTACGATCAG  
TGGGGTGCCTCTGCCTGAAGCCCCAGAGGGATCATGAGTATTGGAGCAGAAAAC  
TTTGCAAGATCCTCGAGACTTATGGAGGCAGGGCGAGTTGAAGATGGAAAAGCTT  
GCCGAGCAATTGAGACCAATGGCGGGGGTATCAAAGGCATCCACATGCAGCAATACGC  
GGTGATTGGGTATCTCCTGACTCTCATCTGAAGTATCCTCTCCTCATGAATGTG  
CTCAAGTATGCTCCTGCATTCACTGCTCCTTGTATTGACAAGTTGGCGTACAAAC  
AAGTTCTGCGGAATTATCTGAAATGCTGGCTTCCTTGTCAAGGCTTGCCAGCTGAT  
CAAACATTGACCGTAGTCATGGCGTATATGGTAGAGGACTTCTTCGTGAAATGCACTG  
ATGGATTTCCAAGAGGGATCTGGTGAGCTTATGGTGCTTGGCGAGAGGAGTGACA  
AAACGTGAGGGGTGTTCCGTGAAGTATCTACATCTGTGGACGAAGTTATTGTTGAGAAT  
GGACGTGCTGTTGGTGAAATTGGCAAAGAGCGGACGTATCATCAAAGCGAAGGAAGCT  
GTTATCAGCAATGCTGATCTTACAACACATAAAGTTGTTCCAGAGGGAAAGCAG  
GGATTGACAAAGAGAGAATTGAGTACCTTGGTCTTACTGCAAAGCCGAAAGATGGCTCA  
GTTCCATTCTGCAAATCATTGACTTGCATCTCGCTGTAAAGGCAGAACTCATACCA  
GAAGATGCGCCTCCACAATGGACTGTTGGTCAAGCAAACCTGATCAGTCATTAGCACC  
GGAAACGTAGTGGTTGATCGGTGGAAGCAAACCTGATCAGTCATTAGCACC  
TATCACGTTATCCATGCTTACACAGCGGGAAATGAATCTTACGAAGACTGGGAAACA  
GAACATCTGATGGATGATGCTGCCGTAGAGACAAAGATGCAGCATACAAACATTCAA  
GACGAGCGAGCTCAGCCATTGGGATGCCATCCAAAAGCGTGCCTGCCGTCAAG  
GGTGTGTTGTTAGAAAAGGTAGCCACCCATTGACTCACGCTGATTCTCAATAGA  
CATCGTGGAAACTACGGATTAGCCATTGCGCCGGATAATGCAAGGCTGGAAGTCCC  
GATGTAAGACGCCCTTGAAGGATACTACAGGTGCGGTGATTCCACAACGTCTGGCATT  
GGAGTTCCGGCGACGGCAAGTAGTGGAGCCGTTGTGCTAATGCGATCATGTCCGTTGG  
GATCAGCTTCATTGAATCAAAGATCAAATGCCGTGAACGAGTAAGTATAATCAATCG  
TTCTTCTGTAATATTTAAACTCAAGCAGCTCAATAC

*Translated:*

MIRSI SAL ALLA ACCPSVFSFAPLSVFRANAPSSLASTTYQDEVDCIVI  
GSGIGGLSCA ALLA ATGRTVRVLEQHYEIGGCAHAFYMDMNGKTPSSALKDDPTKKGEL  
FHFEAGPSLYSGLSEERTPNPLKHIYQMIEEEPEWLTYDQWGAFLPEAPEGYQMSIGAEN  
FCKILETYGGEGAVE DWEKLAEQLRPMAGGIKGIPHAIRGDWGIFLT LILKYPLSF  
LKYAP AFTAPFDLDKLGVNTKFLRNYLEMLAFLLQGLPADQTLTVVMAYMVEDFFRENA  
MDFPKGGS GELMGALARGVTKREGCSVEVTSVDEV VENGRAVGVKLAKSGRIIKAKEA  
VISNADLYNTYKFVPEGKHEGFDKERIEYLGLTAKPKDGSPFCKSF  
MHLHLAVKAEIIP  
EDAPPQWTVVQDWKGIDATGNVVVSVGSKLDQSLAPPGYHVIHAYTAGNESYEDWEQF  
EHLMDDA AVRDKDAAYQTFKDERAQPIWDIAIQKRAPAVVKGACVIEKVATPLTHARFLNR  
HRGNYGLAIAPDNAEGWKFPDVKTPLEGYRCGDSTSGIGVPATASSGAVCANAIMSVW  
DQLSLNQKIKMP-

*Targeting:*

SignalP 3.0 - NN: Yes, Cleavage Site VFS-FA

SignalP 3.0 - HMM: Yes, Cleavage Site VFS-FA, Signal Peptide Probability = 0.998

SignalP 4.1: Yes, Cleavage Site VFS-FA, D = 0.663 (D-cutoff = 0.500)

ChloroP: Yes, Score = 0.517

18) *Thaps3\_25361*

Exon 1:

>Thaps3 chr\_18:367805-365028

```
CTCGCGAAATGAACCTCGTATCCTTCTCGTCAAACCACCAACGCCAACACAAGCACAC  
CGTATTGACATATCCAATACGCTACGCGCTACCAATAGAGCTATACTACTAGACGTATCT  
TGAACCGTCATCATCAAGCAGCTACGCTAACACGAGACACATGCCAACACACAGGACAC  
CATCCATCATGCGTATGGGACGCCAACAAAAAGCTCGCTCCACCTCCAAGCAAACCA  
CCAATCCAATCCACCCAAATACTCTGCCAACATTAGTAGTAGGACAGGTGTCTCCA  
ACGTCATCCATTCCATCTATGGGCCGGCGTTGACGAAGCTGGCGTGGAGAGCGTGGAGG  
AGTATGCAGATGCTGTTTGAGGTGGAGGCGAGTTGCCGGAGGTACTGTCAAGCCAT  
CACAGCTTGTATGCGAGAGGATATTGATGTTGATGCCATGGCACCTTCGAAAAGGGAG  
AGGAGGTTGAAGTCGACCTCGACGGAAGCATTGCTGGCCAGCCACGACAACGACGACGACA  
AGACATCTCACCCACAATGCCACCTCCAACCGCCTTCTCACCACCCAAATCATCCATCG  
ACAACCTCACGCCCTCCTCACGGACACATCCAACACTTCTTACCCACCAACGCGATGGA  
AGATAACACGCCAACGCCGCAAATTGAAACGTCTATTAGATGAAAAATACGGACGTTCC  
GTCCCTTATTGAATCTCATCCAGAGTTAGAGGTGTTATCAAAAAGGTTCAAAGGAAGT  
ATGCCATGGGACAATTGACCCCCCTTAGGAAAGGGAGGGACCGATGAGTACTACCAAGTA  
GTATTATGCTGTTGTTCATGATGCATAGGAATGGGTTCGGAAGGAGTTGGTGGCATTAG  
TGGCGTTGTTCACTCTGGTGGATTGGAGGCCATGGCGTGGTGGATGGTGTGTT  
GAAAGTATTCCGTGGATCAAAGGAGGAGGAAACGGATGGTGGTATGCCAAGAAGGTCA  
AGGTTGTGGAATCGTATTATGCACATGGTGTGGTGGGGAGGAGGAAGAGGAGAGCGAAG  
AAGTGGAACGGAGCAAAAGTATGCTATTGGAAAAGCCGTGGTACCATCTCAATC  
CGCGGATTTAAGTTGAGAGATGAAGAGTACGATGTCATCTGTTGGATGTGGCCGG  
AAAGTGTGCTACTGCATGTTGCTATCACGAGCGGGCAAAAGACGTTGGTATTGTCAC  
CACGAGAGGATGCCCTGGGTGCTGACATTGCAAGAACGGAAAGACGAATGTTCTTTG  
ATATTGACGGAAGTAACATTGCCATTGGCAAGACAACAGTCGCTGTTGGCTCCGGCAC  
TTTGTACAACGACGGATACTCAGGGTGGATTGCGCTTGCACCGCATCGGAAGCGAGGTGG  
ATGGCTATGCTCATTCTATTCTCGGTGCCAGGCCTGGCACGGATTCTATCTGAATG  
AGTGTATTCGATCGTATTGACGGCGGAAGGTGAAGTTGCCTGGCGAGTACTGCTCGA  
CGTATCTGGAGATGCATTCCTGGTACTGATTGGATGGAAACGATAATGGCAACTCTA  
CTTCATTGAGCTATCTCAAGGCATGTGGACAAATCAACGCTGGTCTGGTACTTTACT  
TGGCCAAGCTTTTCCAAGGCAGCTGAATGTTCAAATCTCCGACTCCAATGTCTACC  
AACAAAGCTCTATTGCGCCAGCATCGACATTCTTAACAAGTGCCTACCGCTCAACTC  
ACGTGCGTGCTCTCATGGCGGCCATTGGAATGGCGAATGAGAACTTGAGTCCAGATAAGA
```

CGAGCATGGCGGCTCATGTTACCAATGTTGTGCCATGACTAGTACGGAGGGCTATGCGT  
ATCCTGTTGGAGGTCCGAGGGCGTTGTGCATGCATTGACGAGCGTGATAGAACAGAATG  
GTGGAAGAGTTGTGAGTGGTGTTCAGGAGTTGCTGTTGAGAAGTTGGAAAAGA  
AGGAACCAAAGGAAGAGACTAAAGATGGCGAGTCAAAGGAGCCAAGCCTCGTGCAGG  
GGATAAGATTGGAGAATGGCTTAGAGTTGCGGTTAGACAAGGGAGCTGTCGTTCGT  
TCATGGGAATGATACCCACCTTTGCAACTCGTATCTCCTGATGTACGAAGTGCAGG  
GAGTTCCCTGCCGGCTGCCAGCACTAGAGGAACGCCGTCCTGATGAGGGTCATGATTA  
GTCTCAAAGGAAATAAGGACGACTTGAACCTGACGGGAGCCGATTGGTATCGCTGCCA  
ATGCCACCTTGCGAGGGATGAGTTGATCCAATGACCGGTCAAGGTTAAATCGAACGA  
TTGGTGTAGACGACGATAATACTGGCGCAAGCGAGGGAGTTGATACTTGGCGAAGCTACAG  
ATGAGACAGAACGCAACGACTAGTCACACAGAGGAACGAAACAAAGCAGCCACGTCGA  
AGGCGCCACGATCCAAGTTACATCTGGAGTATCATGGATGAAAGTATCATTCCAAGTG  
CCAAGGATCCAAGTTGGCAAGATCGACATGGAGACGTTCCACTGCGTTGTAACAGTCG  
AGGCAGACGACGACTTGTCAAATGTTGATACAAAGCCAAGATTACTCGGTGTTGA  
AAGCGGGTAATGGCGAGAGAGAACGATTGCGGGACCGAGTGTGAAAGATTATGGAGA  
CATTCCTCAGCTCAAG

Exon 2:

>Thaps3 chr\_18:364943-364515

GCCAGTTGGAGACTGTCCAGATATGTGGACCCGTGCGGTCTGGGCTTACTACAATGGTC  
CCAGATTGCCATCAAAGGAAATCGTCAGAAACTCCGTACCCGGTCTGTACATTGGT  
GAGCGGATCTTACTGTGGGTGATTCTCTCTGGTCAATCGTGGTGGATGGTGGCTG  
CTAATGCGATCATGGTTACAGTTCATGGATCATATGTATCTCGGAAGAACATCACTT  
CGGACCTGCAGCAGTTCATAGAGGAACCGATTGGCAACTGAAAGGAATGGTGTAG  
TGGATGACGTTGCTGTTCTTCAGGAGGGTTGTTGATATGCAGAAAGGAATCACGG  
ATGCAGATAGAACGACCGCAGCTGAATCTAGAAAGAGGAATCGTAATCATAGGATG  
CTATTGAAT

*Translated:*

MRMGRPNKKLRSTSKQTTNPNNPKYSSPLVVGQVSSNVIHSIYGPALTKLAVESVEE  
YADAVLRWEASLPEVLVKPQLDDAEDIDVDADGTFEKGEVEVLDGSILPSHDNDDDK  
TSSPTMPTSNRLLFTQSSIDNLTALLTDTSQHFSTTNAWKIHANAACKERLDEKYGRFR  
PFIESHPELEVFIKKVQRKYAMGQFSPLRKGEPMSTSSIMLLFMMHRNGVRKELVALV  
ALFTLVGLEPWALVGLVCVGKYSVDQRRRKIGGMPKKVWVESYYAHGVVGEEEESEE  
VERSKKYIALEKPVGTFNPADSLRDEEYDVILLGCGPEVLYTASLLSRAGKKTIVLSP  
REDASGCLTLQNGKTNVPFDIDGSNIAHLARQQSLLAPALCTTDQGGIRFARIGSEVD  
GYAHSILSVPGLTDISNECIPIVLTAEGEVALAEYCSTYLGDAFPGTLDGNDNGNST  
SLSYLKACGQINAGSGDFYLAFLPKAAESFKSSDSNVYQQASIRPASTFLNKCLPLNTH  
VRALMAAIGMANENLSPDKTSMAAHVTNVICAMTSTEGYAYPVGGPRALCHALTSVIEQNG  
GRVVSGVLLQELLFEKLEKKEPKEETKDGESKEPKPRCKGIRLENGLELSVSDKGAVVSF  
MGMIPTFLQLVSPDVRTAEGVPAGLPALEERRPLMRVMISLKGKDNLTGADWYRLPN  
ATLPRDELDPMTGQVKFGTIGVDDNTGASEELILGEATDETEATTSHTRGKRKAATSK  
APRSKFTSGVSMKVSFPSAKDPSWQDRHGDVSTCVVTVEADDDFVQMFDTPKPKIYSLK  
AGNGERERLDRVLKDLLETFPQLQGQLETQICGPVRSGLTHNGPRFAIKGNRPETPYP

GLYIGGADLTVGDSFSGAIVGGWLAANAIMGYSFMDHMYLGKNITSSDLQQFIEEPILATE  
RNGVIVDDVAVPFKEVVVDMQKGITDADRSTAESSKEE-

*Targeting:*

SignalP 3.0 - NN: No

SignalP 3.0 - HMM: No, Signal Peptide Probability = 0.004

SignalP 4.1: No, D = 0.101 (D-cutoff = 0.450)

ChloroP: Yes, Score = 0.543

Analysis using peptide sequences starting with any of the next four in-frame methionines downstream the first one did not result in clear predicted ER or chloroplast targeting.

#### 19) Thaps3\_14875

Most of the region was not covered by RNAseq reads. However, there was an open reading frame, that encompassed an approximately 450 base pair region with reads mapped to it.

Open reading frame:

```
>Thaps3 chr_3:2375339-2377698
ATGGACAAAAATAGAGATGCCTGGCCACGAGAACGCCGACCGCGAAAGCATTGGCA
CTCCATCTCACTCATAACCGTGTTCATCATCACTGGCACACCAACGATGGACAATAGACC
TCTCTCTGTCTGACGCCAGAGTGACAATAGATGCCATCCCAACGCTACTACTTCTTC
GTTTCAATCGTTGGAGGTGCAGCAACCTGCAGTGGATCCTCCACTGCATCCACGACGAC
TCATCTACTCCTGTCATCCATTCTCATCGGCCCTCTCTCCCATCATCTCATGTCTCTT
CGTCATTCTGCTCCTCATGTTCTCAAACGACGTCAAACCCGTATGAATTGGAAGGAGG
CAAGTGCAATCTACCCACTGTCGTTGGAGACCAAGATTATGAACTACACGTCCAAGGA
TGAAGGATCCGATGAGGACATTGAGATCGATGATTATGAAGGCATGGGCAAGAGAGTATGC
ACGTTCACTGCAGTCAGACGGCAACAACAGCGGCACATCAACTCATATGAAGAAGTT
GGGATCCTCGGCAATAACCAACATATTACCAAGAATGGAACGCCTCAATGGTCCGTATGG
AATGTACGCCACCGTTACGGAGTGTCCACGAAGGTATTGCACGTGGCTCATCCAGTTCC
CGCCAGAGCTATTCTGACGGGGAGTGGAGTTGAGATGTTGGAGGAATGAACAATGGAAT
CGGAGAATGCTTGAACGACAGAATAGTCGTTTAGGAGAAAATATCACAATCAGTGAC
TCGGCCGTTCAAACGATTGTCATCGGAATGGAGGGTGTGCTATCAGTCATCCGAAGA
ACGAAAACAGCGTCGTAGATCTCTGCACTGCGATTGCTCACCGCTCAACAAAGTATCC
AGCCTATGACCACCTTAAGAACCTTCAAGGGGATGGAGTCTTACCGCTGATGGTCTGA
CTGGAAGCGAAACGTGCTAGCGTCTGCACTGTTATTGAGAAGTGGGGGGCCGATTG
CATGTTGGAAAAGGAGATTAATAGGGCTGCTGACTCTTTGAGAGGGAGGTTACGTGGC
GAAACAAACAATGAATAAGGAGGGCGATGATAAGGATGGTCCAGTGATGAATGTGGTGAC
AATGTTACAAAGGTGACGATTGGTCTCATTTATCGCATCATTACACACCACAATGTGGA
GTTCAGTCCAGACATTGATACAAACGAGCAATTCTTCTCCAAAGAGCTCAGCAGC
ATCTCTCACATCCTGGACAAGAACCAACACAACGGTCTAAGGCATCAGAAGATGATAA
CCACACCAAAACCGATGTAAGAAGGACTCACAGATGAAGTTACTTCTACCAATCTACCT
```

CGATGCAGTCACAAAATACGAATGATTGTCTCGCTCAGTCAGATCTATTGGTATCT  
TCTGCCACGATGGGCTATCGCACATTCTCTCCATGTATCGTGACGAAGAAAGAACAT  
GGTTCCGATTAGACAGTTGCCAGATTGGCGTGTGAGAATGCAGTGGAGGGAGGCCGTT  
GGAATTGCTGAGTCAAAGGAGTAGTCACGCTCAAAAGAGGGCGAAGCGACCAGTCAGT  
CTCGAAGGAGTTGGATGAGGCCATTACTCTCCTATTGCTGGACAGGATACTCTGC  
TGCCACCTGTCGTGGACACTGCATCTACTCATCCACAGGAGCAGCAAAGGT  
AGTGGAGGAGGTTGCTCAGTACTGTCATCTTGATGAGGGCGAAATGGTATCCAAGAA  
CACCATCTCAGCTGCCATATTGGATGCAGTCATCAAGGAATCGATGAGACTTATCC  
TGTTGCACCATTCATCGTCGAAAGCTTACACGGACATGACTATTCCATCGAAAGTC  
GTCTGTAGAAGATGATGCCACAACAACTACCATCCCCGAATCACCTTGATGCATATG  
GATATACGCACTCCAACGAAACCCCAAGCTATGGACAAAACCAGACGAATTCCATCCCCGA  
ACGATGGATCGATCCTGATCTACGAAGCAACGACCTCGGCCAACAAAGAGGTTGGCTCATA  
CATGCCATTGCGCTCGGTCTCGTAATTGCTGGGCAACCAATAGCTCAAGTCATCTT  
AAGAGTACTATTGGCGAGGACTGAACAAGTATGAAGTGAGGGATCCAAGTTGATGC  
CTTGCAGAGGTTGGGGAGGAAACGGGGAGGCATTGATACCAAGTATCTCTCAAGGA  
TATGCAAGCAGGATTACTGTTCTCCTCAAACGGATTGAGAATCAAGTTAGTGGAGAG  
GTGCTAATTGTAGTGGGTT

*Translated:*

MPWPTRTPHRESIWHISLITVFIITGPTMDNRPLSCLTPECTIDRHPNATTSS  
FQSFGGAATCSGSSTASTTHLLSSILIGLSPISCLFVILLMFFKRRQTRHELEGG  
KCNLPTVVWRPRFMNYTSKDEGSDEDIEIDDYEAWAREYARSLQSDDGNNSGTSTHMKKL  
GSSAITNILPRMERLNGPYGMYATVYGVSTKVLHVAHPVPARAILTGSJVVDVGGMNNGI  
GECFERQNSSLGEISQSVPKFRLSSGMEEAISPSEERKQRSSALRLLTGSTKYP  
AYDHFKNFSGDGVTADGSDWKAKRASVLHCLLRSGGADCMLEKINRAADSFEREVW  
KQTMNKEGDDKDGPVMNVVTMLQRSTIGLIYRIITHHNVEFSPDIDTNEQFICSPKSSAA  
SLTSLDKNQHNGAKASEDDNHTKPDVKKDSQMKLPIYLDAVTKIRMIvlaQSRSIW  
LPRWAYRTFSPMYRDEERTMVPIRQFARLACENAVEGSPLELLSQRSSHASKEGEATS  
SKDLLDEAITLLFAGQDTSAATLSWTLHLLSLHPQQKVVEEVRSVLSSLDEGEMVS  
TISQLPYLDAVIKESMRLYPVAPFIVRKLTDMTIPIESQSVEDDATTTIPESTFACIW  
IYALQRNPKLWTKPDEFIPERWIDPDLRSNDLGQQEVGSYMPFALGPRNCLGQPIAQV  
RVLLARILNKYEVDPKFDALQRLGEETGEAFDTKYLLKDMQAGFTVLPNSGLRIKLVER  
C-

*Targeting:*

SignalP 3.0 - NN: Yes, Cleavage Site TPT-MD

SignalP 3.0 - HMM: Yes, Cleavage Site TPT-MD, Signal Peptide Probability = 0.147, Signal Anchor Probability = 0.762

SignalP 4.1: Yes, Cleavage Site ITG-TP, D = 0.475 (D-cutoff = 0.450)

ChloroP: No, Score = 0.473

Analysis using peptide sequences starting with any of the next four in-frame methionines downstream the first one did not result in clear predicted ER and chloroplast targeting.

20) *Thaps3\_bd\_518*

No available RNA-seq data for the unmapped “bottom drawer” sequences.

Gene model predicted by JGI (below) cuts off abruptly on the C-terminal side due to the way the unmapped sequences were assembled. Some C-terminal sequence is likely missing, as evidenced by the lack of an in-frame stop codon. The translated product of the JGI model does not start with a methionine, but can be extended to one upstream. There is only one such methionine that is in frame after the closest stop codon.

JGI Model:

>Thaps3 bd\_35x67:17227-17611

```
AAATGCTATTGGCATTGACTGGGGACTCTCTTGCAATACAACCT  
ACCAATGCTGCAAAAGTGTGATTACCTTGATGCAGTGGCTCGTAAACCGTACGCCATTATCCTCCGGC  
TGCAAGCACTCGTTGGCGACAGATGCAAAGGGTGCAGATGCAGGTGGCTCAACTGGAAAAGAGTGTG  
GTTCATGTCAACTTCTATGCAATTAGCGAGATCCTGACGTTGGAGAACATCCGTCTCGTTGTTCTG  
AACGTTCCCTGGCGAAGAAGGAAGGAGAGGAACTGTCGTATTGTTGCCATTAGTAAAGGATC  
ACGCGACTGCATTGGCAAGT
```

*Translated:*

```
MLLALTGDSLNCNTTYQCLQKCDYLDNAVARETLRLYPPAASRWATDAKGANAGGFNLEKS  
VVHVNFYAIQRDPDVWENPVSFVPERFLGEEGRKRILSYSFLPSKGSRDCIGK  
SignalP 3.0 - NN: =No
```

SignalP 3.0 - HMM: No, Signal Peptide Probability = 0.004

SignalP 4.1: No, D = 0.203 (D-cutoff = 0.450)

ChloroP: No, Score = 0.440

If translated in a different frame, starting downstream the start codon used above, the peptide fragment is not targeted to the ER, and therefore, the chloroplast.

```
MQWLVKRYAFILRLQALVGRQMQRVRMQVASTWKR  
VLFMSTSMQFSEILTFRIPSRLFLNVSLAKKEGRGYCRIRSCHSVKDHALAS
```

*Targeting:*

SignalP 3.0 - NN: Yes, Cleavage Site LVG-RQ

SignalP 3.0 - HMM: No, Signal Peptide Probability = 0.070

SignalP 4.1: No, D = 0.381 (D-cutoff = 0.450)

ChloroP: Yes, Score = 0.531

21) *Thaps3\_6395*

No introns.

>Thaps3 chr\_6:1467629-1469626  
GCTTGATGAGGCTACCATTGGCATTGCTTCAGCTTGACTTCGGCTCATTCGGAATC  
GTCATATCGTCATAGCTTACTTCGGCAGGTACATAGAGATTGCACAGGAATAATCC  
CATCGTTCGCTTCGGGTGTCTCCTACAATGCTCCTCTGATAGACACAGCTACAAC  
TGAATCAACCAAACGACCTCGTCAGGAGAACCATCACACAGTATCATGGCATTGACT  
TGAAGAATAGATCTCGTACGAGAAGAAAATGGAGAGAGTCATTACAGCGTGTCAAAGT  
GTAACGGAGAAGGAAAAGTGCAGCTCCGTTATCAAAGAAGGCTGTGCCAACGCAAAC  
GAATGCAACAGAGCCAACAGGAGATACAACTAATGCACCAATCTGGCTATTCTGAAGA  
AACCGTGTAGGGAGTGTGATGGATCTGGTTGATTGCCATCAATCCTTGGATACAACCG  
AAAGAAAGCAGACACCACAGATTCAACCCAACCTTCGGTAGCCATTGTAGGCAGGTG  
GTATTGGTGGCATTGCATTGGCTGCCGCACTACAGCATCGCAACATTCCATGTATTGTT  
ATGAACGAGATTGTCGTTGAGGAAAGAAAACAGGGATACGGACTAACGATGCAACAAG  
GAGCACGAGCTCTAAGATCCTGGCTTTCTTCTTCATTCTGACGATGGAGAGGAGCACA  
ACAACAATTGTAGTGGAAAAAGCAGTGGATGAGAATACTCAAATACAAGCAAAGT  
TTGGAATCCACTCAACTCGTCACGTAGTTACAAGCCAGATGGAACGTGAGTAGGTGAAT  
GGGGTATGAAAGTCTGGGTGGTCATTGAGAAGAACGGCAGGAAGCACGCCAGCGAC  
AAAATGCACACATCTAGGCAAATCTCGCCAGCTGTTGATGGAGATGCTGCATCCTG  
GTACAATACAATGGGGGCAAAGTTGAGGTTATCGGGACAGTCTAGTGTGACGATT  
CCTCACAGGATCAACCATCATTGCAAGTCAGATTGACGAGTAACGATTGTGATG  
AGGAGGTCGCTACAACCTCGCTGTACTTGTGGATGCGATGGTATCCGATCGTCTGTAC  
GATCTGCAAAGTTGGGTGAGGACGGAACACCAACTCCGTTACCTGGATTGCTATTGCTATT  
TTGGCATTGCTCCGTCGCCAACCTCGCGTTAAGTGGTAACTGATGGTAAACTGTATTGAGACGG  
CAGATGGCATAACTCGTCTGTATGTCATGCCGTTGCGGAAGCTGGAGATGACTCGTCTG  
GTTTATCAACTGACAACACTAAAGGATTGAGCATGTGGCAGCTCTCGTTCCGATGGACG  
AGACTGATGCAACAAGGCTGAGTCACCTGGATGCTGCGTTGAAAGAAGAGGGCCCTCA  
AACGATGTGGTGCATGGCATGATCCAATATTAAAGCTGTTACGTTCCACACCAGAGGATT  
TCATTACTGGATATCCGTATTGATCGTGCCTTGTGAGAGAAAAGAGCTCGAGATG  
GATGTGATAATCTCAATCTGCAAACGCCCTTGTGACTCTACTCGCGATGCTGTAC  
CTATGTCCCCCTTCAAAGGTCAAGGGCGAATCAAGCTCTTGGATGCCGTGCTATTAA  
GCCAAAAGCTTCGATATATCTGTATTGATCACGGAAAACGAACGTCACGAACAGC  
AACCTACCATATCACTCAATGAAAGCACACCACAGGCATTGGCAGAGTCGAAAGTTCTGCATA  
TGCTACAAAGGTGTGAAGTCACAGTTAAAAAGTCGGCAGATGCAAGCTGAAAGTCTG  
GTGACGTCGCTATTCAAGAGGAAACATTACAGGAGCGCAGCGTTGGATGCGAAGG  
GATGAGAGCGAGATTCTTCTGGATCTAGTTGGATACAATCATAAGATAACCTAACGTTAC  
CCCTGTAATGAGCGAACAA

*Translated:*

MRLPLALLSACTSASFRNRHIVHSFTGRSHRDCTGIIPSFRFRVSPTMSSDRHSSQL  
NQPKRPRHEEPSHSIMAFDLKNRSPYEKKMERVITACPKCNGEGKVRAPLSKKARAQRKR  
MQQSQTGDTTNAPNLAILKKPCEDGSGLIAINPLDTERKQTPPQIQPNFSVAIVGGG  
IGGIALAAALQHRNIPCIYERDLSFEERKQGYGLTMQQGARALRSLGFFSFSDGEDDN  
NNCSGKKAVDENTSNTKQKFGIHSTRHVVKPDGTVVGEWMKVWGGRFEKNGRKHAKRQ  
NAHISRNQLRQLLMEMLHPGTIQWGQKFVGYSQSSDDSSQDQPSLQVRFRRRSNCDE  
EVATTASVLVGCDGIRSSVRSAKLGEDGTPRLYLD CIVILGIAPSPTSALTDGETVFQTA  
DGITRLYVMPFAEAGDDSSGLSTDNTKGLSMWQLSPFMDETDA TRLSQLGSSALKEEALK  
RCGAWHDPILKLLRSTPEDFITGYPYDRAVERKELRDGCDKSQSANAFVTLLGDACHP  
MSPFKGQGANQALDAVLLSQKLFDISRIHNGKTNVNEQQPTISLNESTPQALA EFENDM  
LQRCEVKVKKSDAAKFLHSDVAIQEGNITRGAAALDAKG-

*Targeting:*

SignalP 3.0 - NN: No

SignalP 3.0 - HMM: Yes, Cleavage Site VHS-FT, Signal Peptide Probability = 0.974

SignalP 4.1: No, D = 0.207 (D-cutoff = 0.450)

ChloroP: Yes, Score = 0.554

Analysis using peptide sequences starting with either of the next two in-frame methionines downstream the first one did not result in a more clear targeting prediction.

## 22) *Thaps3\_10233*

Exon 1:

>Thaps3 chr\_15:679062-677604  
CGTTGACTCTTTCAACGACGACACCCACCAAGTCATCCATCTAAACTTGTGGTAGT  
ACGCCACTCTGTTGAAAAGTAGATCCAACGACCATGATCGGACGCAAGTACAGTCTCGC  
AGCCTCAGCTCTGGCAATTATCGCCTCCCTCACCTCCACAACCGCATTGACCACCCCTC  
CTCCTCTCCTACGCTCCACTCGCCTCCACTCCACCGCTGAAGAAACCAACGGAGA  
AGCCGCAACAAACACCAATGTCGAACAAATCAAAGACACCTCACGTGACAAAGTAATGAC  
ATTTCTACGACATGTCATTGAACCCAAGTACGAAAAGCCAACGTATCCAGGAACAGG  
CAACGGCATGTCAGGCGACTCTGGTGAATACGACATTATCGTTATTGGATCAGGAATGGG  
CGGACTCGCCTGTCGGCACTCTGCCAAGTACGGCTCACGAGTCTTATGTTGGAAAG  
TCACATTAAAGTGGGAGGAAGTGCTACACCTTAGCCGAATGCACAATGGGGCAAGTA  
CAGTTGAAAGTCGGACCGAGATCTTGAGGGATTGGATGTCCTACGTTGAATCCACT  
GAGAATGATCTTGACATTTGGAGGAACCATGCCGTAAAACGTACAAGGGATTGG  
ATATTGGACTCCTCTGGCTACTGGCGTTCCCCATTGGATCACGTGAGGGATTGAACA  
GTTGTTGATGGAACAGTGTGGT GAGGATGGAGAAAAGGCTATTGGAGAGTGGAAAGCGTT  
GAGAGAGCGATTGAGGACTTGGGTGGAAGTACGCAGGCCGTGGCATTGTTGAATTGAG  
GCAAGATCGGGATTGGCAACTACTGCCGTTCATGCCGTTGTGGTACTCATCC

TGATGTGTTGGGATTGTCATTGACGTTGATGATTGAGCAAGACGGTCATGAGTT  
 TGTGACTGTGCTTCTGAGGAATTATTGATACATGTCATCTTGATGGATTCCC  
 TGCAAAGGGAGCCATGACGGCACACTGTTGACATTCTGAGAGGTTCTTGAGGAGAC  
 TGCAGCTTCTGTTCTATTGGTGGAACATGCGAGCTGGAAACACTCTCAGCGTGG  
 ATTGGAGAAGTATGGAGGTAATTGCAACTCAATGCTCATGTCATGAAATTCTGTAGA  
 GAACGGACGTGCCGTCGGAGTCCGTCTCATGAATGAAATGTCGTCAAGGCACGCAAGGC  
 AGTGGTCAGTAATGCTACTCCCCTTGATACTGTCAAGTTGATGCCAAGGCAGGGTGA  
 GCCCAAGGGATTGACTAAGTGGAGAGAGGAGTGGAAAGCTTCTAGGCATGGAGCTAT  
 CAGTCATTGTTCTGGCATTGATGCGGAGGGCTGGACTTGAGTCATATTAGGATCC  
 TGCTCATTGGTAGTTCAG

**Exon 2:**

>Thaps3 chr\_15:677527-676741

GATTGGGATCGTCTCTCAAGACTCCAAAATCTTGCTCCTCTCATCCCATCCATC  
 CTCGACAAAACGCTATGCCAGAAGGCAAGCACGTCAATTGTCATCTCTGGTGA  
 GAACCTTACGAACCAGGGAAAAGCTCACACCTGGCTCAGAAGAACATCGAACATACAAG  
 AACGAACGTGCCGAGGTTCTGGCGTGTGGAGCGTTGCATTCCGATGTTGTGAT  
 CGTGTGGAGTTCTATGTTGTTCACCTTGGCTCACGAGGCTTCCTCCGAGAGAT  
 AGGGGAACATACGGTATGGCTGGCTGCTGGTCGTCCTCAATCTGGTATCCTT  
 GGAAGTGTCTCCTTCCCATTCCCAACTTGAAGACTCCAGTGGACGGTTGTCG  
 TGTGGTGACTIONGCTCCCTGGTATTGGAACCTCGCTGCTGCTAGTGGTGCCT  
 GCTGCCAATACAATGACTCACGTTGATAACCATTGAAGATGCTGTCGGAGGCGAGTAAG  
 TTGGATCCTATGTACAAATTCTGGATGCTGGTATCATGGGGCAGGTTACAAACCTTG  
 GTGCAGGGATTCACTCCTAGTCCAGAGTTGAGGACCGACCAATACGTTGGTGTGG  
 GTTGCACCTGTCGATTACACTGCCACTGATCCTAGTGTCAAGCAGAGGATTGATTGTA  
 GAGTGGTAAAATAGGGGGTAAATATAGCGTAGTCAGAGTTATTGTCACGTGAAGAGA  
 GCAATTG

*Translated:*

MIGRKYSLAASALAIIASLTSTTAFAPPS  
 SSLLRSTRHLHSTVEETTNGEAATNTNVEQIKDTSRDVKMFTSYDMSIEPKYEKPTYPGTG  
 NGMSGDSGEYDIIVIGSGMGGIACSAKYGSRVLCLESHIKVGSAAHTFSRMHNNGKY  
 SFEVGPSIFEGLDRPSLNPLRMIFDILEETMPVKTYKGLGYWTPSGYWRPIGSREGFEQ  
 LLMEQCQGEDGEKAIGEWKALRERLRTLGGSTQAVALLNLRQDAGFLATTAGSLPVVTHP  
 DVFGDLSTFDDLSKTVDEFVTVPFLRNFDITMCIFCGPAKGAMTAHLLYILERFFET  
 AAFSVPIGGTCELGNTLQRGLEKYGKLQLNAHVDEILVENGRAVGVRLMNGNVVKARKA  
 VVSNATPFDTVKLMPKAEGEPKGLTKWREELGKLPRIHGAISHLFLAIDAEGLDLSHIQDP  
 AHLVVQDWDRSLQDSQNLCFFIPSILDKTLCP EGKVIHVYSSGGEPYEPWEKLTPGSE  
 EYEAYKNERAEVLRWAVERCIPDVDRVEFISIVGSPLAHEAFLRRDRGTYGMAWAAGSSA  
 PQSGILGSVLPPFPNLKTPVDGLLRCGDSCFPGI GTPSAAASGAIAANTMTHVDNHLKM  
 LSEASKLDPMYKFLDAGIMGQVYKPLVQGFTPSPELRTDQYVSGAGVAPVDYTATDPSVS  
 ERIDL-

*Targeting:*

SignalP 3.0 - NN: Yes, Cleavage Site TTA-FA

SignalP 3.0 - HMM: Yes, Cleavage Site TTA-FA, Signal Peptide Probability = 0.998

SignalP 4.1: No, D = 0.619 (D-cutoff = 0.450)

ChloroP: Yes, Score = 0.560

23) *Thaps3\_33926*

Exon 1:

>Thaps3 chr\_4:1242467-1242109

```
TTCGATTTGCTCCTCGTCCTCCCTCACAGCTCATCCATCCAACACCACACACA  
CTACCGCAATGACAATCCCCGGCACCACCAAGCGGTATGCCCTCGGCTCGGCTCCT  
CCACAGGACCATCCGACAACCTCTAACATCGGCTAACATGCCTGCCATCTTCTCCCTCT  
TTTACGCCTCTCGTCCGCCCTAGGACGAAGGGAGGACCATGCACCACCGGTGG  
TTACGTCGAGCCCTGTCTCAAGTCTTCTGCGTGGACTATTGTGGAGTTGGCAAGA  
GTCCTGTGAAGATGGTTAGAGGTGTTATGAGGATTACGGCCTGTGTTACTGTGCCG
```

Exon 2:

>Thaps3 chr\_4:1241947-1240596

```
TTCTCCACAAACGTCTCACCTCCTCATCGGCCCCGAAGCCAAGAACCAATTCTCAA  
GCACCCGACGAAGTCTCTCCAAAACGAAGTCTACGGCTTATGAAACCGTCTTGG  
CCTGGAATCGTCTACGATGCCTCCAAAAGAACCGTCAAGTCAATTCAAATCAATGGCT  
AACGGCCTCGCACTGCTCGTCTAAGGGATACACTGCCAAGATTGAACGTGAGACCGT  
CAGTACCTCGAATCTGGGGAGAGTCCGGAGAGCTGATCTATTCCATGCTCTTCGGAG  
TTGACTATTCTACTGCCTCTCGTTCTACGGAGATGATGTTGTAAGGAAATCTCTC  
AAGGAGGTTCGGAATTGTACGATCTTGACCAGGGCTTGACTCCACTCACCGTGTTC  
TTCCCCAATGCTCTACAAAGTCTCACATGAAACGCAATCGGCCACGTGCCAAAATGGTG  
GAGTTGTTCTCAAAGTGATTAAGAACGATCTGAGGATAATCCTGATGTGCAACACTCGGAT  
GGTACGGATATCCTCTCCATCTTGTGATCGCATTGTTGCTGGCAGCATAACGAGTTGC  
GACGAGCAAGTGACTGGGCTTTGATCGCATTGTTGCTGGCAGCATAACGAGTTGC  
ATTACTTCTACATGGACGAGTCTCTTACTCAACAAACCTGCCATTCTCAAGCGTATT  
ATTGCTGAGCAGAATGACGTCTTGGTTCTCAACCGATGCCATGTGGATTACAAGATG  
GTGAACGAGGATATGCCCTGTTGCACAACCTCGATGAAGGAGGCTTGCCTTGCCCT  
CCGTTGATTCTCTCATCCGTTATGCTCTCAAAGACGTGAAGGTGAAAGCTGCCGAAAG  
GAECTACACCATTCTAAGGGCGATATGGTGCTCATTAGTCATCTGTTGGTATGAGGATT  
CCCGAGGTGTTAAGGAACCTAACCTTGATCGTCTGATCGTGGCTGATAGGGAG  
GAGGACAAGTCAAGTCATTGCTTACATGGGCTTGGAGGAGGTATGCACAGTTGCATG  
GGACAGAACTTGCCTTGTTCAGGTCAAGACGATTCTAGCGTGTGTTCCGTGAGTT  
GAGTTGGAGATGGTTGGAGACGATGCCGACATTGATTATGAAGCCATGGTTGGGA  
CCCAAGGGAGATTGCCGTGTTAGGTACAAGAGGCGTCAGTAGATGATGGTACCATGTC  
AGTTGCAACTGTCTGATCAAACATAGATGTTGAGAAACTGGGTTGATTCATCGTA  
TTGATTTAATTGAATAAGAAGCTAGAGATT
```

*Translated:*

MTIPGTTSGMPFGFSSTGPSDNLLIGLTCLAIFSLF  
YAFFVVRPRTKGGPHAPPVVTSSPVSPLVVGTVIEFGKSPVKMVQRCYEDYGPVFTVPF  
FHKRLLTFLIGPEAQEPFFKAPDEVLSQNEVYGFMKPVFGPGIVYDASKNRQVQFQSMAN  
GLRTARLKGYTAKIERETRQYLESWGSEGEDLFHALSELTLTASRCLHGDDVRENLFK  
EVSELYHDLQGLTPLTVFFPNAPTKSHMKRNAARAKMVELFSKVIKNRRDNPDVQHSDG  
TDILSIFMDVKYKDGSNITDEQVTGLLIAALLFAQQHTSCITSTWTSFLFILNNPAILKRII  
AEQNDVFGSQPDADVYKMNEDMPLLHNSMKEALRLCPPLILLIRYALKDVKVKAAGKD  
YTIPKGDMVLISPSVGMRIPEVFKEPNFTDPDRFGPDREEDKSSPFAYMGFGGGMHSCMG  
QNFAFVQVKTILSVLFREFELEMVSETMPDIDYEAMVVGPKGDCRVRYKRRQ-

*Targeting:*

SignalP 3.0 - NN: No

SignalP 3.0 - HMM: Signal Anchor Predicted, probability = 0.936

SignalP 4.1: No, D = 0.136 (D-cutoff = 0.500)

ChloroP: Yes, Score = 0.543

Analysis using peptide sequences starting with either of the next two in-frame methionines downstream the first one did not result in a more clear targeting prediction.

#### 24) Thaps3\_1549

No introns.

>Thaps3 chr\_1:1808544-1810261

CTCGTCGACATCGAAAGACGGCAAACAGAAACAGCAACACAACGGAACAGCAGATTGATA  
CATGGTGATGTTGATACCATGACAGCGCCATCGTCACCCCTCCTCTCGCTCTGCC  
TCGTCACGGCGGCAGCAGCATCCCTCGTCTCTCCTGCTCTCCATCTACAAGCGTC  
GCCGTACTACGTCCAACAATGAACCTCCCTACCCACCCACCCCTCCGACAGGAACACT  
TCCTCGGCCATGCAATGTCCTCCGACGAGTTCCGGAGAACCAAGAAATCGCACGATC  
TTCTCTTCTGAAGTGGATGAACAAACTCAACAGCAAAGTAGTAATGTTGAGCTCCAT  
TTCTGGACGGCTTCTCGGTCTCGGCGTATGATTGCGTAGGGTATGCCGAGATTGCTC  
GGCACATACTCGTTACGGCGAAGTACAACAAGTCTCCACCTACAGTGTGTTACAGCCAC  
TCATCGGCATGAGTCCATGGTTGCCACGGAGGGAAAGATGTGGAAGGGATCAAAGAAAGT  
TGTACAATCCTGGATTTCTCCAGAGTTCTCGCAATTGTTGATCGACAATTATTGAGA  
AGTGTAAATGATTATCGCCAGATGTGATGGTATGTTGAGAATGGTAGCGACGGATA  
TGTTGGCGAGATCCATTGACCTCACTTCTGATGTGATTGTCAGGTAGCATTGGAGAGG  
ACTGGGGAGTTGATAGCAAGGACAAACATGGTATCGAGACACTGCAAACAAATACGAGATC  
TTACGGTAGCCGTTGGGAAAATATGACCAACCCATTACGCAAATACTTGGATTACGAA  
GCATTGGAGAACGAGGAGACTCTCGGAGCTCTGGATCAGGATATGCAAATCTTGTGA  
AGAGAAGACTTGCTCAGGTGTTGGCTGGAGATGCTGATTAGAGAAGGATATCTTATCAT

TGACGTTGCTGGTGTGGAAAGCAAAACAGGAATCTAAGTCAGGC GCCATCTCGTTGA  
GCAAGGACGAAATGGAAAGGATGACATCGCAACTTAAGACTTTACTCGCTGGCAGC  
ATACCTCTCATCCGCTATCGCATGGCGTATTGGCTGTTGACAAAACATCCAGAACATCAC  
TCCAACGAGCTAGAGAGGAAGTTGATCACACCTCGGAAGAGAGATTGGTCGGACGAGGCAT  
TGACTGGGACTCTTTGCAATACAACCTACCAATGCTGCAAAAGTGTGAGTACCTG  
ATGCAGTGGCTCGTAAACGCTACGCCTTATCCTCCGGCTGCAAGCACTCGTTGGCGA  
CAGATGCAAAGGGTGCAGTCAGGTGGCTCAACTGGAAAAGAGTGTGTTCATGTCA  
ACTTCTATGCAATTAGCGAGATCCTGACGTTGGAGAATCCGACTCGTTGTTCTG  
AACGTTCTGGCGAAGAAGGAAGGAAGAGGATACTGTCGTTCTGCAACTTGCATTCA  
GTAAAGGATCACGCGACTGCATTGGCAAGTACTTTGCTCTTGAATAAAAGATTGCAT  
TGGCTGCTTGATTCTCGGTACGATGCATCAGTTGAAATGAGCAGTATGTTA  
TCCGTTAACATCTGTTCTCACGACGGATGCAAAGTGAATCTCTCGTCGCAGGAAAT  
AAACGTGCTGAAAGAAATCTAAACTAACTTAGTATT

*Translated:*

MFDTMTAPSSPSSRSALVAAAASLVSLSLLSIYKRR  
RTTSNNELPYPPPTPPDRNYFLGHA MSLRRVPGEPKSHDLLFLNWMNKLNSKVVMFELPF  
LGRLFGLGRMICVGDAEIARHILVTANYNKSPVSVLQPLIGMSSMVATEGKMWKDQRKL  
YNPGFSPEFLRNCVSTIIEKCNRFIARCDGDVENGVATDMLARSIDLSDVIVQVAFGED  
WGVDSKDKHGIETLQTIRDLTVAVGENMTNPLRKYFGLRSIWRTRRLSAALDQDMQNLVK  
RRLAQVLAGDADLEKDILSLTSGVLEAKQESKSGAISLKDDEMERMITSQQLTFYFAGHD  
TSSSIAIAWAYWLLTKHPESLQRAREEVVSHLGRDWSDEALTGDSCNTTYQCLQKCEYLD  
AVARETLRLYPPAASTRWATDAKGANAGGFNLEKSVVHVNFYAIQRDPDVWENPDSFVPE  
RFLGEEGRKRILSYFLPFSKGSRDCIGKYFALLEIKIALAALISRYDASVNVNEEQYVI  
RLTSVPHDGCKVNLSRRK-

*Targeting:*

SignalP 3.0 - NN: No

SignalP 3.0 - HMM: Signal Anchor Predicted, probability = 0.936

SignalP 4.1: No, D = 0.136 (D-cutoff = 0.500)

ChloroP: Yes, Score = 0.543

Analysis using peptide sequences starting with either of the next two in-frame methionines downstream the first one did not result in a more clear targeting prediction.

25) *Thaps3\_264647*

Exon 1:

>Thaps3 chr\_19c\_29:130307-130912  
CAAACATCACTATTTGGCAAGGGAGGATGCTTCATTCTGAGTAGTCTCCAATATATT  
TCGCTACAAATCCGGTCATACTCTCCTATAATTTGATATGCCCTTCAAGGTTCGA

TGCTGCTCGATTGTATCTTGGTTACACAGTCAGCAGTGAGAAGTGAGGAGCTCT  
CTCTGCATTGGATATATAAAACTGATAGAAGAGATCAGCCAACACACATAACAATTGG  
TGGAGGAGCGAGAGAGATTCATTGCACCATCGAGAGAGCGGCCAGGCAGGAGGCACGGTG  
CATCCATACTTGATCCATCGCATCGGACGGTCAGATTGCAAATCGGAATCGTACCGAC  
ACATCAACTGCTCCCACCTCCAGTGTCTTCTACCCCTGATCAGTCCTCTCCGCAG  
CAGCGATAGTATGATCAGTAATATGACGATGCCCTCAACACTGGCATTGTATCTTAC  
ACCAACCACAATTATCACCCCTGCTATGTCCTTAGTGACTCGGTTCATCCAATGGAA  
GAATCACCTTGCAGATATGAAGAGCCAGACTCCCTTCTGGAATTCCAGTAGTCCCAG  
TGCTCA

Exon 2:

>Thaps3 chr\_19c\_29:131012-133019

CTGGCTACTCGGCCACTATCCCTGTCGCAACCCGACAAACACCAACCTTCAC  
CGCCACGCCACCCCCCTCCGGCATATCCGCCCTCTGGGGTCCGTCAGTATAAATTCTT  
CTCCTCCGTCGAGCCGATCACTGCCGTTCCATCCTCGTCAAAGCTCCAGTAGAAACTT  
TGTCTCGTTCATGTACGGCATGGACGGAGGACATTGGGAGAGGAGAGTATCATTGAT  
TAACGGAGGAAAGAGGTGGAAGAGGCAACGAAAGGTGATTAGAAGGGCTTCAAGGGCTTCAATTGGA  
GGTTGTGAAAGGTAGGAGGGAGGCTGTGGGGAGGTGGCGGATGTTGTGGATTGGAT  
ACTGAGGGCTTGTAGTGGTAGGAGTGATAGCGGTGTGCATGATGGAGATTGTGGAGGGAG  
ATTGGTTGGTGCAGGGATGGAATGAGAAGGTTGTGGAGGCTGAAGACTTCTTAAGTT  
GTTTGCCTGGAGGTGTTGGAAAGGTAGCAATGGGATATGATTTCGGTGCTTCCTTC  
TCTTGCTACTCGGACGACAACGGCAACAGCAACAGTAATGTTGCCAACACAACAA  
AGATGTGGTGAGCAATGGCACCCATACATACAACGACAACGCGTGCAACTGTCTCAAAT  
GCCACCCGATGCACAGTCCTTGACTTCTGAATGTCGACATCGGGAACCGCTAACACC  
AACGAGCCTGATGAATCCGTGCATGCAATTCTACTCTATACCCACTCCACACAACAAAAA  
GTATCATCATCATGGACAGAATTAAGGGACTGGTGGTAAGATTATCGGACTGCAACT  
GAACAGGTTGTGCAGTGACGGCGGTGTCATGGAAGGCATACAGAACATGATTACCCACTT  
GTTACAATCTACAATCGAAGAGAACTTCAGTCCTACCGATACAGATGGAACACTGGCTG  
TCCATTCTCATCATCCTTACCATCAAAGTCTATTCCAGATACAGTCATCTCAAACCTCAC  
TCCATCAGATAAAGATCAAATCATTGAAAGCGTCTCAAGATGTCATCACATTCTCAT  
GGCAGGCTACGAAACCACTGCAATCTCAATGTCGTTGTAGTGACTTCCTTCAAATA  
CAAACGATGCCAAGAAAGATGTCAGAGGAAGCGAGAAGAGTTCTGGGGCGCTGTGGAGT  
GCATGGAACGGACATTGACGATGACGAGCTGGTAACTGCCGTGTCATGGAAAC  
GATACTGGTGCATGCCAGTCATGTTACAACCTCGTGTGACAGAGAAGGAAATGTCCT  
TGATACAGGGCTGGAGGAAGGCCATAATGTGACAATACCAAGGGAACGAGGTGTGCGT  
TTGTCCTACAGTAGTTCATATGGATGAGCGTAATTGAAACGAGCCGAGGAGTTCTTAC  
TGAGAGATGGGTGCGGTGGAGAGGGGCAGGTGGTTGAACGAGATTACGAAACTGAAGG  
ATTGAAGTCAACAGCATTGCCATCAATTACTGAAGATGAACAAGATTCTCTCCCATATC  
TGCAGAAAGTACGACGAAAGAGAATAATTCTGCCAGTTCAATCTCGGGCTGATCCACACAA  
TTTCTCTCGTTCTCAGATGGAGCAAGGAATTGTGTTGGAAACGTCTGCAATTATGGA  
GTCTACAATCTGATTGCGGTATTGCTCGTGCAGTGTGCGTCAGTCAGAGGAGGG  
ATTGAGAGATGAAAAGGTACGGCGGTCGTACGTGTGCCCTGAGAGTTACCGTCGT  
GTTTGGAGGAGGGAGTGAAGAAAGCTTAGTGTAGTAGGTCTAGTTTTTGAGAAGAAC  
GTAGCGAAATGCGGCTGTAACCAAGCTTCAAGTAGACACACTATTGTGTAAAGTC

GTGATCATGTATTCCATGAAGCCGATCTAATGACTGGAGATGCTGTTAGTTAAGATGCA  
CTTACATGTGAAACTAACAGTTGAGGAC

*Translated:*

MISNMTMALSTLALYLPTTIITLLLCLLVTRFIQWK  
NHLAN MKSQTPFPGPVVPDAHWLLGHYPLFVNPDKHHQFTAATPSGISALWGPSTD  
FFSSVRADHCRSILRQSSSRNFVFIVRHGRRTLGEESIILINGKRWKRQRKVIQKA  
LEVVKGRREAVGEVADVVVDWLIRACSGRSDFGVHDGDCGGRLVGADGNEKVCVEAEDFF  
KLFALEVFGKVAMGYDFRCFPSLATSDDNGNSNSVALHNKQDVVSNGHTYNDNACNCL  
QMPPDAQSFDFLNVDIGNRSTPLSMNPCMFYSIPTPHNKKYHHHMDRIKGLVGKII  
QLNRCLCSDGGVMEGDTNMITHLLQSTIEENFSPTDGTGCFSSSLPSKSIPTD  
LTPSDKDQIESVSKMLITFLMAGYETTAISMFSVYFLSKYKRCQERCAEEARRVLGRC  
GVHGTDIDDDDELVYCRAVFMETIRLHLPVMFTTRVTEKEMSFDTGLEEGHNV  
VVCPTVVHMDERNFERAEEFLPERWVRWERGRWVERDYETEGLKSTALPSITEDEQDSPP  
ISAKYDEENNSASSISAADPHNFFSFSDGARNCVGKRLAIMESTILIAVLLRDVC  
EGFEMKKVRRFTCGPESLPVVFWRRE-

*Targeting:*

SignalP 3.0 - NN: Unclear

SignalP 3.0 - HMM: Signal Anchor Predicted, probability = 0.894

SignalP 4.1: No, D = 0.340 (D-cutoff = 0.500)

ChloroP: No, Score = 0.455

Analysis using peptide sequences starting with any of the next four in-frame methionines downstream the first one did not result in a chloroplast targeting prediction.

## 26) *Thaps3\_4026*

No introns.

>Thaps3 chr\_3:2380128-2379629  
TCAACAAAATCATGTCCAAGAACGCAACTACGCCCTTCACCTCCGCAGCCGAGGCA  
TGGATGGAATCCTAGCCGAACGAATGGCCGAGGGAGGTGGAGCACTCTGCAACGATGAAA  
ACGGATTGTCTAGGTTACGTGGGGATATTGATACTAGTCAGAGTGGTTATACGG  
CAATTGCAAAACTTGCAGTCAGTTGGATAACACGGTGGATGGACAGGGCACTAAGAATA  
ACAACAACAACGGGAAATGCCATTGGTGACCATTCAAGACTGAAAAGCCGGCACTGTTGG  
TGAAGGAATATGGGGAAAGAACGGTGGTCTCGTGTGCCACAGAGGTGAATGTGAACG  
GACAACAATGTGGAGTGAACGGTGTATGAACGGGAGCTGACAATCTGAACGAAGGAG  
TTTGATGGGATGCACTCCGAAACAACAATCCCACTCGGTGTATATTAGGAACGGTATAT  
AATACAAGAGGTTACAACAG

*Translated:*

MSKNATTTPSSPPAAAGMDGILAERMAEGGGALCNDENGLCLGSRGDIDTSQSGCYTA  
IAKLASQLDNTVDGQGTNNNNNGEMPLVTIQTEKAALLVKEYGGRTVVFRVPTEVNNG  
QQCGSELVMNGELDNLNEGV-

*Targeting:*

SignalP 3.0 - NN: No

SignalP 3.0 - HMM: No, probability = 0.011

SignalP 4.1: No, D = 0.139 (D-cutoff = 0.450)

ChloroP: No, Score = 0.447

Analysis using peptide sequences starting with either of the next two in-frame methionines downstream the first one did not result in a more clear targeting prediction.

## 27) Thaps3\_5221

Exon 1:

>Thaps3 chr\_5:652777-650770  
TTTCATCCTCCTTCTACACTCATCAACGTCCGCTAGACTGCCGCCGCTGGCAACACATT  
TGTCCCTCAACTCCTGACACAGCCGAAAGAGAGACTCTGCCATGAAGCTGTTTTGTA  
GCGTCGACGTTGATCGCGTACTCTGTTCACGCCCTCAAGTTCTGACCACACGT  
CATCGGCCACCAGCTCTGTAACTCAGGCGATGCAACAAACGATGGTGGTATGAAGTG  
CACGAAGTCGATATTGCTGTCGTTGGAGCGGGGATAGGTGGTCTGTGCCGGGCCATA  
CTCAACACACTTACGACAAGAAGGTTGGGTGTATGAATCTACTATTAGCCGGAGGA  
TGTGCACACAGTTCAGCCGTAGTGTAAAAATTGGAGACGATGAACAGCCAACAACGTT  
ACATTGACTCTGGGCCTACCATAGTATTGGGATGCAGCAAAGAACCGTACAATCCTCTG  
CAACAAGTACTACGTGCAGTGGGGTAGATGATCAAATAGAGTGGCTCCTACGACGG  
TGGGGAAATGATCGAGCATCCAATGCAACCGAAGGAAAAGAGATGGAAGTTCAAAGTTGGA  
CCGAATCACTTGAGGACGGCCTCTCAAGTGGTGTGATCAAATCTTAATGCTCTTGAG  
GAGTTCAATCAATTGAGAGAAATTACAACGCCTTGTACAGGAGGCCCTACATTCCA  
GCCATGGCCATGAGACCAGGACAATCAGCTCTAGTTCCGTTGAGATATCTTCATCA  
TTGATCTCAATCATTAGCAATGGAGTTGAAGCATCGACTGGACCTTTGCTCCCTACATG  
AACGGCCAATATTACTGTAAAAGATCCGTGGCTACGAAGCTGGTGAATCGTTGGCG  
TTCAGTTGAGTGGCTCCCCGAGATCGTACCGAGTGTGCAATGGCTATGTGCTA  
TTTGATATGCACAGAGAAGGGGAGCGCTAGATTATCCCAGGGAGGACTGGAGAAGTA  
GTCAAAGCATTGGTCAACGGCGTGGAGCAAAAGAGTATTGGATCAAAGTACATCTAGC  
AGACACGTAGAAAGTATTGATACCAACGAAGAAGGGAGATAGAGTCATTGGATTGACTGTT  
CGTAAGAATGGAGGGAAGAAGGTACCGTCAAGGCCAAAGAAGGTGTCGTGTAACGTG  
CCGATGTGGTCACTCCGAAAGTTGATCAAGAATAGGAATGCACTGAGTGTCTGGGTGGA  
GACAAGGCAACTTCTCATCAAGTGGCTGAAAGCAAAACATCTGGATGACGTCTTT

GATACAGACCAAGTACTGGAAGAGGAAGCGTACTTCGTCCAAACCAGCTGAGGACACG  
ACAATAGAAAAAAGTCTCTTAGAGAAGTGTGACTCTGCAGAAATGACTGGCTCATTCTT  
CACCTGCATCTCGCTCTCAATGCTACTGGACTTGATCTCAGTCTTGAGCCTCACTAC  
ACTGTCATGGATCGTGGTTGGAAGGCGATGGGAAAGTTATTGATGGGTTAAGGATGAT  
TCAAGCGGCGAGCTGAATATGATTGCTATCTAATCCTGTGTTGACAATACTTG  
GCACCAGAGGGATTATCATCATGCATGCCATGGTGCAGGTAACGAGCCTTCGAGATA  
TGGAAACCAACTGCAAGTAAAGGCAATGCTCACCAAATACTGCAGGAGAAGGAGAA  
ATTATTGGAGGGAACGATGCTCACCATCGACGTACCAAGGATTGAAAGATAGCCGATCG  
AAGGTACTATGGAGAGCTGTGGAGTCTGTTACCTGACGCACGTGAACGTACTGTGCTT  
GCTCTCATCGGATCTCTCGAACACACGAACGATTCTACGTCGTCCATGCGGCTCGTAC  
GGTGCAGCGTTGAGGATTGTTGAAGGACGGAAGCACTCCAATATCTAACTGGTCTTA  
TCTGGTGACGGTGTCTTCTGGTATTG

Exon 2:

>Thaps3 chr\_5:650680-650446  
GCATTCCTGCTGTAGCACTAACGGGGCTAGCGCAGCGAATGGATTGTTGGCATATTG  
ATCAGTGGAGATGTATGGATTATCTAAGGCCAAGGAATCATTGCCTAGATAGCCGAGA  
AGTTGGACTTCGTCGGCAGCAGTATTTAGGGTCCGTGCCTCTTCAACTGAGTATC  
GCCCATTTACTCAGTCGTTCAAGCTACTGTCCTTCAACGAGTTACAAAT

*Translated:*

MKLLFVASTLIGVLSFTPPQVLTDTR  
HRPPALCNSGDATNDGGDEVHEVDIAVVGAGIGGLCAGAILNTLYDKKVGVYESHYLAGG  
CAHSFSRSVKIGDDEQPTTFTDSGPTIVLGSKEPYNPLQQVLRGVDDQIEWLPYDG  
WGMIEHPMQPKEKRWFVFVGNHFEDGPLQVFASNLNAEEFNQLREITKPLVTGAATIP  
AMAMRPGQSAVPLLRLPSLISIISNGVEASTGPFAPYMNGPIFTVKDPWLRSWLNALA  
FSLSGLPADRTSAGAMAYVLFDMHREGAALDYPRGGLGEVVKALVNGVEQKSIGSKVHLS  
RHVESIDTNEEGDRVIGLTVRKNGGKKVIVAKEGVVCNVPMWSLRKLKNRNALSVLGG  
DKATSSSGLAKQSWMTSFDTDPSTGRGSVLRPKPAEDTTIEKSLLKCDSAEMTGSFL  
HLHLALNATGLDLQSLEPHYTVMDRGLEGDGKVIDGVKDDSSGELNMIAVSNPCVLDNTL  
APEGFIIMHAYGAGNEPFEIKWPPTASKGNASPNTAGEGEIIGGERCSPSTYQALKDSRS  
KVLWRAVESVIPDARERTVLALIGSPRTHERFLRRPCGSYGAAFEDCLKGSTPISNLVL  
SGDGVFPGIGIPAVALNGASAANGFVGIFDQWRCMDYLKAKGIIA-

*Targeting:*

SignalP 3.0 - NN: Yes, Cleavage Site VLS-FT

SignalP 3.0 - HMM: Yes, Cleavage Site VLT-DT, Signal Peptide Probability = 0.999

SignalP 4.1: Yes, Cleavage Site VLS-FT, D = 0.635 (D-cutoff = 0.500)

ChloroP: No, Score = 0.460

Analysis using peptide sequences starting with either of the next two in-frame methionines downstream the first one did not result in a more clear different targeting prediction.

## APPENDIX 2.D ADDITIONAL SEQUENCE-BASED ANALYSES

### 1)PDS

#### Peptide Alignment (With the JGI-Predicted Intron for Thaps3\_bd\_1474)

PDS1 bd_1474	MIITNFILSTVLATSMASFQPHPTIPLSKPSFSNRVHRSPKIGSSNLVMKDFPKPNVEDTDN -----	60 0
PDS1 bd_1474	YRYAEAMSTSFKTSLRVTNDSQKKVAIIGGGLSGLSCAKYLDAGHEPTVYEARDVLGG -----	120 0
PDS1 bd_1474	KVSAWQDEDGDWIETGLHIFFGAYPNVMNMFAELGIHDRLQWKIHQMIFAMQELPGEFTT -----	180 0
PDS1 bd_1474	FDFIPGIPAPFNFGLAILMNQKMLTLGEKIQTAPPPLPMLIEGQSFIDAQDELSVTQFMR -----MNQKMLTLGEKIQTAPPPLPMLIEGQSFIDAQDELSVTQFMR *****	240 42
PDS1 bd_1474	KYGMPERINEEVFIAMAKALDFIDPDKLSMTVVLTAMNRFLNESNGLQMAFLDGNQPDRW KYGMPERINEEVFIAMAKALDFIDPDKLSMTVVLTAMNRFLNESNGLQMAFLDGNQPDRW *****	300 102
PDS1 bd_1474	CTPTKEYVEARGGKVKLNSPIKEIVTNDDGTINHLLRSGEKIVADEYVSAMPDIVKRM CTPTKEYVEARGGKVKLNSPIKEIVTNDDGTINHLLRSGEKIVADEYVSAMPDIVKRM *****	360 162
PDS1 bd_1474	LPTTWQTMPYFRQLDELEGIPVINLHMWFDRKLKAVDHLCFSRSPLLSVYADMSVTCKEY LPTTWQTMPYFRQLDELEGIPVINLHMWFDRKLKAVDHLCFSRSPLLSVYADMSVTCKEY *****	420 222
PDS1 bd_1474	EDPNKSMLELVFAPCSPPIAGGNVNWIGKSDEEIIDATMGEALARLFPTEIANDDKWPATKM EDPNKSMLELVFAPCSPPIAGGNVNWIGKSDEEIIDATMGEALARLFPTEIANDDKWPATKM *****	480 282
PDS1 bd_1474	QGPNGQAKLEYAVVKVPRSVYAAIPGE----- QGPNGQAKLEYAVVKVPRSVYAAIPGRNKYRPSQTSPIPHFTMAGCYTSQKFLGSMEGA *****.	508 342
PDS1 bd_1474	----- TLAGKLAEEVIANRALGNADKPVKEIQQHIIDSASKHVVKEPVGVKGEGAIAFGGGYTVG	508 402
PDS1 bd_1474	----- KKEEDLLRESDPAQYELAVAK	508 423

#### Peptide Alignment (Disregarding the JGI-Predicted Intron for Thaps3\_bd\_1474)

bd_1474_No_Intron PDS1	----- MIITNFILSTVLATSMASFQPHPTIPLSKPSFSNRVHRSPKIGSSNLVMKDFPKPNVEDTDN	0 60
bd_1474_No_Intron PDS1	----- YRYAEAMSTSFKTSLRVTNDSQKKVAIIGGGLSGLSCAKYLDAGHEPTVYEARDVLGG	0 120
bd_1474_No_Intron	-----	0

PDS1	KVSAWQDEDGDWIETGLHIFFGAYPNVMNMFAELGIHDRLQWKIHQMIFAMQELPGEFTT	180
bd_1474_No_Intron PDS1	-----MNQKMLTLGEKIQTAPPLPMLIEGQSFIDAQDELSVTQFMR FDFIPGIPAPFNFGLAILMNQKMLTLGEKIQTAPPLPMLIEGQSFIDAQDELSVTQFMR *****	42 240
bd_1474_No_Intron PDS1	KYGMPERINEEVFIAMAKALDFIDPDKLSMTVVLTAMNRFLNESNGLQMAFLDGNQPDRW KYGMPERINEEVFIAMAKALDFIDPDKLSMTVVLTAMNRFLNESNGLQMAFLDGNQPDRW *****	102 300
bd_1474_No_Intron PDS1	CTPTKEYVEARGGKVKLNSPIKEIVTNDDGTINHLLRSGEKIVADEYVSAMPVDIVKRM CTPTKEYVEARGGKVKLNSPIKEIVTNDDGTINHLLRSGEKIVADEYVSAMPVDIVKRM *****	162 360
bd_1474_No_Intron PDS1	LPTTWQTMPYFRQLDELEGIPVINLHMWFDRKLKAVDHLCFSRSPLLSVYADMSVTCKEY LPTTWQTMPYFRQLDELEGIPVINLHMWFDRKLKAVDHLCFSRSPLLSVYADMSVTCKEY *****	222 420
bd_1474_No_Intron PDS1	EDPNKSMLELVFAPCSIAGGNVNIGKSDEEIIDATMGEALARLFPTEIANDDKWPATKM EDPNKSMLELVFAPCSIAGGNVNIGKSDEEIIDATMGEALARLFPTEIANDDKWPATKM *****	282 480
bd_1474_No_Intron PDS1	QGPNGQAKLEYVAVVKVPRSVYAAIPGE   310 QGPNGQAKLEYVAVVKVPRSVYAAIPGE   508 *****	

### Genomic Alignment (Extended Sequences Contain 10kb downstream the JGI-Predicted Gene Models)

The abrupt start of sequence differences is highlighted in red.

PDS1_Extended PDS1	GCAAAGCGTTCCCTTCGGCGTCAGCCTCCTCCTTCACTGTCAGTCAGTTGTGTT	60
bd_1474_Extended bd_1474	-----	0
-----	-----	0
PDS1_Extended PDS1	GAACACTTCTGCTTCTCATCTCATTACTACCACTGCTATTGCAACTGGCTGC	120
bd_1474_Extended bd_1474	GAACACTTCTGCTTCTCATCTCATTACTACCACTGCTATTGCAACTGGCTGC -----	120 0
-----	-----	0
PDS1_Extended PDS1	CGTATCTGACTCTCCTCAATT CGTCACTCCC ATAGGCCACGTT CACCAT CATT TATCA	180
bd_1474_Extended bd_1474	CGTATCTGACTCTCCTCAATT CGTCACTCCC ATAGGCCACGTT CACCAT CATT TATCA -----	180 0
-----	-----	0
PDS1_Extended PDS1	CCATGATCATTACAATTCAT CCTCTCCACC GT CCTAGCGACATCAATGGCTTTCAAC	240
bd_1474_Extended bd_1474	CCATGATCATTACAATTCAT CCTCTCCACC GT CCTAGCGACATCAATGGCTTTCAAC -----	240 0
-----	-----	0
PDS1_Extended PDS1	CACACACACCCATCCTCTCAAACCATCCTCTCCACC GT CCTAGCGACATCAATGGCTCCCCAAAA	300
bd_1474_Extended bd_1474	CACACACACCCATCCTCTCAAACCATCCTCTCCACC GT CCTAGCGACATCAATGGCTCCCCAAAA -----	300 0
-----	-----	0
PDS1_Extended PDS1	TCGGCTCTCCAACCTCGTTATGAAGGACTTCCGAAACCAAAATGTCGAAGATACAGACA	360
bd_1474_Extended bd_1474	TCGGCTCTCCAACCTCGTTATGAAGGACTTCCGAAACCAAAATGTCGAAGATACAGACA -----	360 0
-----	-----	0

PDS1_Extended	ACTATCGCTACGCAGAGGCCATGTCCACTAGCTTCAAGACGTCTCCGAGTGACGAATG	420
PDS1	ACTATCGCTACGCAGAGGCCATGTCCACTAGCTTCAAGACGTCTCCGAGTGACGAATG	420
bd_1474_Extended	-----	0
bd_1474	-----	0
PDS1_Extended	ATTCACAGAAGAAGAAGGTGGCTATCATTGGAGGAGGATTACAGGTCTGTCTTGCCA	480
PDS1	ATTCACAGAAGAAGAAGGTGGCTATCATTGGAGGAGGATTACAGGTCTGTCTTGCCA	480
bd_1474_Extended	-----	0
bd_1474	-----	0
PDS1_Extended	AGTACCTCTCCGATGCCGGCATGAACCCACCGTATACTGAAGCACGTGATGTACTCGGAG	540
PDS1	AGTACCTCTCCGATGCCGGCATGAACCCACCGTATACTGAAGCACGTGATGTACTCGGAG	540
bd_1474_Extended	-----	0
bd_1474	-----	0
PDS1_Extended	GAAAGGTGTCAGCGTGGCAAGATGAAGATGGAGACTGGATCGAACACAGGTCTCACATCT	600
PDS1	GAAAGGTGTCAGCGTGGCAAGATGAAGATGGAGACTGGATCGAACACAGGTCTCACATCT	600
bd_1474_Extended	-----	0
bd_1474	-----	0
PDS1_Extended	TCTTCGGAGCATACCCCAACGTTATGAACATGTTGCTGAGCTTGGCATCCACGATAGGC	660
PDS1	TCTTCGGAGCATACCCCAACGTTATGAACATGTTGCTGAGCTTGGCATCCACGATAGGC	660
bd_1474_Extended	-----	0
bd_1474	-----	0
PDS1_Extended	TTCACTGGAAAGATTCCACCAATGATTTGCAATGCAGGAACCTCCGGAGAGTTCACTA	720
PDS1	TTCACTGGAAAGATTCCACCAATGATTTGCAATGCAGGAACCTCCGGAGAGTTCACTA	720
bd_1474_Extended	-----	0
bd_1474	-----	0
PDS1_Extended	CCTTTGATTCATCCCTGGTATTCAGCTCCGTTCAACTTGGATTGGCATTCTTATGA	780
PDS1	CCTTTGATTCATCCCTGGTATTCAGCTCCGTTCAACTTGGATTGGCATTCTTATGA	780
bd_1474_Extended	-----	CTTATGA
bd_1474	-----	CTTATGA
	*****	7
	*****	7
PDS1_Extended	ATCAAAAGATGTTGACGTTGGGTAAAAAAATTCAAGACCGCTCCCTCTTCTTATGC	840
PDS1	ATCAAAAGATGTTGACGTTGGGTAAAAAAATTCAAGACCGCTCCCTCTTCTTATGC	840
bd_1474_Extended	ATCAAAAGATGTTGACGTTGGGTAAAAAAATTCAAGACCGCTCCCTCTTCTTATGC	67
bd_1474	ATCAAAAGATGTTGACGTTGGGTAAAAAAATTCAAGACCGCTCCCTCTTCTTATGC	67
	*****	*****
PDS1_Extended	TTATTGAGGGACAGTCATTGATGCTCAGGATGAGTTGAGTGTGACCGAGTTCATGA	900
PDS1	TTATTGAGGGACAGTCATTGATGCTCAGGATGAGTTGAGTGTGACCGAGTTCATGA	900
bd_1474_Extended	TTATTGAGGGACAGTCATTGATGCTCAGGATGAGTTGAGTGTGACCGAGTTCATGA	127
bd_1474	TTATTGAGGGACAGTCATTGATGCTCAGGATGAGTTGAGTGTGACCGAGTTCATGA	127
	*****	*****
PDS1_Extended	GGAAGTACGGTATGCCCTGAGAGAATCAACGAGGGAGGTGTTATTGCGATGCCAAGGCGT	960
PDS1	GGAAGTACGGTATGCCCTGAGAGAATCAACGAGGGAGGTGTTATTGCGATGCCAAGGCGT	960
bd_1474_Extended	GGAAGTACGGTATGCCCTGAGAGAATCAACGAGGGAGGTGTTATTGCGATGCCAAGGCGT	187
bd_1474	GGAAGTACGGTATGCCCTGAGAGAATCAACGAGGGAGGTGTTATTGCGATGCCAAGGCGT	187
	*****	*****
PDS1_Extended	TGGACTTATTGATCCTGATAAGTTGAGTATGACTGTGGTCTTACGGCTATGAACAGGT	1020
PDS1	TGGACTTATTGATCCTGATAAGTTGAGTATGACTGTGGTCTTACGGCTATGAACAGGT	1020
bd_1474_Extended	TGGACTTATTGATCCTGATAAGTTGAGTATGACTGTGGTCTTACGGCTATGAACAGGT	247
bd_1474	TGGACTTATTGATCCTGATAAGTTGAGTATGACTGTGGTCTTACGGCTATGAACAGGT	247
	*****	*****
PDS1_Extended	TCTTGAATGAGAGTAATGGACTTCAGATGGCATTCTGGATGGAATCAGCCTGATAGGT	1080
PDS1	TCTTGAATGAGAGTAATGGACTTCAGATGGCATTCTGGATGGAATCAGCCTGATAGGT	1080
bd_1474_Extended	TCTTGAATGAGAGTAATGGACTTCAGATGGCATTCTGGATGGAATCAGCCTGATAGGT	307

bd_1474	TCTTGAATGAGAGTAATGGACTTCAGATGGCATTCTGGATGGAAATCAGCCTGATAGGT *****	307
PDS1_Extended PDS1 bd_1474_Extended bd_1474	GGTGCACCCACGAAGGAGTATGTGGAAGCACGCGGAGGAAAGGTCAAATTGAECTCTC GGTGCACCCACGAAGGAGTATGTGGAAGCACGCGGAGGAAAGGTCAAATTGAECTCTC GGTGCACCCACCAAGGAGTATGTGGAAGCACGCGGAGGAAAGGTCAAATTGAECTCTC GGTGCACCCACCAAGGAGTATGTGGAAGCACGCGGAGGAAAGGTCAAATTGAECTCTC *****	1140 1140 367 367
PDS1_Extended PDS1 bd_1474_Extended bd_1474	CCATTAAGGAGATTGTGACCAACGACGATGGAACTATCAATCACCTTCTCCTCGATCTG CCATTAAGGAGATTGTGACCAACGACGATGGAACTATCAATCACCTTCTCCTCGATCTG CCATTAAGGAGATTGTGACCAACGACGATGGAACTATCAATCACCTTCTCCTCGATCTG CCATTAAGGAGATTGTGACCAACGACGATGGAACTATCAATCACCTTCTCCTCGATCTG *****	1200 1200 427 427
PDS1_Extended PDS1 bd_1474_Extended bd_1474	GCGAGAAGATTGTGCCGATGAAACAGCTCTGCCATGCCGAGCTTGAGGGCA GCGAGAAGATTGTGCCGATGAAACAGCTCTGCCATGCCGAGCTTGAGGGCA GCGAGAAGATTGTGCCGATGAAACAGCTCTGCCATGCCGAGCTTGAGGGCA GCGAGAAGATTGTGCCGATGAAACAGCTCTGCCATGCCGAGCTTGAGGGCA *****	1260 1260 487 487
PDS1_Extended PDS1 bd_1474_Extended bd_1474	TGCTTCCCACAACGTGGCAGACTATGCCCTACTTCCGTAGCTTGACGAATTGAGGGCA TGCTTCCCACAACGTGGCAGACTATGCCCTACTTCCGTAGCTTGACGAATTGAGGGCA TGCTTCCCACAACGTGGCAGACTATGCCCTACTTCCGTAGCTTGACGAATTGAGGGCA TGCTTCCCACAACGTGGCAGACTATGCCCTACTTCCGTAGCTTGACGAATTGAGGGCA *****	1320 1320 547 547
PDS1_Extended PDS1 bd_1474_Extended bd_1474	TCCCCTGTTATCAACTTGCACATGTGGTCGATCGTAAGTTGAAAGCAGTCGACCATCTT TCCCCTGTTATCAACTTGCACATGTGGTCGATCGTAAGTTGAAAGCAGTCGACCATCTT TCCCCTGTTATCAACTTGCACATGTGGTCGATCGTAAGTTGAAAGCAGTCGACCATCTT TCCCCTGTTATCAACTTGCACATGTGGTCGATCGTAAGTTGAAAGCAGTCGACCATCTT *****	1380 1380 607 607
PDS1_Extended PDS1 bd_1474_Extended bd_1474	GCTTCAGTCGCTCCCCACTCTTCCGTCTACGCCGACATGTCGTACATGCAAGGAGT GCTTCAGTCGCTCCCCACTCTTCCGTCTACGCCGACATGTCGTACATGCAAGGAGT GCTTCAGTCGCTCCCCACTCTTCCGTCTACGCCGACATGTCGTACATGCAAGGAGT GCTTCAGTCGCTCCCCACTCTTCCGTCTACGCCGACATGTCGTACATGCAAGGAGT *****	1440 1440 667 667
PDS1_Extended PDS1 bd_1474_Extended bd_1474	ACGAAGATCCCAACAAGTCATGTTGAATTGGTCTTCGCTCCCTGCTCTCTATTGCCG ACGAAGATCCCAACAAGTCATGTTGAATTGGTCTTCGCTCCCTGCTCTCTATTGCCG ACGAAGATCCCAACAAGTCATGTTGAATTGGTCTTCGCTCCCTGCTCTCTATTGCCG ACGAAGATCCCAACAAGTCATGTTGAATTGGTCTTCGCTCCCTGCTCTCTATTGCCG *****	1500 1500 727 727
PDS1_Extended PDS1 bd_1474_Extended bd_1474	GAGGAAATGTCAACTGGATTGGAAAGTCAGATGAGGAAATCATTGATGCTACCATGGGTG GAGGAAATGTCAACTGGATTGGAAAGTCAGATGAGGAAATCATTGATGCTACCATGGGTG GAGGAAATGTCAACTGGATTGGAAAGTCAGATGAGGAAATCATTGATGCTACCATGGGTG GAGGAAATGTCAACTGGATTGGAAAGTCAGATGAGGAAATCATTGATGCTACCATGGGTG *****	1560 1560 787 787
PDS1_Extended PDS1 bd_1474_Extended bd_1474	AGCTTGCTCGCCTTTCCCTACCGAGATTGCGAATGATGATAAGTGGCTGCTACGAAGA AGCTTGCTCGCCTTTCCCTACCGAGATTGCGAATGATGATAAGTGGCTGCTACGAAGA AGCTTGCTCGCCTTTCCCTACCGAGATTGCGAATGATGATAAGTGGCTGCTACGAAGA AGCTTGCTCGCCTTTCCCTACCGAGATTGCGAATGATGATAAGTGGCTGCTACGAAGA *****	1620 1620 847 847
PDS1_Extended PDS1 bd_1474_Extended bd_1474	TGCAGGGACCTAATGGACAGGCAAAAGCTTGAGAAGTATGCTGTTGAAAGGTGCCAAGGA TGCAGGGACCTAATGGACAGGCAAAAGCTTGAGAAGTATGCTGTTGAAAGGTGCCAAGGA TGCAGGGACCTAATGGACAGGCAAAAGCTTGAGAAGTATGCTGTTGAAAGGTGCCAAGGA TGCAGGGACCTAATGGACAGGCAAAAGCTTGAGAAGTATGCTGTTGAAAGGTGCCAAGGA *****	1680 1680 907 907
PDS1_Extended PDS1 bd_1474_Extended bd_1474	GTGTGTATGCTGCCATTCTGGTGAGTAAAAAATAGTGTGCGGTGAATCTCGTCGCTA GTGTGTATGCTGCCATTCTGGTGAGTAAAAAATAGTGTGCGGTGAATCTCGTCGCTA GTGTGTATGCTGCCATTCTGGTGAGTAAAAAAGAGTGTGCGGTGAATCTCGTCGCTA GTGTGTATGCTGCCATTCTGGTGAGTAAAAAAGAGTGTGCGGTGAATCTCGTCGCTA *****	1740 1740 967 967
PDS1_Extended PDS1	CCTTGGCCAACACTGACTCTTGTCTTTAAATCATATCAGGACGTAACAAATACCGC CCTTGGCCAACACTGACTCTTGTCTTTAAATCATATCAGGACGTAACAAATACCGC	1800 1800

bd_1474_Extended	CCTTGGCCAACACTGACTCTGTTCTTTAAATCATATCAGGACGTAAACAAATACCGC	1027
bd_1474	CCTTGGCCAACACTGACTCTGTTCTTTAAATCATATCAGGACGTAAACAAATACCGC	1027
	*****	*****
PDS1_Extended	CCCAGTCAGACCTCCCCATCCACACTTCACCATGGCTGGATGCTATACTCACAAAAG	1860
PDS1	CCCAGTCAGACCTCCCCATCCACACTTCACCATGGCTGGATGCTATACTCACAAAAG	1860
bd_1474_Extended	CCCAGTCAGACCTCCCCATCCACACTTCACCATGGCTGGATGCTATACTCACAAAAG	1087
bd_1474	CCCAGTCAGACCTCCCCATCCACACTTCACCATGGCTGGATGCTATACTCACAAAAG	1087
	*****	*****
PDS1_Extended	TTCTCGGATCCATGGAGGGTGCACCCCTGCCGGGAAGCTGCTGCCGAGGTCAATTGCC	1920
PDS1	TTCTCGGATCCATGGAGGGTGCACCCCTGCCGGGAAGCTGCTGCCGAGGTCAATTGCC	1920
bd_1474_Extended	TTCTCGGATCCATGGAGGGTGCACCCCTGCCGGGAAGCTGCTGCCGAGGTCAATTGCC	1147
bd_1474	TTCTCGGATCCATGGAGGGTGCACCCCTGCCGGGAAGCTGCTGCCGAGGTCAATTGCC	1147
	*****	*****
PDS1_Extended	AACCGTGCCTCGGAAATCGGATAAGCCAGTCAGGAGATTCAAGGAGATTCAACACATTATCGAC	1980
PDS1	AACCGTGCCTCGGAAATCGGATAAGCCAGTCAGGAGATTCAAGGAGATTCAACACATTATCGAC	1980
bd_1474_Extended	AACCGTGCCTCGGAAATCGGATAAGCCAGTCAGGAGATTCAAGGAGATTCAACACATTATCGAC	1207
bd_1474	AACCGTGCCTCGGAAATCGGATAAGCCAGTCAGGAGATTCAAGGAGATTCAACACATTATCGAC	1207
	*****	*****
PDS1_Extended	TCGGCTAGTAAGCATGTTGAAAGGAGCCAGTGGGTGTGAAGGGAGAGGGAGCGATTGCA	2040
PDS1	TCGGCTAGTAAGCATGTTGAAAGGAGCCAGTGGGTGTGAAGGGAGAGGGAGCGATTGCA	2040
bd_1474_Extended	TCGGCTAGTAAGCATGTTGAAAGGAGCCAGTGGGTGTGAAGGGAGAGGGAGCGATTGCA	1267
bd_1474	TCGGCTAGTAAGCATGTTGAAAGGAGCCAGTGGGTGTGAAGGGAGAGGGAGCGATTGCA	1267
	*****	*****
PDS1_Extended	TTTGGAGGGGGTATACTGTTGAAAGAAGGAGGAGGATTGTTGAGGGAGTCGGATCCT	2100
PDS1	TTTGGAGGGGGTATACTGTTGAAAGAAGGAGGAGGATTGTTGAGGGAGTCGGATCCT	2100
bd_1474_Extended	TTTGGAGGGGGTATACTGTTGAAAGAAGGAGGAGGATTGTTGAGGGAGTCGGATCCT	1327
bd_1474	TTTGGAGGGGGTATACTGTTGAAAGAAGGAGGAGGATTGTTGAGGGAGTCGGATCCT	1327
	*****	*****
PDS1_Extended	GCTCAGTATGAGTTGCAGTAGCCAAGTAAGGAAGAGTATTAAAGTAAACAGCTAGA	2160
PDS1	GCTCAGTATGAGTTGCAGTAGCCAAGTAAGGAAGAGTATTAAAGTAAACAGCTAGA	2160
bd_1474_Extended	GCTCAGTATGAGTTGCAGTAGCCAAGTAAGGAAGAGTATTAAAGTAAACAGCTAGA	1387
bd_1474	GCTCAGTATGAGTTGCAGTAGCCAAGTA--	1357
	*****	*****
PDS1_Extended	TTGATTTGAAGGAGTTGTATGTAGCTTAGTACCTTAAGGTACTTGATGTACTTACT	2220
PDS1	TTGATTTGA-----	2171
bd_1474_Extended	TTGATTTGAAGGAGTTGTATGTAACTTAGTACCTTAAGGTACTTGATGTCTTACT	1447
bd_1474	-----	1357
	-----	-----
PDS1_Extended	TTCCGCTTGGAGAGCCATTCTTGATTATGACAGAATGGAGTTCCCTCATCCTT	2280
PDS1	-----	2171
bd_1474_Extended	TTCCGCTTGGAGAGCCATTCTTGATTACGACAGAATTGAGTTCCCTCATCCTT	1507
bd_1474	-----	1357
	-----	-----
PDS1_Extended	CTCGTGATTGATTGGATCAGATGATATTATGCATCTCACCTGGTGCCTAACAG	2340
PDS1	-----	2171
bd_1474_Extended	CTCGTGATTGATTGGATCAGATGATATTATGCATCTCACCTGGTGCCTAACAG	1567
bd_1474	-----	1357
	-----	-----
PDS1_Extended	ATACATACGAAAGAACCTCCCCCACCTGCCACACCAACTCATTCTCATCTCCTTA	2400
PDS1	-----	2171
bd_1474_Extended	ATACATACGAAAGAACCTCCC-CCACCTGCCACACCAACTCATTCTCATCTCCTTA	1626
bd_1474	-----	1357
	-----	-----
PDS1_Extended	TTTGATTTGTGCTCGAACAGAACTCTCCCTGACAATCGGATCAAATTTACGAA	2460
PDS1	-----	2171
bd_1474_Extended	TTTGATTTGTGCTCGAACAGAACTCTCCCTGACAATTGGATCAAATTTACGAA	1686
bd_1474	-----	1357
	-----	-----
PDS1_Extended	CTTGAACCTCTGGTGTCTCGATACGTTCGTGTGGTGTAGAAGAACAGTCCC	2520

PDS1	-----	2171
bd_1474_Extended	CTTGAACCTCTGGTGTCTCGATACTGTTCTCGTCGTGTGGTAGAAGAACCCAGTC	1746
bd_1474	-----	1357
PDS1_Extended	CGCCGAGCTTAAGAGCTGCCTGTTAACGACGTGAATGGAAAGAGGAGTCAGTCAGT	2580
PDS1	-----	2171
bd_1474_Extended	CGCCGAGCTTAAGAGCTGCCTGTTAACGACGTGAATGGAAAGAGGAGTCAGTCAGT	1806
bd_1474	-----	1357
PDS1_Extended	GGATGAGATGATATGCAGCATAGCCACACCTCTTCAATCATACAAAGGCTGATTGCACA	2640
PDS1	-----	2171
bd_1474_Extended	GGATGAGATGATATGCAGCATAGCCACAACTCTTCAATCATACAAAGGCTGATTGCACA	1866
bd_1474	-----	1357
PDS1_Extended	CAACGTGTACCGTCACCTCATCTGACGGAACAGCACCTCCACTCACTTGATGGGATC	2700
PDS1	-----	2171
bd_1474_Extended	CAACGTGTACCGTCACCTCATCTGACGGAACAGCACCTCCACTCACTTGATGGGATC	1926
bd_1474	-----	1357
PDS1_Extended	GTCTTGCCTCCCTCTGGCCATGTGAAGAATAGCGGTCGGCTGCATGGTATTTACTCT	2760
PDS1	-----	2171
bd_1474_Extended	GTCTTGCCTCCCTCTGGCCATGTGAAGAATAGCGGTCGGCTGCATGGTATTTACTCT	1986
bd_1474	-----	1357
PDS1_Extended	TCTCGATAATGCAAACGTTTCTAAGATGGGTGTTGCCGGTTGGTGAAGGGGTGACG	2820
PDS1	-----	2171
bd_1474_Extended	TCTCGATACTGCAGACGTTTCTAAGATGGGTGTTGCCGGTTGGTGAAGGGTGGCG	2046
bd_1474	-----	1357
PDS1_Extended	GTGGTGGTGGTTGGTTGTTGTTGTGCGTGACGAGTTGTGATGTTGGTTTGT	2880
PDS1	-----	2171
bd_1474_Extended	GTGGTGGTCGTTGGTTGTTGTGCGTGACGAGTTGTGATGTTGGTTTGT	2106
bd_1474	-----	1357
PDS1_Extended	GAACAGTTCACTGTTGTCGTGACGGACTAACGTGATTCCGTGGATACCAAGAAC	2940
PDS1	-----	2171
bd_1474_Extended	GAACAGTTCTGTAACGTGTTGTCGTGACGGACTAACGTGATTCCGTGGATACCAAGAAC	2166
bd_1474	-----	1357
PDS1_Extended	ACTAACATGGTAACCCCC--CCCCCAGACCAACAAATCATTGATCCCCACCAACTCCAT	2998
PDS1	-----	2171
bd_1474_Extended	ACTAACATAGTAACCCCACCCCCCAGACCAACAAATCATTGATCCCCACCAACTCCAT	2226
bd_1474	-----	1357
PDS1_Extended	CACACTCCCTCATCGATACATCCAGCACAAACCATGATAGTTGATAGTCCTCATTGATT	3058
PDS1	-----	2171
bd_1474_Extended	CACACTCCCTCATCGATACATCCAGCACAAACCATGATAGTTGATAGTCCTCATTGATT	2286
bd_1474	-----	1357
PDS1_Extended	CTCGTCGCACTGCTACAGCGATGCCTCCACAAACAGCCGTACGATGATAAACATTGT	3118
PDS1	-----	2171
bd_1474_Extended	CTCGTCGCACTGCTACAGCGATGCCTCCACAAACAGCCGTACATTGATAAACATTGT	2346
bd_1474	-----	1357
PDS1_Extended	ACTCCCACTCCAGACTGGGTGGAGTCGACAGTGAAGTCAGATGATGAATGTTGGCT	3178
PDS1	-----	2171
bd_1474_Extended	ACTCCCACTCCAGACTGGGTGGAGTCGACAGTGAAGTCAGATGATGAATGTTGGCT	2406
bd_1474	-----	1357

PDS1_Extended	GCAAACGCACAACCCGAGCCAAGTGAACGATGGCACTACAATCATCCGCCGCATGC	3238
PDS1	-----	2171
bd_1474_Extended	GCAAACGCACAACCCGAGCCAAGTGAACGATGGCACTACAATCATCCGCCGCATGC	2466
bd_1474	-----	1357
PDS1_Extended	CTTGAAACCAATTCACTAGACCCTGCAGAACACCACCTTGTGCCTACGAAAATGTTCA	3298
PDS1	-----	2171
bd_1474_Extended	CTTGAAACCAATTCACTAGACCCTGCAGAACACCACCTTGTGCCTACGAAAATGTTCA	2526
bd_1474	-----	1357
PDS1_Extended	ACCAGTCCTCGAGATGATGGCGAAGCAGTCAACCATCTCACGTCAACCATAATGTTACGCATCTG	3358
PDS1	-----	2171
bd_1474_Extended	AACAGTCCTCGAGATGATGGCGAAGCAGTCAACCATCTCACGTCAACCATAAGTTACGCATCTG	2586
bd_1474	-----	1357
PDS1_Extended	GGATCCGTATTATTGCGATGGGACTGTCAAGCAACATCTAGCCTCTTGGGATACGATCG	3418
PDS1	-----	2171
bd_1474_Extended	GGATCCGTATTATTGCGATGGGACTGTCAAGCAACATCTAGCCTCTTGGGATACGATCG	2646
bd_1474	-----	1357
PDS1_Extended	TGTGATTAACGAAAACCTTGACTTTACAAGCGAGTAGAGGACAACACTATCCCCGAGCA	3478
PDS1	-----	2171
bd_1474_Extended	TGTGATTAACGAAAACGTTGACTTTACAAGCGAGTAGAGGACAACACTATCCCCGAGCA	2706
bd_1474	-----	1357
PDS1_Extended	CGATGTCTTGTGACGAATCCTCCGTACAGCGGCATCACATCGAACGATTGCTTAAGTT	3538
PDS1	-----	2171
bd_1474_Extended	CGATGTCTTGTGACGAATCCTCCGTACAGCGGCATCACATCGAACGATTGCTTAAGTT	2766
bd_1474	-----	1357
PDS1_Extended	TGTTACGACGGTGAATGATAAGCCATTGCTACTAATGCCAATTGGGTTGCGAGAAA	3598
PDS1	-----	2171
bd_1474_Extended	TGTTACGACGGTGAATGATAAGCCATTGCTACTAATGCCAATTGGGTTGCGAGAAA	2826
bd_1474	-----	1357
PDS1_Extended	GAAGGAGTACAAATCCATCATTGGTAAACGAATCTGTTACGTATCCCCATCGAGGT	3658
PDS1	-----	2171
bd_1474_Extended	GAAGGAGTACAAATCCATCATTGGTAAACGAATCTGTTACGTATCCCCATAGAGGT	2886
bd_1474	-----	1357
PDS1_Extended	ATACACGTATGCTATGCCAACTTGGAAATCGAACACGTCGACGGAGAGACGGG	3718
PDS1	-----	2171
bd_1474_Extended	ATACACGTATGCTATGCCAACTTGGAAATCGAACACGTCGACGGAGAGACGGG	2946
bd_1474	-----	1357
PDS1_Extended	AAAGACGACTCCCTATTGAGTTCTGGTATGTCGTTAAAGCAATAGTGAGGCAAC	3778
PDS1	-----	2171
bd_1474_Extended	AAAGACGACCCCTATTGAGTTCTGGTATGTCGTTAAAGCAATAGTGAGGCAAC	3006
bd_1474	-----	1357
PDS1_Extended	GAGTAGGATAGAGAATAAGCTTGGTATTGCAAAACGGCAGCAACCACCTGTTGGGT	3838
PDS1	-----	2171
bd_1474_Extended	GGGTAGGATAGAGAATAAGCTTGGTATTGCAAAACGGCAGCAACCACCTGTTGGGT	3066
bd_1474	-----	1357
PDS1_Extended	TGTAGCCAAGACGGTCAAA <del>CG</del> CTAAAGTGGAAAGATTCAAAAGGTGAAAGAAAAGAG	3898
PDS1	-----	2171
bd_1474_Extended	TGTAGCCAAGACGGTCAAA <del>CG</del> CACAGGAGCACCAATTCTGACAACATTGTTGTGT	3126
bd_1474	-----	1357

PDS1_Extended	GTGATTGGAGATTT-----CTCCTCGGAGATGCTAAATCGCTTAGCAATGGAAGTGAGA	3953
PDS1	-----	2171
bd_1474_Extended	CTCAATGGGAGCGATGAAATCGCATGGGACAATCTCGTGCCTGATGCAATAATTGATA	3186
bd_1474	-----	1357
PDS1_Extended	A-----CTGAATTGTCATGATACACGTTATATGTCATAAACTGAAGTAC	4000
PDS1	-----	2171
bd_1474_Extended	GCTAGGACCAAGTGGTGCAGACTGTGAGGTTAGATTATGGCT-----AGTTTACGAAC	3241
bd_1474	-----	1357
PDS1_Extended	CCATCCCACACTCAATCGACA---ATAAG-----AGTCATACCCAACGA---AC	4042
PDS1	-----	2171
bd_1474_Extended	TACGAGAACGAATGCCAGCATCTGAGAACTCAGTCAGTCTATGACCTACGAAGGACA	3301
bd_1474	-----	1357
PDS1_Extended	GGTTTCCCCGTTTATCACTCCGGAGTTGCTCACTCGAGGACGAGTCGATTGTTGC	4102
PDS1	-----	2171
bd_1474_Extended	GACACCCCCCATCATGCACTTGACAACAAAT----GTCGCCAGAAC-----	3345
bd_1474	-----	1357
PDS1_Extended	TTGATGGTAGTCATTACTCCGTTGCCTCTCTCAAAGTTGTTGTTGACTTGATACTC	4162
PDS1	-----	2171
bd_1474_Extended	-----TACATAGATGAGAGATGGTGTCAATTGCAATGACAACACT	3382
bd_1474	-----	1357
PDS1_Extended	TATCCCCCCAACCGTCGCACCCCTACAAAGCTTCGTTCATTCATTCATTGCCAGC	4222
PDS1	-----	2171
bd_1474_Extended	GTTGCGAACAGCAAGTCCAAA----GAGAAGATTGGAAGGC---AGAACGCGAAGA	3437
bd_1474	-----	1357
PDS1_Extended	CCCCTCCAATGTGCCGTTTATTGAGTCATCCTGTTCTTGATCCCCATCAA	4282
PDS1	-----	2171
bd_1474_Extended	CATGAAGAAGCTGACCGGGTACGTGTACCTGACTCC----GGGAGTGGTGGCCAGTCA	3491
bd_1474	-----	1357
PDS1_Extended	AAGTAACATAATTAGAAAGTGAGATGGTCAGATTCACCTCACAGTGTACATGAACAA	4342
PDS1	-----	2171
bd_1474_Extended	GTG----AGACTTAGA----GCGGTGGTGTGACCCG-----GACCA	3524
bd_1474	-----	1357
PDS1_Extended	TCGTCTCACCTCTCCTCTCCACCCAATCCTCACCACCTACCAAACCTCGCTAACTTT	4402
PDS1	-----	2171
bd_1474_Extended	TGTGATGATGTCTTGTATCTGGCGTGAAGGATACACGAGGAGGAGATGATAGTACTG	3584
bd_1474	-----	1357
PDS1_Extended	CCAT-----AGGAGCAGCACCTCCACCACTAAATCAGCAGCCTTCACATA-----C	4449
PDS1	-----	2171
bd_1474_Extended	GAGTCAGTGCTAACGGTAGTGGTGTATGGGATAATGACCGAGCAACGCATTGACGA	3644
bd_1474	-----	1357
PDS1_Extended	AACACATTATTACACCGAATCAACACCTCCCCAACGTACCGCAAACGTCCATCAATG	4509
PDS1	-----	2171
bd_1474_Extended	AATGAAGAATAACGGGACATGAAAGAGTC-----GCGAAGATGGCGAAAATG	3691
bd_1474	-----	1357
PDS1_Extended	AACTCCTCCGTCTCCTCCAATTGTAATTGTCATGAGGCATCCGAGGAGGGAGCTTGCCT	4569
PDS1	-----	2171
bd_1474_Extended	AGCACTGTCTTCATCTCTTGT-----TGAAAAGATCCGGGGATTGATCTTGCCTA	3743
bd_1474	-----	1357

PDS1_Extended	TGGTATTCTGGCCCCAC-----TTGA-----GACGGACGCGGACGTGTTGCC	4613
PDS1	-----	2171
bd_1474_Extended	GAAACATGTTCACTTCAATGAGTTGTGCTGCACCCACTCGCGCACAGCGTTCTTC	3803
bd_1474	-----	1357
PDS1_Extended	TGTTAACGTCGGC-----TAGGA-----AGGGTTGGGGTGACGATTAG	4652
PDS1	-----	2171
bd_1474_Extended	AGTTCCATGTGTCGAATAGCTTGAAGTTGTGTTGGTCCATGAGACGCAAGATTCA	3863
bd_1474	-----	1357
PDS1_Extended	TTGTGACTGTTGATGAGAGTTGGTGGAGGAGGAGTTATAGGTGAGAAGGTGGC	4712
PDS1	-----	2171
bd_1474_Extended	TTGTAATTCCAGATACTAGTG-----	3884
bd_1474	-----	1357
PDS1_Extended	AGAGGCATCAGACGAAGGCATCGCCTCACCATGAAACGAGCAGATAATAGATTAACTAA	4772
PDS1	-----	2171
bd_1474_Extended	-GCACCGTCAGCGTCAGAAATGGGAACGCCAATAGAACAGAAACCATTGGCGATGTTGCG	3943
bd_1474	-----	1357
PDS1_Extended	TCCCTCTAGATGGGCTTACCATTGTATTGGGGCGTTAGCGTCGAAAGAGTGAAGCG	4832
PDS1	-----	2171
bd_1474_Extended	AATAGCCAAAGTGAGTTCCCAGCGACATTGGTG-----GCTCGAATCTCTGCTTCA	3995
bd_1474	-----	1357
PDS1_Extended	GG-----TAAAGGCACCGACCGTCTTGTCTCGTCGTGGTGAACCAAATGGTCCGCC	4888
PDS1	-----	2171
bd_1474_Extended	CAAGAACTTAGTGAAGTTCTGTCTGGCGTCTGATGCCAT---GAAATCGGTCCGCC	4051
bd_1474	-----	1357
PDS1_Extended	GTTCCTGAAAACAACAAAT---AGTGACAATATGCTGTTAACGAGAGGTGGAGTAACC	4945
PDS1	-----	2171
bd_1474_Extended	AGATCGAAACACAATAGCACCCTCATACTACGAAGCTTGAAGAGGGGAAGGAGCGTT-C	4110
bd_1474	-----	1357
PDS1_Extended	AAGCCAAGCCCGCAACGAAGGCAACAGGAGACCAACAA-----	4983
PDS1	-----	2171
bd_1474_Extended	CTTCATGTACCGCGTTGCCGATTGACTACCCAACATGCATCACTGTAAGTAGTCAGTT	4170
bd_1474	-----	1357
PDS1_Extended	--ACAACCAGAACTGATCAAAACAGCCAAACACCCAACAATGAACACGCTAATTGCACG	5041
PDS1	-----	2171
bd_1474_Extended	TGCTTCCATACCTGATCTGGGGTGTGCACTACAATAAGCTTCA-----GTGTCCGA	4225
bd_1474	-----	1357
PDS1_Extended	TGGCGCCGAGAAGTCAAGGTGTT--GTTGCGCACTAGCATCAAAT-----	5085
PDS1	-----	2171
bd_1474_Extended	GGAATCAGGAAAGTGAAGATATGTATGGAGAGGATTACGGTTCTGACGTGAAGGTAAAT	4285
bd_1474	-----	1357
PDS1_Extended	-----CAAGTGCACCTCGACGTCGGCGGG-----TGCATCCT---CTCC	5122
PDS1	-----	2171
bd_1474_Extended	GCCATAGTCATGGGTAGAATGGATATAGTGCAGTGCATGAAGGGCTGCTTCATGTGACC	4345
bd_1474	-----	1357
PDS1_Extended	AAGAAGTGATGTG---TCAGCACGTAATCAGCCGCACATGATGCATGCTACAACATCATC	5179
PDS1	-----	2171
bd_1474_Extended	AGGAGAAGGCTTGTGTTGACGATGATAAGAAGGAGTGGACTGGAGCAATGTCAGGACG	4405

bd_1474	-----	1357
PDS1_Extended PDS1 bd_1474_Extended bd_1474	GGCGTCTGGCAACTGCTACACTAACATCCAACCATTCTCGGC-----CAATACC ----- AGTCATTGTGCCAACCA--TCCAATAGATCCAACAAGACTCATATATGCCCTCGAGCAT -----	5231 2171 4463 1357
PDS1_Extended PDS1 bd_1474_Extended bd_1474	TCCAGTTGGACCCGCAACT---TCTCATC---GGAAGCACCCCTACAACAACAACAACAA ----- CGTTGGGGCAGTCGAATGCCTTCATTGGAGTCAGCGATTGCATCAATAGGAATG -----	5285 2171 4523 1357
PDS1_Extended PDS1 bd_1474_Extended bd_1474	CAACAAACGTCCCAGGCCATCGAAAAAGCCAACCCCCCCCCTCTAACACCCGGACACGCC ----- CCAGATCGATACTGGAGTGATGGTAGGAGAAG---GAGTCTTAGAATCA-ACTTGGAAATCG -----	5345 2171 4579 1357
PDS1_Extended PDS1 bd_1474_Extended bd_1474	ATCCGCATCCTTCAAATCCACGGAGCCAACCAAGCACAACTCATCCGTCGTCAGACTTT ----- TTCCCGCAAGATTT-----GCTGCAAAACCAGCCTGATTCAATGTGCACTTTAATGTT -----	5405 2171 4631 1357
PDS1_Extended PDS1 bd_1474_Extended bd_1474	GTCAAACTATG-----TGAATCATCCCGTCCTGGAAAGAACGGGATGCCAAGGTGATT ----- GATGGAGTAAGACTCCAAGAGAAGTGTGTCGCCAAAAACATTCAACACCCCATGAAG -----	5459 2171 4691 1357
PDS1_Extended PDS1 bd_1474_Extended bd_1474	GCTACGGCTTGAGGGAGTTCAAACGCAATAACAAGTTGTGCTTCATAGGGAGGGAGCG ----- TCAACGGCGATGAGGTTTGACAGAATTCTGGAACTTGTC---TCTACAGAGTCGTCG -----	5519 2171 4748 1357
PDS1_Extended PDS1 bd_1474_Extended bd_1474	AGTGCCGCTGTGGGGGATGATGAGGTCCAGTATTCCAATTATAAGGTGGTTATGGA ----- GGTG-----AGTAATACACGAAGTCATCAACATACAAACCAAGTGTAGTG -----	5579 2171 4794 1357
PDS1_Extended PDS1 bd_1474_Extended bd_1474	AAGCCTAGGGTGGAGGCTCGGTGTTGTGGCGGAGCAGGTTTGGATGAGAGTACGGGG ----- GTGCCGTGGACCGG-----TGGTACAGATGGATTG---TTAGGGTC---G -----	5639 2171 4832 1357
PDS1_Extended PDS1 bd_1474_Extended bd_1474	TTGTACTTGCAGTGAAGATTGAGGATGTGGATGGTGTGAGTGAGTTGCAGCAGGGG ----- ATGATGTGTCGAGTAAAGAGGGCATGGATCCGA-----TGGATTGGTTGCAAACCCAT -----	5699 2171 4885 1357
PDS1_Extended PDS1 bd_1474_Extended bd_1474	TTGAGTGAGTTGGAGGAACGGGTATGAACGTTAGACTTGCAGCTCAAATGAAGAAGAG ----- CGACA---TGAGGATGGAGCGGATCTTATCGTACCGAGTGACGGGGCT-ACGACGAAGAC -----	5759 2171 4941 1357
PDS1_Extended PDS1 bd_1474_Extended bd_1474	GTCGAAGAGAGTGGTATGAGTGCAAGATGCTACAAG----- CGTACAATGTCTTGTGAGAAGCCAGTATTGCCAGGCTAGCGTCGGATCACCGGATG -----	5796 2171 5001 1357
PDS1_Extended PDS1	-----ATG-----CTCAGCGTGTACCGAAGGATTGATGAAGCTATTGGTA- -----	5837 2171

bd_1474_Extended	GAGGGCGGACGTGGTACTTCGTCAAGTGGCAAAATGCCATTGCAGAAGGCATTTGC	5061
bd_1474	-----	1357
PDS1_Extended	-----AAGCGAAGATCTCGTCCAGAGAACAGATGAAGAAGAGAGCAAAGC	5883
PDS1	-----	2171
bd_1474_Extended	AATCACCTGCTTGAGGACACGACATTGTCGATAGCCAACATG-ACAAGGTACCGGAGG	5120
bd_1474	-----	1357
PDS1_Extended	GAGGGTATCTCAAACCTCCTCACTGAAC----GATGGCCCGAAGACAGCACCTGAA	5938
PDS1	-----	2171
bd_1474_Extended	GAGTCTGA-CGAAGAACACTGGTGCCTAACGTTGAGATTCGACCAAGAGCGATCTCGAG	5179
bd_1474	-----	1357
PDS1_Extended	ACTGGCAACACAAATCGCTTTGCTATTGGGGATCTGCTCTGCGAGGAAGAACATTAT	5998
PDS1	-----	2171
bd_1474_Extended	GTTACCAAGGACAACGATGCGTGATTTGC-----ACGAAGCGGCATGAGATT	5229
bd_1474	-----	1357
PDS1_Extended	TGCTCCGTATGCTGATGC----CTTTGGAGTGGAGAGGTTGACGAGTCTATTCTCAG	6053
PDS1	-----	2171
bd_1474_Extended	CATCCTTTTGATGTTAAGAACACACATGGTAGGTATGGCTTGGGAGCACCTTCTCAC	5289
bd_1474	-----	1357
PDS1_Extended	TTGGTTGCGGATGCTGAG---GCGAAGGAGTTGGCGAGAAGGAGAGTGTGAGGCTGC	6109
PDS1	-----	2171
bd_1474_Extended	GCAATGCCGATATTAACCGACAGTGAGGCGTGGAAAGGTACCCATACTTCAATAGAAC	5349
bd_1474	-----	1357
PDS1_Extended	CGCCGCCGCAGCTGCTGCTGCAGAAGAGGAGGCATCTGAAGCGGGGATGGTGAAGT	6169
PDS1	-----	2171
bd_1474_Extended	CCT-----TTCTTCATAGTAACCTGAAGCCATATT	5382
bd_1474	-----	1357
PDS1_Extended	ACACGATGGCAGTGAAATGATTCAAGAACATCAGAAGAGTCACGGAGGAAACTAAGTC	6229
PDS1	-----	2171
bd_1474_Extended	-CTCGATCGGGATGGTTGTCGGCGAGAGCACGAAGGAGAGTGGCAGGA---C---AATC	5434
bd_1474	-----	1357
PDS1_Extended	TTAAGGTAATATACTGTGTAAGGTAGTACTACACCTGTTATCCGATGGGTCCGGTT	6289
PDS1	-----	2171
bd_1474_Extended	TTGATG-----GAGGTTGATGGCACTGACGTGATGTGCACTGGATCAAACG	5481
bd_1474	-----	1357
PDS1_Extended	GCTTGGCTGTCGAGGTAGGGGGAGAGGTGTCAGCCTCGTCACTGGTGGTTGTAACAC	6349
PDS1	-----	2171
bd_1474_Extended	TGCTACCGGTAGAGGAATGCAAAGG--AATGA-----TGAATGATGACCCGGAAGAA	5532
bd_1474	-----	1357
PDS1_Extended	GCCTTCCTCACGCTCCGCCTCCCCCCCACCAACCACAATCCAAAGCAAACGCCGCCA	6409
PDS1	-----	2171
bd_1474_Extended	GAATGCCTGAAACACATAGATCAGTCCAATTGATGGCAGGTAGGAAGAGCAACCCCCC	5592
bd_1474	-----	1357
PDS1_Extended	CTGCATCGTCCTACCCCTGTTGTC----TTCCTGACAGCGCCACTCTTAAATTGACCT	6465
PDS1	-----	2171
bd_1474_Extended	ATTCCCTTTGCGTGCATTGGATGGCTTATACACAAACGGTATCCATTGTCGGACT	5652
bd_1474	-----	1357
PDS1_Extended	TACACTGCTGATATGCCATCGGTGCCGTATTGATTGAAACGTCGTCCTACGATTGCAA	6525

PDS1	-----	2171
bd_1474_Extended	TACCCAAGTAACCTTGTAGTATTGTCCTCATGCTCATAAGTGTACTGTTCAAGTT	5712
bd_1474	-----	1357
PDS1_Extended	-----	
PDS1	ACATTAAT---CAGAGAACATCAGCTCACACATCATGGCATCGGTGCACGTCAACAACC	6582
bd_1474_Extended	-----	2171
bd_1474	GAAGAAACGGTGGAGGAGAGTGGAGGAGTCATCTGACGAGGGAGCTG-----	5763
-----	-----	1357
PDS1_Extended	ACCGCAATCATGCTTCCGAAACAGGCCAAACAGTCCTAGAACAAAGTCCTACACCCCTC	6642
PDS1	-----	2171
bd_1474_Extended	-----	5815
bd_1474	GAGGCGTTGGGATTAAGTTGGGATGTCCGAGAGGGAGATATAGGCAGTCGT-----	1357
PDS1_Extended	-----	
PDS1	AACATGGTGGAGTACGATTCGAGAACTATGCTCTTACCAAGGTAAGAAATCCGCCTAT	6702
bd_1474_Extended	-----	2171
bd_1474	AGAGTCAT---CAAATTGGATGAGATAGTCAGTGAGAAGGGAGGAC-----	5861
-----	-----	1357
PDS1_Extended	-----	
PDS1	GACTTGCCCAAGTGATCTACGATGCAGTAGTCAGCAGAGTAATTGTAATGATCCTAA	6761
bd_1474_Extended	-----	2171
bd_1474	GGGAGGGGGATGTCCATGACAGTGCCTGGAGGATAGGGTCG-TCGAAGGAAGGAGTGGTGTACGATA	5918
-----	-----	1357
PDS1_Extended	-----	
PDS1	CCTGTTAATCACTGCCATGAACGAATGACGTCTTGCCTTCACCCAGGTATTCCCGAA	6821
bd_1474_Extended	-----	2171
bd_1474	CGTTCTACCGAGTGCCTGGAGGATAGGGTCG-TCGAAGGAAGGAGTGGTGTACGATA-----	5977
-----	-----	1357
PDS1_Extended	-----	
PDS1	ACACTCGACCCCTCCCCAACCGCAAGGCTGGCTCG-----TCTTCGCCACGGCGAAGA	6877
bd_1474_Extended	-----	2171
bd_1474	TAAGGAGCAGAACAGCCCCATCATAGGTGATTGTAGGATAAACCGAAACTGGCAAACG	6037
-----	-----	1357
PDS1_Extended	-----	
PDS1	GGCCGAGCCGGTATTAACCTCCGCCAAGCACGATCCTAGGTTACGTACCGTGGTGTGTCG	6937
bd_1474_Extended	-----	2171
bd_1474	AAACGGATCAA--TACGATAGCTGTCAGGCTCATAGTACTGTTGCTGGATTGTAG-----	6095
-----	-----	1357
PDS1_Extended	-----	
PDS1	TCACTGGTGCCTGATTGTGTATGAAGG---GAGCGCGTGTGAGTTTGATCAATA	6994
bd_1474_Extended	-----	2171
bd_1474	ACCCGAATAGCATTGGATGTAGTGGAACGACCGATGACGATACCATCCATCGTATGAGCC	6155
-----	-----	1357
PDS1_Extended	-----	
PDS1	TGATTTATCCAA-----GATGCCACTGTGTCGCCATG-----	7026
bd_1474_Extended	-----	2171
bd_1474	TGATTCTAGAACGAAACACAAGAGCCGTCTTGTGGAGTAACAGACGGAGAAG-----	6215
-----	-----	1357
PDS1_Extended	-----	
PDS1	-----	7079
bd_1474_Extended	---GCGATCGGTGTAAAGTGAAGGATTGT---CCATTAGACACATCAACGAAGCGGAT	2171
bd_1474	-----	6275
-----	ATAGGGATCCAAGTACGCTGATCAGCTTCACCGTGTACGAGCATGAAGGGTGTGCT-----	1357
PDS1_Extended	-----	
PDS1	CGGTTGGAGTGTCTTTACAGTCAGGGATTCTGCATTCAAGGTCCATTCTGCAGGTAT	7139
bd_1474_Extended	-----	2171
bd_1474	AATTTACCGTGGAACTTT-----CCTGGAATCATG-TTCATCATGCG---AG-----	6318
-----	-----	1357

PDS1_Extended	AGGCACGTGAGGAGGGAGAGGGCCGACTTGCCAGTGGTGGCTGATTTACATTGGGTTG	7199
PDS1	-----	2171
bd_1474_Extended	CGGCATGAGAGAT-GGAGTGAACCAAAAGCAGCGCGCATTGTTTCAGTGAGGTAAC	6377
bd_1474	-----	1357
PDS1_Extended	AGTCAAATGCAAGCTGGGAAGGATGGAGTGTCTGGCTGTACGACGACCTGCTCCGAAGCCA	7259
PDS1	-----	2171
bd_1474_Extended	GCA---CGAGACATGTGAACCACATCACC-----TTCCAATGGCTTCAACCAAACCG	6425
bd_1474	-----	1357
PDS1_Extended	AATGAGTTCTT-----CA---AAGTTAGTTGTGTAAGCACTTTTGAGTG--GGGAG	7307
PDS1	-----	2171
bd_1474_Extended	TTGGAGGACTGGCGCCCTGCAGGAGCGGAATAATGTTGAATCTTGTCTGGAGGTAAC	6485
bd_1474	-----	1357
PDS1_Extended	TGTCCCTTGG-AGATGGATGTCACTTGCTCATG-----	7341
PDS1	-----	2171
bd_1474_Extended	GCTCGGATGGCAGTACCGAAGAGCTTCGTCACAGTCACAGCAGAAAACATTGGCGAAA	6545
bd_1474	-----	1357
PDS1_Extended	-GGGAGGCAGAGTTGAGGAGGCCAGGGCAAGAACCGACGAAGACTGTGGGGAGGATGGG	7400
PDS1	-----	2171
bd_1474_Extended	CGGCCGGCTTCACTCCTGAATTGTTGAAAGCAGCGATGATGTCAGTGGAGAGCGAG	6605
bd_1474	-----	1357
PDS1_Extended	GAAATTGCGGAGAAC-----ATGTTGGGACGCAGGAGACGACTACGGTGGATTAT	7451
PDS1	-----	2171
bd_1474_Extended	CGAAGACCAAAGACCCAAGTGTATCTGGTTGCTCCATCTGCGAAGACAAGAGCATA	6661
bd_1474	-----	1357
PDS1_Extended	TATCAGGGTGGAGCTGCCGGTGGGGTAAGCCAACG-----CCCATTGGAACCCGAG	7505
PDS1	-----	2171
bd_1474_Extended	CATCGTGCCACCAAGGGCAACCCATCACCAAAACCAATGTCAACATGAAC	6712
bd_1474	-----	1357
PDS1_Extended	AATGCATCATTCTTATTCTGCCGGCGCGACCTATCGT-----ATTGTGCCATCTC	7558
PDS1	-----	2171
bd_1474_Extended	GATGTCCAATACCTG---TAACGAGTACGATCGATTGGGTACCACTGGCTTGCCTTGG	6769
bd_1474	-----	1357
PDS1_Extended	TACTGTCGAATGAATGGATGGTACAACGAAAGCATGCAGAGGAATCAAC---AAAGC	7615
PDS1	-----	2171
bd_1474_Extended	TATAGTAGCGTACGATCCAAGAGCTAATGGAAACTCACCGAAATCCGTCCACACTCCATC	6829
bd_1474	-----	1357
PDS1_Extended	TCATGAGGGTGGAGACAAGTCATGTTCTTACAGTTGGGATTCCAACCCACATTCA	7675
PDS1	-----	2171
bd_1474_Extended	GCGAGAAAGTTGGAGAAGGTGCTTGAGTTCTGAAACGACGGC---AACCAGTGATA	6884
bd_1474	-----	1357
PDS1_Extended	GGGGGCAGCACTGCTGACTTCCTCCGCATCGTAT-----GTTGAATCGGCAGATCACAA	7729
PDS1	-----	2171
bd_1474_Extended	CGGTGGAGTTCCCTCTGCTGACCAATGGGTTTGGTGTCACTCCATTGGCGTGTACAT	6944
bd_1474	-----	1357
PDS1_Extended	ACAACCAAAGAACGGAGCTCCTACAAACGCCAACGCAAACAAAGATGGAGCATCTGCTA	7789
PDS1	-----	2171
bd_1474_Extended	GGACGGATGGGA-----GGAGGAGACGTACCGGGATGGTGGATGAGGCGG	6989
bd_1474	-----	1357

PDS1_Extended	CCGATCAA---GTGTGAATGGT---ATCGTACTTGTGAGCTGCCCATCTCACTGCATT	7843
PDS1	-----	2171
bd_1474_Extended	AGGATGTCGGTGGAAATGGTGGAAAGGAGCCGAGGTGCTGCGATACGGGCTTGCA	7049
bd_1474	-----	1357
PDS1_Extended	GGAAGCTGCTCCCGATCTCTGCTTCCCACATCAACTACACAATTCTGTCAAGATATGAA	7903
PDS1	-----	2171
bd_1474_Extended	ACAAGTGGGATGC---GTTGTTGATCTCATCAGGAGCCAAGTCAGACATTGAA---	7100
bd_1474	-----	1357
PDS1_Extended	GCTCTAAAATGGGGAAAGCAGTGATGAAGGCAATTGGAACTCGCCTCTTGTACGTTGA	7963
PDS1	-----	2171
bd_1474_Extended	-----CGAGGC-----CT-GAGTTGGAAGGAGGCTGGGTGTCAGGTGGA	7139
bd_1474	-----	1357
PDS1_Extended	CGAGTCATGGAATGGAGGGACTACGATGAAATGGCGGGAAAGGACTCACGTCCCTCC	8023
PDS1	-----	2171
bd_1474_Extended	A-TGACATGTAGTACCGCGGAGATGACGAAGTGGCTGCATTGTCCACA-----ATG	7190
bd_1474	-----	1357
PDS1_Extended	GCCAGTGGGAGATGCAATATTGACAGACTTCGTTGTCCTTGCCGGAGGAGGT---GTC	8080
PDS1	-----	2171
bd_1474_Extended	GCAACCGGGCGAGCAGAGA-CCCGAGGCTGAGCGTAATCTAACCTCGAAGCGATGACGTT	7249
bd_1474	-----	1357
PDS1_Extended	GTGGCCTACGCTTCCA-----GGTCCGGGTTCATATTGG-GTGCAACTCGCAGACTA	8133
PDS1	-----	2171
bd_1474_Extended	GGTGCCTAACGGTTCATATAAAAGATGACAGTCAAGGTTGTTGACAGTGAGAATGAA	7309
bd_1474	-----	1357
PDS1_Extended	TGGATGAATGTTAGGAAGAGGATTGTTGGCTACCAGCTATGAAAGGTGAGACTTT	8193
PDS1	-----	2171
bd_1474_Extended	TGAAGGAAAGTAGACATACATACCCCCCATGTCAGCGTCACCAATGAAACCGCAGC	7369
bd_1474	-----	1357
PDS1_Extended	GTTGGGA---GGGCACAATGTAGTTGAGACTATTCCTTAAT-GCTCACTGGACTCG	8248
PDS1	-----	2171
bd_1474_Extended	CTGGAGTAAGTGAGACCGGAGACTGTAGAGAGGATTGCGAAGAGCCGAAATGCA	7429
bd_1474	-----	1357
PDS1_Extended	TTTGCAAC-----TATTCTCTAGATTGCTGCTGCAGGTATCCGACCAG-----	8292
PDS1	-----	2171
bd_1474_Extended	GTTCCGAACCATAATCTCTTCATTGAGAGAGAACGGCAGTACCCACCCACAGAC	7489
bd_1474	-----	1357
PDS1_Extended	--GCTCTCCATCTT-TCTCTACAACGTCAGTGAACGTCTCATCTTGGATCTTGAAG	8349
PDS1	-----	2171
bd_1474_Extended	TGGAGCCAACGACTTGTCTCCATGCGCACCTGCAG-GTGAGTGTGGTTGTAGGAGA	7548
bd_1474	-----	1357
PDS1_Extended	CTCTTACACCGGCTATCATGAACATGGAACCAAAGGCATTCTCAAAGAACCTAAAGCTC	8409
PDS1	-----	2171
bd_1474_Extended	CAAATACCGACTTGTCAAGGAACATGTGA-----TCAGTCGCACCAGAGTCAG	7596
bd_1474	-----	1357
PDS1_Extended	AAACCTCACCTTCCCTGTACAAATCCGTGTACGAATCAGTTGGAGTGTCCCTCCGTCC	8469
PDS1	-----	2171
bd_1474_Extended	CAACCAAAAGTGTGAGGATG---GAGTGGAGGTGGTGTAGTGGCTGGTGTAGTGTCC	7652
bd_1474	-----	1357

PDS1_Extended	ATGAC---G-----ACGATCCAGCGTTGA-----ATGATGTGTTG	8501
PDS1	-----	2171
bd_1474_Extended	GAAATGGAGCCCTCCAATAAGAGACGGACCAGTAGGGAGGCCAACACAGTAGTGGTG	7712
bd_1474	-----	1357
PDS1_Extended	AGAGCTCGTGTGGCGGAAGAATTGGACACTGACGTTGCACAGTCGGAGGCATTGGCA	8561
PDS1	-----	2171
bd_1474_Extended	GAGGACGATGCCGATGGAGGAGATGGACGAATGGGAGAAGGACAAGAAGGGCAGTGGAG	7772
bd_1474	-----	1357
PDS1_Extended	AGTTTGATTGCCAACCAATGTGGGGCATTGAGTTACATGACAGAGTATGCCGTAGTATT	8621
PDS1	-----	2171
bd_1474_Extended	GAGACAATGTACTTGGAACTGGAGTCGTTATGTTAGCGACAACA--GAAGCATAAGAGG	7830
bd_1474	-----	1357
PDS1_Extended	GAAACCGAGACAGTTGAACGTTGCA--GCTCCTCCAATTGCATTGCCCTCGTAAAATT	8678
PDS1	-----	2171
bd_1474_Extended	CAGACGAAGTCGTATGATCTATAACAGCCTCATGCCATCCAAAGCAAAGTCATTGAAC	7890
bd_1474	-----	1357
PDS1_Extended	GGAACGGCTTAAGGGGGACAATCTGACTGTTAAAAGTACACATGAATTGATATTTAA	8738
PDS1	-----	2171
bd_1474_Extended	CCTCAGGCCTCGAGTACCCCCTATCGTCC----GCACCAGATGACG----CGGTAA	7938
bd_1474	-----	1357
PDS1_Extended	CGATACTTCTTGTCTCCTCAGTATTACAATATATGCCATGCTTCGAAAGAGCTTATAC	8798
PDS1	-----	2171
bd_1474_Extended	CCTGACTGACAG----CTGGCTGTGCTAGACAGTAGGTTGGACAGCAGCAGGTTGAGCGGA	7993
bd_1474	-----	1357
PDS1_Extended	A-TAAGGGAATGTCCACACTCGTCAGTGCCCATCCATGAGATTGAAGCCG-----	8847
PDS1	-----	2171
bd_1474_Extended	AGAAGAGGGAGGAGGTGAAGGGTCAGTGACAGTAGGTTGGACAGCAGCAGGTTGAGCGGA	8053
bd_1474	-----	1357
PDS1_Extended	GCAACACTTTAAATTCATCTGGCAAAACCTGCATCGTGTGCTGTCACTGAAAT	8907
PDS1	-----	2171
bd_1474_Extended	GGGAAGAGACGACTTGCCTCGCGAGTGACGGTGA----GATGTGCCTTTTCAGCAAC	8108
bd_1474	-----	1357
PDS1_Extended	GGGTCTGGAGTACTTCTGCTGCTACCTCAGCTTGGTGTTCGTTAGCTCCA	8967
PDS1	-----	2171
bd_1474_Extended	TGGCACTTGTGATGTTGTGACAGCGACGTGCGATGCA--GATGCAGTTGGACTTCTGA	8166
bd_1474	-----	1357
PDS1_Extended	GCAGCGAGGTAAGCTCTT-----CGGGTACAATAACTGGGAATGATATTGGA	9015
PDS1	-----	2171
bd_1474_Extended	GAAAGAAGGCAAGAACGTCCCTGCTTGAGGGCACCAATCCACGGAGTCTGA	8226
bd_1474	-----	1357
PDS1_Extended	AAAGAG---AACGGAGCGTGTGGAGAAGAGGGTGTGATGCTTGACGGGTCG	9071
PDS1	-----	2171
bd_1474_Extended	AGGTTGAAGGGGCCTGGCTACTGGAAGGAGTGGTGGAAAGCTGCTGCAGCTGCAGGAGCAG	8286
bd_1474	-----	1357
PDS1_Extended	CAGAGCACTCGGCAGAACTCCCTCACACCCCTCGGGAGTTATGTTCTCGCTTGTGACGTG	9131
PDS1	-----	2171
bd_1474_Extended	GAGCAGGAGTAGCCCGGGCAGATCGAGTCCCAGGAGCATCGG-----TCGAACAAGG	8338

bd_1474	-----	1357
PDS1_Extended PDS1 bd_1474_Extended bd_1474	AGTATTCTAATGTGTGTTACCAACCAAGCTAATTGCCAATCCCCTCAATACTTCATTG ----- AGCCCGATCAAACCTCTGGACAAGATCAGACACCTT-----AGACATTGTCATGGAGTC -----	9191 2171 8392 1357
PDS1_Extended PDS1 bd_1474_Extended bd_1474	GTAACCGCGTTGCAACCGAGATCGACAACCTCTAGCAATGTGTGGTTACTTGAA----- ----- G---AAGGAGAGCTACCAGAGCGAAA---ACGGTCAATGAGTGGCTCGTATTCAACGAC -----	9247 2171 8446 1357
PDS1_Extended PDS1 bd_1474_Extended bd_1474	--GACCGTCGACAACAACGACTGCAATCCAGCTGCAGTAAGACTACGATTGTCGGATAA--- ----- AAGACCCATTACAAAGAACATGACCTGAAGTTGGAAGACACCAATTGTCGGAGGAGGA -----	9301 2171 8506 1357
PDS1_Extended PDS1 bd_1474_Extended bd_1474	---ATCGAGA---CGCCTCAACTGGAGTTGGTTATTAATCATTGTCATGCAAGCA ----- AGTACGGAGGAACATCCCCTCCAACCGAGATTGGTAGGAAGTGACTGGTCCGACAC -----	9353 2171 8566 1357
PDS1_Extended PDS1 bd_1474_Extended bd_1474	TAGCTCGTCTTCAAACGTGATTGCTTGATACCACAAGAGTCTCCATTGCTGTGGAT ----- -----TTGGCGGTTGTTGGTAAATCACGGAGAATCTCAAATGTAACCATATCAT -----	9413 2171 8616 1357
PDS1_Extended PDS1 bd_1474_Extended bd_1474	TTTGCAGTATGGAGGACGAAAGAACGCGTGAACATCCTCGCTGTCGCTCTCCGTTG ----- CAC-----ACGGAGAGAAATGGTTGT-----TGATTGCATCAACCCTCAAATCCT -----	9473 2171 8663 1357
PDS1_Extended PDS1 bd_1474_Extended bd_1474	TACCGAGAGTTAAAGTCTTCAGGTTGTGTTGCAGCGAGCCCATTGCCAAAGACAGAA ----- TTGCCATCATACAATC---AC-----CCTGTTCGCAAAGAGCAACT -----	9533 2171 8703 1357
PDS1_Extended PDS1 bd_1474_Extended bd_1474	GTGATTCGTCGTCAAGACCACAGCATGAGCGTTCAATTCTTCAACGCTGAATTGGCA ----- GTGCCTCGGAGCCATCGACA-----	9593 2171 8723 1357
PDS1_Extended PDS1 bd_1474_Extended bd_1474	TAACTTCTGAAAGCGCTGCCAACCAACTGTTTATATCAGGATTCAAGCTCATAGTCA ----- -----AGGCAGGTGTGTACCTTCAAACCTCC -----	9653 2171 8747 1357
PDS1_Extended PDS1 bd_1474_Extended bd_1474	ATGTTTCAATGTGAAATTGCTGCTCAACCATGTGATAATGCG-----GCAATA ----- AGCTGACGACTCTGAGCAGCGTTGCAACAGTGGTGAACAGAGGGTCACTTGAGGAGACA -----	9703 2171 8807 1357
PDS1_Extended PDS1 bd_1474_Extended bd_1474	TCTTCATCCGTCAAGCCCCAGACGAGATGATGATCAGGTGCTCCACTGTGAAAGTACTCAA ----- TTGTAGTAGCTGCGGAGGAAGAACGAGTGCTGAAGATCCAAGAGGGAGTAAGAAG -----	9763 2171 8862 1357
PDS1_Extended PDS1	GCAGATGCAAGTGACTGCCATGTTCT-----TCACCGTTGAGAACAAAGCAATTGCG -----	9814 2171

bd_1474_Extended	AGAGATCCGAAAGTTCGGAAGCTCATACTTACGAGCTTGAATGGCATCGTAGAGGGAGA-----	8922 1357
PDS1_Extended	--AGGTTCAATGTTGCAGTGTGAGTTGCCACTCAAACCACAGAGAGCATTGATATT-----	9872
PDS1	-----	2171
bd_1474_Extended	GCTGGTGTATGGAGACTGAATCAAATTGGTGGTAGAG-ACCTCGAGAGCAAGACCCCTCC-----	8981 1357
bd_1474	-----	
PDS1_Extended	CATCGTCATTCATCTC-----A-----TTATTGCTGAGGTCAAGCCG-----	9909
PDS1	-----	2171
bd_1474_Extended	AATTGGCCTCCTCAGGGCACACAATGACAACAGAAGCGGGATGGTCGAAGGCCACAGTG-----	9041 1357
bd_1474	-----	
PDS1_Extended	TTTCAATTGGAATTGAGCTTTCAGCATGTTAGATACTCCGTATGAGTACACAGTA-----	9969
PDS1	-----	2171
bd_1474_Extended	CTAGAACCGAAGGTGGAGCCGGCGAGGGTGCAGGATGACCGTTAGAAGGG-----	9092 1357
bd_1474	-----	
PDS1_Extended	TGAACGATTGTGAGCGAGCTTGCATCAGAGAGTACTAATGTTCAAGAGCCGAAGCTGT-----	10029
PDS1	-----	2171
bd_1474_Extended	GGGAGGATAGAGGAAGAACATCAATG-----TCGTCCACCTCATCATCGAATCGGA-----	9145 1357
bd_1474	-----	
PDS1_Extended	CAATCCATTAGACAGGGCACCAATC-----CCT-----C--TACCATCT-----	10066
PDS1	-----	2171
bd_1474_Extended	CCCCCCATGATCGCGGCAAGACTCTCGATGCCAATGCTGAGCCGCGACGCCGTGT-----	9205 1357
bd_1474	-----	
PDS1_Extended	GAAAGGCTATCTTGATTGTAAGCGTTCTCATATTGTTACTGGAAAGAAGAGTCTCA-----	10126
PDS1	-----	2171
bd_1474_Extended	ACGTTGTGATTCTCTCCGAGATTGATAAGATTGTTGTATAACGCCGATGGAGG-----	9265 1357
bd_1474	-----	
PDS1_Extended	ATTGCTCGCAGTTTCTTCGACGTAGCTACCCATCACAGAGAGACTGGCTAGATTG-----	10186
PDS1	-----	2171
bd_1474_Extended	CTCCA---GCTGAACCCGGGCCGCAGAGGACAAGATGACACTGAAG-TGCGTCCACTG-----	9320 1357
bd_1474	-----	
PDS1_Extended	GGGTTGGCAGCCAATGCCTCTATTATAAGCCTGTTGCTTCGTCGGTACGAACAATACGT-----	10246
PDS1	-----	2171
bd_1474_Extended	GAGGGGGTAG-----ACCGAAGGGAGC-GGGCAGGCGAGAAACAACAAGT-----	9363 1357
bd_1474	-----	
PDS1_Extended	ACCT-----CCCATTGATGTTGGTGAATATTCACACGTTTCAGGGATGTG--TTTCCTAG-----	10299
PDS1	-----	2171
bd_1474_Extended	GCTGAGGCACGAAGTCGTATCAGGAGGATCCACGCCAAGCCGAGAAGGGGGCTGAGTGG-----	9423 1357
bd_1474	-----	
PDS1_Extended	GAGCATCGATGCAATACATGATGGATGAATGACAAGACATTCCCAAGTCGAGTCGGT-----	10359
PDS1	-----	2171
bd_1474_Extended	AAGGAAG---AGGACCGAGTTGATG-----CAGAACGCTCGCAGAGAAGCCAAGTAGGAG-----	9474 1357
bd_1474	-----	
PDS1_Extended	AAGATGCCCGTCTCGAACAGGGGCTCAAGTTCTGACCAATCAGCTCCGATAAGCACCT-----	10419
PDS1	-----	2171
bd_1474_Extended	GAGACCGCATGGGGTTGCGTGAAGGTGTATTC-----CACAGCCACGGAAAAGGATG-----	9528 1357
bd_1474	-----	
PDS1_Extended	GCATAACTGCAGCCTTATGATTGATCTGTTGCGA-----GATACCCCCT---CACAAAAG-----	10471

PDS1	-----	2171
bd_1474_Extended	ACTGAGAGGGATGGTCATACTCCCTGCTGAATTGGCGATGCAGGAGAGAGACGAC	9588
bd_1474	-----	1357
PDS1_Extended	-----	10531
PDS1	-----	2171
bd_1474_Extended	CCTCATGGAAGATGACAGGGCTACTCTGGAGGAGATCGCGAGAAGGTGACGGGTGCAC	9648
bd_1474	-----	1357
PDS1_Extended	-----	10583
PDS1	-----	2171
bd_1474_Extended	CAATTGGCGTCTGTGAGGAGATGGCGACGGTGCCTGTGTCAGGGAAAGTGGCGATCG	9708
bd_1474	-----	1357
PDS1_Extended	-----	10633
PDS1	-----	2171
bd_1474_Extended	CAGGTGTG-AGTGATGACACATCCCGTGTCCCTCAAGGTAGGAATGAGAGATAGGGCATCA	9767
bd_1474	-----	1357
PDS1_Extended	-----	10693
PDS1	-----	2171
bd_1474_Extended	GGGTGGAGGGATCAGGGCAGAACAGCTGCCGATAAGACCAGCACCGTCGGAGGGGTG	9827
bd_1474	-----	1357
PDS1_Extended	-----	10753
PDS1	-----	2171
bd_1474_Extended	GACGAAACGAGATCGGTGAGCAAATCTCATCATAAGATGCCGTGAGCCTCGCTATTG	9878
bd_1474	-----	1357
PDS1_Extended	-----	10808
PDS1	-----	2171
bd_1474_Extended	CTCAA-----GAGATCTCAACCGCGTTGAAGCTATCCATTGTACTAGTTCTAGACGTCA	9936
bd_1474	-----	1357
PDS1_Extended	-----	10837
PDS1	-----	2171
bd_1474_Extended	AAG-----TGAGCCGTTGTGGTTGAGTATC-----GGTA	9996
bd_1474	-----AGGAAGGATAGCGAGATAACGGTGCTGCCATTGGAGGGGAGCACCGTCTCGTCGGTATC	1357
PDS1_Extended	-----	10896
PDS1	-----	2171
bd_1474_Extended	ATCTTG-GGCCCGAATCCGTGCAGGGGAAGGAATGGAAGGGGACCGTGTGTGAAGAAA	10051
bd_1474	-----AAGTTACCGCGCTCAATTGAGGTTCACTGAGGTTAGT-----TTATGGCTA-GTTTACGAAC	1357
PDS1_Extended	-----	10956
PDS1	-----	2171
bd_1474_Extended	GATACGTTGTTGTCTCCTCGTAATATCGTTACCTGTAGAGGGGCTATATGTAGAGACA	10111
bd_1474	-----AGAAACGAATGCCAGCATCTGAGAACTCAGTCAGTCAAGTCTAGGACCTACGAAGGACAGACA	1357
PDS1_Extended	-----	11016
PDS1	-----	2171
bd_1474_Extended	GGGTGGCGCGGAGAGGGG-----GAGGAGAGGAGAGATGTTGCCCCCTTA--ATG	10161
bd_1474	-----	1357
PDS1_Extended	-----	11063
PDS1	-----	2171
bd_1474_Extended	AAACACACACTTAAAGGAAACTTATTGTACCCATACAATAGAAATAATTATATTAG	10221
bd_1474	-----	1357

PDS1_Extended	TAGACAATTTATGGACACGATC-TCCCCACGGTGCTCGTGTCAAGCAAACCG-CAACGAAC	11121
PDS1	-----	2171
bd_1474_Extended	GGGATTAAAATGGACAATAAGATGGATGCCGAGTTCATAACCAACAAAAAAATGGTAC	10281
bd_1474	-----	1357
PDS1_Extended	CCTCT-CTT--CCGTTCCCTACCCTCCCTCCACGCCACCACTAACATGTCG	11178
PDS1	-----	2171
bd_1474_Extended	CCTTCACCTTCACCCCTGCTGCTCATCCTCCCTATGCAAT----CGACTCGAATCTTCA	10336
bd_1474	-----	1357
PDS1_Extended	ACCCCCTCCCAGCTCCACA----ACCCCAAAGCAGTATGGTTCTCGGTGCACCAGTCT	11233
PDS1	-----	2171
bd_1474_Extended	ATGGCCTACTTCATCAGTAAGCATGGCGACATCACATCTCTACGTGAG---GT	10392
bd_1474	-----	1357
PDS1_Extended	CCAAAGCAATAGCTGCATCAACCGCTGCGATTATGTGTTGGCGGAGATGAACAAATGGC	11293
PDS1	-----	2171
bd_1474_Extended	CGAGCCCAAGTCTTG-ATGTCCGAGGAGGAAGTCAATGT----GGCTCGGAAGGTGGC	10445
bd_1474	-----	1357
PDS1_Extended	ACGAGGCTTTGTGTTGGTGAGTGGTGCATGTGATCTGTGTTAG--GGATGTGGCGTT	11351
PDS1	-----	2171
bd_1474_Extended	AACAGTCAGTGGATTGGG----GTAATTGATCTTCGTCAGAAGCTGAACCCGAT	10496
bd_1474	-----	1357
PDS1_Extended	GCTATTGAGCT-----TGTAGTTCTGAAGCCGTTGTTGTTGTCTTTC	11396
PDS1	-----	2171
bd_1474_Extended	AGTATTACGTTGGTCCAAGACAATTCAACAGTTACTGAAAGAGCTGTATTGCTCTGAT	10556
bd_1474	-----	1357
PDS1_Extended	TAATT-AA--TGTCACAACCTCTA-----GATACCT	11424
PDS1	-----	2171
bd_1474_Extended	ACAAGTACCGTCATCACAGCTGTTGGTAGTGAAGCTGAAACGATTCAACAAACAGCAGCT	10616
bd_1474	-----	1357
PDS1_Extended	CCAAGATATTGACCAGGCTCAGTTCTACAGAATCTTGCAATTGACGTTGCGT	11484
PDS1	-----	2171
bd_1474_Extended	GCCTTCTCCATTGGCAAGCTCAGTTCAACCATAATCTGTGATATCCTATGACTTT-GA	10675
bd_1474	-----	1357
PDS1_Extended	CGATTGGAGAACTCGTCTCGGGTTGTTGGCTCTGTGTCC---TTTGATGCGTCGATTT	11540
PDS1	-----	2171
bd_1474_Extended	GCATGGGA--AGACAGTGGCATCGTACACTGGGTGGCAGCAAGTTGATGAATTGTG	10733
bd_1474	-----	1357
PDS1_Extended	GAACGTGAGGTATGTTACGTT---TAACTTATTGATATCCGCTGAATTGCAATTGATTCT	11597
PDS1	-----	2171
bd_1474_Extended	GAT-GGAATGCGAGAACGGTGGAACGAACCTCATGCACAAATCAATTGGTACTTGTCT	10792
bd_1474	-----	1357
PDS1_Extended	CTTGCTTGTCTTCAACTCATACGAAACGTATCCAC---TTCTTCACTCACAAGATGGG	11654
PDS1	-----	2171
bd_1474_Extended	CGAGCCTTCTCGGGAGCTGCAACATCGTCTTCTTCTGCCTCCCTCAAGTACTGA	10852
bd_1474	-----	1357
PDS1_Extended	TAGCAGAAAGTTGGTCATTCTATCAGTCAGTCCTCTCAACGATATTGAGTT	11714
PDS1	-----	2171
bd_1474_Extended	TGATAAGGAGAGCGAGGAAACAAACAAACGAAACCTGGGGCATTGCAAACACGGTGGCGTT	10912
bd_1474	-----	1357

PDS1_Extended	GGTATT-CTTCAATATATTCTTGACACAGAGCGATACTCCGGTCCATATCCACAACCTGG	11773
PDS1	-----	2171
bd_1474_Extended	GGGTCTCACAGCACACACTGAATG-----GAAT-----ACCAC	10945
bd_1474	-----	1357
PDS1_Extended	GGGCAGTCCTTGCAATGTATCACAAATTCGCACCTCGGCTGCATCCTAAGTTCTGGAG	11833
PDS1	-----	2171
bd_1474_Extended	GGGCAGAGATCACCTTGTG-----AAAG---GC---TGGTGACATACTTCAGC	10989
bd_1474	-----	1357
PDS1_Extended	TGCTAGGATACGACTTCTCTGAGAAGTCACTCACGTATGGTTATGTGCTCA-AGTGATT	11892
PDS1	-----	2171
bd_1474_Extended	TGGGAGGAGAACAAATACGC-----CAATATCAATCCATTCAAGGTGGAC	11036
bd_1474	-----	1357
PDS1_Extended	CTTTCGGGTGGTTGAGCACGGCTATCCCTACAATCTTGGCTCATCTCGGGTATGCTT	11952
PDS1	-----	2171
bd_1474_Extended	GTTATTGGTGCTTGG-GATAGACAG-----AAGGAGCATAGTGAATCAGATG	11082
bd_1474	-----	1357
PDS1_Extended	AGTGTGAGCCTCAGTCAGCAGGAGCTACCAAGAAATCGTGTACACTGCTGCTGGAACCTTT	12012
PDS1	-----	2171
bd_1474_Extended	AAAA-----CAAGCAAAGCAAGCTAGACGAC---TCCA---CGATGAAGGTAATCTT	11128
bd_1474	-----	1357
PDS1_Extended	GG-----TAAAGCATTGTGGACGATGCACCCGCAATCATGATGGCACGGACAGTACA	12065
PDS1	-----	2171
bd_1474_Extended	ACGCCATGCCGAGTTGTTCAAGCTGACGTTGGTGCATCACCT-----CCAACAAA	11180
bd_1474	-----	1357
PDS1_Extended	GCGT-GGAGGAAGGAATCAGCAAAGACGAGCTTCCACCGGTGCAAGGGGAGGAAGGGATG	12124
PDS1	-----	2171
bd_1474_Extended	GAGTCATTCCAAGCTGTCACTCAAGAGGTGTTGAATCTGTTGGTGGAAAAGGATGCTTG	11240
bd_1474	-----	1357
PDS1_Extended	C-----CACGGCGGGA-----G--CTC-----	12139
PDS1	-----	2171
bd_1474_Extended	ACTTTCTCTGAGATACTATGGTCGTTGACTACTAACCTCTCTGATATATCCCTTG	11300
bd_1474	-----	1357
PDS1_Extended	-----CGGCAGCGGCACCTCCTGCTGTGCAGCCTC-----CT	12171
PDS1	-----	2171
bd_1474_Extended	TCTATTCTTGCAAACACACTCAATCATCCCACGCTGACATGATCTCGCAAAGCT	11357
bd_1474	-----	1357

### Peptide Alignment (62.9% Sequence Identity)

PDS1	MIITNFILSTVLATSMAFQPHTPILSKPSFSNRVHRSPKIGSSNLV---MKDFP-KPNVE	56
PDS2	---MKFLPLLPALVAGAFSI-THLSQHPSLRLMHQSLSTSLYSSSSSTSQRPRRPTPDRIR :<*: * : *..: **. * : .: **: : * ..: **. * ..	56
PDS1	DTDNRYRAEAMSTSFKTSL---RVTNDSQKKVAIIGGLSGLSCAKYLSDAGHEPTVYE	113
PDS2	NTQNFKEAKELSQKFITDFQQLQVKGSPEPKRVAIFGGGLSGLSCAKYLSDAGHIPTLYE :<*: * : * : * ..: : .....: *:****:*****:*****:***:***	116
PDS1	ARDVLGGKVSAWQDEDGDWIETGLHIFFGAYPNVMNMFAELGIHDRLQWKIHQMIFAMQE	173
PDS2	ARGVLGGKVSAWQDEDGDTVETGLHIFFGAYPNIHNLFGLKIQDRLQWAPHRTMFAMQE **.*****:*****:*****: *: * ..: *: * ..: *: * ..: *	176

PDS1	LPGEFTTFDFIPGIPAPFNFGLAILMNQKMLTLGEKIQTAPPPLPMLIEGQSFIDAQDEL	233
PDS2	LPGQFTTFFFPAGVPAPLNMAAAILGNTEMLTLEEKIKMVPGLLPMLLEGQSFIDEQDEL ***:****: * * :****: * . *** * :**** * * : . * ****:*****:****	236
PDS1	SVTQFMRKYGMPERINEEVFIAMAKALDFIDPDKLSMTVVLTAMNRFNLNESNGIQLQMAFLD	293
PDS2	SVLQFMRKYGMPERINEEIFIAMGKALDFIDPDLLSMTVVLTAMNRFINEADGSQTAFLD ** *****:*****:*****.*****:*****:*****:*****:*****:*****:*****	296
PDS1	GNQPDRWCTPTKEYVEARGGKVKLNSPIKEIVTNDDGTINHLLLRSGEKIVADEYVSAMP	353
PDS2	GNPPERLCQPMKESIEKKGGEVVCNSPVVEIQLNEESNVKSLKLANGTEITADYYVSAVP ** *: * * * * : * : * : * ***: * * * : * : * : * . * : * . ** ****: *	356
PDS1	VDIVKRMLPTTWQTMPYFRQLDELEGIPVINLHMWFDRKLKAVDHLCFSRSPLLSVYADM	413
PDS2	VDVFKRLVPTQWSTMPYFRQLDELEGIPVINIQIWFDRKLNSVDGLCFSRSPLLSVYADM **:.*: * * . *****:*****:*****:*****:*****:*****:*****:*****	416
PDS1	SVTCKEYEDPNKSMILELVFAPCSPPIAGGNVNWIGKSDEEIIDATMGELARLFPTEIANDD	473
PDS2	STCCEEYASNDKSMILELVFAPCSPPEAGSPLNWIAKPDSIDIATMKELERLFPLEIGPDA . *: * . :*****: * . :*****. * . :***** * * * * . *	476
PDS1	KWPATKMQGPNGQAKLEYAVVKVPRSVYAAIPGE-----	508
PDS2	PE-----EKRANVVKSTVVVRVPRSVYAAVPGRNKYRPSQESPIENFIMAGDYATQKY . :*: * :*:*****:***.	528
PDS1	----- 508	508
PDS2	LGSMEGAVLSGKLAEEVICDKFMGRAERKGVKEVHSSVLTQIEERTPAGIAMEKGRVSP TSYGGGQQGGFENP 602	588

## 2)β-carotene hydroxylase, BCH

Plant and Green Algal BCH Sequences (non-heme di-iron):

*Vitis vinifera*, GenBank accession number AAM77007.

```

1 matgisasln smscrlgrns ftatgpssvi slssfltpvt hlkggnifplq rrrslkvclv
61 lekeiedgie ieddspessn raserlarkk aerytylva mmsslgitms aivavyyrls
121 wqmeggeipv lemlegtfals vgaavgmefw arwahkalwh aslwhmhesh hrpregpfel
181 ndvfainav paisllsygl fnkglvpgle faglgitvf gmaymfvhgld lvhrrfpvgp
241 ianvpylrkv asahqlhhsd kfngvpyglf lgpmeleevg gmeelekeis rrikssdss

```

*Haematococcus pluvialis* (*Haematococcus lacustris*), GenBank accession number AAO53295.

```

1 ittmlsklqs isvkarrvel arditrpkvc lhaqrcslvr lrvaapqtee avg tqqaaga
61 gdehsadval qqldraiaer rarrkreqls yqaaaiaasi gvsgiaifat ylrfamhmtv
121 ggavpwgeva gp1llvvvggq lgmemaryya hkaiwespl gwllhkshht prtgpfeand
181 lfaiikglpa mllctfgfwl pnvlgtacfg aglgitygm aymfvhdglv srrfpptgpi
241 glpymkrltv ahqlhhsgky ggapwgmflg pqelqhipga aeeverlvle ldwskr

```

*Capsicum annuum*, CAA70888.

1 ttgryhyqlv wcqisfssts rtsyyrhspf lgpkptptp svypitpfsp nlgsilrcrr	
61 rpsftvcfvl eddkfktqfe ageediemki eeqisatrla eklarlkser ftylvaavms	
121 sfgitsmavm avyyrfywqm eggevpfsem fgtfalsvga avgmefwarw ahkalwhasl	
181 whmheshhkp regpfelndv fainavpai alldyffffhk glipglcfga glgitvfgma	
241 ymfvhgdglvh krfpvgpvan vpylrkvaaa hslhhsekfn gypyglflgp keleevggle	
301 elekevnrrt ryikgs	
 T_pseudonana	-----
V_vinifera	-----matgisaslnsmcsrclgrnsftatgpssvislssfltpvthlkgnifplqr
C_annuum	ttgryhyqlvwcqisfsstsrtsyrrhspflgpkptptpsvypitpfspnlgsilrcrr
H_pluvialis	-----ittmlsklqsisvkarrvelard
 T_pseudonana	-----
V_vinifera	rrslkvclvle-----kei-----ed-gieeddspessnraserlar
C_annuum	rpsftvcfvl-----ddkfktqfeagee-diemkieseqisatrlaeeklar
H_pluvialis	itrpkvclhaqrcslvrlrvapqteeeavgtqqaagagdehsadvalqqldraiaerrar . : : *
 T_pseudonana	LLSKLFPVIATYIIAKYALPHINTI---LH-----CSNTLSNFVRITYTVLFAIAM
V_vinifera	kaerytylvaammssligitsmaivavyr1swqme-ggeipvlemlgtfalsvgaavgm
C_annuum	kkserftylvaavmssfsgitsmavmavyyrfywqme-ggevpfsemfgtfalsvgaavgm
H_pluvialis	rkleqlsyqaaaiaasigvsgiaifatylrfamhmtvvgavpwgevagplllvvggqlgm . : : . : : : . : : . : : . : : . : * * ..*
 T_pseudonana	EYISRYSHCYLWHGKFLWINGSHHHQYPAVGSTPVYGHNNPYVSPAIELNDAFFAT
V_vinifera	efwarwahkalwhas--lwhmheshhr-pr-----egpfelndvfaiinav
C_annuum	efwarwahkalwhas--lwhmheshhk-pr-----egpfelndvfaiinav
H_pluvialis	emyaryahkaihesplgwllhkshht-pr-----tgpfeandlfaiikgl * : *::* : ** . * . ** * : * : * * *::* .
 T_pseudonana	IATLAMWIGSEPPSTLTKDCSIGIGLVTLGYLSYFVGHDIVAHERLGKGVANLRAFP
V_vinifera	paisllsyglfnkglv-pglcfgaglgityvfgmaymfvhgdlvhrrfpvgpia----nvp
C_annuum	paialldyffffhkgli-pglcfgaglgityvfgmaymfvhgdlvhkrfpvgpva----nvp
H_pluvialis	pamlctfgfwlpnv1-gtacfgaglgitygmaymfvhgdlvsrfptgpia---glp * * . : . : . : * : * : * : * : * : * : * . *
 T_pseudonana	YMEQCASVHIRYHHKLTKRSNDSDPYGAPYGFWLGPSEVECLNRGQWYAPMPMSLKAISW
V_vinifera	ylrkvasahqlhh-----sdkfngvpyglflgpmeleevggmeele--keisrriks
C_annuum	ylrkvaahs1hh-----sekfngvpyglflgpkeleevggleele--kevnrrtry
H_pluvialis	ymkrltvahqlhh-----sgkyggapwgmflgpqelqhipgaaev--erlvleldw *::: : . * : * . . *.*: * : * : * : .
 T_pseudonana	IATLIFFASTIHSSLSPAQAQAIVLGGCVGWCGSGTLSDNNTTSRRIGKLLSLNWQSTPSR
V_vinifera	sdss-----
C_annuum	ikgs-----
H_pluvialis	skr-----
 T_pseudonana	LMPHGLSGLISVGIGSYLIFGHSLVGDLPYTMQQPPYLIIILYATATSWNALGGYMIVNT
V_vinifera	-----
C_annuum	-----
H_pluvialis	-----
 T_pseudonana	APPNTRMLFRRCAILQVCLSYFIVRFLPHSSVLLIRLESNTITSLRCLDLIVTISAVVC
V_vinifera	-----
C_annuum	-----
H_pluvialis	-----
 T_pseudonana	TLSFFDAVVDMSKQSVVLGQSIAFGIIGILLSVYPIQLSLQGEWWSCIQNRYPMQASG
V_vinifera	-----
C_annuum	-----
H_pluvialis	-----

T_pseudonana	MIAYIYVPATVTFSLFLFGATLYQRKIMSASEYGIISLMVILVCLLATVLSQEIHIPDVS	534
V_vinifera	-----	299
C_annuum	-----	316
H_pluvialis	-----	296
T_pseudonana	TQRIYLPCEDPAMDSLEEKVLEALDFSRYARSILTTVLGIKFESPA	580
V_vinifera	-----	299
C_annuum	-----	316
H_pluvialis	-----	296

### *T. pseudonana* BCH (Appendix C)

MHQQLSRLLSKLFPVIATYIIAKYALPHINT  
ILHCSNTLSNFVRITYTVLFAIAAMEYISRYSHCYLWHGKFLWWINGSHHHQYPAVGSTPV  
YGHNNPYVSPAIELNDAFAVFFATIALMAMIGSEPPSTLTKDCSIGIGLVTLGYGLSYF  
VGHDIVAHERLGKVANALRRAFPYMEQCASVHIRYHHKLTKRNSNDSPYGAPYGFWLGP  
SEVECLNRGQWYAPMPMSLKAISWIATL IFFASTIHSSLSPAAQAIIVLLGCVGWCGSGTL  
SDNTTTSRRIGKLLSLNWQSTPSRLMPHGLSGLISVGIGSYLIFGHSLVGDLPYTMQQP  
PYLIILYATATSWNALGGYMIVNTAPPNTRMLFRCAILQVCLSYFIVRFLPHSSVLLIR  
LESNTITTSRCLDLIVTISAVVCTLSDLAVVDMMSKQSIVLGQSIAGIIIGILLSVYP  
IQLSLQGEWWSCIQNRYPMQASGMIAIYIYVPATVTFSLFLFGATLYQRKIMSASEYGII  
SLMVILVCLLATVLSQEIHIPDVSTQRIYLPCEDPAMDSLEEKVLEALDFSRYARSILTT  
VLGIKFESPA-

The underlined portion is what corresponds to BCHs from other organisms in the above alignment.

### Percent Identity Matrix

1: T_pseudonana	100.00	25.73	26.21	27.05
2: V_vinifera	25.73	100.00	68.56	42.96
3: C_annuum	26.21	68.56	100.00	42.45
4: H_pluvialis	27.05	42.96	42.45	100.00

### Cyanobacterial BCH Sequences (non-heme di-iron):

*Prochlorococcus marinus* subsp. *marinus* str. CCMP1375, GenBank accession number AAP99312.

```

1 mtntlnttih ndlppkfqss sfwqkrikdy ldppnfnpt lglfiggyai aflsiwqwyk
61 gvwplpvlvg laflslhmeg tvihdachka ahpnkwinga mghgaaillg fsfpvftrvh
121 lqhhshvndp kndpdhvst fgpvwliapr ffyheyffffq rklwrkyelm qwglersifi
181 tivlagvhfn fmnnviynlwf gpalmvgvtl giffdylphr pfmarnkwn srvypsrvmn
241 ilimgqnyhl vhhlwpsipw feykpayeat kplldqkgsp qrmgifeskk dsfnflydii
301 lgirshkksr skmrplanli ptkkrrkw1 yilhktaip dkid

```

*Thermosynechococcus elongatus* BP-1, GenBank accession number NP\_682690.

```

1 miteaaipat vpkeflgppv gfnptlvmff aafaaialst wgyvqghwpg glsfvanmla
61 lhlmgtvihd ashnvahrhp imnaimghgs almlgfvfpv ftrvhmqhha hvndpendpd
121 hyvskggplw liaprfyhe ifffkrrlwr kyellewfsl rltlvgitf aalngyldyi
181 lnywfplagv vglmglffd yfphrphter drwhnarvyp srllnlifg qnyhlihhwl
241 pnipwykvqp ayyavkp11d ahgckqt1gi lepgnflpfl ydalvglhf rprss

```

*Cyanidioschyzon merolae* strain 10D, GenBank accession number NP\_848964.

```

1 mnsllfflsv sltlvsligy vhmplsvcf vfnvislhla gslihdashk sahsneying
61 iighvcgfl gfsfvvfkf hmqhhahvnq akydpdhyvs tggpiwliap rffyheiyff
121 qrrlyrnhel lewmarglf flvlmaawkf galtyvrcw fcaallvgtf lglcfdfylph
181 ypfvqthrwh naciqendml nwlihgnyh lvhhlwpsep wykyqqkyqa hqqlftpqtc
241 vlgwptqig dlcfglrig

```

T_pseudonana	MHQSLRLLSKLFPVIATYIIAKYALPHINTILHCSNTLSNFRITYTVLFAIAMEYISRY	60
C_merolae	-----	0
P_marinus	-----	0
T_elongatus	-----	0
T_pseudonana	SHCYLWHGKFLWWINGSHHHQYPA-VGSTPV-YGHNNPYVSPAIELNDAFVFATIAT-	117
C_merolae	-----mnsllfflsvslt	13
P_marinus	-----mtntlnntihndlppkfqsssfwqkrikdyldppnfnptlglfiggyia	51
T_elongatus	-----miteaaipatvpkeflgppvgfnptlvmffaafaaia	36
	:*: : :	
T_pseudonana	-LAMW--I-GSEPPSTLTKDCSIGIGLGVTLYGLSYFVGH-----DIVAHERLGKGVAN	167
C_merolae	lvsligiyv-mhmplsfcvfvn----islhlagslihdashksahsneyingiighvcgf	68
P_marinus	fliwiqwykgvwplpvlgaf---lshmegtvihdachkaahpnkwinqamghgaa	107
T_elongatus	ilstwgvyqghwpgglsfvanm---lalhmgtvihdashnvahrhpimnaimhgsal	92
	: : * : . : . : : * : . : : * : .	
T_pseudonana	ALRRAFPYMEQCASVHIRYHHKLTKRSNDSDPYGAPYG-FWLGPS----EVECLNRGQW	221
C_merolae	llgfsfvf---kkvhmqhhahvnqakypdhvstggpiwliaprfyheiyffqrly	125
P_marinus	llgfsfpvf---trvhqlqhshvndpkndpdhivstfgpvwliaprfyheyfffqrklw	164
T_elongatus	mlgfvfpvf---trvhmqhhahvndpendpdhyvskggplwliaprffyheiffkrllw	149
	* * : **::* : : . * * : * .** * : : * : :	
T_pseudonana	YAPMPMSLKAISWIATLIFFASTIHSSLSPAAQAIVLLGCVGWCGSGTLSDNNTTSRRIG	281
C_merolae	r-----hellewmarglfvlvmaawkfagt-yvl--rcwfcaal-----lvg	168
P_marinus	rk----yelmqwglerisifitivlagvhfnfmn-viy--nlwfqpal-----mvg	207
T_elongatus	rk----yellewflsrltvgivtfaalngyld-yil--nywfplag-----vvg	192
	: .. * : : . : : * . : * . : * : :	
T_pseudonana	KLLSLNWQSTP-----SRLMPHGLSGLISVGIGSYLIFGHSL--VGDL--KP	324
C_merolae	tflglcfdfylphypfvqthrwhnaciqendmln-----wlhgqnyhlvhhlpsep	220
P_marinus	vtlgiffdfylphrpfmarnkwknsvrpsrvmn-----ilimgqnyhlvhhlpsep	259
T_elongatus	lmlglffdypfrphpterdrwhnarvypsrln-----ilifgqnyhlhhlwpnip	244
	* .. : * : : . : * : : . : * : . * : *	
T_pseudonana	YTMQQPPYLILYATATSWNALGG--YMIVNTAPPNTRMLFRRCAILQVCLSYFIVRFL	381
C_merolae	wykyqqkyqah---qqlftpqtcvlwgpt-----qigydlc----fgl---rig	259
P_marinus	wfeykpayeat---kplldqkgspqrmgifeskdsfnflydi----lgi---rsh	306
T_elongatus	wykvqpayyav---kplldahgckqtlgilepg-nflpflydal----vg1---hfh	290
	: : * : : .. : :	
T_pseudonana	PHSSVLLIRLESNTIT-TSLRCLLDLIVTISAVVCTLSFFDAVVDM SKQS VVLGQSIAFGI	440
C_merolae	-----	259
P_marinus	kksrskmrpl-anliptkllrkwyi-----lhktaiipdkid---	344
T_elongatus	rprss-----	295
T_pseudonana	IGILLLSVYPIQLSLQGEWWSCIQNRYPMQASGMIAIYIVPATVTFSLFLFGATLYQRK	500
C_merolae	-----	259
P_marinus	-----	344
T_elongatus	-----	295
T_pseudonana	IMSASEYGIISLMVILVCLLATVLSQEIHIPDVSTQRIYLPCEDPAMDSLEEKVLEALDF	560
C_merolae	-----	259

P_marinus	-----	344
T_elongatus	-----	295
T_pseudonana	SRYARSILTTVLGIKFESPA580	
C_merolae	-----259	
P_marinus	-----344	
T_elongatus	-----295	

Percent Identity Matrix:

1: T_pseudonana	100.00	17.49	21.71	22.27
2: C_merolae	17.49	100.00	45.17	49.81
3: P_marinus	21.71	45.17	100.00	53.90
4: T_elongatus	22.27	49.81	53.90	100.00

Non-Photosynthetic Eubacterial BCH Sequences (non-heme di-iron):

*Pantoea stewartia*, GenBank accession number AAN85601.

```

1 mlwiwnaliv fvtvvgmevv aalahkyimh gwgwgwhlsh heprkgafev ndlyavvfa
61 vsialiyfgs tgiwplqwig agmtaygllly fmvhgdglvhq rwpfryiprk gylkrlymah
121 rmhhavrgke gcvsfgflya pplsklqatl rerhaarsga ardeqdgvdt sssgk

```

*Pseudomonas putida*, GenBank accession number KT2440 NP\_745389.

```

1 mlfnlailfg tlvamegvgt lahkyimhg gwwlhrshhe phlgmletnd lylvalglia
61 talvalgksg yaplqwvggg vagygalyvl ahdgffhrhw prkprpvnry lkrlhrahrl
121 hhavkgrtgs vsfgffyapp lkvlkqqlrs rrsqs

```

*Flavobacterium* sp. ATCC 21588, GenBank accession number AAC44852.

```

1 mstwaailtv iltvaamelt aysvhrewmh gplgwghks hhdedhdhal ekndlygvif
61 avisivlfai gamgsdlaww lavgvtcygl iyyflhdglv hgrwpfryvp krgylrrvyq
121 ahrmhahvg rencvsfgfi wapsvdsika elkrsgallk dregadrnt

```

T_pseudonana	MHQLSRLLSKLFPVIATYIIAKYALPHINTILHCSNTLSNFVITYTVLFAIAHEYISRY	60
Flavobacterium	-----mstwaailtviltvaameltays	23
P_stewartia	-----mliw-nalivfvtvvgmevvaal	23
P_putida	-----mlf-nlailfgtlvamegvgtl : .. . . ** .	21
T_pseudonana	SHCYLWHGKFLWWINGSHHHQYPAVGSTPVYGHNNPYVSPAIELNDAFAVFATIATLAM	120
Flavobacterium	vhrwimhgplgwghkshded-----hdhalekndlygvifavisivlf	68
P_stewartia	ahkyimhg-wgwgwhlshhe-p-----rkgafevndlyavvfaivsiali	66
P_putida	ahkyimhg-wgwwlhrshhe-p-----hlgmletdnlylvalgliatalav *: ** * : ***. : * ** : * .. :: .	64
T_pseudonana	WIGSEPPSTLTKDCSIGIGLVTLGYLSYFVGHDIVAHERLGKGVANALRRAFPYMEQCA	180
Flavobacterium	aigamgsd-----lawlwavgvtcygliyyflhdglvhgrwpfryvpk---rgylrrvy	119
P_stewartia	yfgstgiw----plqwigagmtayglllyfmvhgdglvhqrwpfryipr---kgylkrly	117
P_putida	algksgya----plqwvgggvagygalvylahdgfffrhwprkprpv---nrylkrlh : * .. * : * * . ** . * : * : ..	115
T_pseudonana	SVHIRYHHKLTKRSNDSDPYGAPYGFWLGPSEVECLNRGOWYAPMPMSLKAISWIATLIF	240
Flavobacterium	q-ahrmhhahvg-----encvsfgfiwapsvdsikaelk-----	153
P_stewartia	m-ahrmhhavrgk-----egcvsfgflyapplsklqatlr-----	151
P_putida	r-ahrlhhavgr-----tgsvsfgffyapplkvtkvqlqqr----- * ** : : .. * : ** * :	149

T_pseudonana	FASTIHSSSLSPAAQAIVLLGCVGCGSGTLSNDNTT--TSRRIGKLLSLNWQSTPSRLMPH	298		
Flavobacterium	-----rsga-----11kdregadrnt-----	169		
P_stewartia	-----erhaa-----rsgaardeqdgvdtsstgk-----	175		
P_putida	-----srsrq-----s-----	155		
	:			
T_pseudonana	GLSGLISVGIGSYLIFGHSLVGDLKPYTMQQPPYLILYATATSWNALGGYMIVNTAPPN	358		
Flavobacterium	-----	169		
P_stewartia	-----	175		
P_putida	-----	155		
T_pseudonana	TRMLFRRCAILQVCLSYFIVRFLPHSSVLLIRLESNTITSLRCLDLIVTI SAVVCTLSF	418		
Flavobacterium	-----	169		
P_stewartia	-----	175		
P_putida	-----	155		
T_pseudonana	FDAVVDMMSKQSVVLGQSIAGFIIGILLLSVYPIQLSLQGEWWSCIQNRYPMQASGMIA Y	478		
Flavobacterium	-----	169		
P_stewartia	-----	175		
P_putida	-----	155		
T_pseudonana	IYVPATVTFSLFGLFGATLYQRKIMSASEYGIISLMVILVCLLATVLSQEIHIPDVSTQRI	538		
Flavobacterium	-----	169		
P_stewartia	-----	175		
P_putida	-----	155		
T_pseudonana	YLPCEDPAMDSLEEKVLEALDFSRYARSILTTVLGIKFESPA	580		
Flavobacterium	-----	169		
P_stewartia	-----	175		
P_putida	-----	155		
1: T_pseudonana	100.00	29.34	28.90	27.74
2: Flavobacterium	29.34	100.00	50.60	41.18
3: P_stewartia	28.90	50.60	100.00	52.90
4: P_putida	27.74	41.18	52.90	100.00

#### Archaeal BCH Sequence (non-heme di-iron):

*Sulfolobus solfataricus* P2, GenBank accession number NP\_344225.

1	mmliyvgma vltfgmefv arlmhkyvmh gllwfihedh hkekqaelek ndlfglvfas	
61	vsvylfflgi qgsyvalsia igmssygiay ffi hdmvihd rhlrlrswgl khrpfkdlil	
121	vhdihhkegk gnwgflfvik gldkvplkd e	
S_solfataricus	-----mmliyvgmavltfgmefvarl	23
T_pseudonana	MHQLSRLLSKLFPVIA TYIIAKYALPHINTILHCSNTLSNFVRITYTVLFAIAMEYISRY	60
	: : : :** :.*: :*::: :	
S_solfataricus	mhkymhg-llwfihedhhkekq-----aelekndlfglvfasvsvylf	66
T_pseudonana	SHCYLWHGKFLWWINGSHHHQYPAVGSTPVYGHNNPYVSPAIELNDAFAVFFATIATLAM	120
	* * : ** :**:* : .***: : * ** * ..**::: . :	
S_solfataricus	flgiqgs----yvalsiaigmssygiayffi hdmvihd rhlrlrswgl khrpfkdlilv	121
T_pseudonana	WIGSEPPSTLT KDCS I GIGLGV TL GSYFVGHDIVAH ERLGKVAN ALR-RAFPYMEQC	179
	::* : : :..*: : * :** : : * : : .*: * * :	
S_solfataricus	hd----ihhke-----gkgnwgflfvik gldkvplkd e-----	151
T_pseudonana	ASVHIRYHHKLTKRSNDSDPYGA PYGFWLGP---SEVECLNRGQWYAPMPMSLKAI SWIA	236
	*** . :** : . :* * :	

S_solfataricus	-----	151
T_pseudonana	TLIFFASTIHSSLSPAAQAIIVLLGCVGCGSGTLSNDNTTSRRIGKLLSLNWQSTPSRLM	296
S_solfataricus	-----	151
T_pseudonana	PHGLSGLISVGIGSYLIFGHSLVGDLKPYTMQQPPYLILYATATSWNALGGYMIVNTAP	356
S_solfataricus	-----	151
T_pseudonana	PNTRMLFRRCAILQVCLSYFIVRFLPHSSVLLIRLESNTITTSRCLDLIVTISAVVCTL	416
S_solfataricus	-----	151
T_pseudonana	SFFDAVVDMSKQS VVLGQSIAFGIIGILL SVYPIQLSLQGEWWSCIQNRYPMQASGMI	476
S_solfataricus	-----	151
T_pseudonana	AYIYVPATVTFSFLFGATLYQRKIMSASEYGIISLMVILVCLLATVLSQEIHIPDVSTQ	536
S_solfataricus	-----	151
T_pseudonana	RIYLPCEDPAMDSLEEKVLEALDFSRYARSILTVLGIKFESPA	580

#### Percent Identity Matrix:

```

1: S_solfataricus   100.00   28.57
2: T_pseudonana      28.57   100.00

```

#### Cytochrome 450-type BCH Sequences:

*Thermus thermophilus* HB8, GenBank accession number BAD71899.

```

1 mkrlslreaw pylkdlqqdp lavllewgra hprlfplpr fplalifdpe gvegallaeg
61 ttkatfqtyra lsrltgrgll tdwgkswkea rkalkdpflp ks vrgyream eeeawaffge
121 wrgeerdldh emlalsrl11 gralfgkpls ps laehalka ldrimaqtrs plalldlaae
181 arfrkdrgal yreaealivh pp lshlprer alseavtllv aghetvasal twsfl1lshr
241 pdwqkrvaes eeaalaafqe alrlyppawi ltrrlerpll lgedrlpqgt tlvlspvvtq
301 rlyfpegeaf qperflaerg tpsgryfpfg lgqrlclgrd fallegpivl raffrrfrld
361 plpfprvlaq vtlrpeggip arpregvra

```

*Xanthophyllomyces dendrorhous*, GenBank accession number CDN65464.

```

1 mfilvlltga lglaafswas iaffslylap rrsslynlg pnhtnyftgn fldilsartg
61 eehakyreky gstlrfagia gapvlnstdp kfvnhvmkea ydypkpgmaa rvlriatgdg
121 vvtaegeahk rhrrimipsl saqavksmvp iflekgmelv dkmmmedaaek dmavgesage
181 kkatrleteg vdvkdwg rldvmalagf dyksdlsqnk tnelyvafvg ltdgfaptld
241 sfkaimwdfv pyfrtmkrrh eipltqglav srrvgielme qkqavlgsa sdqavdkkdv
301 qgrdilsl1v raniaanlpe sqklsdeevl aqisnllfag yetsstvltw mfhrledska
361 vqdklreeic qidtdmp tld elnalpylea fvkeslrdp pspyanrecl kd edfiplae
421 pvigrdgsvi nevritkgm vmlplfninr skfiygedae efrperwled vtdslnsiae
481 pyghqasfis gpracf gwravaemkaclf vtlrrvqfep iishpeyehi tliisrpriv
541 grekegyqmr lqvkpve

```

T_pseudonana	MHQLSRLLSKLFPIATYIIAKYALPHINTILHCSNTLSNF--VRITYTVLFAI----AM	54
T_thermophilus	-----	0
X_dendrorhous,	-----mf-----il-----vlltgalglaafswasiaffslylaprrssl	35

T_pseudonana	EYISRYSHCYLWHGKFLWWIN---GSHHHQY-----PAVGSTPVYGHNNPYVSPA	101
T_thermophilus	-----mkrl	4
X_dendrorhous,	ynlqgpnhnyftgnfldilsartgeehakyrekygstlrfagiagapvlnstdpkvfhn	95
	:	
T_pseudonana	IELNDAFAVFATIATLAMWIGSEPPSTLTKDCSIGIGLVLYGLSYFVGHDIVAHRL	161
T_thermophilus	-slreawpy-----lk-dlqqdp----lavlle----wgr--ahprl	34
X_dendrorhous,	-vmkeaydy-----pk-pgmaarvlriatgdgvta---egeahkrhrri	135
	: : * : : : . * . * * :	
T_pseudonana	GKGVA--NALRRAF-----PYMEQCASVHIRYHHKL-TKRSNDSDPYGAPYGF	206
T_thermophilus	flplprf---plalifdpegveg--allaegttka---tfqyralsrltgrg-lltd	82
X_dendrorhous,	mipslsaqavksmvpiflekgmelvdkmmedaaekdmavgesagekkatrletegvdkd	195
	: : : . : . * :	
T_pseudonana	WLGPSEVECLNRGQ--WY-----AP----MPMSILKAISWIAT	237
T_thermophilus	wgks-----wkea-----rkalkdpflpksvrgyreameeeawaff	118
X_dendrorhous,	wvgratldvmalagfdyksdqlqnktnelvyafvgltdgfap---tldsfkaimwdfv	250
	* : : * : : : * :	
T_pseudonana	LIFFASTIHSSLSPAAQAIVLLGCVGCGSGTLSNDNTTSRRIGKLLSLNWQSTPSRLMP	297
T_thermophilus	gewrgeerd-lhem---l-----alslrligral-----fg	146
X_dendrorhous,	pyfrtmkrr-heipltqgl-----avs-rrvgiel-----me	280
	: : * : * * : :	
T_pseudonana	HGLSGLISVGIGSYLIFGHSLVGDLKPYTMQQPPYLI-ILYATATSWNALGGYMIV---	352
T_thermophilus	kpls-----pslaehalkaldrimaqrtrsplatllaearfrkdrgalyreaea	196
X_dendrorhous,	qkkq-----avlgasasdqavdkkdqvgrdils-----llvrani	314
	: . : .. * * : :	
T_pseudonana	-NTAPPNTRM-----LFRRCAILQVCLSYFIVRFLPHSSVLLIRL--ESNTIT	397
T_thermophilus	livhppplshlpreralseavtl vaghetvasaltwsflll-shrdwqkraeeseaa-	254
X_dendrorhous,	aanlpesqklsdeevlaqisnllfagyetsts vtwmfhrl-sedkavqdklreeicqid	373
	* : : * . * : * : : . : : . :	
T_pseudonana	TSLRCLDLIVTISAVVCTLSFFDAVVDMSKQ-----SVVL	432
T_thermophilus	-----laafqealrlyppawiltrl-----er-----plll	281
X_dendrorhous,	tdmptl del--nalpyleafvkeslrl dpsspyanreclkdedfiplaepvigrdgsvi	430
	: .. : :	
T_pseudonana	G-QSIAFGIIGILLLSVYPIQ-----LSIQGEWWSCIQNRYPMQASGMIAIYIV	481
T_thermophilus	gedrlpqg--ttl v l spvvtq---rlyfpegeafqperflaer-----gt	321
X_dendrorhous,	nevrkitg--tmvmlplfninrskf i ygedaaefrperwledvtdsl-----nsiae	480
	. : * : * : : : : * .. .	
T_pseudonana	PATVTFSILFLFGATLYQRKIMSASEYGIISLMVILVCLLATVLSQEIHIPDVSTQRIYLP	541
T_thermophilus	psgryfp-fglgqrlcl----grdfalle gpivlraffrrfrldplpfprvla-qvtr	374
X_dendrorhous,	pyghqas-fisgpracf---gwrfavaemka lfvtlrrvqfepiishpeye-hitli	533
	* * . : .. . * : . : : : * :	
T_pseudonana	CEDPAMDSLE-EKVLEALDFSRYARSILTTVLGIKFESPA	580
T_thermophilus	-pegg lparpregvra-----	389
X_dendrorhous,	isrprivgrekeyg qmrlqvpve-----	557
	: . *	

### Percent Identity Matrix:

1: T_pseudonana	100.00	16.77	20.09
2: T_thermophilus	16.77	100.00	26.98
3: X_dendrorhous_	20.09	26.98	100.00

### 3) LUT1-like, LTL

Peptide alignment of the two *T. pseudonana* LTls.

LTL1	--MKFTT--ALA--VLCWTSVTNAFVPPSSFTSPA-----LKNEQQQVRASSPLYALDTK	48
LTL2	MCTKLSSRRTLLALYFAFTGCTAFQLPSATPSRASITKAYSTHLDKEIKSKTPLVNPSKI	60
	*::: * :* ::*: * * :**: * * .. ::::::: ** ..	
LTL1	EKEETTTATSASSTDSTSSTPAA--AATEESEGLPWWWEI-----WK---	88
LTL2	YTQADIDTDLSSYEN-ELLAAWDTDSSLQRGFDEWEIEKLRRNFAGLRQREDGQWVRKPS	119
	. : . * * : . * * : . . *: * * :	*
LTL1	-LPVMQPAE-----PGTDIFADSARVLRT-----	112
LTL2	LFDFLVTNTPSNVVGVSNTGERYESPPKPVNMLDVGLLITKNLLNTLGFGPSLGMAAVPD	179
	: . : * . : .	
LTL1	-NIEQIYGGFPSLDQCPLAEGEITDIADGTMFIGLQRYQQQYGSPYKLCFGPKSFLVISD	171
LTL2	AVIQKYEGSFFSF-IGKVLLGGDLQTLAGGPFLLLAKYYQDYGPIFIQLNSFGPKSFLVISD	238
	*:: *.* *: : * :*. * :* : * * :** :*:*****	
LTL1	PVQAKHVLRDAN-TLYDKGILAEILKPIMGKGLIPADPETWSVRRRAIVPAFKAWLNHM	230
LTL2	PVMARHILRDSSPEQYCKGMLAEILEPIMGDGLIPADPKIWVKVRRRAVVPGFHKWLNNM	298
	** * :*:****: . * ***:*****:****.*****: * .*****:***.*** ****:*	
LTL1	VGLFGYCNEGLIASLEEAKKNDAPNGQQGGKIELMEEKFCVALDIIGLSVFNYEFGSVS	290
LTL2	VTLFGDCGERLVNLDARAT-----AKTPVDMEERFCSTLDIIGKAVFNYDFGSVT	350
	* *** *.* *: .*: *. : :****:****:***** :****:****:	
LTL1	EESPVIKAVYSALVEAEHRSMTPAPYWDLPFANEVVPRLRKFNSDLKVLLDDVLTDLIDRA	350
LTL2	KESPIVKAVYRVLREAHRSSSFIPYWDLPYADKWMGGQVERFRKDMGMLDDILTKLINRA	410
	:****:**** .* *****: * :*****:***: : :*..*: :***:***.***:*	
LTL1	KNSRQVEDIEELEKRDYANVKDPSSLRLFLVDMRGADIDNKQLRDDLMTMLIAGHETTAAV	410
LTL2	IETRDEASVEELEDRDVG--DDPSLRLFLADMRGEDLTSKVLRDDLMTMLIAGHETTAAM	468
	:*: . :****.** . .*****.**** *: . * *****:*****:*****:	
LTL1	LTWALFELTKHPE-QMAKVRAEIDSVLGDR-PTYDDIKEMQYLRLVVAETLRLYPEPPL	468
LTL2	LTWTVFGLVSNDGSLMKEIQAERVTVMDKLRPDYDDIAKMKMRYALIEALRLYPEPPV	528
	***: * * . . * :***: :*:***: * **** :*: :* . : * :*****:	
LTL1	LIRRRCRTENKLPKGGR---EATVIRGMIDFLSLYNLHHDERFWPEPNFKPERWESKYI	525
LTL2	LIRRAREDNLPGAGSGLSSGVKVLRGTDIFISTWNHLRAPEYWENPEKYDPTWRERRFK	588
	****. * :* :*** **. .*:*** ***: * :***: .*: :*: :*. *** :	
LTL1	NPEVPEWAGYDPAKWINTNLYPNEVASDFAYLPFGGGARKCVGDEFATLEATVTLAMLLR	585
LTL2	NPGVKGWNGYDPEKQSSESSLYPNEITADYAFLPFGAGRKRCIGDQFAMLEASVTLAMIIN	648
	*** * * **** * : :****: :*:***: * ***: * ***: ***: ****: :.	
LTL1	RFEFEFDASKLAAKSIDIMHPEDLEHAVGMRTGATIHTRKGLHMVIRKREL-----	637
LTL2	KFDFTLVGS-----PKDVGMMKTGATIHTMNGLNLVVSRRSEDNPETN	692
	:*: * : . : ***:***** :*:***: * :*.	
LTL1	-----	637
LTL2	DYWIQQHLSRGLENVNGRPYSTNEDAAWTASSRDKNEGVVSRNV	736

Percent Identity Matrix

1: LTL1	100.00	47.78
2: LTL2	47.78	100.00

## APPENDIX 2.E PLASMID MAPS AND PRIMERS

- 1) VDL2 overexpression, nitrate reductase promoter and terminator.

Created with SnapGene®



Primers for amplifying the VDL2 open reading frame:

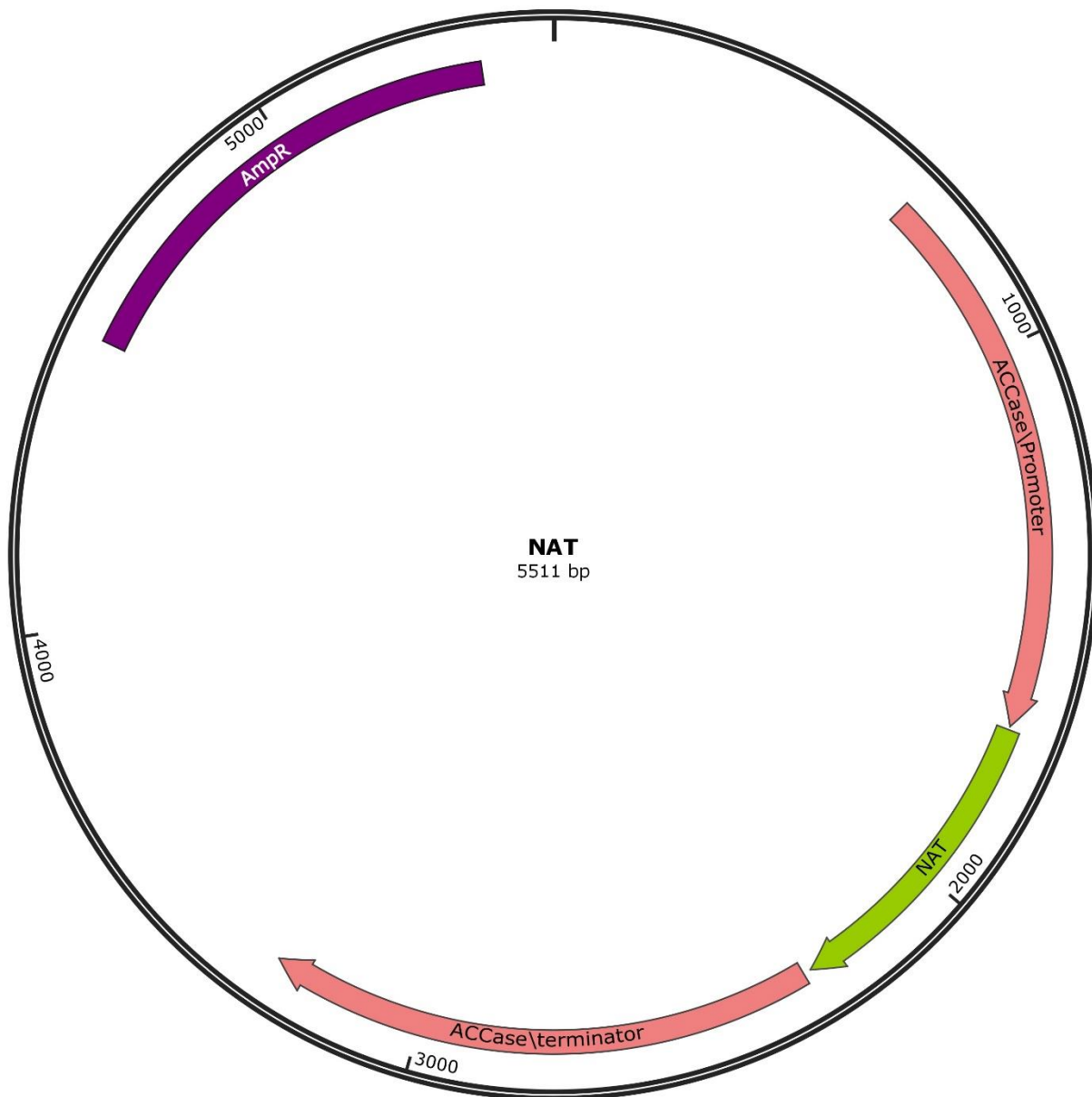
Fwd: 5'ggggacaagttgtacaaaaaaaggcaggctATGTCGGCATCATCATCATCAAC3'

Rev: 5'ggggaccactttgtacaagaagctgggtATCACCAATTCTTCTTTGATATAAT3'

Lower case sequences add Att sites for Gateway cloning.

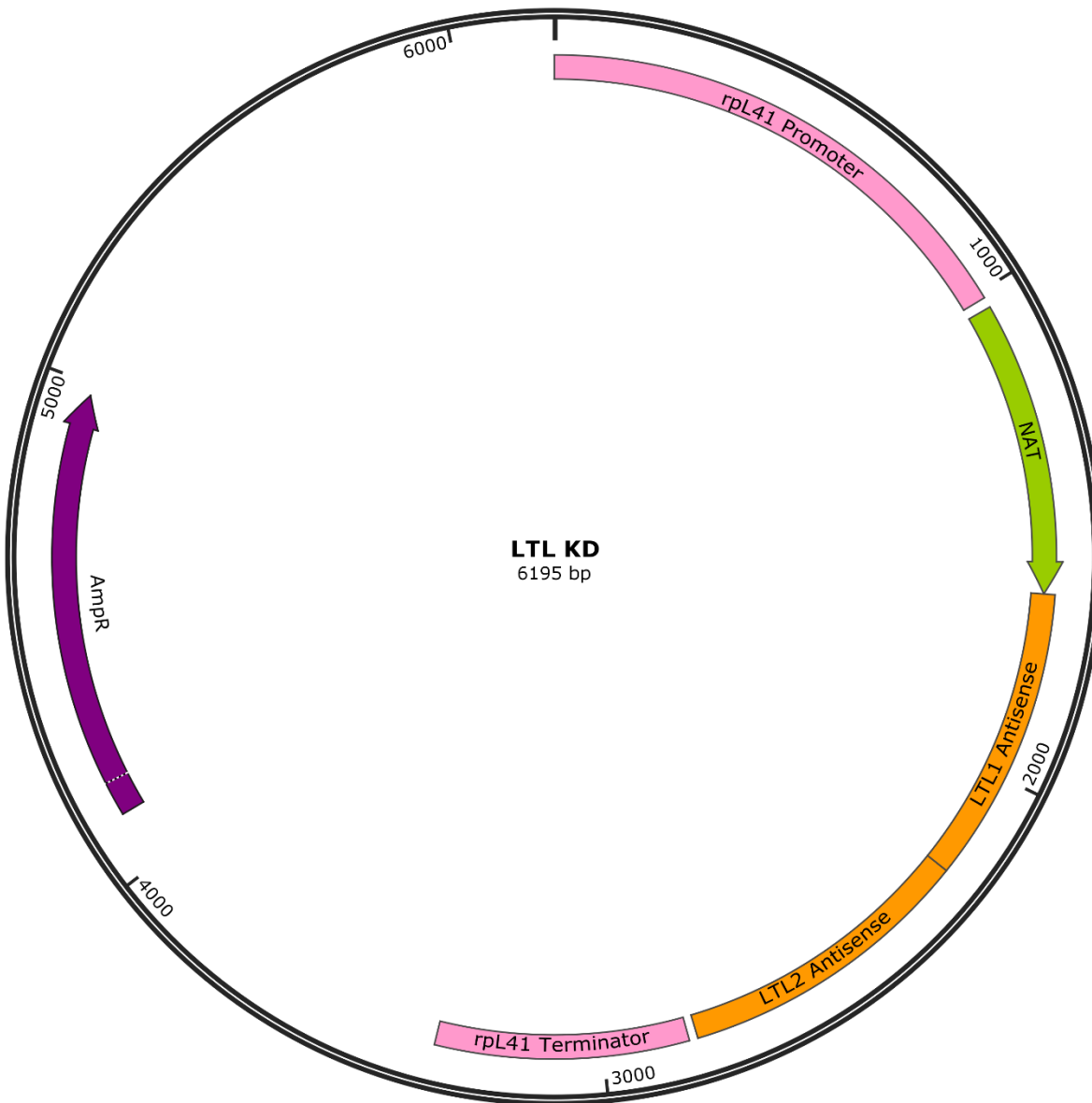
2) NAT, acetyl CoA carboxylase promoter and terminator.

Created with SnapGene®



- 3) LTL KD, ribosomal protein 41 promoter and terminator, NAT on the same transcript.

 Created with SnapGene®



Primers to amplify antisense regions:

Fwd, LTL1: 5'ggggacaagttgtacaaaaaaaggcgtccatgaccatagtgttg3'

Rev, LTL1: 5'ggggacaactttgtatacaaaggttgcagagacttgggtgg3'

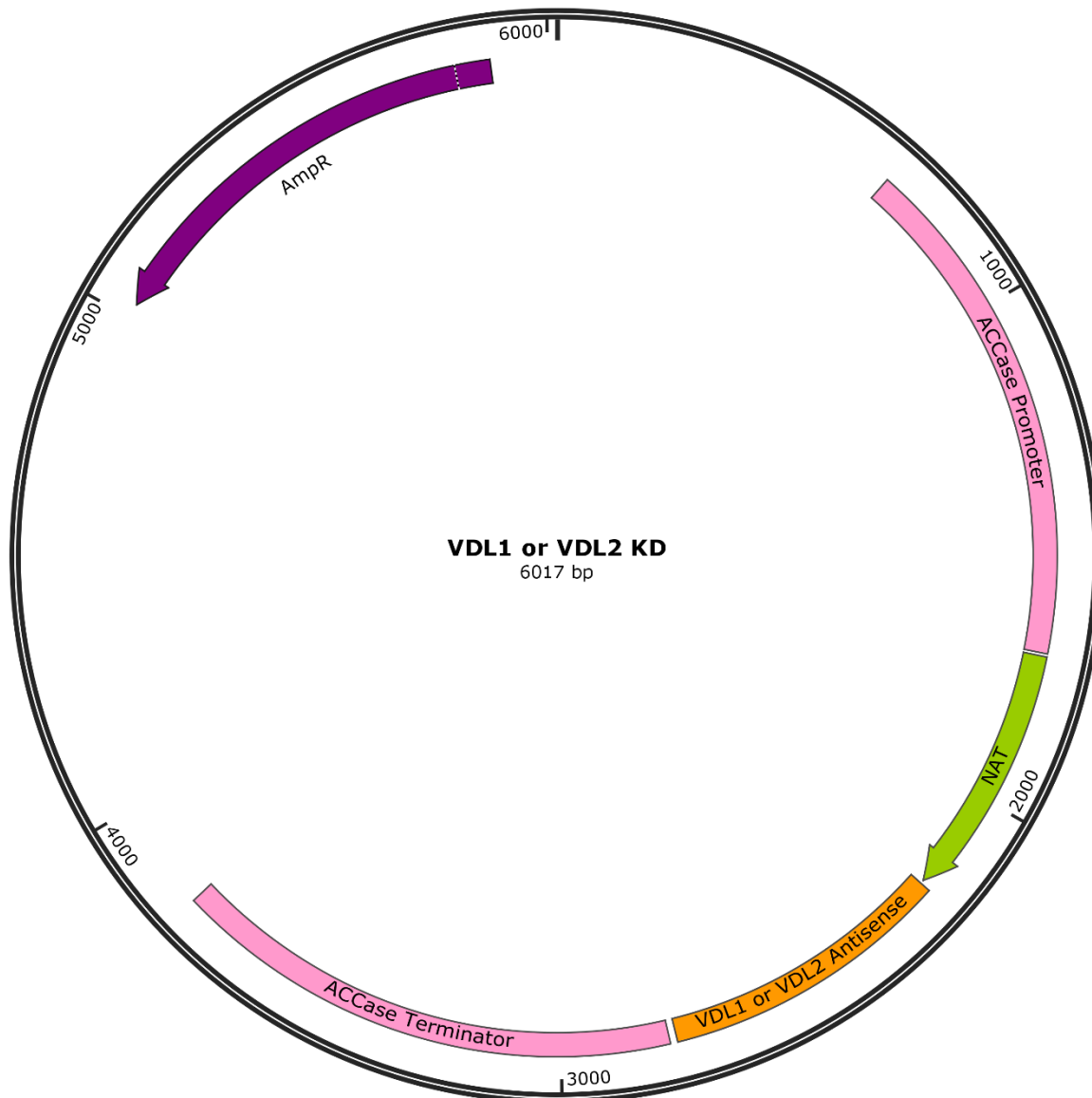
Fwd, LTL2: 5'ggggacaactttgtatacaaaaggcttccttatatccatgttt3'

Rev, LTL2: 5'ggggaccacttgtacaagaaggctgggtgggtgggtgg3'

Lower case sequences add Att sites for Gateway cloning.

4) VDL1 or VDL2 KD, acetyl CoA carboxylase promoter and terminator, NAT on the same transcript.

Created with SnapGene®



Primers to amplify antisense regions:

VDL1, Fwd: 5'ggggacaagttgtacaaaaaaggcaggctCAGTTGTCAAATCCTCGCTCC3'

VDL1, Rev: 5'ggggaccacttgtacaagaaaggctggtaACAGTCGTCTAGGCACCATTG3'

VDL2, Fwd: 5'ggggacaagttgtacaaaaaaggcaggctCCAAACACTTGGCAGTACACG3'

VDL2, Rev: 5'ggggaccacttgtacaagaaaggctggtaTCAATGCCTACTCGGTCGATAC3'

Lower case sequences add Att sites for Gateway cloning.

## **CHAPTER 3**

**Enhanced triacylglycerol (TAG) and protein accumulation in transgenic diatom *Thalassiosira pseudonana* with altered photosynthetic pigmentation**

### 3.1 ABSTRACT

Microalgal productivity in mass cultures is limited by the inefficiency with which available light energy is utilized for photochemistry. In dense cultures, cells closest to the light source absorb more light energy than they can use and dissipate the excess while light penetrance into the culture is steeply attenuated. Reducing microalgal light harvesting and/or dissipating capacity may improve the efficiency with which light is utilized by mass cultures. In this study, two transgenic lines of the diatom *Thalassiosira pseudonana* with altered photopigmentation are evaluated with respect to photosynthetic parameters, growth, and productivity. In one line, violaxanthin de-epoxidase-like 2 is overexpressed (VDL2 OE), resulting in a reduction of the diadinoxanthin cycle pigments, which are involved in light energy dissipation (non-photochemical quenching, NPQ), accompanied by a stoichiometric increase in the light-harvesting pigment fucoxanthin. No differences in the maximum potential quantum yield of photosystem II (Fv/Fm) or light-limited photosynthetic rate ( $\alpha$ ) were found. However, when adapted to 30  $\mu\text{mol}$  photons  $\text{m}^{-2} \text{ sec}^{-1}$ , the VDL2 OE maximum relative electron transport rate ( $r\text{ETR}_{\max}$ ) upon exposure to saturating light intensities was 86-95% of wild type (WT). When adapted to 300  $\mu\text{mol}$  photons  $\text{m}^{-2} \text{ sec}^{-1}$ , VDL2 OE saturated photosynthesis at 62-71% of the light intensity needed to saturate WT ( $E_k$ ). NPQ was substantially lower at and below 300  $\mu\text{mol}$  photons  $\text{m}^{-2} \text{ sec}^{-1}$ . VDL2 OE accumulated up to 3.4 times as much triacylglycerol (TAG) as WT during exponential growth, and up to twice as much protein. Growth was up to 7% slower, but harvesting could be timed to achieve improved yields. TAG and protein accumulation inversely correlated with NPQ. The second strain evaluated was obtained by using antisense to simultaneously silence or knock down (KD) both LUT1-like genes, hypothesized to catalyze an intermediate carotenoid biosynthesis step of converting  $\beta$ -carotene to zeaxanthin. Overall reduction of photopigment content without altering photopigment ratios resulted. No significant differences from WT in photosynthetic performance were found. LTL KD grew at a rate comparable

to WT and accumulated up to 40% more TAG during exponential growth, while protein content was reduced by 11-19%. LTL KD cells were elongated and 5-10% smaller than WT, and cultures contained auxospores, indicating stress that may relate to a cell cycle progression defect.

### **3.2 INTRODUCTION**

Microalgae are a promising production platform for sustainable biofuels and other bioproducts. They do not compete with plant crops for arable land and require only modest nutrient input and light energy to synthesize biomolecules of commercial interest and accumulate biomass [Mata et al. 2010]. A major challenge for the economic feasibility of microalgal production is the inefficient utilization of light by microalgal cultures grown at scale [De Mooij et al. 2015]. Microalgae have evolved extensive photopigmentation, which confers a competitive advantage in the wild by maximizing a cell's light absorption capacity in environments where light may be limited, while minimizing the light available to cells below. In dense cultures such as those used for production, this results in a suboptimal distribution of light energy. At high light intensities such as direct sunlight, algae closest to the light source capture more light than the cells are able to utilize. Excess light is dissipated as heat and fluorescence. Because of the efficiency of light capture, there is a steep attenuation of light penetrance into the culture. Thus, the cells closest to the light source are subject to photosystem-damaging light-induced stress, while the cells deeper in the culture have less light available for photosynthesis [De Mooij et al. 2015]. In theory, reducing cellular light-harvesting and/or dissipation capacity could improve light distribution and therefore productivity in dense cultures, making their cultivation for commercial purposes more cost-efficient. Cells closest to the light source would suffer less light-induced stress and light penetrance would increase. Thus, a greater proportion of the culture would be photosynthetically active [De Mooij et al. 2015].

Numerous efforts have been made in chlorophytes to reduce the size of photoantennae, which serve to capture light energy and funnel it to the photosynthetic reaction centers where it is used to drive photochemistry. This has generally resulted in improved photosynthetic parameters, such as saturation of photosynthesis at higher irradiances, greater light-saturated rates of oxygen evolution on a per-chlorophyll basis [Beckmann et al. 2009, Cazzaniga et al. 2014, Jeong et al. 2017, Kirst et al. 2012a, Kirst et al. 2012b, Mitra and Melis 2008, Nakajima et al. 2001, Shin et al. 2016, Shin et al. 2017], increased quantum yield and lower photoinhibition [Mussgnug et al. 2007]. In some cases, higher maximal culture density [Polle at. al. 2003], faster growth [Mussgnug et al. 2007], and better biomass productivity in laboratory conditions have been reported [Beckman et al. 2009, Shin et al. 2016, Shin et al. 2017]. Several strains that appeared promising based on laboratory performance did not show improved biomass productivity in mass culture conditions simulated in laboratory-scale panel photobioreactors, possibly due to unintended effects of the genetic modifications or higher vulnerability to photodamage [De Mooij et al. 2015]. Cazzaniga et al. [2014], however, reported improved biomass productivity in laboratory conditions as well as in 7 L hanging bag photobioreactors deployed outdoors. As a different strategy, Berteotti et al. [2016] explored downregulation of light energy dissipation through non-photochemical quenching (NPQ) in the chlorophyte *Chlamydomonas reinhardtii*, and found that if it is reduced, but not completely abolished, improved biomass productivity in a small scale photobioreactor results.

Non-chlorophyte eukaryotic microalgae have been largely unexplored with respect to light utilization efficiency improvement through biological modification. Because microalgae are incredibly diverse and have evolved different strategies for interacting with their environment, different taxa may respond to such modifications with varying degrees of success. Diatoms, for example, are brown microalgae belonging to the Stramenopile or heterokont class, whose light-harvesting and photoprotective strategies differ substantially from chlorophytes [Wilhelm et al.

2006]. Chlorophytes rely predominantly on chlorophylls a and b (Chl a, Chl b) for light capture, the ratio of which adjusts dynamically in response to changes in light intensity. Diatoms use Chl a in association with chlorophyll c (Chl c) and the more abundant carotenoid-derived accessory photopigment fucoxanthin (Fx) to capture light energy [Wilhelm et al. 2006]. The ratio of Chl a to Fx, and thus photoantenna size, does not change much with light intensity [Lepetit et al. 2012]. Diatoms appear to rely on their capacity to induce NPQ faster and to a higher extent than chlorophytes when adjusting to short-term irradiance increases and coordinately reduce the abundance of photosynthetic reaction centers and photoantennae during long-term adaptation to higher light [Lepetit et al. 2012]. NPQ in diatoms relies predominantly on the diadinoxanthin (Ddx) cycle that is absent in chlorophytes, wherein the carotenoid derivative Ddx is reversibly converted to diatoxanthin (Dtx) via de-epoxidation when it is necessary to dissipate excess light energy [Lepetit et al. 2012, Wilhelm et al. 2006]. Because diatoms are very promising in terms of biomass productivity and triacylglycerol (TAG, neutral lipid of interest for biofuels) accumulation [Hildebrand et al. 2012], it is intriguing to explore improving their productivity by modulating culture light utilization efficiency. So far, only one such study has been published. A *Cyclotella* sp. strain was obtained through two subsequent rounds of mutagenesis, employing ethylmethylsulfonate and ultraviolet radiation [Huesemann et al. 2009]. Its green color indicated that it had drastically reduced carotenoid abundance, including the main accessory light-harvesting photopigment Fx and the photoprotective Ddx cycle pigments. It also had a substantially higher Chl a/Chl c ratio, indicating a smaller photoantenna size. The mutant required higher light intensity to saturate photosynthesis on a per chlorophyll basis but was less stable in culture and had reduced biomass productivity. It was not fully characterized, but the observed lack of fitness could be attributed to too much reduction in carotenoids and thus susceptibility to photodamage and oxidative stress, and

possible additional undesirable mutations [Huesemann et al. 2009]. More exploration is necessary to determine the utility of reducing light absorption and/or dissipation in diatoms.

In this study, we evaluate photosynthetic parameters, growth, carbon partitioning, and macromolecule accumulation in two transgenic (TG) lines of the diatom *Thalassiosira pseudonana* in which the abundance of two carotenoid biosynthesis enzymes is manipulated (Chapter 2). In one line, VDL2 OE, the violaxanthin de-epoxidase 2 is overexpressed, resulting in a decrease of the photoprotective Ddx cycle pigments (Ddx+Dtx) and a stoichiometric increase in the light-harvesting Fx. In the other line, LTL KD, both copies of LUT1-like, hypothesized to convert β-carotene to zeaxanthin, are simultaneously knocked down, resulting in an overall reduction of total cellular photopigment content (Tot) with conserved ratios of individual pigments. Four clones of each TG line were selected for characterization and compared to wild type (WT) in low light (LL, 30 μmol photons m<sup>-2</sup> sec<sup>-1</sup>) and high light (HL, 300 μmol photons m<sup>-2</sup> sec<sup>-1</sup>). There were four experimental culture sets: VDL2 OE vs. WT in LL, VDL2 OE vs. WT in HL, LTL KD vs. WT in LL, and LTL KD vs. WT in HL. Each set was independently acclimated to cultivation conditions and used to obtain samples and data, which were then processed independently of each other. Thus, our findings will be discussed as comparisons within but not between the sets.

### 3.3 RESULTS

#### 3.3.1 Photosynthetic Parameters

Photosynthetic parameters were determined for LL and HL-adapted cultures via rapid light-response curves (RLCs) obtained with a pulse amplitude modulation (PAM) fluorometer. This approach involves measuring dynamic rather than steady state responses of a culture to gradual increases in light intensity, and allows, therefore, an assessment of the photosynthetic performance of a culture as it relates to the light intensity it had previously adapted to [Malapascua et al. 2014,

Ralph and Gaderman 2005]. The parameters assessed were Fv/Fm (maximum potential quantum yield of photosystem II),  $\alpha$  (initial slope of the RLC curve, light-limited photosynthetic rate), rETR<sub>max</sub> (maximum light-saturated relative electron transport rate), E<sub>k</sub> (rETR<sub>max</sub>/ $\alpha$ , minimum saturating light intensity), and NPQ (non-photochemical quenching, dissipation of photon energy) [Malapascua et al. 2014, Ralph and Gaderman 2005].

No significant differences in Fv/Fm were found between the TG lines and WT in either LL or HL (**Table 3.1**).  $\alpha$ , rETR<sub>max</sub>, and E<sub>k</sub> were derived from rETR measurements over a range of irradiance, depicted in **Fig. 3.1**. LL-adapted VDL2 OE clones had a reduced rETR<sub>max</sub>, calculated to be 86-95% of the WT average (p-value = 0.02) (**Fig. 3.1A, Table 3.1**). Nevertheless, rETR values did not vary between the TG lines and WT in any tested condition when measured at the irradiance they were adapted to (**Fig. 3.1**). Additionally, HL-adapted VDL2 OE clones had reduced E<sub>k</sub> values, calculated to saturate photosynthesis at 62-71% of the average WT minimum saturating light intensity (p-value = 0.008) (**Fig. 3.1B, Table 3.1**). Although some trends in parameter differences between the TG lines and WT could be observed, no other significant differences were found.

NPQ values measured over a range of irradiance are depicted in **Fig. 3.2**. A high degree of variability between different TG clones and WT cultures was observed, and no claims about statistically significant differences consistent between all TG clones within any condition could thus be made, with one exception. At lower irradiances, the HL-adapted VDL2 OE clones had substantially less NPQ than WT (**Fig. 3.2B**). At 125  $\mu\text{mol photons m}^{-2} \text{ sec}^{-1}$ , VDL2 OE clone 6 had 53% of the average WT NPQ, while the other three clones were at 1-8% of the WT average (p-value = 0.01). At 191  $\mu\text{mol photons m}^{-2} \text{ sec}^{-1}$ , VDL2 OE clone 6 measured at 64% of the WT average NPQ, while the other three clones had 16-18% of the WT average (p-value = 0.02). At 282  $\mu\text{mol photons m}^{-2} \text{ sec}^{-1}$ , VDL2 OE clone 6 had 82% of the average WT NPQ, while the other three clones were at 27-36% (p-value = 0.08 with clone 6, and 0.03 without).

### *3.3.2 Morphology, Cell, and Chloroplast Dimensions*

The VDL2 OE clones appeared morphologically similar to WT (data not shown). LTL KD clones, on the other hand, were elongated and formed numerous auxospores, indicating sexual reproduction (**Fig. 3.3A, B**). The elongation phenotype and auxospore formation were more prominent in HL, but observable in LL as well. Incubating with PDMPO, a fluorescent dye that incorporates into newly synthesized silica, confirmed that the elongated cells were single cells, not multiple cells that have failed to separate, as no cell wall could be observed within the cells (**Fig. 3.3C, D**). The LTL KD cells with a high degree of elongation appeared to have numerous chloroplasts distributed throughout (**Fig. 3.3E, F**).

The average cell area was not significantly different between WT and VDL2 OE clones but was reduced in LTL KD clones in HL, measuring at 90-95% of the WT average (p-value = 0.03) (**Table 3.2**). The chloroplast to cell area ratio in LTL KD clones did not significantly differ from WT in LL or HL (**Table 3.2**). In HL-adapted VDL2 OE clones, the chloroplast to cell area ratio was reduced to 93-96% of the WT average (p-value = 0.02).

### *3.3.3 Growth Rates and Maximal Culture Density*

During exponential growth in LL, the specific growth rate of the VDL2 OE clones was approximately 98% of the WT average (p-value = 0.0006) (**Table 3.2**). When light-limiting culture densities were reached around day 6, the disparity between the KD clones and WT cultures became more pronounced (**Fig. 3.4A**). The stationary phase culture densities reached by the VDL2 OE clones in LL were 72-88% of the WT average (p = 0.02).

In HL, VDL2 OE clones also experienced slowing (**Fig. 3.4B**). During exponential growth, the specific growth rate of the VDL2 OE clones was 93-96% of the WT average (p-value = 0.009) (**Table**

**3.2).** At stationary phase, HL clones VDL2 OE3 and OE5 reached 54% of the average WT culture density, OE2 was at 84% of WT, and OE6 did not differ from WT. Interestingly, all the HL-adapted VDL2 OE clones were substantially lower in culture density than WT during day 5 (34-57% of the WT average, p-value = 0.002) and day 6 (45-69% of the WT average, p-value = 0.007), as the light-limited cultures were transitioning to stationary phase.

The LTL KD clones had some slowing in growth compared to WT in LL and in HL (**Fig. 3.4C, D**). Unlike the VDL2 OE clones that had the most substantial slowing during the light-limited transition from exponential to stationary phase, the slowing in LTL KD clones was more uniform, from inoculation to stationary phase (**Fig. 3.4**). The specific growth rates of the LTL KD clones in LL were 97-99% of the WT average (p-value = 0.04), and not significantly different in HL (**Table 3.2**). Stationary phase culture densities of the LTL KD clones did not significantly differ from WT.

### *3.3.4 Lipid, Protein, Carbohydrate, and Photopigment Content*

The cellular abundance of neutral lipids (triacylglycerol, TAG, quantified by BODIPY fluorescence), proteins, carbohydrates, and photopigments was assessed during exponential growth.

The TAG content of VDL2 OE clones was found to be 21-81% greater than the WT average (p-value = 0.05) in LL, and 2-3.4 times greater than the WT average in HL (p-value = 0.04) (**Fig. 3.5A, B**). The LTL KD TAG content did not significantly differ from WT in LL. In HL, LTL KD clone 49 had TAG content similar to WT, while the other 3 clones had 25-40% more (**Fig. 3.5C, D**). When normalized to average cell area, TAG content was 17-46% greater than the WT average in HL (p-value = 0.03) (**Fig. S3.1A**).

No significant differences were found when comparing total cellular protein between TG lines and WT in LL (**Fig. 3.6A, C**). HL-adapted VDL2 OE clones contained approximately 1.5-2 times as much protein as WT (p-value = 0.02) (**Fig. 3.6B**). HL-adapted LTL KD clones had 81-89% of the average WT total cellular protein content (p-value = 0.01) (**Fig. 3.6D**). When normalized to average cell area, total cellular protein content did not significantly differ between HL-adapted LTL KD clones and WT (**Fig. S3.1B**).

No significant differences in total carbohydrate content were found between TG lines and WT, in either LL or HL (**Fig. S3.2**). Cell area-normalized carbohydrate content also did not differ significantly between LTL KD clones and WT in HL (**Fig. S3.1C**).

Average cell area (3.3.2) and total cellular photopigment content (**Chapter 2**) did not significantly differ between VDL2 OE clones and WT. LL-adapted LTL KD clones had 75-93% total photopigments of the WT average (p-value = 0.2), and 60-76% of the average WT total photopigments in HL (p-value = 0.009) (**Chapter 2**). In HL, cell area-normalized total photopigment content was reduced in LTL KD clones to 63-81% of the WT average (p-value = 0.02).

### *3.3.5 Inverse Relationship Between NPQ and TAG, Protein Content*

Plotting NPQ measured at the light intensity closest to the irradiance to which the cultures were adapted (125  $\mu\text{mol photons m}^{-2} \text{ sec}^{-1}$  for LL, 282  $\mu\text{mol photons m}^{-2} \text{ sec}^{-1}$  for HL) (**Fig. 3.2**) against BODIPY fluorescence (**Fig. 3.5**), revealed an inverse trend between the two variables for VDL2 OE clones and WT in LL and HL (**Fig. 3.7**). The Pearson correlation coefficient (R), where 0 signifies no correlation and -1 means that there is a perfect negative correlation, was -0.3 in LL and -0.4 in HL. No such trend could be observed for LTL KD at LL, as there was no significant variance in TAG or NPQ in that condition, nor for LTL KD in HL, as there was no significant variance in NPQ (**Figs. 3.2C, D, 3.5C**).

Significant difference from WT in protein content was found only for VDL2 OE in HL (**Fig. 3.6B**). When plotted against NPQ as described above, an inverse trend, stronger than that for TAG, was observed as well ( $R = -0.7$ ) (**Fig. 3.8A**). LL-adapted LTL KD clone 51 had approximately 40% less cell area-normalized protein than the average of the other LTL KD clones and WT cultures (**Fig. 3.6C**). This correlated with approximately 1.9 times more NPQ than the average of the other LTL KD clones and WT cultures at the measured value closest to the irradiance to which the cultures were adapted, (**Fig. 3.2C**), thus confirming the trend of an inverse relationship between NPQ and protein accumulation ( $R = -0.9$ ) (**Fig. 3.8B**).

### 3.4 DISCUSSION

#### 3.4.1 Photosynthesis

In VDL2 OE clones, Tot did not exhibit a trend with respect to WT, and the ratios of Chl a, Chl c, and  $\beta$ -carotene to Tot were unchanged (**Chapter 2**). This indicates that the stoichiometric increase in Fx/Tot at the expense of (Ddx+Dtx)/Tot did not affect the cellular abundance of photosynthetic reaction centers and photoantennae. Rather, Fx had replaced some of what would have been Ddx cycle pigments, which are present in distinct pools. Some are bound to photoantenna proteins, while others are dissolved in the lipid shield around photoantennae [Lepetit et al. 2010]. Without further investigation outside the scope of this study, it is not possible to directly discern which pool(s) of the Ddx cycle pigments were at least partially replaced with Fx in the VDL2 OE clones.

Photosynthesis in VDL2 OE clones was not negatively impacted in LL or HL, as indicated by no change in Fv/Fm,  $\alpha$ , and rETR measured at the irradiance to which the cultures were adapted with respect to WT (**Table 3.1, Fig. 3.1A, B**). The lowered rETR<sub>max</sub> in LL-adapted VDL2 OE clones

means that in the short term, LL-adapted VDL2 OE clones would have an impairment in photosynthetic electron transfer through photosystem II compared to WT upon being exposed to saturating irradiance (**Table 3.1, Fig. 3.1A**) [Malapascua et al. 2014, Ralph and Gaderman 2005]. This is not the case with HL-adapted VDL2 OE clones, the  $rETR_{max}$  of which did not significantly differ from WT (**Table 3.1, Fig. 3.1B**). Photosynthetic electron transport of the HL-adapted VDL2 OE clones, however, would, in the short term, saturate at a lower irradiance than in WT, as indicated by lower  $E_k$  values (**Table 3.1, Fig. 3.1B**) [Malapascua et al. 2014, Ralph and Gaderman 2005]. The mechanism by which altered photopigmentation in VDL2 OE clones causes the observed defects in short-term adaptation to higher irradiance needs to be investigated further. It may be attributable to the excess, misplaced Fx.

As discussed in Chapter 2, the overall photopigment reduction in LTL KD clones is most likely due to the destabilization of light-harvesting complexes caused by Fx insufficiency, as carotenoids are known to be crucial for their assembly and stabilization [Moskalenko and Karapetyan 1996, Santabarbara et al. 2013]. Nevertheless, in comparison to WT, photosynthetic parameters as indicated by  $Fv/Fm$ ,  $\alpha$ , and  $rETR$  at the irradiance to which the cultures were adapted were not adversely affected in the LTL KD clones in LL or HL (**Table 3.1, Fig. 3.1C, D**). In contrast to the VDL2 OE clones, short-term adaptation to increases in irradiance was also not impaired, as demonstrated by  $rETR_{max}$  and  $E_k$  values not differing between the LTL KD clones and WT (**Table 3.1, Fig. 3.1**).

The high degree of variance between different TG clones in NPQ responses over a range of irradiance, especially in the LL-adapted state in which WT cultures had a highly replicable response (**Fig. 3.2**), may be explained by potential inter-clonal differences in adaptation to altered photopigmentation. The substantially reduced NPQ in HL-adapted VDL2 OE lines at lower irradiance

levels (**Fig. 3.2B**) may be attributed to the reduced Ddx cycle pigment abundance, as the largest part of NPQ in diatoms requires the presence of Dtx [Lepetit et al. 2012]. The extent of NPQ induction depends on the light adaptation state and incident irradiance, and it appears that despite the reduced abundance of Ddx cycle pigments, HL-adapted VDL2 OE clones were able to induce WT-equivalent NPQ levels at higher irradiance levels (**Fig. 3.2B**) [Lepetit et al. 2012].

#### 3.4.2 Auxospore Formation in LTL KD

Frequent auxospore formation and cell elongation, as observed for the LTL KD clones (**Fig. 3.3**), are both markers of stress. Under typical laboratory conditions, auxospore formation, which indicates sexual reproduction, is rarely if ever observed in *T. pseudonana* [Moore et al. 2017]. In some diatom species, sexual reproduction serves as a way to reconstitute cell size, as it diminishes with every division. However, *T. pseudonana* appears to maintain a relatively constant cell size. Sexual reproduction in diatoms may also be triggered by growth stress that leads to cell cycle arrest, such as nutrient depletion and oxidative stress [Moore et al. 2017]. Because the LTL KD clones were grown in the same nutrient-replete media as WT, which did not form abundant auxospores, nutrient depletion is not a likely cause of the observed sexual reproduction in LTL KD clones. Oxidative stress is also unlikely, since it would be expected to lead to reduced Fv/Fm, which was not observed (**Table 3.1**). A small portion of LTL KD cultures consisted of cells that were smaller than typical (data not shown), and it is possible that sexual reproduction was induced in those cells to restore size. However, stress evidenced by elongation (**Fig. 3.3**) was present in the majority of LTL KD cells, and we suggest that it was a contributor to auxospore formation. The elongated phenotype has been documented in *T. pseudonana* subject to various stresses that impede cell cycle progression, such as copper toxicity and limitation in silica or selenium. It has not been observed in response to nitrate or phosphorus limitation and is thus not a universal stress response

[Davis et al. 2005]. The cause of the stress in our study is not clear. We hypothesize that it may relate to a defect in chloroplast division, stemming from light-harvesting assembly impairment and destabilization by Fx deficiency in LTL KD clones. Microalgae coordinate cell and chloroplast division to ensure that both daughter cells have chloroplasts upon cytokinesis [Sumiya et al. 2016]. Depending on the timing, an arrest in chloroplast division may cause cell cycle arrest, or chloroplasts may continue dividing without concomitant cell cycle progression if cells are arrested in S-phase, resulting in numerous chloroplasts per cell [Sumiya et al. 2016]. A deregulated coordination between chloroplast division and cell cycle progression in the LTL KD clones could thus account for cell elongation and auxospore formation, which may result from a cell cycle progression defect, as well as the overaccumulation of chloroplasts observed in some of the highly elongated cells (**Fig. 3.3**).

#### *3.4.3 Growth, Carbon Partitioning, and Macromolecule Accumulation*

The most disparity in growth rates between VDL2 OE clones and WT was observed during the light-limited linear portions of the growth curves in LL and HL (**Fig. 3.4A, B**). This may be explained by excess Fx reducing light availability or energy transfer efficiency in the culture when light became limiting. The disparity lessened at higher culture densities, likely because at that point the difference in shading experienced by VDL2 OE clones and WT cultures diminished.

Exponential growth rates for VDL2 OE clones were up to 7% lower than in WT in HL and 2% lower in LL, and average cell area was not statistically different (**Table 3.2**). However, VDL2 OE clones accumulated substantially more TAG per cell than WT in LL and HL (**Fig. 3.5A, B**), and HL-adapted VDL2 OE clones also accumulated more protein per cell than WT (**Fig. 3.6B**). This suggests that VDL2 OE clones may have been fixing more carbon than WT, and preferentially storing it as

TAG (and producing more protein in HL), rather than using it to fuel faster growth or storing it as carbohydrate (**Fig. S3.2B**). Thus, excess fixed carbon was diverted to glycolysis, which eventually feeds into TAG and amino acid biosynthesis, rather than gluconeogenesis, which results in carbohydrate biosynthesis [Smith et al. 2012].

NPQ dissipates absorbed light energy and is inversely correlated with the amount of photons available for photochemistry. Because NPQ was measured as part of an RLC curve on dark-adapted cultures rather than in real time during cultivation, the measurements at the light intensity closest to what cultures had been adapted to (cultivation irradiance) are estimates of the NPQ response in cultures. We observed an inverse correlation between NPQ at the cultivation irradiance and TAG levels for VDL2 OE clones and WT cultures in LL and HL (**Fig. 3.7**). The most striking difference in TAG accumulation as well as in NPQ closest to cultivation irradiance as compared to WT was measured for HL-adapted VDL2 OE clones (**Figs. 3.2B, 3.5B**). HL-adapted VDL2 OE clones were also the only condition that accumulated significantly more protein per cell than WT (**Fig. 3.6B**), and an inverse relationship between cellular protein content and NPQ closest to cultivation irradiance was also found for that condition (**Fig. 3.8A**). In LL, LTL KD clone 51 had substantially less protein per cell than the other clones and WT cultures, and this correlated with substantially higher NPQ as well (**Figs. 3.2C, 3.6C, 3.8B**). Additionally, that clone exhibited markedly slower growth in LL than the other cultures (**Fig. 3.4C**). We suggest that diminished NPQ in cultivation conditions allowed the VDL2 OE clones to utilize more photons for carbon fixation, which was then used to synthesize additional TAG and protein. Conversely, excess NPQ at cultivation irradiance for LL-adapted LTL KD clone 51 would have reduced the amount of light energy available for photosynthesis, resulting in slower growth and reduced protein content. For VDL2 OE clones and WT at LL and HL, extent of NPQ measured closest to irradiance correlated with  $(Ddx+Dtx)/Tot$  ( $R = 0.7$  in LL and  $0.8$  in HL, where  $0$  signifies no correlation and  $1$  a perfect positive correlation) (**Fig.**

**S3.3).** No such correlation was found for LTL KD clone 51, and the increased magnitude of NPQ it exhibited compared to the other LTL KD clones may be attributed to a clonal difference in adapting the light-harvesting machinery to reduced photopigmentation.

HL-adapted LTL KD clones had higher TAG than WT (**Figs. 3.5D, S3.1A**), but no significant variation in NPQ. We suggest that in this case, enhanced TAG accumulation occurred due to growth stress (3.4.2), with some of the fixed carbon stored as TAG instead of being used to fuel growth due to a defect in cell cycle progression. The observed reduced abundance of proteins and photopigments per cell area and smaller cell size could result from such stress as well. Additionally, improved light penetrance into the culture due to reduced cellular pigmentation in LTL KD clones may have contributed to increased carbon fixation and storage as TAG. The milder phenotype observed for LTL KD clones in LL may be explained by a lesser extent of photopigment reduction with respect to WT than in HL.

#### 3.4.4 Concluding Remarks

Our results indicate that reducing the photoprotective Ddx cycle pigments without reducing light-harvesting pigmentation may be a promising strategy for improving TAG and protein productivity in diatoms. Ddx cycle pigments are necessary for NPQ induction and preventing photoinhibition due to excess absorbed light energy and resultant oxidative stress [Lepetit et al. 2010]. However, diatoms may accumulate them in excess of what is needed to protect cells without unnecessarily reducing the amount of light energy available for photochemistry. A similar concept has been reported by Berteotti et al. [2016], who found that downregulating but not completely abolishing NPQ in the chlorophyte *Chlamydomonas reinhardtii* improved biomass productivity in laboratory conditions.

As detailed in Chapter 1, strain performance in laboratory conditions does not always relate to productivity in a production setting. Therefore, it will be important to assess the performance of VDL2 OE in production conditions and explore diel changes in TAG and protein abundance under sinusoidal light and temperature encountered outdoors, as well as productivity throughout the growth curve, to find optimal harvesting conditions. Our preliminary data are promising: in HL, which was closer to production conditions that typically utilize even higher irradiance, harvesting could be timed so as to obtain improved TAG yields, despite the slight growth rate reduction in VDL2 OE clones. For example, VDL2 OE clone 6 grew at the same rate as WT prior to reaching a light-limiting density, while accumulating more TAG and protein (**Figs. 3.4B, 3.5B, 3.6B**). Thus, if harvested prior to slowing, VDL2 OE clone 6 would yield approximately 3-fold more TAG and 2-fold more protein (**Fig. 3.5B, 3.6B**). Other clones were slower than WT throughout the growth curve (**Fig. 3.4B**) but could be harvested to yield an equivalent or increased amount of TAG and protein compared to WT harvested a day later, for example, reducing operating costs. The enhanced protein content in VDL2 OE clones could be used as a high-value co-product for applications such as animal feed, further offsetting the costs of TAG production [Moreno-Garcia et al. 2017]. Although it is not yet known how VDL2 OE clones will perform in a production setting, it is encouraging that Cazzaniga et al. [2014] found that their *Chlorella sorokiniana* mutant with reduced photoantenna size had better biomass productivity than WT outdoors as well as in laboratory conditions.

The ability to enhance TAG production without adversely affecting growth is an important goal for advancing biofuels, as currently their commercialization is stymied by production inefficiency [Trentacoste et al. 2013]. Our VDL2 OE clones suffered somewhat from slower growth compared to WT, especially in light-limiting culture densities. This may be at least partially attributed to excess Fx reducing the light utilization efficiency in cultures. Reducing Ddx cycle pigments without increasing the amount of Fx may result in an improvement over VDL2 OE by

reducing NPQ without impairing growth. As described in Chapters 1 and 2, the abundance of Ddx cycle pigments increases with cultivation irradiance. Some Ddx cycle pigments are bound to photoantenna proteins, while others, including the majority of those synthesized in response to increased irradiance, are dissolved in the lipid shield that surrounds photoantennae [Lepetit et al. 2012]. Light-induced biosynthesis of Ddx cycle pigments appears differentially regulated from the induction of carotenoid biosynthesis when photoantenna proteins need to be populated during chloroplast division (Chapter 1). In Chapter 2, we hypothesized that the two copies of phytoene synthase (PSY, catalyzes the first committed step of carotenoid biosynthesis) found in the *T. pseudonana* genome may serve to differentially activate carotenoid biosynthesis in response to different cellular needs, with PSY1 serving during chloroplast division and PSY2 during irradiance increase. Thus, knocking down PSY2 may be a promising strategy for reducing Ddx cycle pigments without affecting Fx content. It may prove especially useful in sinusoidal light, such as encountered outdoors. As described in Chapter 1, Ddx cycle pigment abundance closely follows light intensity changes when a sinusoidal light regime is applied. Reducing the amplitude of that response by knocking down PSY2, if it functions as hypothesized, may improve light utilization efficiency throughout the photoperiod under sinusoidal light. Another useful approach may be to target proteins involved in NPQ, such as LHCX3 [Hao et al. 2018].

Reducing overall photopigment content may also be considered for TAG productivity improvement in diatoms. Although the LTL KD clones had a slightly reduced protein content and did not accumulate as much additional TAG as VDL2 OE clones did, there was an approximately 25-40% improvement over WT in three out of the four clones (**Fig. 3.5D**). The LTL KD clones had an advantage over VDL2 OE clones in that their growth was not substantially different from WT, even when light-limited (**Fig. 3.4**). The disadvantage of the LTL KD clones was the apparent stress experienced by the cells, which may potentially lead to reduced culture stability in production

conditions. Nevertheless, it will be interesting to evaluate the performance of LTL KD clones in production conditions to assess the utility of overall photosynthetic pigment reduction for improving productivity in diatoms.

### 3.5 METHODS

#### 3.5.1 Cultivation, Sampling, and Growth Curves

WT and TG *T. pseudonana* cultures were cultivated at either 30 or 300  $\mu\text{mol photons m}^{-2}$   $\text{sec}^{-1}$  (natural white LED lighting, superbrightleds.com, NFLS-NW300X3-WHT-LC2), using a 12:12 light:dark regime, at 18°C. 50 mL cultures in Erlenmeyer flasks were maintained in Artificial Sea Water (ASW) medium [Darley and Volcani 1969] with rapid stirring. Each experimental set included 2 WT cultures and 4 TG clones. After inoculation, the cultures were grown to  $1-3 \times 10^6$  cells/mL, then allowed to adapt to the cultivation conditions by daily dilutions that maintained exponential growth with culture density under  $2.5 \times 10^6$  cells/mL for a minimum of 2 weeks prior to sampling. Cultures were rotated between stir plates each day to minimize any position-specific differences and transferred to clean flasks once a week. Sampling for protein content, carbohydrate content, cell/chloroplast dimensions and lipid content, and photosynthetic measurements was performed on separate days, within the first two hours of the light period. After sampling was completed, the cultures were inoculated into fresh 50 mL of ASW for growth curves at approximately  $8-11 \times 10^3$  cells/mL. Cell counts were performed in triplicate daily, including immediately upon inoculation, with the MUSE® Cell Analyzer (EMD Millipore, Billerica, MA) and averaged. Specific growth rates were calculated as  $\ln(x_1-x_0)/t$ , where  $x_1$  = number of cells at the end of exponential growth,  $x_0$  = number of cells at the beginning of exponential growth,  $t$  = number of exponential growth days.

### *3.5.2 Photosynthetic Parameter Measurements*

Photosynthetic parameter measurements were performed using a Walz WATER-PAM fluorometer (Heinz Walz GbmH, Eichenring, Germany). The fluorometer was calibrated by using ASW as a blank. Cultures at  $1\text{-}3 \times 10^6$  cells/mL were dark-adapted for at least 45 minutes prior to measurements. Measurements were performed on 3-4 replicate aliquots from the same culture stocks.  $F_v/F_m$ ,  $\alpha$ ,  $rETR_{max}$ , and  $E_k$  were calculated by the WinControl-3 software (Heinz Walz GbmH, Eichenring, Germany).

### *3.5.3 Silica Staining and Microscopy*

PDMPO (2-(4-pyridyl)-5-((4-(2-dimethylaminoethylaminocarbamoyl)methoxy)phenyl)oxazole), a fluorescent dye that binds to freshly incorporated silica [Shimizu et al. 2001], was used to monitor cell wall formation. 5 mL aliquots of exponentially growing cultures were incubated with .125  $\mu\text{M}$  PDMPO in 40 mL glass culture tubes under the cultivation conditions for 24 hours, allowing for approximately two cell doublings. Cells were imaged using a Zeiss Axio Observer Z1 Inverted Microscope (Carl Zeiss Microimaging Inc., USA). The Zeiss#05 (Ex 395–440 nm, FT 460 nm, Em 470nm LP) filter was used for chlorophyll autofluorescence and Zeiss #21HE (Ex 387/15 nm, FT 409, Em 510/90 nm) was used for PDMPO. Images were acquired using a 40x objective and processed with the AxioVision 4.7.2 software (Carl Zeiss Microimaging Inc., USA).

### *3.5.4 Cell/Chloroplast Dimensions and BODIPY Fluorescence*

$2.5\text{-}8.3 \times 10^7$  exponentially growing cells per sample were harvested by centrifugation and stored at -20°C until processing. Pellets were thawed on ice and resuspended in 0.5 mL 2.3% NaCl. 1.3  $\mu\text{L}$  of 1 mg/mL stock of the lipophilic fluorescent dye BODIPY (4,4-difluoro-4-bora-3a,4a-diaza-s-

indacene, 493/503, Molecular Probes, ThermoFisher Scientific, USA) per sample was added to stain for neutral lipids (TAG). Following a 30 min incubation on ice in the dark, data for 10,000 cells per sample were collected using an ImageStream X imaging flow cytometer with the INSPIRE™ software package (Amnis Corp., Seattle, WA, USA). 0.6 and 1.0 neutral density filters and 488 nm excitation were used during data acquisition. Post-acquisition spectral compensation and data analysis were performed with the IDEAS™ software (Amnis Corp., Seattle, WA, USA) [Hildebrand et al. 2015]. After debris, unfocused cells, and images containing more than one cell were discarded, 1200-7200 cells were analyzed per sample.

### *3.5.5 Protein Content*

1.5-7.2x10<sup>7</sup> cells per replicate were harvested by centrifugation and stored at -20°C until processing. Pellets were thawed on ice and resuspended in 6x volume of extraction buffer (4% SDS, 125 mM Tris-Cl pH 6.8), incubated at 95°C for 5 min, then centrifuged at maximum speed for 3 min. Supernatants were transferred to clean tubes. Protein concentrations were measured using the DC™ Protein Assay (Bio-Rad, Hercules, CA, USA), based on the Lowry method for protein quantification, according to manufacturer's instructions. Absorbance measurements at 750 nm were performed in triplicate using a SpectraMax M2 microplate reader (Molecular Devices LLC, San Jose, CA, USA). A bovine gamma globulin standard (Bio-Rad, Hercules, CA, USA) set was used to generate a standard curve for calculating protein concentrations in the samples.

### *3.5.6 Carbohydrate Content*

Total cellular carbohydrate content was determined using a method adapted from Granum and Myklestad [2002]. 1.8-6.3x10<sup>7</sup> cells per replicate were harvested by centrifugation, washed in

2.3% NaCl, and stored at -20°C until processing. Pellets were thawed on ice, resuspended in 1 mL 0.05 M H<sub>2</sub>SO<sub>4</sub>, incubated in a 60°C water bath for 10 min, then centrifuged at 4000 g for 2 min. Two 400 µL supernatant aliquots per sample were transferred to clean 1.5 mL microfuge tubes for duplicate analysis. 100 µL of 3% freshly prepared aqueous phenol and 1 mL concentrated H<sub>2</sub>SO<sub>4</sub> were added to each tube, followed by vortexing. After a 30 min incubation at room temperature, samples absorbance at 485 nm was measured in a 1 cm quartz cuvette using a DU<sup>TM</sup> 730 spectrophotometer (Beckman Coulter, Brea, CA, USA). 155, 38.75, 9.68, and 2.42 mg/L glucose solutions were used to generate a standard curve for calculating carbohydrate concentrations in the samples.

### 3.5.7 Statistical Analysis

An online one-way ANOVA calculator (<https://www.socscistatistics.com/tests/anova/default2.aspx>) was used to assess the statistical significance of the difference or lack thereof between measurements obtained for TG lines and WT cultures. An online Pearson correlation coefficient calculator (<https://www.socscistatistics.com/tests/pearson/Default2.aspx>) was used to assess two-variable correlations.

## 3.6 ACKNOWLEDGEMENTS

Chapter 3, in full, is material currently being prepared for submission for publication. Gaidarenko, Olga; Yee, Daniel; Hildebrand, Mark. "Enhanced triacylglycerol (TAG) and protein accumulation in transgenic diatom *Thalassiosira pseudonana* with altered photosynthetic pigmentation." Olga Gaidarenko was the principal researcher and author of this work. We thank Dr. Andrew E. Allen and members of his lab for providing access to the Water PAM used in this work.

We also thank Ms. Corinne Sathoff for assistance with cultivation chamber set-up and Image Stream data analysis. Additionally, we thank Dr. James Golden for critically reading this work and providing helpful input. This work was supported by U.S. Dept. of Energy grant DE-FOA-0001471.

**Table 3.1.**

Photosynthetic parameters. VDL2 overexpression (OE) and LTL knockdown (KD) clones are compared to wild-type (WT) cultures in low light ( $30 \mu\text{mol photons m}^{-2}\text{sec}^{-1}$ , LL) and high light ( $300 \mu\text{mol photons m}^{-2}\text{sec}^{-1}$ , HL). Fv/Fm = maximum quantum yield of photosystem II (PSII),  $\alpha$  = light-limited photosynthetic rate, rETR<sub>max</sub> = maximum relative electron transport rate, E<sub>k</sub> = minimum saturating irradiance.

		Fv/Fm	$\alpha$	rETR <sub>max</sub>	E <sub>k</sub>
VDL2 OE LL	WT1	$0.698 \pm 0.009$	$0.214 \pm 0.032$	$119.0 \pm 6.3$	$570.3 \pm 99.7$
	WT2	$0.707 \pm 0.007$	$0.185 \pm 0.021$	$118.3 \pm 6.7$	$652.3 \pm 112.6$
	OE2	$0.697 \pm 0.005$	$0.166 \pm 0.006$	$112.3 \pm 5.6$	$676.9 \pm 34.9$
	OE3	$0.714 \pm 0.030$	$0.158 \pm 0.010$	$102.1 \pm 9.2$	$653.7 \pm 96.1$
	OE6	$0.713 \pm 0.003$	$0.191 \pm 0.031$	$104.3 \pm 10.8$	$570.3 \pm 162.5$
	OE7	$0.688 \pm 0.003$	$0.196 \pm 0.002$	$102.9 \pm 11.7$	$524.5 \pm 64.1$
	p-value	0.9	0.3	0.02	0.9
VDL2 OE HL	WT1	$0.699 \pm 0.008$	$0.158 \pm 0.008$	$217.1 \pm 36.3$	$1368.6 \pm 179.4$
	WT2	$0.679 \pm 0.007$	$0.135 \pm 0.000$	$151.0 \pm 5.9$	$1119.9 \pm 49.0$
	OE2	$0.685 \pm 0.008$	$0.175 \pm 0.019$	$146.9 \pm 7.8$	$850.5 \pm 113.7$
	OE3	$0.680 \pm 0.002$	$0.173 \pm 0.026$	$133.7 \pm 16.5$	$803.6 \pm 194.3$
	OE6	$0.678 \pm 0.005$	$0.156 \pm 0.024$	$115.8 \pm 10.4$	$770.8 \pm 166.4$
	OE7	$0.685 \pm 0.008$	$0.164 \pm 0.031$	$136.4 \pm 19.4$	$882.8 \pm 257.9$
	p-value	0.4	0.1	0.09	0.008
LTL KD LL	WT1	$0.711 \pm 0.009$	$0.184 \pm 0.018$	$125.4 \pm 8.2$	$692.9 \pm 95.9$
	WT2	$0.713 \pm 0.007$	$0.210 \pm 0.007$	$119.9 \pm 10.3$	$573.5 \pm 67.1$
	KD49	$0.693 \pm 0.009$	$0.194 \pm 0.022$	$110.7 \pm 3.9$	$578.6 \pm 68.4$
	KD51	$0.703 \pm 0.011$	$0.190 \pm 0.010$	$104.5 \pm 4.3$	$550.7 \pm 33.8$
	KD60	$0.706 \pm 0.007$	$0.197 \pm 0.020$	$119.9 \pm 5.8$	$617.0 \pm 95.4$
	KD71	$0.709 \pm 0.009$	$0.183 \pm 0.017$	$117.3 \pm 8.9$	$650.3 \pm 111.5$
	p-value	0.2	0.6	0.2	0.5
LTL KD HL	WT1	$0.639 \pm 0.006$	$0.141 \pm 0.007$	$97.9 \pm 17.9$	$702.8 \pm 150.5$
	WT2	$0.625 \pm 0.002$	$0.147 \pm 0.003$	$85.0 \pm 5.0$	$581.4 \pm 44.2$
	KD49	$0.609 \pm 0.004$	$0.158 \pm 0.008$	$81.8 \pm 11.2$	$517.4 \pm 55.4$
	KD51	$0.628 \pm 0.009$	$0.153 \pm 0.016$	$72.2 \pm 11.0$	$483.1 \pm 113.4$
	KD60	$0.625 \pm 0.004$	$0.172 \pm 0.023$	$92.3 \pm 10.5$	$554.6 \pm 131.9$
	KD71	$0.647 \pm 0.027$	$0.154 \pm 0.014$	$92.9 \pm 15.1$	$617.0 \pm 138.9$
	p-value	0.7	0.08	0.5	0.2

**Table 3.2.**

Average cell and chloroplast (Chl) area measurements, their ratio, and specific growth rates. VDL2 overexpression (OE) and LTL knockdown (KD) clones are compared to wild-type (WT) cultures in low light ( $30 \mu\text{mol photons m}^{-2} \text{sec}^{-1}$ , LL) and high light ( $300 \mu\text{mol photons m}^{-2} \text{sec}^{-1}$ , HL).

		Cell Area	Chl Area	Chl/Cell Area	Specific Growth Rate ( $\mu, \text{day}^{-1}$ )
VDL2 OE LL	WT1	$37.8 \pm 4.8$	$22.7 \pm 4.5$	0.60	2.26
	WT2	$39.4 \pm 5.0$	$23.7 \pm 4.5$	0.60	2.27
	OE2	$40.2 \pm 5.8$	$23.7 \pm 5.1$	0.59	2.22
	OE3	$39.0 \pm 6.3$	$22.1 \pm 5.5$	0.57	2.22
	OE6	$37.1 \pm 5.8$	$19.5 \pm 5.5$	0.53	2.22
	OE7	$37.3 \pm 6.0$	$21.4 \pm 5.2$	0.57	2.21
	<i>p-value</i>	0.9	0.3	0.1	0.0006
VDL2 OE HL	WT1	$38.2 \pm 5.9$	$23.1 \pm 4.7$	0.60	3.86
	WT2	$39.5 \pm 5.8$	$23.1 \pm 5.0$	0.59	3.85
	OE2	$38.0 \pm 7.0$	$21.0 \pm 6.8$	0.55	3.62
	OE3	$36.5 \pm 6.9$	$20.6 \pm 6.5$	0.56	3.71
	OE6	$38.2 \pm 6.3$	$21.6 \pm 6.1$	0.56	3.58
	OE7	$39.8 \pm 6.8$	$22.7 \pm 6.8$	0.57	3.68
	<i>p-value</i>	0.5	0.08	0.02	0.009
LTL KD LL	WT1	$41.6 \pm 5.8$	$20.7 \pm 5.7$	0.50	1.83
	WT2	$43.3 \pm 6.5$	$22.8 \pm 6.1$	0.53	1.83
	KD49	$40.4 \pm 6.7$	$23.9 \pm 6.7$	0.59	1.79
	KD51	$41.2 \pm 6.8$	$24.5 \pm 7.5$	0.59	1.77
	KD60	$40.8 \pm 7.1$	$24.6 \pm 7.7$	0.60	1.80
	KD71	$39.5 \pm 6.7$	$20.4 \pm 6.1$	0.52	1.81
	<i>p-value</i>	0.06	0.4	0.1	0.04
LTL KD HL	WT1	$48.4 \pm 7.4$	$24.9 \pm 6.2$	0.51	3.80
	WT2	$48.0 \pm 8.3$	$26.0 \pm 6.6$	0.54	3.72
	KD49	$43.2 \pm 6.9$	$22.3 \pm 5.1$	0.52	3.68
	KD51	$45.3 \pm 8.3$	$24.2 \pm 6.4$	0.53	3.59
	KD60	$45.5 \pm 8.3$	$24.0 \pm 7.0$	0.53	3.66
	KD71	$46.0 \pm 8.7$	$23.1 \pm 7.0$	0.50	3.54
	<i>p-value</i>	0.03	0.05	0.6	0.06

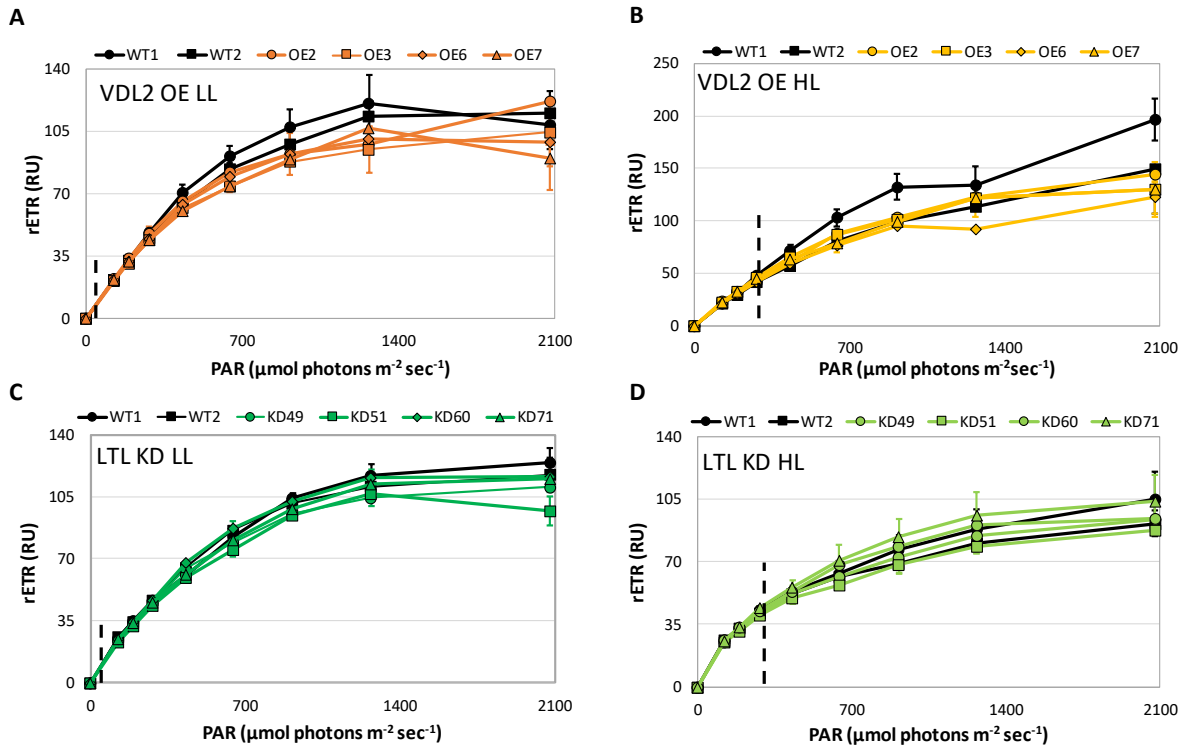


**Figure. 3.1.**

Rapid light curves, relative electron transfer rates (rETR – relative units, RU) vs. photosynthetically active radiation (PAR). Vertical dashed black lines indicate irradiance to which the cultures were adapted. Data are presented as averages of 3-4 replicates  $\pm$  standard deviation. **A.**  $30 \mu\text{mol photons m}^{-2} \text{sec}^{-1}$  (low light - LL)-adapted VDL2 overexpression (OE) clones vs. wild-type (WT); **B.**  $300 \mu\text{mol photons m}^{-2} \text{sec}^{-1}$  (high light - HL)-adapted VDL2 OE clones vs. WT; **C.** LL-adapted LTL knockdown (KD) clones vs. WT; **D.** HL-adapted LTL KD clones vs. WT.

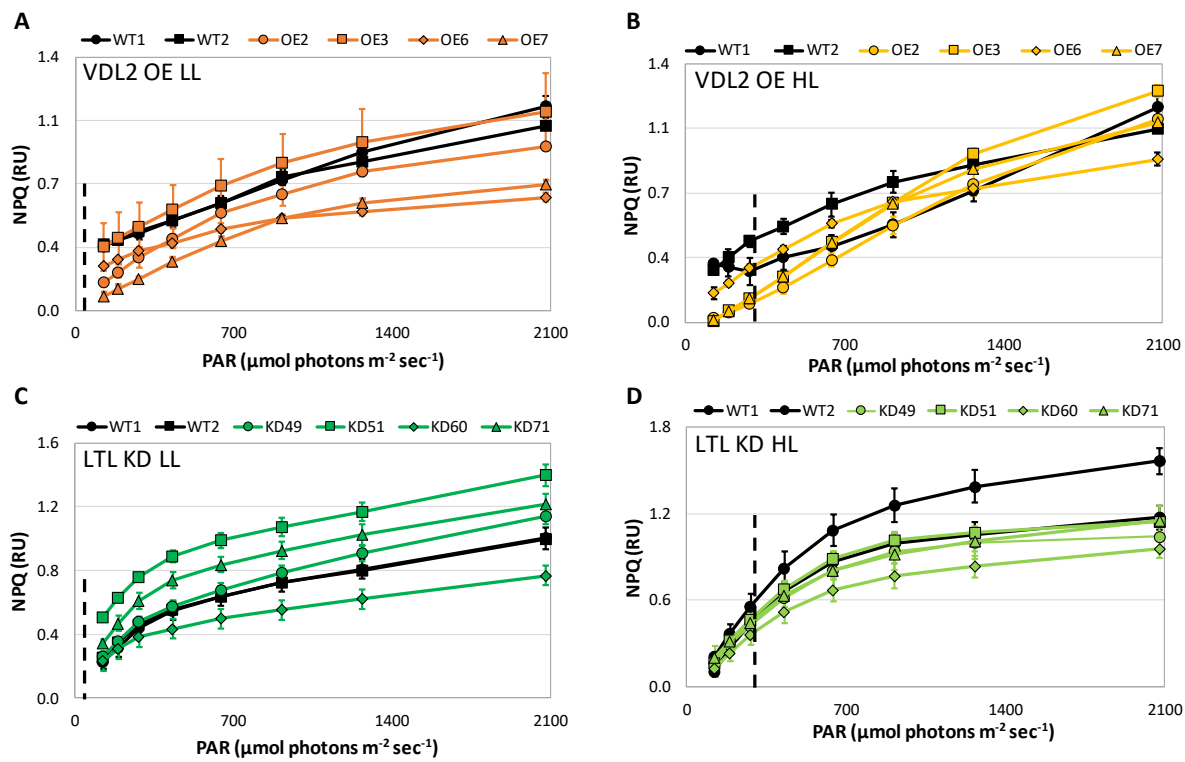


**Figure. 3.2.**

Rapid light curve-derived non-photosynthetic quenching values (NPQ – relative units, RU) vs. photosynthetically active radiation (PAR). Vertical dashed black lines indicate irradiance to which the cultures were adapted. Data are presented as averages of 3-4 replicates  $\pm$  standard deviation. **A.** 30  $\mu\text{mol photons m}^{-2} \text{sec}^{-1}$  (low light - LL)-adapted VDL2 overexpression (OE) clones vs. wild-type (WT); **B.** 300  $\mu\text{mol photons m}^{-2} \text{sec}^{-1}$  (high light - HL)-adapted VDL2 OE clones vs. WT; **C.** LL-adapted LTL knockdown (KD) clones vs. WT; **D.** HL-adapted LTL KD clones vs. WT.

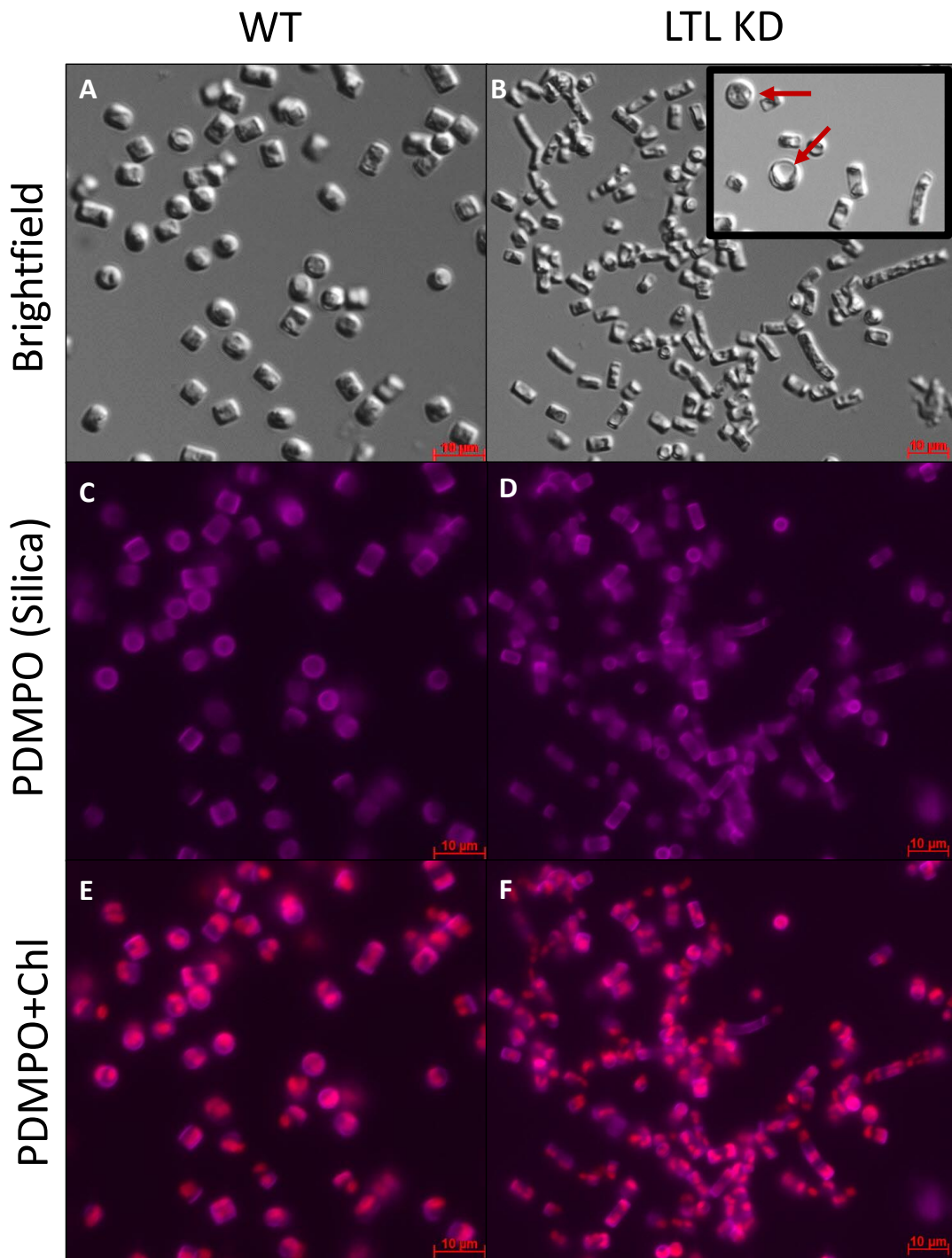


**Figure. 3.3.**

Wild-type (WT) (A, C, E) and LTL knockdown (KD) (B, D, F) cultures, cultivated at  $300 \mu\text{mol}$  photons  $\text{m}^{-2} \text{sec}^{-1}$  (high light - HL). A, B. Brightfield. Red arrows indicate auxospores; C, D. PDMPO staining for silica; E, F. PDMPO and chlorophyll fluorescence (Chl).

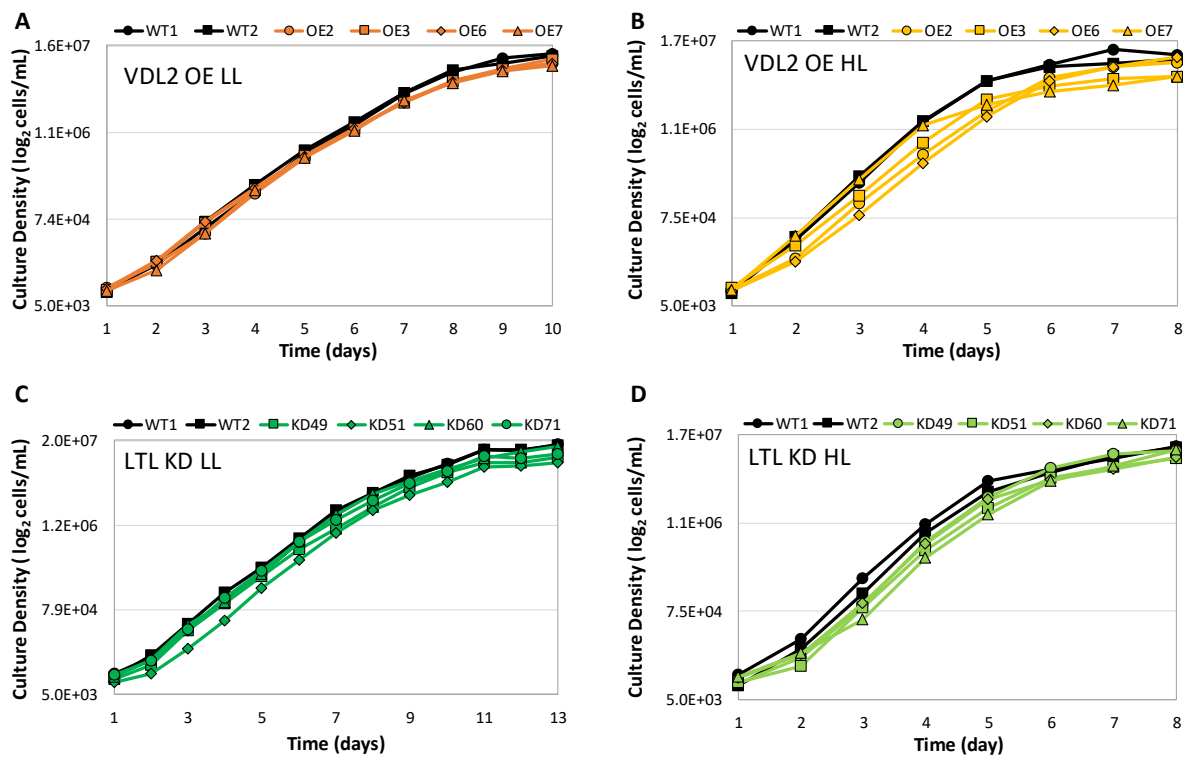


**Figure. 3.4.**

Growth curves. Each data point represents an average of three technical replicates.

**A.**  $30 \mu\text{mol photons m}^{-2} \text{sec}^{-1}$  (low light - LL)-adapted VDL2 overexpression (OE) clones vs. wild-type (WT); **B.**  $300 \mu\text{mol photons m}^{-2} \text{sec}^{-1}$  (high light - HL)-adapted VDL2 OE clones vs. WT; **C.** LL-adapted LTL knockdown (KD) clones vs. WT; **D.** HL-adapted LTL KD clones vs. WT.

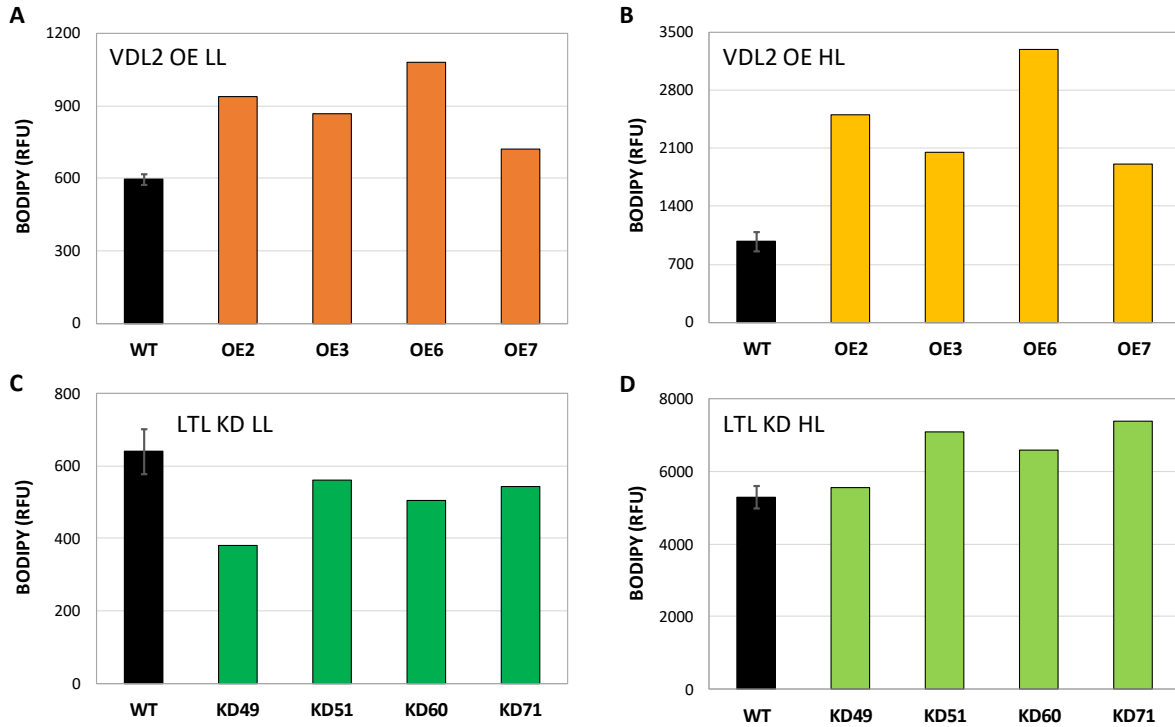


**Figure. 3.5.**

Average BODIPY fluorescence (relative fluorescence units – RFU). Wild-type (WT) data are presented as averages of two independent cultures  $\pm$  standard deviation. **A.** 30  $\mu\text{mol}$  photons  $\text{m}^{-2} \text{ sec}^{-1}$  (low light - LL)-adapted VDL2 overexpression (OE) clones vs. wild-type (WT); **B.** 300  $\mu\text{mol}$  photons  $\text{m}^{-2} \text{ sec}^{-1}$  (high light - HL)-adapted VDL2 OE clones vs. WT; **C.** LL-adapted LTL knockdown (KD) clones vs. WT; **D.** HL-adapted LTL KD clones vs. WT.

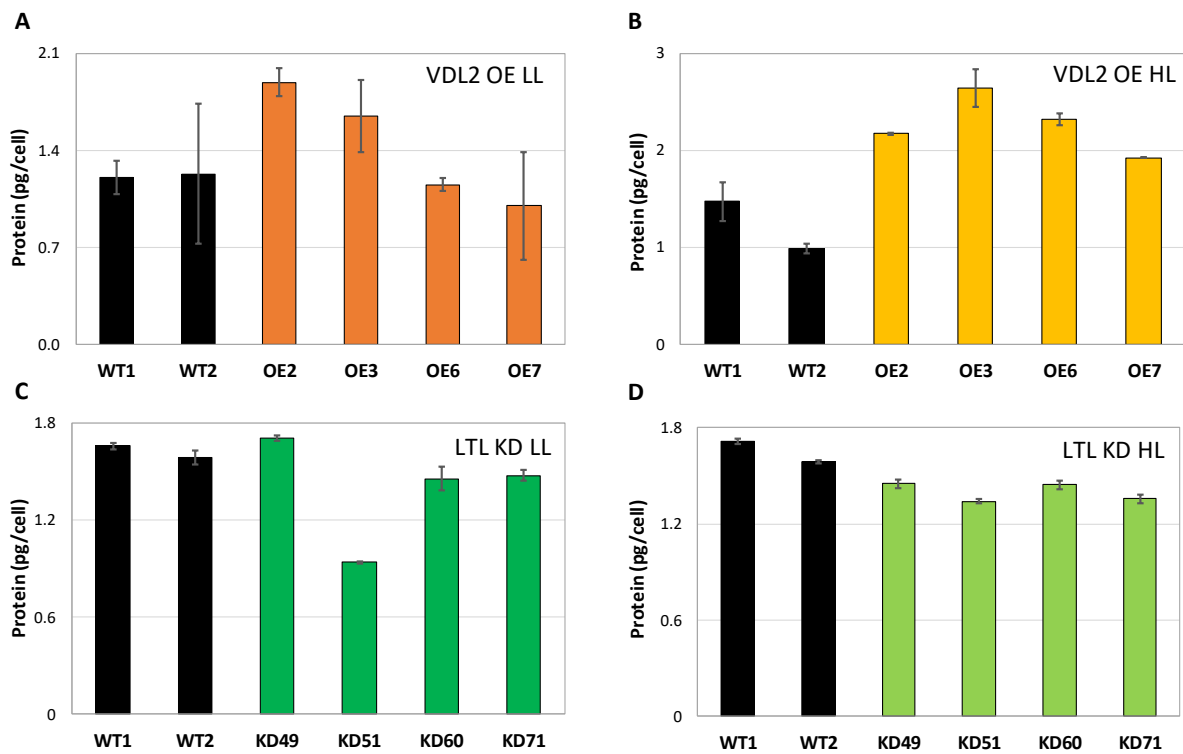


**Figure. 3.6.**

Average total cellular protein content. Data are presented as averages of two technical replicates  $\pm$  standard deviation. **A.**  $30 \mu\text{mol photons m}^{-2} \text{ sec}^{-1}$  (low light - LL)-adapted VDL2 overexpression (OE) clones vs. wild-type (WT); **B.**  $300 \mu\text{mol photons m}^{-2} \text{ sec}^{-1}$  (high light - HL)-adapted VDL2 OE clones vs. WT; **C.** LL-adapted LTL knockdown (KD) clones vs. WT; **D.** HL-adapted LTL KD clones vs. WT.

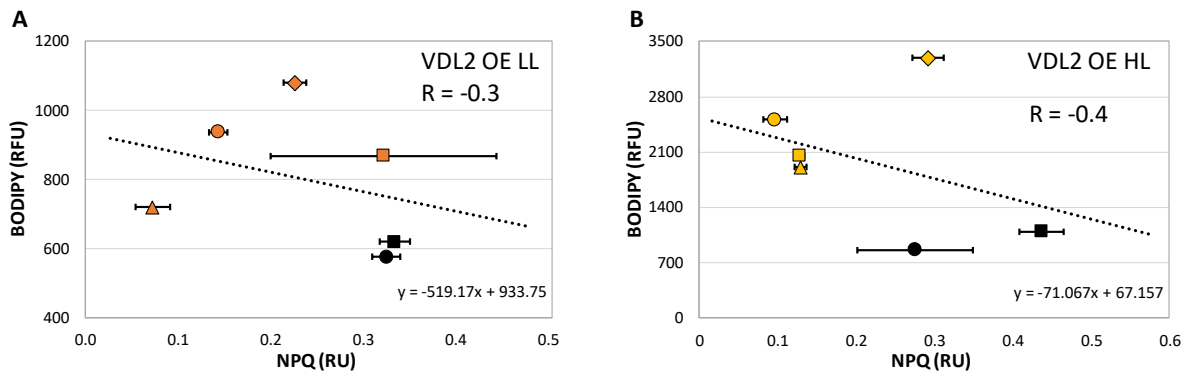


**Figure 3.7.**

Relationship between non-photochemical quenching (NPQ, relative units - RU) at irradiance to which the cultures were adapted and average BODIPY fluorescence (relative fluorescence units, RFU). Data are presented as averages of 3-4 technical replicates  $\pm$  standard deviation for NPQ. Pearson correlation coefficient (R) is indicated on the plots. Wild-type (WT) cultures are represented by black circles (WT1) and squares (WT2). VDL2 overexpression (OE) clones are represented by orange circles (VDL2 OE2), squares (VDL2 OE3), rhombuses (VDL2 OE6), and triangles (VDL 2 OE7). **A.**  $30 \mu\text{mol photons m}^{-2} \text{sec}^{-1}$  (low light - LL)-adapted VDL2 OE clones vs. WT; **B.**  $300 \mu\text{mol photons m}^{-2} \text{sec}^{-1}$  (high light - HL)-adapted VDL2 OE clones vs. WT.

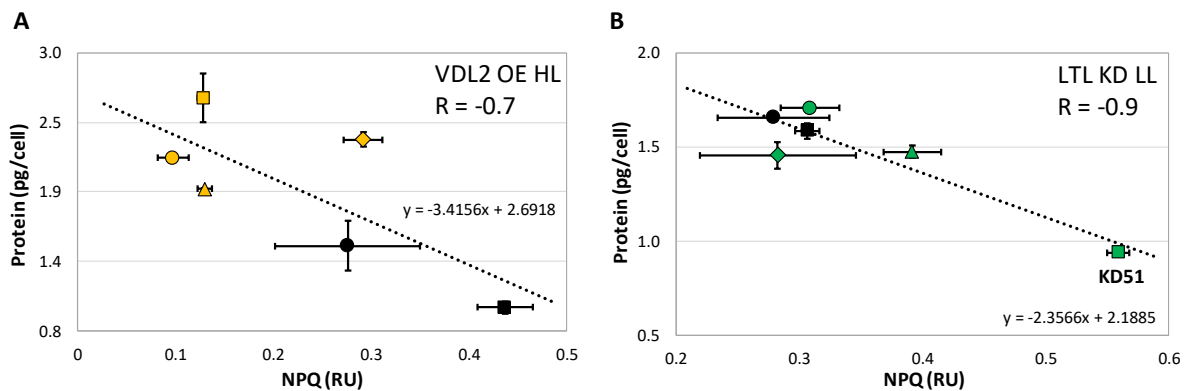


**Figure 3.8.**

Relationship between non-photochemical quenching (NPQ – relative units, RU) at irradiance to which the cultures were adapted and average cellular protein content. Data are presented as averages of two technical replicates  $\pm$  SD for protein content, and as averages of 3-4 technical replicates  $\pm$  SD for NPQ. Pearson correlation coefficient (R) is indicated on the plots. Wild-type (WT) cultures are represented by black circles (WT1) and squares (WT2). VDL2 overexpression (OE) clones are represented by orange circles (VDL2 OE2), squares (VDL2 OE3), rhombuses (VDL2 OE6), and triangles (VDL 2 OE7). LTL knockdown (KD) clones are represented by green circles (LTL KD49), squares (LTL KD51), rhombuses (LTL KD60), and triangles (LTL KD71). **A.**  $300 \mu\text{mol photons m}^{-2} \text{sec}^{-1}$  (high light - HL)-adapted VDL2 OE clones vs. WT; **B.**  $30 \mu\text{mol photons m}^{-2} \text{sec}^{-1}$  (low light - LL)-adapted LTL KD clones vs. WT. Clone LTL KD51 is labeled on the plot.

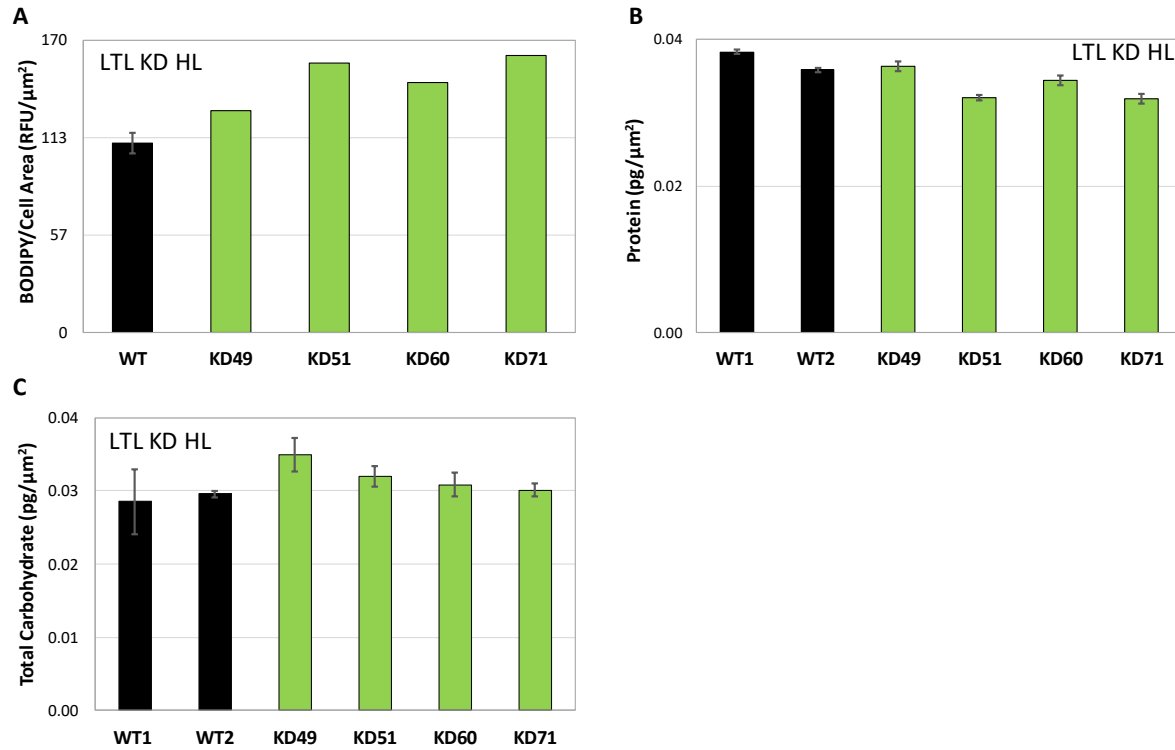


**Figure. S3.1.**

**A.** Average BODIPY fluorescence (relative fluorescence units – RFU) normalized by average cell area.  $300 \mu\text{mol photons m}^{-2} \text{sec}^{-1}$ (high light - HL)-adapted LTL knockdown (KD) clones vs. wild-type (WT). WT data is presented as an average of two independent cultures  $\pm$  standard deviation; **B.** Average cellular protein content normalized by average cell area. HL-adapted LTL KD clones vs. WT. Data are presented as averages of two technical replicates  $\pm$  standard deviation. **C.** Average total cellular carbohydrate content normalized by average cell area. HL-adapted LTL KD clones vs. WT. Data are presented as averages of two technical replicates  $\pm$  standard deviation.

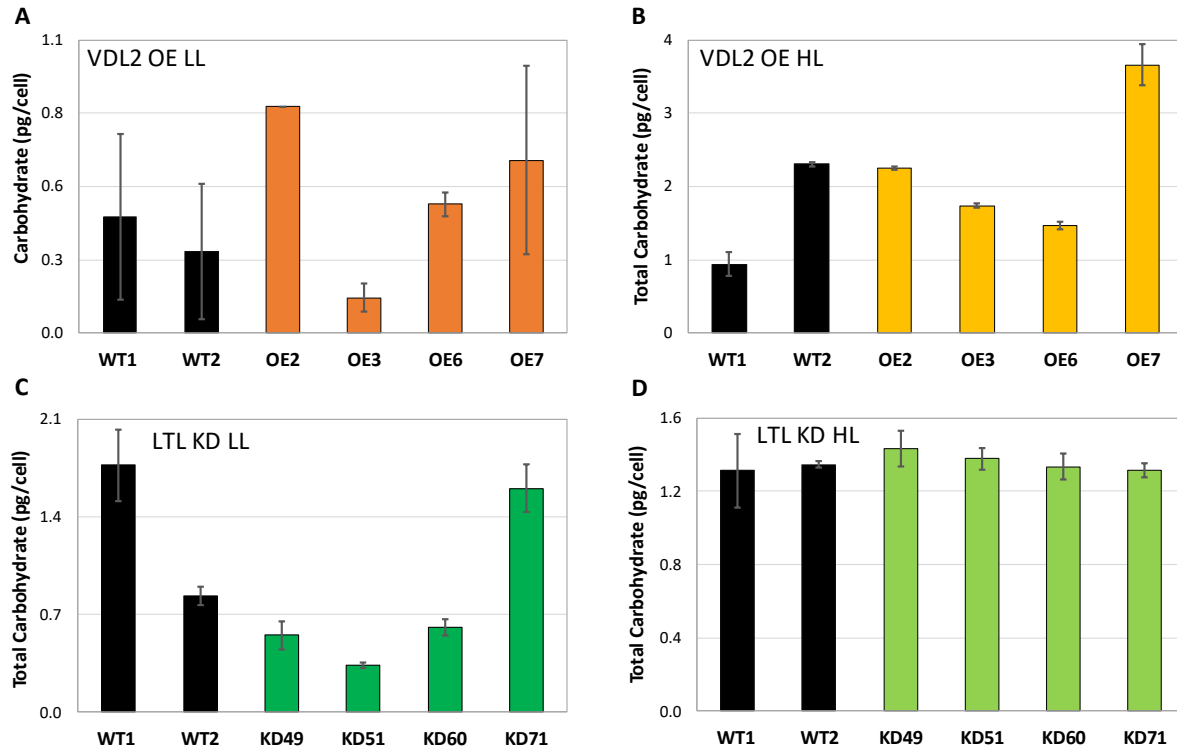


**Figure. S3.2.**

Average total cellular carbohydrate content. Data are presented as averages of two technical replicates  $\pm$  standard deviation. **A.**  $30 \mu\text{mol photons m}^{-2} \text{ sec}^{-1}$  (low light - LL)-adapted VDL2 overexpression (OE) clones vs. wild-type (WT); **B.**  $300 \mu\text{mol photons m}^{-2} \text{ sec}^{-1}$  (high light - HL)-adapted VDL2 OE clones vs. WT; **C.** LL-adapted LTL knockdown (KD) clones vs. WT; **D.** HL-adapted LTL KD clones vs. WT.

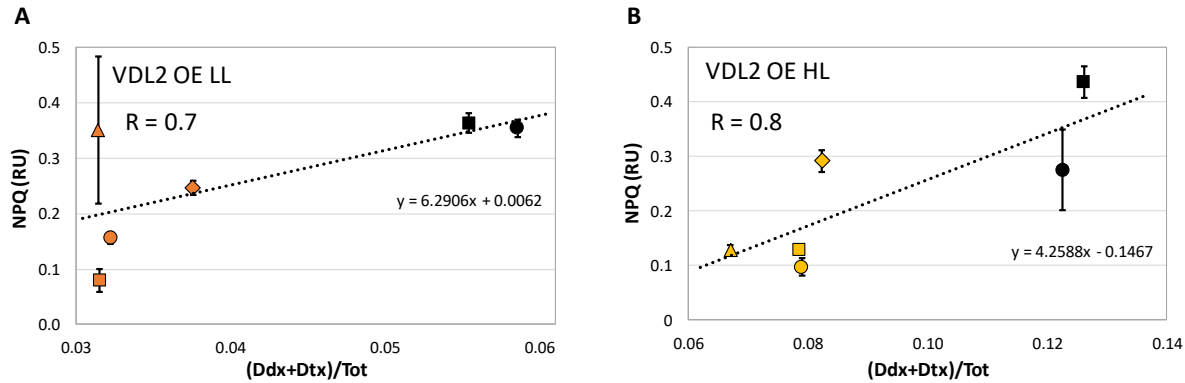


**Figure. S3.3.**

Relationship between the ratio of diadinoxanthin cycle pigments to total cellular photopigment content ( $(Ddx+Dtx)/Tot$ ) and non-photochemical quenching (NPQ, relative units - RU) at irradiance to which the cultures were adapted. Data are presented as averages of 3-4 technical replicates  $\pm$  standard deviation for NPQ. Pearson correlation coefficient (R) is indicated on the plots. Wild-type (WT) cultures are represented by black circles (WT1) and squares (WT2). VDL2 overexpression (OE) clones are represented by orange circles (VDL2 OE2), squares (VDL2 OE3), rhombuses (VDL2 OE6), and triangles (VDL2 OE7). **A.**  $30 \mu\text{mol photons m}^{-2} \text{sec}^{-1}$  (low light - LL)-adapted VDL2 OE clones vs. WT; **B.**  $300 \mu\text{mol photons m}^{-2} \text{sec}^{-1}$  (high light - HL)-adapted VDL2 OE clones vs. WT.

### 3.7 REFERENCES

- Beckmann J., Lehr F., Finazzi G., Hankamer B., Posten C., Wobbe L., Kruse O. (2009) Improvement of light to biomass conversion by de-regulation of light-harvesting protein translation in *Chlamydomonas reinhardtii*. *J Biotechnol* 142: 70-77.
- Berteotti S., Ballottari M., Bassi R. (2016) Increased biomass productivity in green algae by tuning non-photochemical quenching. *Sci Rep* 6:21339.
- Cazzaniga S., Dall’Osto L., Szaub J., Scibilia L., Ballotari M., Purton S., Bassi R. (2014) Domestication of the green alga *Chlorella sorokiniana*: reduction of antenna size improves light-use efficiency in a photobioreactor. *Biotechnol Biofuels* 7:157.
- Darley W., Volcani B. (1969) Role of silicon in diatom metabolism: a silicon requirement for deoxyribonucleic acid synthesis in the diatom *Cylindrotheca fusiformis* Reimann and Lewin. *Exp Cell Res* 58: 334–42.
- Davis A. K., Hildebrand M., Palenik B. (2005) A stress-induced protein associated with the girdle band region of the diatom *Thalassiosira pseudonana* (Bacillariophyta). *J Phycol* 41: 577-589.
- de Mooij T., Janssen M., Cerezo-Chinarro O., Mussgnug J. H., Kruse O., Ballottari M., Bassi R., Bujaldon S., Wollman F., Wijffels R. H. (2015) Antenna size reduction as a strategy to increase biomass productivity: a great potential not yet realized. *J Appl Phycol* 27: 1063-1077.
- Granum E., Myklestad S. M. (2002) A simple combined method for determination of β-1,3-glucan and cell wall polysaccharides in diatoms. *Hydrobiologia* 477: 155-161.
- Hao T., Jiang T., Dong H., Ou L., He X., Yang Y. (2018) Light-harvesting protein LhcX3 is essential for high light acclimation of *Phaeodactylum tricornutum*. *AMB Expr* 8: 174.
- Hildebrand M., Davis A., Abbriano R., Pugsley H. R., Traller J. C., Smith S. R., Shrestha R., Cook O., Sanchez-Alvarez E. L., Manandhar-Shrestha K., Alderete B. (2016) Applications of imaging flow cytometry for microalgae. In: Barteneva N., Vorobjev I. (eds.), *Imaging Flow Cytometry. Methods in Molecular Biology* vol. 1389. Humana Press, New York, NY.
- Hildebrand M., Davis A., Smith S. R., Traller J. C., Abbriano R. (2012) The place of diatoms in the biofuels industry. *Biofuels* 3(2): 221-240.
- Huesemann M. A., Hausmann T. S., Bartha R., Aksoy M., Weissman J. C., Benemann J. R. (2009) Biomass productivities in wild type and mutant of *Cyclotella* (sp.) (diatom). *Appl Biochem Biotechnol* 157: 507-526.
- Jeong J., Baek K., Kirst H., Melis A., Jin E. (2017) Loss of CpSRP54 function leads to a truncated light-harvesting antenna size in *Chlamydomonas reinhardtii*. *Biochim Biophys Acta* 1858: 45-55.
- Kirst H., Garcia-Cerdan J. G., Zurbriggen A., Melis A. (2012) Assembly of the light-harvesting chlorophyll antenna in the green alga *Chlamydomonas reinhardtii* requires expression of the *TLA2-CpFTSY* gene. *Plant Physiol* 158: 930-945.

Kirst H., Garcia-Cerdan J. G., Zurbriggen A., Ruehle T., Melis A. (2012) Truncated photosystem chlorophyll antenna size in the green microalga *Chlamydomonas reinhardtii* upon deletion of the *TLA3-CpSRP43* gene. *Plant Physiol* 160: 2251-2260.

Lepetit B., Goss R., Jakob T., Wilhelm C. (2012) Molecular dynamics of the diatom thylakoid membrane under different light conditions. *Photosynth Res* 111(1-2): 245-257.

Lepetit B., Volke D., Gilbert M., Wilhelm C., Goss R. (2010) Evidence for existence of one antenna-associated, lipid-dissolved and two protein-bound pools of diadinoxanthin cycle pigments in diatoms. *Plant Physiol* 154: 1906-1920.

Malapascua J. R. F., Jerez C. G., Sergejevova M., Figueroa F. L., Masojidek J. (2014) Photosynthesis monitoring to optimize growth of microalgal mass cultures: application of chlorophyll fluorescence techniques. *Aquat Biol* 22: 123-140.

Mata T. M., Martins A. A., Caetano N. S. (2010) Microalgae for biodiesel production and other applications: a review. *Renew Sust Energ Rev* 14: 217-232.

Mitra M., Melis A. (2008) Optical properties of microalgae for enhanced biofuels production. *Opt Express* 16(26): 21807-21820.

Moore E. R., Bullington B. S., Weisberg A. J., Jiang Y., Chang J., Halsey K. H. (2017) Morphological and transcriptomic evidence for ammonium induction of sexual reproduction in *Thalassiosira pseudonana* and other centric diatoms. *PLoS One* 12(7): e0181098.

Moreno-Garcia L., Adjalle K., Sarbane S., Raghavan G. S. V. (2017) Microalgae biomass production for a biorefinery system: recent advances and the way towards sustainability. *Renew Sust Energ Rev* 76: 493-506.

Moskalenko A. A., Karapetyan N. V. (1996) Structural role of carotenoids in photosynthetic membranes. *Z Naturforsch* 51c: 763-771.

Mussgnug J. H., Thomas-Hall S., Rupprecht J., Foo A., Klassen V., McDowall A., Schenk P. M., Kruse O., Hankamer B. (2007) Engineering photosynthetic light capture: impacts on improved solar energy to biomass conversion. *Plant Biotechnol J* 5: 802-814.

Nakajima Y., Tsuzuki M., Ueda R. (2001) Improved productivity by reduction of the content of light-harvesting pigment in *Chlamydomonas perigranulata*. *J Appl Phycol* 13: 95-101.

Polle J. E. W., Kanakagiri S., Melis A. (2003) *tla1*, a DNA insertional transformant of the green alga *Chlamydomonas reinhardtii* with a truncated light-harvesting chlorophyll antenna size. *Planta* 217: 49-59.

Ralph P. J., Gaderman R. (2005) Rapid light curves: a powerful tool to assess photosynthetic activity. *Aquat Bot* 82(3): 222-237.

Santabarbara S., Casazza A. P., Ali K., Economou C. K., Wannathong T., Zito F., Redding K. E., Rappaport F., Purton S. (2013) The requirement for carotenoids in the assembly and function of photosynthetic complexes in *Chlamydomonas reinhardtii*. *Plant Physiol* 161: 535-546.

Shimizu K., Del Amo Y., Brzezinski M. A., Stucky G. D., Morse D. E. (2001) A novel fluorescent silica tracer for biological silicification studies. *Chem Biol* 8: 1051-1060.

Shin W., Lee B., Jeong B., Chang Y. K., Kwon J. (2016) Truncated light-harvesting chlorophyll antenna size in *Chlorella vulgaris* improves biomass productivity. *J Appl Phycol* 28: 3193-3202.

Shin W., Lee B., Kang N. K., Kim Y., Jeong W., Kwon J., Jeong B., Chang Y. K. (2017) Complementation of a mutation in *CpSRP43* causing partial truncation of light-harvesting chlorophyll antenna in *Chlorella vulgaris*. *Sci Rep* 7:17929.

Smith S. R., Abriano R. M., Hildebrand M. (2012) Comparative analysis of diatom genomes reveals substantial differences in the organization of carbon partitioning pathways. *Algal Res* 1(1): 2-16.

Sumiya N., Fujiwara T., Era A., Miyagishima S. (2016) Chloroplast division checkpoint in microalgae. *PNAS* 113(47): E7629-E7638.

Trentacoste E. M., Shrestha R. P., Smith S. R., Gle C., Hartmann A. C., Hildebrand M., Gerwick W. H. (2013) Metabolic engineering of lipid catabolism increases microalgal lipid accumulation without compromising growth. *PNAS* 110(49): 19748-19753.

Wilhelm C., Buchel C., Fisahn J., Goss R., Jakob T., LaRoche J., Lavaud J., Lohr M., Riebesell U., Stehfest K., Valentin K., Kroth P. G. (2006) The regulation and nutrient assimilation in diatoms is significantly different from green algae. *Protist* 157(2): 91-124.

## **CONCLUSIONS**

Microalgae present a promising solution to the increasing need for sustainable production of food, fuel, and chemical products [Mata et al. 2010]. The objective of this dissertation was to contribute information towards the goal of improving microalgal productivity and therefore making microalgal production economically competitive. One issue that was addressed is the disconnect often observed between the performance of microalgal strains in the laboratory versus production conditions (Chapter 1). The other issue was the suboptimal light utilization efficiency in dense microalgal cultures, which is currently a major hurdle to the economic viability of large-scale microalgal production (Chapters 2 and 3).

Promising microalgal strains that have been developed or screened in the laboratory often fail to deliver when tested in production conditions [e. g. de Mooij et al. 2015]. This has to do with differences in numerous variables, including light and temperature. In the laboratory, light and temperature are often constant, or the light is switched on and off abruptly. To take advantage of sunlight, most commercial microalgal cultivation happens outdoors, where light and temperature follow sinusoidal diel patterns. Changes in temperature and light have been found to affect microalgal growth and productivity [Bonnefond et al. 2016, Edmundson and Huesemann 2015, Ogbonna and Tanaka 1996, Orefice et al. 2016, Yang et al. 2016], and it is thus important to understand diel metabolic and physiological changes microalgal cultures experience when cultivated outdoors in order to optimize their performance. Chapter 1 followed cell cycle progression and changes in optical density (proxy for biomass), triacylglycerol (TAG, neutral lipid of interest for biofuel production), and photopigments in the production candidate diatom *Cyclotella cryptica* subject to diel sinusoidal changes in light and temperature, mimicking outdoor conditions. A major finding was that hypothetical product yields differ substantially throughout the day. This relates to the timing of light energy availability, as well as various physiological and metabolic processes such as synchronous cell cycle progression typical of microalgal cultures grown on a

light/dark cycle. Generally, TAG and biomass yields would be greatest towards the end of the light period, regardless of the species and conditions used. This is because at that time, carbon fixation for the day would be complete, but night-time energy-requiring processes would not have yet started. In our system, harvesting in the evening rather than in the morning would have increased TAG yield 4-6-fold, biomass yield 2-3-fold, and photopigment yield 1.5-3-fold. Taxonomic differences that affect the timing of various processes, as well as variables that need to be optimized for maximal yields in a microalgal production system were discussed.

Additionally, photopigment dynamics were recorded with unprecedented resolution, providing insight into how their cellular abundance responds to cell cycle progression (and therefore chloroplast division) and irradiance changes. Notably, the major diatom photoprotective pigment diadinoxanthin (Ddx), together with its de-epoxidized form diatoxanthin (Dtx), followed the sinusoidal changes in light intensity closely, while the abundance of other photopigments was affected by cell cycle progression. These results indicate that the abundance of Ddx+Dtx is regulated separately from the main accessory light-harvesting photopigment fucoxanthin (Fx). This is intriguing, because Ddx/Dtx and Fx are end products of a branched carotenoid biosynthesis pathway that is still poorly understood in diatoms [Bertrand 2010, Coesel et al. 2008].

Chapters 2 and 3 focused on improving light utilization efficiency, and therefore productivity, in diatom cultures. Dense microalgal cultures suffer from uneven light distribution because microalgae evolved very efficient light harvesting and dissipation of excess light energy. Cells closest to the light source absorb too much light and dissipate what they do not use, and cells deeper into the culture are shaded [de Mooij et al. 2015]. As a solution, reducing the light-harvesting or dissipating capacity of microalgal cells has been explored, with some success, mostly in chlorophytes. Diatoms differ in light-harvesting and dissipation strategies from chlorophytes and are highly productive [Hildebrand et al. 2012, Wilhelm et al. 2006]. Thus, we aimed to explore

improving light utilization efficiency in diatom cultures as a means of further increasing productivity. Because the main diatom accessory light-harvesting pigment Fx and the pigment pool responsible for photoprotection and dissipation of excess light energy (Ddx/Dtx) are products of understudied diatom carotenoid biosynthesis [Bertrand 2010, Coesel et al. 2008], Chapter 2 focused on elucidating the pathway in order to identify genetic manipulation targets. The model diatom *Thalassiosira pseudonana* was chosen based on the availability of genomic, transcriptomic, and physiological data, as well as a suite of genetic manipulation tools. A major finding was the identification of a novel violaxanthin de-epoxidase-like enzyme (VDL2, Thaps3\_11707), that participates in Fx biosynthesis. Heretofore, no enzymes responsible for Fx biosynthesis have been identified. Furthermore, this is the first documented function for a VDL. VDLs have been hypothesized to participate in photoprotective xanthophyll cycling wherein pigments are interconverted by epoxidation and de-epoxidation based on their similarity to the enzyme violaxanthin de-epoxidase that catalyzes the de-epoxidation reactions [Bertrand 2010]. Our findings do not support that hypothesis and demonstrate a separate role for a VDL. Additionally, another candidate that may also participate in Fx biosynthesis was identified (Thaps3\_10233).

Another major finding was that reducing Fx results in an overall reduction in photopigments including chlorophylls, which are products of a separate biosynthetic pathway. Ratios of photopigments to each other were not changed. We hypothesize that Fx plays a role in the assembly and stabilization of diatom light-harvesting complexes, as other carotenoids have been found to do in other organisms [Moskalenko and Karapetyan 1996, Santabarbara et al. 2013]. One outcome of this finding is it appears to not be possible to selectively reduce Fx abundance without affecting the content of other photopigments as a possible strategy to improve light utilization efficiency. Three separate lines silencing VDL1, VDL2, and both copies of LUT1-like (LTL) simultaneously with antisense resulted in the overall reduced photopigmentation phenotype. Thus,

another outcome of this finding is that it appears that knocking down the expression of carotenoid biosynthesis genes will, with few exceptions discussed in Chapter 2, not be helpful in elucidating the function of their products, unless it is possible to perform a chemical rescue. Finally, this finding implicates LTLs in diatom carotenoid biosynthesis. They have been hypothesized to replace  $\beta$ -carotene hydroxylase (BCH) in diatoms [Bertrand 2010], but this has not been previously assessed experimentally. While the results do not conclusively assign the LTLs to a specific step of diatom carotenoid biosynthesis, they do indicate that they are part of the pathway.

Chapter 2 also identified several evolutionary curiosities. One of those is finding that VDL2 has a domain with only very limited similarity based on sequence or predicted structure to currently known proteins. It will be interesting to characterize it, as it may catalyze previously unobserved chemistry. Another relates to the partial BCH sequence found in *T. pseudonana* and no other currently available diatom genomes. We found that it had gained a C-terminal domain with limited similarity to uncharacterized proteins in diverse organisms, and lost chloroplast targeting. The C-terminal domain is also unique to *T. pseudonana* among available sequenced diatom genomes. Why *T. pseudonana* has retained a partial BCH sequence is unknown but studying this could bring additional insight into diatom evolution. Additionally, it would be interesting to learn what its new function is, and what the novel C-terminal domain does. Finally, it appears that a portion of a chromosome containing a phytoene desaturase gene had been duplicated by insertion into a different chromosome. The duplicated region contains at least two other genes, and it is not possible given the currently available genomic information to determine the full span of the duplicated region. Nevertheless, this duplication was retained in the population, possibly conferring an evolutionary advantage.

Finally, a model for how diatom carotenoid biosynthesis may be differentially regulated in response to chloroplast division and irradiance increase was developed, based on transcriptomic

and physiological data. Not all hypotheses generated in Chapter 2 were tested, but they lay a foundation for further investigation of the still enigmatic pathway. Orthologues of all the enzymes identified in this chapter were found in the five other currently available diatom genomes. Thus, our findings are relevant to diatom carotenoid biosynthesis in general, beyond our model organism.

In Chapter 3, we took advantage of two transgenic *T. pseudonana* lines generated in Chapter 2 to evaluate the impact of altered photosynthetic pigmentation on growth and productivity. In one line, the novel VDL2 was overexpressed (OE). A reduction in the photoprotective Ddx/Dtx, which are involved in light energy dissipation, resulted, along with a stoichiometric increase in the abundance of the light-harvesting Fx. This proved to be a promising strategy for improving diatom productivity, resulting in a substantial increase in TAG and protein accumulation during exponential growth compared to wild type (WT) (up to 3.4-fold and 2-fold, respectively). This negatively correlated with light energy dissipation through non-photochemical quenching (NPQ), most of which relies of Ddx+Dtx content. It will be important to evaluate VDL2 OE performance in production conditions, utilizing the concepts discussed in Chapter 1.

VDL2 OE grew up to 7% slower than WT, which may be due to the presence of additional misplaced Fx. Because Ddx+Dtx abundance appears to be regulated separately from Fx, as discussed in Chapters 1 and 2, it may be possible to selectively reduce it. The model for differential diatom carotenoid biosynthesis regulation developed in Chapter 2 suggests that this may be accomplished by knocking down phytoene synthase 2 (PSY2). If PSY2 is indeed responsible for activating diatom carotenoid biosynthesis in response in increased irradiance as hypothesized, knocking it down should also downregulate the extent to which Ddx+Dtx accumulate in response to sinusoidal light as observed in Chapter 1, thus increasing productivity throughout the photoperiod in cultures grown outdoors. Another option to explore is targeting proteins involved in NPQ, such as LHCX3 [Hao et al. 2018].

The other transgenic line evaluated in Chapter 3 was created by simultaneously knocking down (KD) both copies of *T. pseudonana* LTL with antisense. The LTL KD lines had an overall reduction of photosynthetic pigmentation without a change in pigment ratios. This turned out to be not as conducive to improving diatom productivity as the VDL2 OE phenotype. The upside of LTL KD was that growth was comparable to WT, and there was an increase in TAG content of up to 40%, substantially less than in VDL2 OE. The downside was a reduction in protein content and apparent sustained cellular stress. Protein can be co-harvested along with TAG as a high-value co-product, and VDL2 OE is poised to provide both in substantially higher quantities than WT. LTL KD, on the other hand, would provide a comparably modest increase in TAG yield with a concomitant decrease in protein. Additionally, the stress observed in LTL KD may result in reduced fitness in production conditions.

To summarize, Chapter 2 delved into the diatom carotenoid biosynthesis pathway, identifying potential targets for altering cellular photopigment content in hopes of improving light utilization efficiency, and therefore productivity, in dense cultures. Chapter 2 has substantially advanced the understanding of diatom carotenoid biosynthesis and identified numerous next steps that need to be undertaken to further elucidate the biosynthetic pathway. Chapter 3 investigated the effectiveness of two photopigment manipulation strategies identified in Chapter 2 for increasing productivity in diatom cultures. One of those strategies was found to be promising. The utility of that strategy for improving performance in production conditions can be evaluated using the concepts presented in Chapter 1. Taken together, this work advances our understanding of diatom metabolism and provides strategies for a potentially substantial improvement in product yields, one based on improved light utilization efficiency in dense cultures, the other based on understanding and taking advantage of diel changes in metabolic and physiological processes in cultures grown outdoors.

## REFERENCES FOR THE CONCLUSIONS

- Bertrand M. (2010) Carotenoid biosynthesis in diatoms. *Photosynth Res* 106: 89-102.
- Bonnefond H., Moelants N., Talec A., Bernard O., Sciandra A. (2016) Concomitant effects of light and temperature diel variations on the growth rate and lipid production of *Dunaliella salina*. *Algal Res.* 14: 72-78.
- Coesel S., Obornik M., Varela J., Falciatore A., Bowler C. (2008) Evolutionary origins and functions of the carotenoid biosynthetic pathway in marine diatoms. *PLoS One* 3(8): e2896.
- de Mooij T., Janssen M., Cerezo-Chinarro O., Mussgnug J. H., Kruse O., Ballottari M., Bassi R., Bujaldon S., Wollman F., Wijffels R. H. (2015) Antenna size reduction as a strategy to increase biomass productivity: a great potential not yet realized. *J Appl Phycol* 27: 1063-1077.
- Edmundson S. J., Huesemann M. H. (2015) The dark side of algae cultivation: characterizing night biomass loss in three photosynthetic algae, *Chlorella sorokiniana*, *Nannochloropsis salina* and *Picochlorum* sp. *Algal Res.* 12: 470-476.
- Hao T., Jiang T., Dong H., Ou L., He X., Yang Y. (2018) Light-harvesting protein Lhcx3 is essential for high light acclimation of *Phaeodactylum tricornutum*. *AMB Expr* 8: 174.
- Hildebrand M., Davis A. K., Smith S. R., Traller J. C., Abbriano R. (2012) The place of diatoms in the biofuels industry. *Biofuels* 3(2):221-240.
- Mata T. M., Martins A. A., Caetano N. S. (2010) Microalgae for biodiesel production and other applications: a review. *Renew Sust Energ Rev* 14: 217-232.
- Moskalenko A. A., Karapetyan N. V. (1996) Structural role of carotenoids in photosynthetic membranes. *Z Naturforsch* 51c: 763-771.
- Ogbonna J. C., Tanaka H. (1996) Night biomass loss and changes in biochemical composition of cells during light/dark cyclic culture of *Chlorella pyrenoidosa*. *J Ferment Bioeng.* 82(6): 558-564.
- Orefice I., Chandrasekaran R., Smerilli A., Corato F., Caruso T., Casillo A., Corsaro M. M., Piaz F. D., Ruban A. V., Brunet C. (2016) Light-induced changes in the photosynthetic physiology and biochemistry in the diatom *Skeletonema marinoi*. *Algal Res.* 17: 1-13.
- Santabarbara S., Casazza A. P., Ali K., Economou C. K., Wannathong T., Zito F., Redding K. E., Rappaport F., Purton S. (2013) The requirement for carotenoids in the assembly and function of photosynthetic complexes in *Chlamydomonas reinhardtii*. *Plant Physiol* 161: 535-546.
- Wilhelm C., Buchel C., Fisahn J., Goss R., Jakob T., LaRoche J., Lavaud J., Lohr M., Riebesell U., Stehfest K., Valentin K., Kroth P. G. (2006) The regulation and nutrient assimilation in diatoms is significantly different from green algae. *Protist* 157(2): 91-124.
- Yang W., Zou S., He M., Fei C., Luo W., Zheng S., Chen B., Wang C. (2016) Growth and lipid accumulation in three *Chlorella* strains from different regions in response to diurnal temperature fluctuations. *Bioresour Technol.* 202: 15-24.